

A Thesis Submitted for the Degree of PhD at the University of Warwick

Permanent WRAP URL:

<http://wrap.warwick.ac.uk/87745>

Copyright and reuse:

This thesis is made available online and is protected by original copyright.

Please scroll down to view the document itself.

Please refer to the repository record for this item for information to help you to cite it.

Our policy information is available from the repository home page.

For more information, please contact the WRAP Team at: wrap@warwick.ac.uk

Electronic Nose Technology as a Point-of-Care Solution for the Detection of Colorectal Cancer

By

Eric William Westenbrink

A thesis submitted in fulfilment of the requirements for the degree of Doctor of Philosophy
in Engineering

University of Warwick, School of Engineering

September 2016

Table of Contents

List of Tables	vii
List of Illustrations.....	ix
Acknowledgements.....	xiv
Declarations	xiv
Abstract.....	xviii
Abbreviations.....	xix
1. Introduction	1
1.1. Clinical Scope	1
1.2. Basis of Approach	5
1.3. Project Aims.....	7
1.4. Thesis Structure	7
1.5. References.....	9
2. Literature Review: Volatile Analytics in Digestive Disease	12
2.1. Overview of Lower Gastrointestinal Disease	12
2.1.1. Non-Inflammatory Disease: Irritable Bowel Syndrome	13
2.1.2. Inflammatory Bowel Disease (IBD)	17
2.1.3. Colorectal Cancer	23
2.2. Overview of Electronic Nose Technology	30
2.2.1. Sensor Technologies	31
2.2.2. Ion Mobility Spectrometry	38
2.2.3. Electronic Nose Statistical Methods	42

2.2.4. Commercial Electronic Noses	48
2.2.5. Gas Chromatography – Mass Spectrometry	49
2.3. Review of Analytical Disease Detection by Gases and Volatiles	51
2.3.1. Biomarkers discovered using Gas Chromatography	56
2.3.2. Studies using Commercial Electronic Noses	57
2.4. Conclusions	59
2.5. References	61
3. Volatile Content of Urine Samples by Gas Chromatography – Mass Spectrometry	79
3.1. Scope and Disease States Studied	79
3.2. Methods and Materials.....	80
3.2.1. Instrument and Pre-concentration Method.....	80
3.2.2. Experimental Method	81
3.2.3. Data Analysis Method.....	82
3.3. Results	83
3.3.1. System Artefact Peaks.....	83
3.3.2. Sample Variation	87
3.3.3. Common Urine Peaks.....	90
3.4. Discussion and Conclusions	98
3.4.1. Metabolic and Dietary Links	98
3.4.2. Disease Incidence of Common Peaks	100
3.4.3. Conclusions and Future Work	101

3.5. References.....	104
4. Commercial Electronic Noses for Detection of Colorectal Cancer	107
4.1. Scope and Objectives	107
4.2. Fox 4000 Electronic Nose	107
4.2.1. Methods and Materials	107
4.2.2. Urine Samples.....	110
4.2.3. Experimental Methods.....	111
4.2.4. Statistical Methods	114
4.2.5. Volatile Sample Results	117
4.2.6. Urine Sample Results	120
4.3. Owlstone Lonestar FAIMS.....	126
4.3.1. Methods and Materials	126
4.3.2. Urine Samples.....	127
4.3.3. Experimental Methods.....	128
4.3.4. Statistical Methods	130
4.3.5. Urine Sample Results	131
4.4. Conclusions and Further Work	133
4.5. References.....	134
5. Development and Construction of the WOLF 4.1 Desktop Electronic Nose	137
5.1. Requirements and Objectives	137
5.2. System Overview.....	138
5.3. Sensor Technology.....	140

5.3.1. Gas Sensor Array	141
5.3.2. Environmental Sensing.....	142
5.3.3. Sensor Drive	143
5.4. Final Construction	145
5.5. Experimental Testing of WOLF 4.1 with Single-Volatile Samples	147
5.5.1. Introduction.....	147
5.5.2. Methods and Materials	147
5.5.3. Results and Discussion	149
5.6. Conclusions	159
5.7. References.....	161
6. Development and Construction of the WOLF 3.1 GC/E-Nose Instrument	162
6.1. Requirements and Objectives.....	162
6.2. System Overview.....	163
6.2.1. Airflow Sub-system.....	164
6.2.2. Chromatography Sub-system	165
6.2.3. Micropacked Column	167
6.2.4. User Interface	168
6.3. Sensor Technology.....	169
6.3.1. E2V MICS Sensors.....	170
6.3.2. AppliedSensors AS_MLV_P Sensors.....	172
6.3.3. Environmental Monitoring	175
6.4. Full Assembly.....	176

6.5. Development and Construction of a Humidity Generator for the Sensor Testing Rig	179
6.5.1. Requirements and Objectives	179
6.5.2. Control and Measurement System for Humidity Unit	181
6.5.3. Assembly and Integration	184
6.6. Experimental Testing of GC/E-Nose WOLF 3.1 with Single Volatile Samples	186
6.6.1. Introduction	186
6.6.2. Materials and Methods	188
6.6.3. Results and Discussion	195
6.7. Conclusions	208
6.8. References	211
7. Experimental Testing of WOLF 4.1 and WOLF 3.1	214
7.1. WOLF 4.1 Colorectal Cancer Distinction from Healthy and Diseased Controls	214
7.1.1. Methods and Materials	214
7.1.2. Statistical Analysis	215
7.1.3. Results and Discussion	216
7.1.4. Conclusions	221
7.2. WOLF 3.1 Colorectal Cancer Distinction from Healthy and Diseased Controls	222
7.2.1. Introduction	222
7.2.2. Materials and Methods	222

7.2.3. Results and Discussion	225
7.2.4. Conclusions and Future Work	230
7.3. References.....	231
8. Conclusions and Further Work.....	233
8.1. Recommendations and Further Work	238
Appendix 1: Additional GC-MS Chromatograms and Mass Spectra	241
Common Peak Mass Spectra in Urine Samples	243

List of Tables

Table 1.1: List of deliverables for a new screening/ diagnostic triage tool being introduced to clinic – Page 6

Table 2.1: Pathological criteria for distinction of IBS – Page 15

Table 2.2: Alarm features for indicating negative diagnosis of IBS – Page 16

Table 2.3: List of macroscopic features for UC and CD diagnosis – Page 21

Table 2.4: List of personal and environmental risk factors for CRC – Page 25

Table 2.5: List of macroscopic symptoms of CRC – Page 26

Table 2.6: List of features extracted directly from sensor responses in electronic nose studies – Page 44

Table 2.7: List of features extracted from curve fitting parameters in electronic nose studies – Page 45

Table 2.8: Classification methods used in electronic nose studies – Page 47

Table 2.9: List of commercially-available electronic noses on the market – Page 49

Table 2.10: List of studies investigating olfactory response for detection of biological diseases and pathogens – Page 55

Table 3.1: List of disease groups analysed by GC-MS and pre-concentration techniques employed – Page 80

Table 3.2: List of top three candidate NIST classifications for chromatogram peaks (chosen candidates in bold) and rates of incidence (low in red, normal in black, high in green) – Page 92-93

Table 3.3: List of candidate volatiles found in this study and their presence in the results of Wahl et al. (2) and Mills et al. – Page 98

Table 3.4: Compounds found at abnormal rates of incidence within samples of each disease group – Page 101

Table 4.1: List and description of sensors included in the Fox 4000 electronic nose – Page 109

Table 4.2: Patient demographics for urine sample cohort run through the Fox 4000 – Page 111

Table 4.3: Patient demographics for urine sample cohort run through the Owlstone Lonestar FAIMS – Page 128

Table 5.1: List of sensor manufacturers, mechanisms, and target gases included in the array – Page 142

Table 5.2: Volatile groups tested in aqueous solution to determine WOLF sensor sensitivities – Page 149

Table 6.1: List of sensor manufacturers, mechanisms, and target gases included in the array – Page 169

Table 6.2: Corresponding response colours for WOLF 3.1 sensors in Section 6.6.3 – Page 196

Table 7.1: Patient demographics for urine sample cohort run through the WOLF 4.1 – Page 215

Table 7.2: Average discriminant function scores for 3-group LDA classification – Page 219

Table 7.3: Average discriminant function scores for 2-group LDA classification – Page 221

Table 7.4: Patient demographics for urine sample cohort run through the WOLF 3.1 – Page 223

Table 8.1: List of volatile chemicals found in urine headspace by GC-MS in this study – Page 234

Table 8.2: Comparison of the tested electronic noses against original deliverables – Page 237

List of Illustrations

Figure 1.1: Illustration of the proportions of screening and diagnostic (symptomatic consulter) populations that suffer from CRC (yellow) and do not (white) out of 100 – Page 2

Figure 1.2: Patient pathways from first contact to resolution for screening (left) and symptomatic (right) populations – Page 3

Figure 2.1: Chart showing relative global prevalence of digestive disease – Page 12

Figure 2.2: Venn diagram of environmental factors with an effect on UC and CD development – Page 19

Figure 2.3: Type 1 – 4 classifications of colorectal carcinoma – Page 27

Figure 2.4: Paris classification of superficial colorectal carcinoma – Page 28

Figure 2.5: Comparison between the human and electronic nose – Page 31

Figure 2.6: Band gap energy diagram for aluminium oxide, chromium oxide and Cu with H₂S – Page 32

Figure 2.7: Structural diagram of a thick film metal oxide gas sensor – Page 33

Figure 2.8: Structural diagram of a thin film metal oxide gas sensor – Page 34

Figure 2.9: Internal structure of a modern electrochemical gas sensor – Page 35

Figure 2.10: Sensing chamber of a Non-Dispersive Infrared gas sensor – Page 36

Figure 2.11: Pellistor catalytic gas sensor internal structure – Page 37

Figure 2.12: Wheatstone bridge circuit for pellistor sensor – Page 38

Figure 2.13: Diagram showing the operation of Ion Mobility Spectrometry by drift tube, (a) during the initial baseline halt state, (b) after opening the ion shutter, and (c) typical response – Page 40

Figure 2.14: Illustration of the operation of a Field Asymmetric Ion Mobility Spectrometer – Page 42

Figure 2.15: Illustration showing the operation of a mass spectrometer – Page 50

Figure 2.16: Diagram of methods for sample acquisition and processing – Page 53

Figure 3.1: Example of chromatogram of a blank air sample run with ITEX pre-concentration – Page 84

Figure 3.2: Example of chromatogram of a blank air sample run with SPME pre-concentration – Page 85

Figure 3.3: Example of the mass spectrum of an artefact peak found at 3.39 minutes – Page 86

Figure 3.4: Example of the mass spectrum of an artefact peak found at 5.14 minutes – Page 87

Figure 3.5: Example chromatogram of a typical urine sample – Page 88

Figure 3.6: Example chromatogram of a heavily-diluted urine sample – Page 89

Figure 3.7: Example chromatogram of a urine sample with unique dietary peaks – Page 90

Figure 3.8: Example mass spectrum of an ITEX peak found at 1.74 minutes – Page 94

Figure 3.9: Example mass spectrum of an ITEX peak found at 4.56 minutes – Page 95

Figure 3.10: Example mass spectrum of a SPME peak found at 4.54 minutes – Page 96

Figure 3.11: Example mass spectrum of a SPME peak found at 9.76 minutes – Page 97

Figure 4.1: Photograph of the Fox 4000 in the laboratory – Page 110

Figure 4.2: Raw sensor output data from a urine headspace sample – Page 114

Figure 4.3: Average sensor responses to acetone between 4th May 2013 and 23rd April 2015 – Page 118

Figure 4.4: Average sensor responses to isopropanol between 4th May 2013 and 23rd April 2015 – Page 119

Figure 4.5: Average sensor responses to 1-propanol between 4th May 2013 and 23rd April 2015 – Page 120

Figure 4.6: LDA plot of CRC against IBS and volunteer samples run through the Fox 4000 – Page 122

Figure 4.7: LDA plot of CRC against IBS samples run through the Fox 4000 – Page 124

Figure 4.8: Polar plot of average response from each sensor to CRC and IBS samples – Page 125

Figure 4.9: Labelled photograph of the Owlstone Lonestar setup in the laboratory – Page 127

Figure 4.10: Raw data from the Lonestar FAIMS for a colorectal cancer patient – Page 130

Figure 4.11: FDA plot of CRC against healthy control samples run through the Lonestar – Page 132

Figure 5.1: System block diagram for the WOLF 4.1 electronic nose – Page 139

Figure 5.2: Front End of the LabVIEW control software for the WOLF 4.1 – Page 140

Figure 5.3: 3-Dimensional diagram of the SHT15 temperature/humidity sensor – Page 143

Figure 5.4: Potentiostatic circuit for driving an electro-chemical sensor – Page 144

Figure 5.5: Photograph of the interior of the WOLF 4.1 – Page 146

Figure 5.6: Photograph of the user interface and exterior of the WOLF 4.1 – Page 146

Figure 5.7: High variance average sensor response to acetone – Page 150

Figure 5.8: Low variance average sensor response to acetone – Page 151

Figure 5.9: High variance average sensor response to ethyl acetate – Page 152

Figure 5.10: Low variance average sensor response to ethyl acetate – Page 153

Figure 5.11: High variance average sensor response to propan-1-ol – Page 154

Figure 5.12: Low variance average sensor response to propan-1-ol – Page 155

Figure 5.13: High variance average sensor response to propan-2-ol – Page 156

Figure 5.14: Low variance average sensor response to propan-2-ol – Page 157

Figure 5.15: High variance average sensor response to toluene – Page 158

Figure 5.16: Low variance average sensor response to toluene – Page 159

Figure 6.1: Illustration of the air flow system layout and the control algorithm used for the WOLF 3.1 – Page 165

Figure 6.2: Model of the GC temperature control assembly in the WOLF 3.1 (NiCr wire and thermocouple wrapped around hollow bar) – Page 167

Figure 6.3: Chromatogram of HAYESEP R micropacked column separation of MAPP gases – Page 168

Figure 6.4: SGX Sensortech MICS sensor body – Page 170

Figure 6.5: Typical MICS sensor heating and measurement circuits – Page 171

Figure 6.6: Appliedsensor AS-MLV-P sensor body – Page 172

Figure 6.7: Appliedsensor AS-MLV-P sensor circuit layout – Page 173

Figure 6.8: Scaled Solidworks model of the MICS sensor chamber – Page 174

Figure 6.9: Photographs of fully assembled sensor chambers for the WOLF 3.1 – Page 175

Figure 6.10: Full assembly Solidworks model for the WOLF 3.1 system – Page 177

Figure 6.11: Final implementation of the WOLF 3.1 with exposed interior – Page 178

Figure 6.12: Final implementation of the WOLF 3.1 in operation – Page 179

Figure 6.13: Diagram of the air flow pathways and control algorithm of the humidity rig control system – Page 183

Figure 6.14: Photograph of the assembled full testing rig – Page 185

Figure 6.15: Schematic of the pneumatic system in the WOLF 3.1 – Page 188

Figure 6.16: LabVIEW PC control front-end of the volatile testing rig – Page 189

Figure 6.17: Graph of the relationship between sensor response and relative humidity at 10 ppm acetone concentration – Page 196

Figure 6.18: Graphs showing the relationship between sensor responses and 10 – 100 ppm concentrations of acetone at relative humidity levels of 0%, 5%, 10%, 15% and 20% – Page 198

Figure 6.19: Graphs showing the relationship between sensor responses and 10 – 100 ppm concentrations of ethanol at relative humidity levels of 0%, 5%, 10%, 15% and 20% – Page 199

Figure 6.20: Graphs showing the relationship between sensor responses and 10 – 100 ppm concentrations of toluene at relative humidity levels of 0%, 5%, 10%, 15% and 20% – Page 201

Figure 6.21: Graphs showing the relationship between sensor responses and 10 – 100 ppm concentrations of valeraldehyde, at relative humidity levels of 0% and 5% – Page 202

Figure 6.22: Graphs of WOLF 3.1 sensor response to acetone concentrations of 10 ppm, 20 ppm and 50 ppm at 5% relative humidity – Page 204

Figure 6.23: Graphs of WOLF 3.1 sensor response to ethanol concentrations of 10 ppm, 20 ppm and 50 ppm at 5% relative humidity – Page 205

Figure 6.24: Graphs of WOLF 3.1 sensor response to toluene concentrations of 10 ppm, 20 ppm and 50 ppm at 5% relative humidity – Page 207

Figure 6.25: Graphs of WOLF 3.1 sensor response to valeraldehyde concentrations of 10 ppm, 20 ppm and 50 ppm at 5% relative humidity – Page 208

Figure 7.1: Voltage signals produced by the ISBs of a subset of WOLF sensors from a urine sample – Page 216

Figure 7.2: Radial plot of the average normalised response of all 13 WOLF 4.1 sensors to CRC (full line) and IBS (dashed line) urine samples – Page 217

Figure 7.3: LDA classification separating all three sample groups of CRC, IBS and healthy controls (Ctl) – Page 218

Figure 7.4: Box plot of LDA classification separating IBS and CRC sample groups – Page 220

Figure 7.5: WOLF 3.1 sensor response to a CRC urine headspace sample (CRC232) – Page 226

Figure 7.6: WOLF 3.1 sensor response to an IBS urine headspace sample (IBS150) – Page 227

Figure 7.7: LDA classification of CRC and IBS samples from WOLF 3.1 data – Page 228

Figure 7.8: Mean values of “Sig-base3” for CRC and IBS samples across 20 included time slices – Page 229

Figure 7.9: Mean values of “Average” for CRC and IBS samples across 20 included time slices – Page 230

Acknowledgements

I would like to express my gratitude to my main supervisor James Covington, who has helped me develop myself in the lab and earn my stripes for three and a half exciting years. His diligence in reviewing the written work for publications, university submissions and this thesis at all hours of the day has been invaluable. Thanks are also gratefully given to my medical supervisor Ramesh Arasaradnam, who has given me extremely useful clinical insight and drive. I must also thank Karna “Chandu” Bardhan, who gave me unique insight as a mentor and inspired me with his fervent imagination and sense of wonder towards all areas of science.

Many thanks go to Christopher Pursell, Frank Courtney and Ian Griffith, who all had to bear with me on the many occasions I sought their greater technical experience. I am also grateful to Nicola O’Connell, Catherine Bailey and Subiatu Wurie for their support from the hospital in sending the urine samples that were vital to this work.

I’d like to thank my family for their constant support leading me to this point. Finally, I thank my partner and best friend, Helen, without whose immense patience, support and love I would not have completed this thesis.

Declarations

This thesis is submitted to the University of Warwick in support of my application for the degree of Doctor of Philosophy. It has been composed by myself and has not been submitted in any previous application for any degree.

The work presented (including data generated and data analysis) was carried out by the author except in the cases outlined below:

- The Computer Aided Design models for the humidity unit (Chapter 4) were completed by Christopher Jefferies
- The experimental testing of urine samples on the Fox 4000 and Owlstone Lonestar (Chapter 4) was completed by Courtney Ryan-Fisher
- The statistical analysis for the Owlstone Lonestar urine cohort (Chapter 4) was completed by James Covington
- The PC test control software for the volatile testing rig (Chapter 6) and for the WOLF 4.1 (Chapter 5) were developed by James Covington
- The interface circuit boards in the WOLF 4.1 (Chapter 5) and the sensor circuit boards in the WOLF 3.1 (Chapter 6) were designed in part by Ian Griffith
- The sensor chamber in the WOLF 4.1 (Chapter 5) was designed by Frank Courtney
- The mixing chambers in the humidity unit and the WOLF 3.1 (Chapter 6) were designed by Christopher Pursell

Parts of this thesis have been published by the author:

- 1) Westenbrink, E., Arasaradnam, R.P., O'Connell, N., Bailey, C., Nwokolo, C., Bardhan, K.D., Covington, J.A., Development and application of a new electronic nose instrument for the detection of colorectal cancer. 2014, Biosens Bioelectron 67, 733-738.
- 2) Westenbrink, E., O'Connell, N., Bailey, C., Nwokolo, C., Bardhan, K., Arasaradnam, R., Covington, J., Detection of colorectal cancer from urinary volatile organic compounds using a new chromatograph/electronic nose instrument – WOLF system. 2016, British Society of Gastroenterologists Annual Meeting 2016. (Submitted)
- 3) Westenbrink, E., O'Connell, N., Bailey, C., Nwokolo, C., Bardhan, K., Arasaradnam, R., Covington, J., Detection of colorectal cancer from urinary volatile organic

compounds using a new chromatograph/electronic nose instrument – WOLF system. 2016, Biosens Bioelectron. (In Draft)

- 4) Arasaradnam, R.P., Westenbrink, E.W., MacFarlane, M., Harbord, R., Chambers, S., O'Connell, N., Bailey, C., Nwokolo, C., Bardhan, K.D., Savage, R.S., Covington, J.A., Differentiating Coeliac Disease from Irritable Bowel Syndrome by Urinary Volatile Organic Compound Analysis – A Pilot Study. 2014, PLOS ONE 9(10), E107312.
- 5) Covington, J.A., Westenbrink, E.W., Ouaret, N., Harbord, R., Bailey, C., O'Connell, N., Cullis, J., Williams, N., Nwokolo, C., Bardhan, K.D., Arasaradnam, R.P., Application of a Novel Tool for Diagnosing Bile Acid Diarrhoea. 2013, Sensors 13(9), 11899-11912.
- 6) Covington, J.A., Westenbrink, E.W., O'Connell, N.C., Bailey, C., Thomas, M., Nwokolo, C., Harmston, C., Bardhan, K.D., Arasaradnam, R.P., Towards the Non-Invasive Detection of Colorectal Cancer: The Role of Electronic Noses (E-Nose) and Faims. 2013, Gastroenterology 144(5), S-879.
- 7) Covington, J.A., Westenbrink, E.W., Thomas, M., O'Connell, N.C., Bailey, C., Nwokolo, C., Bardhan, K.D., Arasaradnam, R.P., Towards the Detection of Bile Acid Diarrhea: A Novel Non-Invasive Approach Using Electronic Noses (E-Noses) and Field Asymmetric Ion Mobility Spectroscopy (FAIMS). 2013, Gastroenterology 144(5), S-655.
- 8) Covington, J.A., Harbord, R., Westenbrink, E.W., Bailey, C., O'Connell, N., Dhaliwal, A., Nwokolo, C., Foley, A., Marya, N., Baptista, V., Bardhan, K.D., Cave, D.R., Arasaradnam, R.P., Detection of Urinary Volatile Organic Compounds in Patients With Inflammatory Bowel Disease and Controls by an Electronic Nose – A Transatlantic Study. 2014, Gastroenterology 146(5), S-796.
- 9) Arasaradnam, R.P., MacFarlane, M., Ryan-Fisher, C., Westenbrink, E.W., Hodges, P., Thomas, M.G., Chambers, S., O'Connell, N., Bailey, C., Harmston, C., Nwokolo, C.,

Bardhan, K.D., Covington, J.A., Detection of Colorectal Cancer (CRC) by Urinary Volatile Organic Compound Analysis. 2014, PLOS ONE 9(9), E108750.

- 10) Arasaradnam, R.P., McFarlane, M., Daulton, E., Westenbrink, E.W., O'Connell, N., Wurie, S., Nwokolo, C., Bardhan, K.D., Savage, R., Covington, J.A., Non-Invasive Distinction of Non-Alcoholic Fatty Liver Disease using Urinary Volatile Organic Compound Analysis: Early Results. 2015, J Gastrointest Liver 24(2), 197-201.

Abstract

This thesis presents a comparative study of electronic nose technologies for the detection of colorectal cancer from healthy and disease controls using gases/volatiles in urine headspace. A review is made of the clinical features of lower gastro-intestinal diseases and the sensing technologies available to electronic noses. The literature surrounding the detection of cancers and other diseases by sensing of gases and volatiles is also reviewed. An investigation into the common volatile components of urine headspace is conducted experimentally using a gas chromatograph – mass spectrometer (451 Scion SQ, Bruker Corp), resulting in 10 candidate chemicals with links to gut bacteria and diet. A humidity generation unit was developed and integrated with a volatile testing rig to aid in assessing the response of different electronic nose technologies to volatile chemical groups.

Four electronic nose systems were tested in parallel studies using urine headspace samples from patients of colorectal cancer (CRC) and irritable bowel syndrome (IBS), as well as healthy volunteers. This involved pre-classified multivariate analysis techniques followed by K-Nearest-Neighbour validation for sensitivity and specificity. A commercial electronic nose based on metal oxide sensors (Fox 4000, AlphaMOS Ltd) analysed 93 urine samples giving a sensitivity and specificity to colorectal cancer of 54% and 48%. A field asymmetric ion mobility spectrometer that is commercially available (Lonestar, Owlstone Ltd) was tested using 133 samples of CRC and volunteer samples, yielding 88% disease sensitivity and 60% specificity. A new electronic nose system was developed using state-of-the-art amperometric and optical sensors and tested against 92 urine samples, giving a respective sensitivity and specificity to CRC against IBS controls of 78% and 79%. A final instrument was developed that includes a micro-packed GC column and an array of micro-hotplate metal oxide sensors, which analysed 49 samples to give a 92% sensitivity and 77% specificity to CRC against IBS.

Abbreviations

Abbreviation	Definition
ADC	Analogue-Digital Converter
BAD	Bile Acid Diarrhoea
BAM	Bile Acid Malabsorption
CAD	Computer-Aided Design
CH ₄ or CH ₄	Methane
CD	Crohns Disease
CO	Carbon Monoxide
CO ₂ or CO ₂	Carbon Dioxide
CRC	Colorectal Cancer
CS	Chip Select
CT	Computer Tomography
Ctl	Healthy Controls
E-nose	Electronic Nose
EPA	Environmental Protection Agency
ETO	Ethylene Oxide
FAIMS	Field Asymmetric Ion Mobility Spectrometer
FDA	Fisher Discriminant Analysis
FIT	Faecal Immunochemical Testing
GI	Gastro-intestinal
GC	Gas Chromatograph
H ₂ S or H ₂ S	Hydrogen Sulphide
IBD	Iritable Bowel Disease
IBDU	Iritable Bowel Disease Unclassified
IBS	Iritable Bowel Syndrome
IBS-A	Alternating IBS
IBS-C	Constipation-Based IBS
IBS-D	Diarrhoea-Based IBS
IC	Integrated Circuit
IMS	Ion Mobility Spectrometry
IR	Infrared
ISBs	Individual Sensor Boards
ITEX	In-Tube Extraction
KNN	K-Nearest-Neighbour
LDA	Linear Discriminant Analysis
MFC	Mass Flow Controller
MOX	Inorganic Metal Oxides
MS	Mass Spectrometry
NAFLD	Non-Alcoholic Fatty Liver Disease
NDIR	Non-Dispersive Infrared
NH ₃ or NH ₃	Ammonia
NICE	National Institute for Health and Care Excellence

Abbreviation	Definition
NiCr	Nickel Chromium
NI-DAQ	National Instruments Data Acquisition
NIST	National Institute of Standards and Technology
NIH	National Institute of Health
NO	Nitrogen Dioxide
O ₃ or O ₃	Ozone
PC	Personal Computer
PCA	Principle Component Analysis
PCB	Printed Circuit Board
PDMS	Polydimethylsiloxane
PID	Photo-Ionisation Detector
PLS	Partial Least Squares
ppb	Parts per Billion
ppm	Parts per Million
PS	Adenomatous Polyps
PTFE	Polytetrafloripheline
SAW	Surface Acoustic Wave
SD	Secure Digital
SO ₂	Sulphur Dioxide
SPME	Solid Phase Microextraction
TIC	Total Ion Count
UHCW	University Hospital of Coventry and Warwickshire
UC	Ulcerative Colitis
USB	Universal Serial Bus
V	Volunteer
VOC	Volatile Organic Compound

1. Introduction

1.1. Clinical Scope

Colorectal cancer is a highly prevalent form of cancer with a high associated mortality, especially in the Western world and increasingly in those areas that are acquiring the modern Western lifestyle (1). There was an average annual incidence of the disease in developed, Western countries of 13.4% of total cancer cases, with an average of 7.8% elsewhere in the world. The UK has seen a rising incidence of this cancer from 1990 to 2010 of over 125% (2), and there are similar trends being shown in the USA and in the rest of Europe (1). The quality of life for patients both before and after successful treatment of tumours can be severely impacted, with typical symptoms including: mobility, pain/discomfort, psychological well-being, bowel control, urination, body image and sexuality (3). It has been shown that 50 – 80% of patients have some form of complication even after treatment has finished, depending on their age group. The 5-year survival rate is relatively high (93.2%) for Stage 1 colorectal cancer, however this rate is reduced with every subsequent stage of cancer severity resulting in a minimum 5-year survival rate of 8.1% for stage four cancers (4). The global mortality rate for this disease was recently estimated at 394,000 deaths per year, which is the fourth highest amongst cancer-related deaths (1). It is important to have a diagnostic method that can reliably distinguish this disease in the earliest stage of development possible.

The symptoms presented by patients can include rectal bleeding, abdominal pain, weight loss, anaemia and a variety of different deviations from normal bowel habit (5). However there is a high level of variation between sufferers, and symptoms are often very similar to those for many other disease of the lower gastro-intestinal tract such as ulcerative colitis (UC), Crohns disease (CD) and irritable bowel syndrome (IBS). The first two of these can be

Introduction

highly debilitating and aggressive diseases in their own right, with many overlapping features and an associated mortality (6). Irritable bowel syndrome is potentially a series of condition affecting a much larger fraction of the population compared to colorectal cancer, although it has much better overall prognosis and very different treatment regime (7).

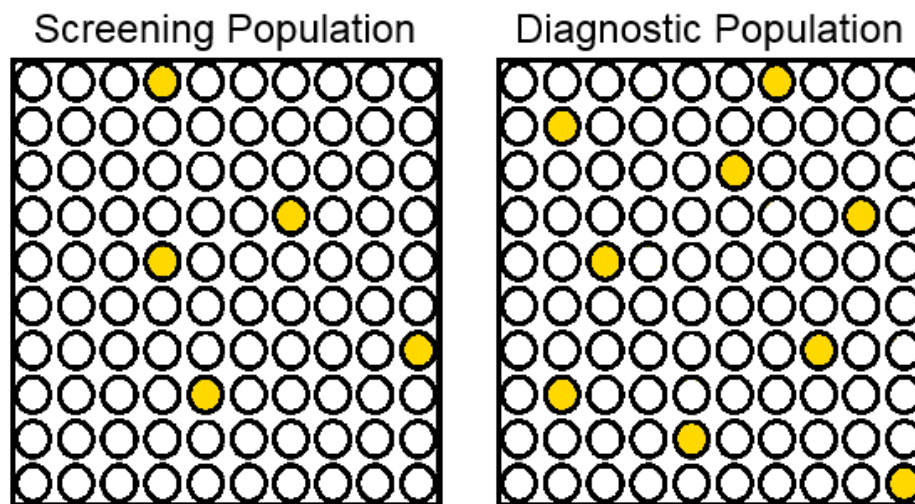


Figure 1.1: Illustration of the proportions of screening and diagnostic (symptomatic) populations that suffer from CRC (yellow) and do not (white) out of 100.

The current definitive diagnostic method for colorectal cancer is colonoscopy with biopsy, which is a highly invasive technique that requires both skill and time to complete successfully and incurs a high associated cost for each procedure. The typical fraction of patients who undergo a colonoscopy and have malignant carcinomas is shown in Figure 1.1. The prevalence of colorectal cancer is three orders of magnitude lower than that of irritable bowel syndrome (1, 8), but there are some distinctive symptoms (such as rectal bleeding) that allow many patients in the diagnostic population to be triaged away from colonoscopy. The screening population has been specifically chosen from a high risk age group (over 60's in the UK), and so proportional numbers will also be higher than in the full population.

Introduction

There is a number of different scanning and chemical technologies that have been highlighted as non-invasive screening and diagnostic triage tools for colorectal cancer including computer tomography (CT) colonoscopy and tests on patient faecal samples (9). While improvements are being made in these techniques, they generally do not provide reliable sensitivity to the disease to provide a definitive diagnosis. In addition, the current popular screening and triage methods (Faecal Occult Blood and Faecal Immunochemical Testing) require patients to collect a stool sample of significant size to hand in to clinical staff. This process is known to have a very low acceptance level among patients, meaning that either quality of diagnosis or patient ease is affected.

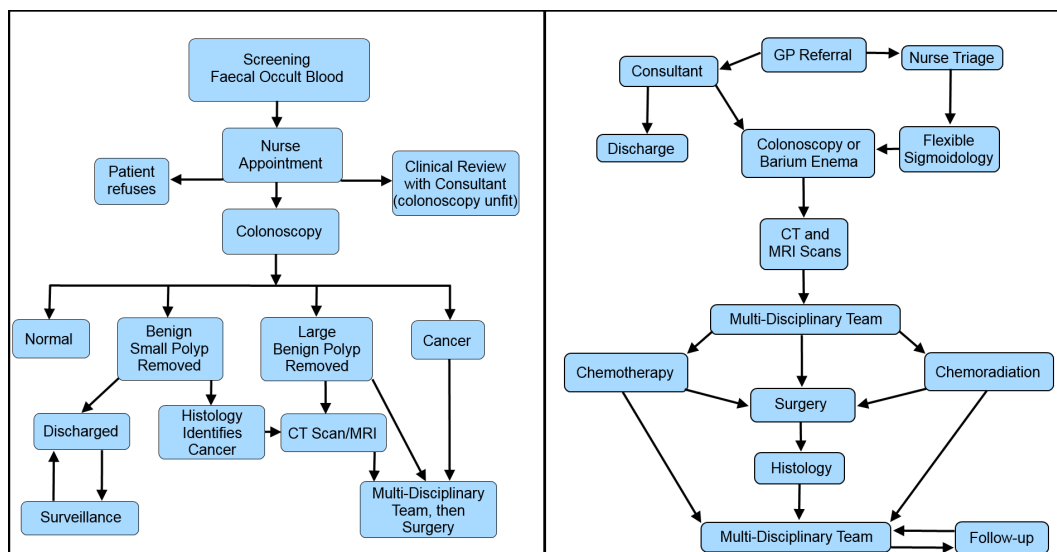


Figure 1.2: Patient pathways from first contact to resolution for screening (left) and symptomatic (right) populations (10)

The current process of definitive colorectal cancer diagnosis requires patients to visit primary healthcare centres multiple times, often with lengthy wait times for sample testing by specialist groups (10). The full processes of diagnosis for patients in the screening and symptomatic populations are shown in Figure 1.2. The average length of time between symptom initiation and diagnosis for a population of Spanish patients during 2006 – 2009

Introduction

was 128 days, with a further 155 days of treatment time (11). The main factors that affected these time intervals were related to the perceptions of the patient and consulted healthcare professionals to their symptoms. There is also a very high monetary cost to look after patients of colorectal cancer, with individual costs of surgical procedures in the UK ranging between £4493 and £8308 in 2012 (10). The associated per-instance cost of colonoscopy is also very high, with estimated figures in the US from 2000 being nearly \$700 per session (approximately £500 if it were in the UK) (12).

In this light, it would be highly beneficial for both patients and healthcare providers if another technique was available to be used at the point of initial screening (Figure 1.2 top left) or triage (Figure 1.2 top right) to better and more rapidly distinguish between cancer and non-cancer cases. This technique could be employed during the two week wait period between initial appointments and further review in the NHS, which would enhance its ability in such an enriched population (10). This could greatly reduce the number of colonoscopies required in primary healthcare centres, resulting in both lower costs and shorter waiting times. This should aid patient mortality rates and help reduce severe symptoms by achieving earlier diagnosis before the disease can develop. There is therefore a need for new non-invasive diagnostic tools that can be used at the point of care, preferably by non-specialist medical staff, to perform reliable diagnostic triage and/or screening. Patient urine samples have been collected at the University Hospital of Coventry and Warwickshire prospectively during a period just prior to bowel preparation for colonoscopy, as shown in the symptomatic population diagram in Figure 1.2. These are available for investigation, along with healthy urine samples from among volunteer hospital staff, under the Ethical Approval Number 09/H1211/38.

1.2. Basis of Approach

Associations between the aromas given off by biological media and underlying disease of patients suffering from pulmonary tuberculosis and bladder ulcerations have been mentioned in the Hippocratic writings (13). The popularity of techniques involving peripheral factors that can add to diagnostic information, such as the smell emanating from patients, was boosted in modern times by a report in the 1980's (14). This report highlighted that particular effluvia from biological waste products and exhaled breath could be linked to metabolic disease, uremia and many others. In that same decade, a technology was newly developed that employed an array of gas sensors to behave as an olfactory unit similar to a biological nose (15). There have been a large number of studies released since then that have strived to use this 'electronic nose' technology in biomedical applications (16). There have also been numerous reviews of these investigations, but very few of these have any direct experimental comparisons of different instruments using the same test methodology and timeframe. There are a wide variety of commercial electronic noses available (detailed in Chapter 2), and many of these have been used in investigations into the detection of cancers (including colorectal cancer specifically). However, the instruments currently studied do not include all of the recent sensor technologies that could be utilised in this approach. There remains a large degree of uncertainty in which combination of technologies would be the most suitable for the distinction between lower gastro-intestinal diseases such as colorectal cancer, inflammatory bowel disease and irritable bowel syndrome. A significant step can be made in clarifying this situation by comparative experimental assessment of multiple different technologies, using parallel testing methodologies.

For a new technology to be adopted within clinical practice, it must be accepted to have made an improvement in at least one aspect (such as disease sensitivity) displayed by current methods while at least maintaining the level of other aspects (such as usability). A

Introduction

number of deliverables should ideally be set based on clinical demand, to be used as a metric for comparing the technologies under test. A list of such pre-requisite features has been compiled for a diagnostic triage tool for detecting colorectal cancer in Table 1.1, taken from discussions with gastroenterologists that are experts in this clinical pathway. The aim for a candidate technology is to be a non-invasive point-of-care solution for the distinction of colorectal cancer from controls. The highest priority is given to sensitivity to disease, with other features such as rapid analysis, portability and robustness of design given a secondary level of importance.

Deliverables	Clinical Reasoning
Sufficient sensitivity to detect patients that are suffering from colorectal cancer	Highest priority, as paramount to maintaining an acceptable level of patient care and safety
Sufficient specificity to screen out patients not suffering from colorectal cancer	Reduces the number of patients undergoing unnecessary endoscopy
Ability to be used as a stand-alone device	Allows for use within clinic without any need for prior setup or external analysis
Non-invasive technique	Higher patient acceptance, giving higher quality of life and lower refusal rate
Use of 'acceptable' medium for analysis	Higher patient acceptance, giving higher quality of life and lower refusal rate
Reasonable degree of portability	Allows transport between rooms and areas without excessive effort
Low technical knowledge required for analysis	Potential for front-line clinical staff to use without extensive training
Relative low cost per treatment compared to colonoscopy	Improves overall cost of lower gastro-intestinal (GI) disease diagnosis for healthcare centres
Reasonable analysis time	Increases the speed at which patients can be triaged, with potential for analysis as they wait
Ability to be serviced and maintained easily	Provides quick turn-around to minimise the time that the device is out-of-use
Ability to store patient data for later use and updates	Each confirmed diagnosis can be added to training set for improved diagnostic strength
Robust design that cannot be easily damaged by contact	Minimises chance of device being put out-of-use by unexpected damage

Table 1.1: List of deliverables for a new screening/ diagnostic triage tool being introduced

to clinic

1.3. Project Aims

This study presents an investigation into the use of 'electronic nose' technology as a point-of-care solution for the detection of colorectal cancer. The biological medium used for this investigation is the headspace of urine. Urine is already a widely collected biological sample, and thus has a high level of patient acceptance. There have been a wide variety of studies conducted on the gaseous and volatile contents of urine (17, 18). There is some degree of consensus of constituent chemicals between these studies, which adds some confidence in using this biological medium as a valid method for discriminatory test for colorectal cancer.

Candidate technologies are compared by their ability to distinguish urine samples taken from known patients of colorectal cancer from controls taken from irritable bowel syndrome sufferers and healthy volunteers. The included technologies constitute a variety of the 'state-of-the-art' in terms of sensing and separation techniques. Some of these were found in commercially-available instruments, while others were acquired individually and constructed into systems that were designed and built in-house to achieve the deliverables described in Section 1.2. A significant amount of background work was also carried out to construct appropriate testing rigs for the instruments, and to determine the common content of urine headspace for determining the validity of the approach. The electronic noses under test will analyse a cohort of urine samples with a common test methodology, aiming to distinguish colorectal cancer samples from healthy and diseased controls. At the end of this project, the candidate technologies will be compared against their success in fulfilling the deliverables.

1.4. Thesis Structure

Chapter 2 is a review section, which first outlines the current clinical situation of related lower gastro-intestinal diseases with regards to prevalence, pathological features and

Introduction

current diagnostic methods. The technologies and techniques available within the field of electronic noses is then reviewed, followed by a literature review of research looking into the use of volatile biomarkers for disease.

A body of new experimental research into the volatile content of urine headspace by gas chromatograph-mass spectrometer is presented in Chapter 3. This section has a focus on finding commonality among the chemicals found in the patient samples of many different gastro-intestinal diseases, as well as some degree of distinction between them using chemical incidence levels.

Chapter 4 presents new comparative experimental research on two commercially-available instruments (AlphaMOS Fox 4000, Owlstone Lonestar). This made use of single volatile samples to check the sensitivity and drift of the sensors, and then analysed cohorts of urine samples from colorectal cancer patients as well as controls of irritable bowel syndrome and healthy volunteers.

The next chapter (Chapter 5) details the design and construction of a new electronic nose, with an array of electrochemical and optical gas sensors that have previously not been used in commercial instruments. This system is developed as a test platform that achieves some of the pre-requisite deliverables. Single volatile samples are then used to check sensitivity levels and develop an experimental method.

Chapter 6 presents the design and construction of another new instrument building on lessons learnt from the work in Chapter 5, which combines the retention-based temporal separation of gas chromatography with the pattern-based discrimination techniques used in electronic noses. The micro-hotplate metal oxide sensors used in this instrument have not yet been used with a chromatography column. This instrument has been developed

Introduction

with the point-of-care application in mind, and aims to meet the deliverables for a new diagnostic triage tool. Single volatile samples were again used to determine a suitable method, as well as sensitivity and separation levels.

The experimental testing of the two in-house built electronic noses using comparative urine sample sets is detailed in Chapter 7. The ability of both machines to distinguish colorectal cancer from irritable bowel syndrome and healthy controls is presented.

The results of all of the tested technologies are compared in the concluding chapter, and the merits and limitations of the investigation are explored.

1.5. References

- 1) Haggard, F.A., Boushey, R.P., Colorectal Cancer Epidemiology: Incidence, Mortality, Survival, and Risk Factors. 2009, *Clin Col Rect Surg* 22(4), 191-197.
- 2) Wilkinson, J.R., Morris, E.J.A., Downing, A., Finan, P.J., Aravani, A., Thomas, J.D., Sebag-Montefiore, D., The rising incidence of anal cancer in England 1990-2010: a population-based study. 2014, *Colorectal Dis* 16, 234-239.
- 3) Downing, A., Morris, E.J.A., Richards, M., Corner, J., Wright, P., Sebag-Montefiore, D., Finan, P., Kind, P., Wood, C., Lawton, S., Feltbower, R., Wagland, R., Vernon, S., Thomas, J., Glaser, A.W., Health-Related Quality of Life After Colorectal Cancer in England: A Patient-Reported Outcomes Study of Individuals 12 to 36 Months After Diagnosis. 2015, *J Clin Oncol* 10.1200/JCO.2014.56.6539
- 4) O'Connell, J.B., Maggard, M.A., Ko, C.Y., Colon Cancer Survival Rates With the New American Joint Committee on Cancer Sixth Edition Staging. 2004, *J Natl Cancer Inst* 96(19), 1420-1425.

Introduction

- 5) Astin, M., Griffin, T., Neal, R.D., Rose, P., Hamilton, W., The diagnostic value to symptoms for colorectal cancer in primary care: a systemic review. 2001, *Br J Gen Pract*, 231-243.
- 6) Magro, F., Langner, C., Driessen, A., Ensari, A., Geboes, K., Mantzaris, G.J., Villanacci, V., Becheanu, G., Borralho Nunes, P., Cathomas, G., Fries, W., Jouret-Mourin, A., Mescoli, C., de Petris, G., Rubio, C.A., Shepherd, N.A., Vieth, M., Eliakim, R., European consensus on the histopathology of inflammatory bowel disease. 2013, *J Crohns Colitis* 7, 827-851.
- 7) Spiller, R., Aziz, Q., Creed, F., Emmanuel, A., Houghton, L., Hungin, P., Jones, R., Kumar, D., Rubin, G., Trudgill, N., Whorwell, P., Guidelines on the irritable bowel syndrome: mechanisms and practical management. 2007, *Gut* 56, 1770-1798.
- 8) Canavan, C., West, J., Card, T., The epidemiology of irritable bowel syndrome. 2014, *J Clin Epidemiol* 6, 71-80.
- 9) Levin, B., Brooks, D., Smith, R.A., Stone, A., Emerging Technologies in Screening for Colorectal Cancer: CT Colonography, Immunochemical Fecal Occult Blood Tests, and Stool Screening Using Molecular Markers. 2003, *CA Cancer J Clin* 53, 44-55.
- 10) Goom, J., Lingard, S., Ellis-Brookes, L., Barnes, M., Francis, N., A Costed Pathway for Colorectal Cancer. 2012, National Cancer Intelligence Network, Public Health England.
- 11) Esteve, M., Leiva, A., Ramos, M., Pita-Fernández, S., González-Luján, L., Casamitjana, M., Sánchez, M.A., Pértega-Díaz, S., Ruiz, A., Gonzalez-Santamaría, P., Martín-Rabadán, M., Costa-Alcaraz, A.M., Espí, A., Macià, F., Segura, J.M., Lafita, S., Arnal-Monreal, F., Amengual, I., Boscá-Watts, M.M., Manzano, H., Magallón, R., Factors related with symptom duration until diagnosis and treatment of symptomatic colorectal cancer. 2013, *BMC Cancer* 13(87).

Introduction

- 12) Sonnenberg, A., Delco, F., Inadomi, J.M., Cost-Effectiveness of Colonoscopy in Screening for Colorectal Cancer. 2000, *Ann Intern Med* 133, 573-584.
- 13) Adams, F., Hippocratic writings: Aphorisms IV, V. 1994, *The Internet Classic Archive*, pp. 1-10.
- 14) Fitzgerald, F.T. Tierney, L.M., Jr., The bedside Sherlock Holmes. 1982, *West J Med*, 169-175.
- 15) Persaud, K., Dodd, G.H. Analysis of discrimination mechanisms of the mammalian olfactory system using a model nose. 1982, *Nature*. 299, 352-355
- 16) Wilson, A.D., Baietto, M., Applications and advances in electronic-nose technologies developed for biomedical applications. 2011, *Sensors* 11, 1105-1176.
- 17) Wahl, H.G., Hoffmann, A., Luft, D., Liebich, H.M., Analysis of volatile organic compounds in human urine by headspace gas chromatography-mass spectrometry with a multipurpose sampler. 1999, *J Chromatogr A* 847(1-2), 117-125.
- 18) Bouatra, S., Aziat, F., Mandal, R., Guo, A.C., Wilson, M.R., Knox, C., Bjorndahl, T.C., Krishnamurthy, R., Saleem, F., Liu, P., Dame, Z.T., Poelzer, J., Huynh, J., Yallou, F.S., Psychogios, N., Dong, E., Bogumil, R., Roehring, C., Wishart, D.S., The Human Urin Metabolome. 2013, *PLOS ONE* 8(9), E73076.

2. Literature Review: Volatile Analytics in Digestive Disease

2.1. Overview of Lower Gastrointestinal Disease

The main initiative behind this investigation is to compare the feasibility and development potential of a low-cost, non-invasive method for diagnosing lower GI diseases at the point of care. There are an increasing number of cases of GI disease patients within the developed world, and therefore it is becoming a common health issue in later life for individuals in the UK, United States and other Western countries (1). The relative global prevalence of these diseases over the years of 2013 and 2014 are shown in the pie chart in Figure 2.1. A large majority – approximately 11% of the international population – of lower GI patients suffer from IBS, with much smaller proportions of relatively equal size have ulcerative colitis (UC) or colorectal cancer (CRC). Finally, the smallest proportion of the global population suffers from Crohns disease, with an overall prevalence of 0.0322% (2).

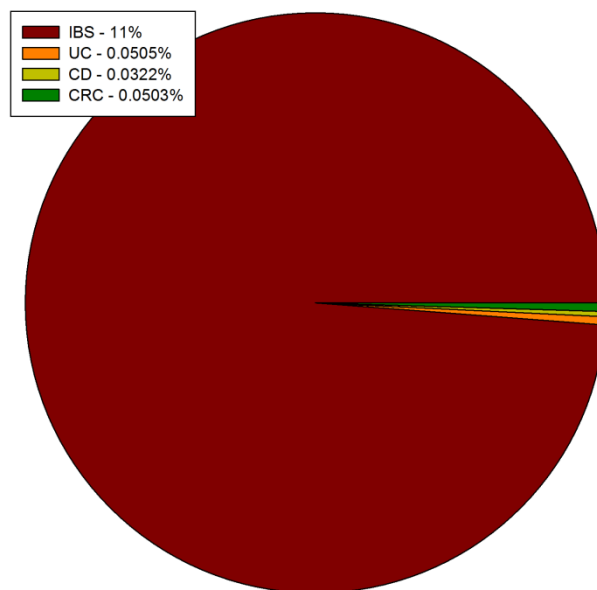


Figure 2.1: Chart showing relative global prevalence of digestive disease (2, 3, 4)

2.1.1. Non-Inflammatory Disease: Irritable Bowel Syndrome

Affecting approximately 20% of adults in the western world, this is the most prevalent lower gastro-intestinal disease. There are three categories based on the manner in which stool frequency is altered, either by diarrhoea (IBS-D), constipation (IBS-C) or an alternating mix of the two (IBS-A) (1).

2.1.1.1. Disease Prevalence

The prevalence of IBS varies between 0 – 20 % of the total population in different regions internationally (2). This difference is generally associated with prevalence of the modern “western” diet in the country of study, with populations of the USA and UK both being on the high end of the scale. Countries with a simpler, less excessive diet such as France and Thailand have a much lower reported prevalence of 4.7 – 5.7%. However, there is not a high level of confidence in the numbers quoted as the metrics of actual disease prevalence must usually be estimated. This is due to a number of investigational studies showing that up to 70% of the symptomatic population do not consult with a physician (5). There have been a large number of studies that estimate the percentage of the population being affected by IBS by community survey, leading to end estimates that are highly varied. For example, estimates of UK prevalence (a country with relatively high levels of medical standards, awareness and access) have included values in a range between 6.1% and 21.6% depending on the population being surveyed (6, 7). This leads to a large degree of uncertainty in the patient demographics and population magnitude for this disease.

By far the majority of reported cases suffer from IBS-D, with the most documented cause being Bile Acid Malabsorption (BAM) or the dysfunction of the bowel to re-absorb bile acids that are secreted to aid in the digestion process. There have been links to other means of dysfunction, such as Fat Malabsorption, but these are less well-attributed (1). Many studies featuring large population sizes have seen similar relative prevalence of the three

IBS sub-types, where just over half of the reported sufferers being classed with IBS-D with the remainder being fairly equally divided between IBS-C and IBS-A (8).

There are some significant features in the demographics of patients reporting IBS symptoms that are consistent on the international scale. Disease rates are seen to be 67% higher in women than in men in a large number of regions (9), with a female prevalence of 14.0% compared to that of 8.9% for the male population. There are others areas such as South Asia and South America where the gap between sexes is less distinguished; this could be due to a more equal likelihood for men and women with symptoms to seek primary care advice. There is another shift in likelihood of symptoms with increasing age, where those under 50 years of age have a 25% higher prevalence than those who are older (10). This result points to a potential easing of symptoms with increasing age, or to an increase in overall epidemiology in newer generations. Studies have shown that IBS prevalence could be associated with both lower and higher end socioeconomic status, with an additional negative relationship between the percentages of the population employed in manual labour jobs (11, 12). Finally, there could be a hereditary component in the disease, with risk of IBS being approximately twice as high if an individual has a biological relative with the disease (13).

2.1.1.2. Associated Pathology

Table 2.1 shows the criteria that are used clinically to constitute a diagnosis of the disease state of IBS. These have been adjusted and re-released in the years, indicated on the top row of the table, as the understanding of the disease by the medical community grew. The key symptoms shown below include pain or discomfort in the abdominal region that is associated with a change in stool frequency, consistency and an inability to temporarily relieve these complications. In most cases, these only present themselves in intermittent periods of a few days with subsequent remission, though this is not always the case (14).

The wide variety in the symptomatic patterns of IBS patients is captured in the Rome classifications, where the subjects can experience any combination of alteration in stool frequency, consistency, straining and urgency of defaecation. The classification of a patient into the three sub-categories is solely based on whether over 25% of their stools are ‘loose’ (IBS-D), ‘hard’ (IBS-C) or both (IBS-A). There are a large number of links to the daily routine of the patients and the onset or ‘flaring’ of IBS symptoms. These include reports of increased defaecation in the morning, increased onset after meals, and aggravation of symptoms by stress created by a number of different factors.

Manning (1978)	Rome I (1989)	Rome II (1999)	Rome III (2006)
<p>2 or more of the following symptoms:</p> <ul style="list-style-type: none"> - Abdominal distension - Pain relief with defecation - Frequent stools with pain - Looser stools with pain - Passage of mucus - Sensation of incomplete evacuation 	<p>At least 3 months of continuous or recurrent abdominal pain:</p> <ul style="list-style-type: none"> - Relieved with defecation <p>or</p> <ul style="list-style-type: none"> - Associated with change in stool consistency <p>With at least 2 of the following on at least 25% of days:</p> <ul style="list-style-type: none"> - Altered stool frequency - Altered stool form - Altered stool passage - Passage of mucus - Bloating or abdominal distension 	<p>At least 12 weeks in past 12 months of continuous or recurrent abdominal pain or discomfort</p> <p>With at least 2 of the following:</p> <ul style="list-style-type: none"> - Relief with defecation - Altered stool frequency - Altered stool form - Onset of symptoms more than 12 months before diagnosis 	<p>At least 3 days per month in past 12 weeks of continuous or recurrent abdominal pain or discomfort</p> <p>With at least 2 of the following:</p> <ul style="list-style-type: none"> - Relief with defecation - Altered stool frequency - Altered stool form - Onset of symptoms more than 6 months before diagnosis

Table 2.1: Pathological criteria for distinction of IBS (14)

An important factor in IBS distinction is the lack of a number of alarm features that, if present, would point a clinician away from this disease and potentially to another with much higher severity, as shown in Table 2.2 (14). These have also been shown to add to the accuracy of diagnosis for all digestive disease, with a much lower risk of later escalation

another disease (15). These alarm features include a number of criteria based on symptoms and demographics of the patient. Distinction of IBS is important clinically as it leads to the least complication in terms of overall health as compared to most other lower gastrointestinal diseases. The severity of IBS does not extend much beyond the symptoms themselves, although these can cause a large degree of discomfort, pain and reduced quality of life (16).

Alarm Features List:
Age >50 years
Short history of symptoms
Documented weight loss
Nocturnal Symptoms
Male sex
Family history of colon cancer
Anaemia
Rectal bleeding
Recent antibiotic use

Table 2.2: Alarm features for indicating negative diagnosis of IBS (14)

2.1.1.3. Current Diagnostic Methods

There are no currently-known consistent biological markers that can be used for diagnosis of IBS in general, and the accepted method involves the positive distinction of symptom criteria and the absence of alarm features described above (17). However, a number of diagnostic tests may be performed in order to rule out the presence of other gastrointestinal diseases with additional severity of pathological complications. A complete blood count may be executed in order distinguish anaemia, and stool tests can be performed to check for bacterial infection, parasites or faecal occult blood. There are more invasive procedures that can be undertaken as a more definitive test for negative diagnosis, such as direct visual colonoscopy, capsule endoscopy and barium enema. The final category of tests that are commonly performed are psychological in nature and used to indicate anxiety, depression or other problems that may be linked to the pathology. The main arguments for

performing these tests include a deviation from the standard IBS characteristics such as inclusion of one or more alarm features. There are also wider factors that affect the inclusion of these tests in the diagnostic approach involving their availability and cost within the clinical environment.

The most common subset of the disease is IBS-D, for which one underlying cause that is better understood is the inability of the GI tract to effectively re-absorb bile acids and is denoted bile acid diarrhoea (BAD) (18). This subset of the disease has been indicated in several studies that 68% of IBS-D patients in a large population had mild to severe BAD. The current 'gold standard' diagnostic method for BAD is the SeHCAT retention test, which involves injecting a photo-fluorescent tag that binds to bile acids and detecting how much is retained by the body after a period of one week (2). However, this technique is not employed internationally and many countries including the US omit it due to its cost implications.

2.1.2. Inflammatory Bowel Disease (IBD)

This group actually incorporates a variety of conditions which are based around the inflammation of different areas of the bowel. The most observable of these includes ulcerative colitis and Crohns disease, which are both centred in the colon and lower bowel. Another large portion of IBD cases do not have a clearly-identified region of effect in the GI tract, and so are denoted IBD unclassified (IBDU) (19).

2.1.2.1. Disease Prevalence

Both UC and CD have a high prevalence within the Western developed world, with the highest figures internationally being found in Europe at 505 and 322 per 100,000 per person years respectively (20). The prevalence in many other countries in developing economic areas are also increasing, such as East Asia and Africa (21). This ratio is also likely

to be on the rise in all countries, due to high incidence levels and the chronic nature of IBD with low associated mortality. The emergence of IBD in developing countries in Asia has been manifested by an initial rise in UC followed by an increase in CD prevalence. This pattern supports the theory that shifts in lifestyle are key factors in the epidemiology of IBD (2). Further links can be made between specifically the diet and lifestyle of a region and the prevalence of IBD by the demonstration of particular studies, which showed that paediatric emigrants to British Columbia had an even higher incidence of IBD than the general paediatric population (22).

IBD prevalence in the paediatric population has been found to be dominated by CD incidence, with studies showing a higher level as compared to UC in countries such as Sweden, Norway, Finland and Canada (2). The rates of IBD have been found to be relatively similar across both sexes, although some have shown a higher incidence in males when aged 5-14 years. Investigations into the change in incidence levels of IBD with age have shown a peak between 20 and 39 years (23) with the potential for a second rise at approximately age 60 (24).

A wide variety of environmental factors have been shown to influence the development of UC and CD, a large number of which are illustrated on the Venn diagram in Figure 2.2. There are many dietary factors that can affect IBD prevalence, with a high carbohydrate/fat content causing detrimental effects and the inclusion of foods with high fibre and vitamin D having a protective influence. Other ingested products such as antibiotics and oral contraceptives can also lead to an increased risk, as well as a more complex relationship with breast feeding in infants (25). Other risk factors include those relating to the general environment experienced in many economically developed countries, such as an urban setting, stress, smoking and air pollution. Interestingly, it has also been noted that smoking may have a protective effect from ulcerative colitis (26).

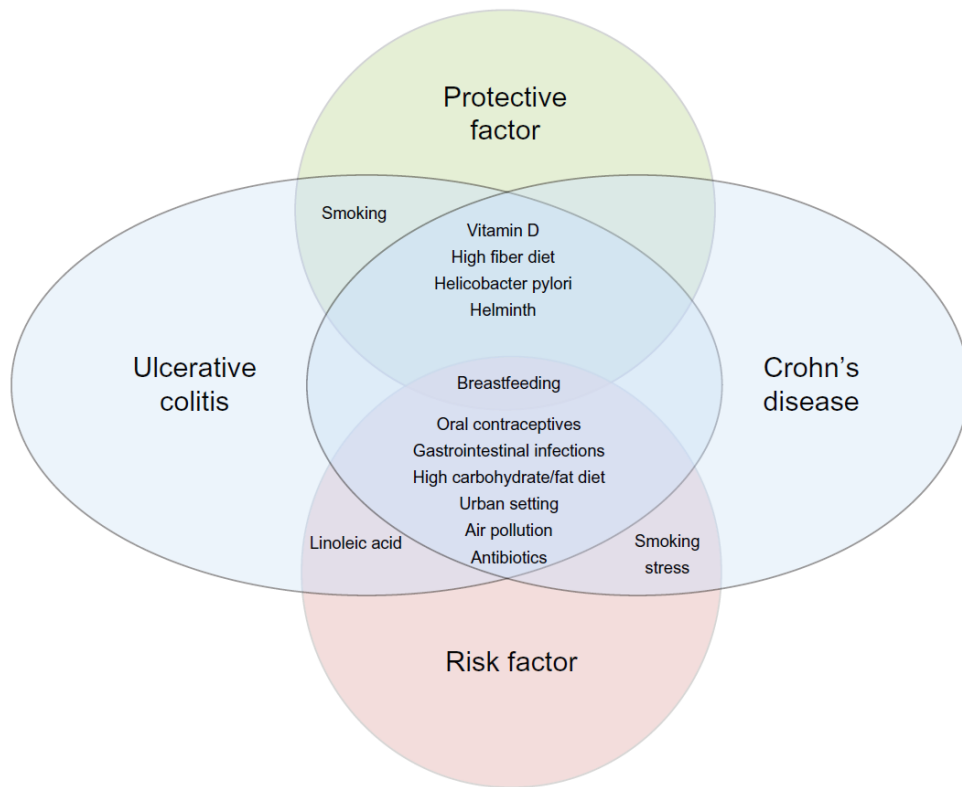


Figure 2.2: Venn diagram of environmental factors with an effect on UC and CD development (2)

2.1.2.2. Associated Pathology

Both forms of IBD are characterised by a chronic inflammation of the lower GI tract that can “flare” for periods of up to two weeks with subsequent months with only mild symptoms. The pathology of UC and CD affects the right and left colon at varying degrees, and is presented in symptoms including bloody diarrhoea (main symptom), abdominal pain, fever, and a large number of other potential signs (2). There is a wide range of severities associated with both of these disease modes, but in most cases of CD or severe UC there is a very significant impact on the well-being and quality of life of patients. In the former case, a terminal form of inflammation often occurs and resolution of severe symptoms is only achieved by surgical treatment or removal of the lower GI tract (19).

Many of the macroscopic features of both UC and CD are included in Table 2.3, which shows a degree of commonality between the two but also highlights areas of distinction. Both modes of disease involve inflammation of some regions of the GI tract with ulcers, lesions and/or polyps lining the interior walls, the aggravation of which being the main cause of pain and bleeding (27). Ulcerative colitis is more localised within the colon and rectum, with a diffuse distribution of ulcers and pseudopolyps in these areas with a relatively low risk for complication (as compared to CD). A degree of atrophy of mucosa can be seen in this form of IBD, producing well-like ulcers that penetrate through the GI tract layers (28). There are rare cases where “backwash-ileitis” can occur, in which the inflammation extends up to the ileum and can be very difficult to distinguish from the more terminal form of ileitis found in CD (29). CD contrasts this with a more segmented inflammation that can cover the whole GI tract, commonly including the ileum while the rectum is usually spared of symptoms. There is also the potential for a large host of features to classify this disease visually, including lesions, fissures, deep ulcers, strictures and an associated increase in the wall thickness of the GI tract. There are also a large number of microscopic pathological features for UC and CD that supports the distinction of the two by the regional continuity of inflammation (both chronic and acute) (27). There are also specific complications associated with each disease mode, such as hyperplasia or metaplasia of particular tissue cells.

Macroscopic features used for the diagnosis of IBD.		
	Ulcerative colitis	Crohn's disease
Localization GI tract	Especially colon and rectum	Whole GI tract
Ileum	Not except in backwash-ileitis	Often involved
Colon	Left > right	Right > left
Rectum	Commonly involved	Typically spared
Distribution GI tract	Diffuse (continuous)	Segmental (discontinuous)
Ulcers	Superficial ulcers	Aphthoid ulcers, confluent deep linear ulcers
Pseudopolyps	Common	Uncommon
Skip-lesions	Absent	Present
Cobblestone-pattern	Absent	Present
Deep fissures	Absent except in fulminant colitis	Present
Fistulae	Absent except in fulminant colitis	Present
Mucosal atrophy	Marked	Minimal
Thickness of the wall	Normal	Increased
Fat wrapping	Absent	Present
Strictures	Uncommon	Present

Table 2.3: List of macroscopic features for UC and CD diagnosis (27)

2.1.2.3. Current Diagnostic Methods

The current methods for diagnosis include a variety of indicators, including differentiation by intra- and extra-intestinal symptoms, sensing of relevant biomarkers, cross-sectional imaging and various forms of endoscopy. Both forms of IBD can include symptoms such as faecal blood, chronic diarrhoea and abdominal pain, but with other features that differentiate them statistically from each-other (19). Ulcerative colitis patients are more likely to report visible blood in the stool and rectal urgency, with Crohns disease presenting from more systemic symptoms such as a significant weight loss, fever and tachycardia (30). Extra-intestinal manifestations such as enteropathic arthritis and metabolic osteopathy can be seen in patient fractions of 24 - 40% (31) and 22 - 67% (32) respectively, with the prevalence being greater in CD for the former case and roughly equal in the latter. Stool samples are often examined to look for a variety of biomarkers normally constituent in serum, intestinal mucosa and cellular sources (19) to indicate some of the pathologies described in Section 2.1.2.2, as well as to check for infection as an alternate explanation for

symptoms (2). Cross-sectional imaging is used primarily upon first diagnosis of CD to stage the inflammatory and obstructive natures of the disease as well as for follow-up monitoring (33).

The definitive initial examination for diagnosis and classification of IBD has continued to be ileo-colonoscopy for a number of decades (34). There are a significant number of macroscopic features that distinguish both UC and CD specifically (as shown in Section 2.1.2.2), that can also be seen visually using an endoscope and lead to a high confidence diagnosis in at least 75% of cases. Many of the differentiating characteristics described can be used to accurately distinguish CD from UC in the vast majority of cases, with a marked minority of studies presenting atypical and mixed features (35). Additional confidence may be gained from histopathology of terminal ileum and colorectal specimens to check for the distinctive microscopic features that are also present. This confidence is such that examination of specimens from at least 5 sites along the colon, rectum and ileum during ileo-colonoscopy the recognised “gold-standard” diagnostic and classification tool for IBD. In addition, endoscopy of the small bowel (36) and upper GI tract (37) may also increase confidence in classification of CD due to its potential to present itself throughout the entire system.

The main issues with the level of complexity involved in the current diagnostic method is the time period from initial report of symptoms to definitive diagnosis from the patient point of view, and the cost required for this confidence level for the healthcare centre. The first of these has been addressed by a number of studies; one of these reported that delay in diagnosis of CD was the most severe with only 75% of patients being diagnosed within 24 months (38). The cost models for IBD modes are very significant due to their chronic, severe nature with a lower relative morbidity. A recent UK investigation into annual costs

for NHS trusts showed an average estimated £3084 per UC patient and £6256 per CD patient, increasing to £10760 and £10513 for severe cases of the respective diseases (39).

2.1.3. Colorectal Cancer

Colorectal cancer (CRC) remains one of the leading causes of cancer-related death in Europe and the USA (40) (41), and is becoming more prevalent in these areas as time goes on.

2.1.3.1. Disease Prevalence

Over 9% of cancer incidence internationally can be attributed to CRC, which is currently the third leading form of cancer in terms of commonality while being fourth in levels of cancer-related death (42). In the USA alone the 2005 annual rate of new cases has been 108,100, with 40,800 deaths in that same year. Prevalence of the disease seems to be nearly equal between men and women, with the fraction of incident cancer caused by CRC in men and women being 9.4% and 10.1% respectively (43). However, CRC is much more common in developed Western-cultured countries, with these regions experiencing incidence rates up to 10 times what is seen in those that are less developed (44). This variation may be due to the potential for extreme underreporting in the latter category, but may also relate to differences in diet and/or lifestyle between these geographical areas. Mortality from CRC has significantly decreased in developed nations in North America, Western Europe and Australia (45). Meanwhile, in developing countries that are beginning to experience a more western lifestyle such as in Eastern Europe, associated mortality has increased by 5 – 15 % every 5 years (46).

There are a variety of factors associated with the risk of developing CRC, which can be broadly divided into two categories: those that cannot be modified by a change in lifestyle, and those that will decrease chance of incidence if an adjustment is made. A list of

affecters in both categories is shown in Table 2.4. The chance of diagnosis of CRC increases from the age of 40 to a progressively greater extent with increasing years, whereby 90% of cases are found in those aged 50 or older (47). However, there is an increasing shift of incidence within the population aged 10 – 49 (48). Adenomatous polyps are precursors to colorectal cancer, with nearly 95% of cases developing from them after an estimated 5 to 10 years to become malignant (49). Adenoma removal may reduce the chance of CRC incidence, but there is also an associated increase in additional cancer development in this area. There is also a relationship between IBD sufferers and future development of CRC, with the risk of malignancy being increased an estimated 4 – 20 times (46). There also seems to be some inherited risk of CRC development, with approximately 5 – 10% of incidences being attributed to recognised conditions such as familial adenomatous polyposis and hereditary nonpolyposis colorectal cancer (50). Overall, 20% of those diagnosed with CRC have one or more family members that also suffer from the disease, but it is not clear which of these are purely hereditary and which are as a result of shared environmental factors (51).

There are a wide variety of environmental factors involved in increased CRC risk, which are not fully understood, but can be managed in order to reduce the chance of incidence in individuals. There are very strong links to changes in dietary practices and reduction in risk of diagnosis by up to 70% (52). Negative dietary factors include consumption of high fat content foods (46) and large quantities of meat (53), while the dietary intake of fruits, vegetables and other foods that are high in fibre has a positive effect (46, 54). Many of these aspects that are associated with increased risk are common constituents of a western diet. In addition to this, physical inactivity and excess body weight are two more environmental factors that could heavily affect up to a third of CRC cases (49). There has been a well-reported inverse association between risk of diagnosis and physical activity

intensity and frequency. Smoking of tobacco cigarettes also has a very negative effect on the lower GI system; up to 12% of CRC deaths have been reported to be attributed to smoking (55). The habit has also been linked to the formation of adenomatous polyps (56). Heavy consumption of alcohol has been found to factor into the diagnosis of CRC at a younger age, with an additional negative interaction with smoking (55).

Risk Factors	
Unaffectable	Environmental
Age in years	Diet and nutrition
Adenomatous polyps (PS)	Physical activity and obesity
Inflammatory Bowel Disease (IBD)	Cigarette smoking
Family history of CRC or PS	Heavy alcohol consumption
Inherited genetic risk	

Table 2.4: List of personal and environmental risk factors for CRC (42)

The survival rate of CRC varies with the stage of disease found at diagnosis, with a range of 5-year survival rate for local, regional and distant metastatic cancers being at 90%, 70% and 10% respectively (57). The average 5-year survival rate in the United States has risen considerably in recent years, with a change from 1995 to 2000 of 11-14% for both men and women (58).

2.1.3.2. Associated Pathology

There are a variety of symptoms related to CRC, all of which can be also associated with other lower GI diseases. Therefore, it is difficult for clinicians to determine the exact symptoms that will point to CRC specifically, especially in cases where the patient does not fit into the higher risk age range of 40 years or greater. A systematic review of the likelihood of symptoms to be attributed to a positive cancer diagnosis has been compiled from a total of 23 independent studies with hundreds of thousands of patients in 2011 (59). The statistical results of this review are shown in Table 2.5, including the sensitivities, specificities and positive/negative likelihoods of all of the common CRC-associated

symptoms. Boundaries for a Confidence Interval have been added on either side of each statistical value for each symptom, such that 95% of all cases would have values within the range given in brackets. All of the symptoms included had a relatively poor sensitivity, highlighting the difficulty in using pathology to classify the disease. In addition to these results, paired symptoms were also studied to determine if a match could be made to maximise positive likelihood. However, the results of this analysis were a relatively poor sensitivity to CRC from other lower GI diseases. This study concluded a similar situation to that implied by current National Institute for Health and Care Excellence (NICE) guidelines (60), that those suffering from CRC are very likely to present almost all of the symptoms shown in Table 2.5 but this will not specifically indicate this condition.

Symptom	Sensitivity % (95% CI)	Specificity % (95% CI)	Positive likelihood ratio (95% CI)	Negative likelihood ratio (95% CI)
Rectal bleeding	17 (16.4 to 18.4)	98 (98.3 to 98.6)	5.31 (1.65 to 17.07)	0.77 (0.57 to 1.03)
Abdominal pain	31 (29.6 to 32.0)	91 (91.1 to 91.6)	2.47 (1.09 to 5.61)	0.75 (0.62 to 0.90)
Weight loss	11 (10.6 to 12.3)	96 (95.7 to 96.1)	3.48 (2.08 to 5.80)	0.82 (0.69 to 0.97)
Diarrhoea	19 (18.3 to 20.3)	94 (93.8 to 94.2)	2.44 (1.57 to 3.79)	0.86 (0.70 to 1.04)
Constipation	27 (25.9 to 28.2)	89 (88.7 to 89.3)	1.74 (1.11 to 2.72)	0.84 (0.79 to 0.88)
Anaemia	37 (35.7 to 39.1)	92 (91.2 to 92.3)	4.62 (3.03 to 7.06)	0.68 (0.65 to 0.71)
Change in bowel habit	11 (10.4 to 12.1)	99 (98.9 to 99.1)	11.47 (10.12 to 13.00)	0.90 (0.89 to 0.91)
Bloating	54 (38.7 to 67.9)	39 (33.4 to 45.6)	0.88 (0.63 to 1.15)	1.18 (0.79 to 1.64)

Table 2.5: List of macroscopic symptoms of CRC (59)

The key pathologies that are used to classify CRC in a specific way are those presented on the interior of the colon as discovered by colonoscopy (61). Colorectal carcinomas can be classified into Types 0 – 4, which are distinguished on an approximate scale of the depth of infiltration into surrounding tissue in the colonic wall. Type 0 carcinomas are in the early stage of development and the rest are in more advanced stages. A cross-sectional diagram showing Types 1-4 of advanced carcinomas is shown in Figure 2.3. The range includes protuberant tumours (Type 1), as well as ulcerative lesions with either clear margins (Type

2) or infiltration of the surrounding tissue to a marginal (Type 3) or diffuse (Type 4) level. Type 2 is the most common class of carcinoma found clinically, and can potentially be detected from other examinations aside from endoscopy.

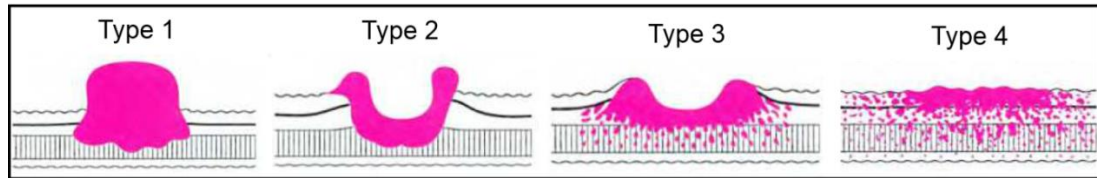


Figure 2.3: Type 1 – 4 classifications of colorectal carcinoma (61)

Colonoscopy can yield discovery of a range of different carcinomas and adenomatous polyps that appear to be very similar, with an adenoma width of 2 cm having a 40% chance of being malignant (62). The factors that have a relationship with risk of malignancy include carcinoma size, number, and some components of morphology (63). A widely-used method for distinguishing between different forms of early colorectal carcinomas is the Paris classification, for which a flow diagram is included in Figure 2.4 (64). The candidate lesions are first classified as “polypoid” (Type 0-I) or “non-polypoid” (Type 0-II), with the former having two sub-classes based on the morphology of the polyp in question. The “non-polypoid” lesions are sub-classified by their elevation level as compared to the surrounding colonic wall, giving a final denunciation of Type 0-IIa, b or c.

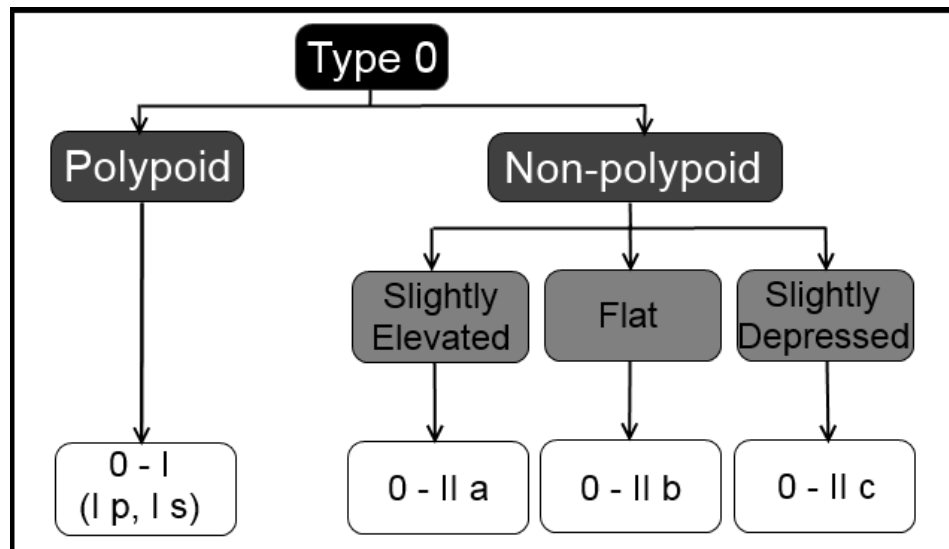


Figure 2.4: Paris classification of superficial colorectal carcinoma (61)

These classification systems are used to predict the level of tissue invasion by the carcinomas present, helping to stage the disease and estimate the risk of metastasis to the lymph nodes. This provides a suitable basis for selection of treatment, usually between endoscopic treatment and surgical removal of some or all of the colon (61). For example, Type 0-I lesions have an increased risk of invasion to the submucosal layer of the colon with increasing size, while Type 0-IIc lesions have a tendency for deeper infiltration despite a much smaller size.

2.1.3.3. Current Diagnostic Methods

There is a need for an effective and unobtrusive method for screening at risk individuals. This is largely due to the broad overlap of symptoms exhibited from patients suffering from CRC and from those with other lower GI diseases such as IBS. The definitive diagnostic test for this disease is colonoscopy, which is well-established in informing treatment choices based on the criteria described above (4). It has been shown that a large-scale colonoscopy screening program for a national population of individuals aged 55 or older would be highly effective in detecting adenomas and Type 0 carcinomas (65) However, this technique is

highly invasive, with disruptive bowel preparations required beforehand and not sufficiently cost effective for large-scale screening purposes. The cost of a single colonoscopy as estimated by American Medicare payments in 2000 is approximately \$695.95 (66). This has led to costs simply becoming too high to establish an effective screening method for colon cancer in the UK, and only the beginnings of a program in the USA (67).

Current non-invasive options for CRC diagnosis have shifted from the traditional method of measuring faecal occult blood due to a relatively low sensitivity to the disease (68). However, a relative cost of faecal occult blood testing in the USA is significantly less than colonoscopy at \$3.50 for a single treatment, giving it the potential to be a useful tool in clinical triage as an inclusion criterion (66). The recent preferred diagnostic tool is Faecal Immunochemical Testing (FIT) for haemoglobin at specific cut-off thresholds. A comparative study of the diagnostic value of the technique against the NICE referral criteria for colonoscopy has reported it to be more accurate than these symptom-based guidelines (69). This method shows an impressive specificity of 87-96% towards the disease, but has a high variation in reported sensitivity with the potential to produce reasonably low values (66-88%) (67). Another technique that has been employed more recently is multi-target stool DNA testing against some of the genetic components found in malignant and polypoid lesions (70). A comparative study on an asymptomatic screening population has shown a higher sensitivity to malignant, advanced pre-cancerous and polypoid lesions as compared to FIT. This technique looks to be promising as a screening and diagnostic tool, but has not been fully qualified for large-scale implementation.

Despite these clinical diagnostic tools, the initial discovery of CRC-associated symptoms does not lead directly to a path towards definitive diagnosis. There is a complicated psychological relationship between the presence of symptoms and the response to these

by both the patient and any consulted physicians (71). These factors can lead to very significant delays in the diagnostic process, with studies finding a waiting period of over 4 months for half of patients and over 6 months for a third (72). Endoscopic treatment and surgical resection of primary carcinomas has been reported to be very beneficial to the survival time of CRC patients, but there is a large negative impact on this time for cases of more advanced stages of the disease (4, 73). Therefore, it is imperative that the clinical community strives to minimise the time from initial discovery of CRC symptoms to final diagnosis.

2.2. Overview of Electronic Nose Technology

An electronic nose can be considered an umbrella term, which can be used to describe any instrument formed from an array of sensors with overlapping sensitivity. First developed in the 1980's (74), it is an attempted to mimic the biological olfactory system by evaluating the total chemical profile of a complex mixture of chemical compounds, instead of detecting each individually. An overview on the functionality of an electronic nose system is shown in Figure 2.5; direct comparisons are made with the biological counterparts in the human olfactory system. A traditional electronic nose is formed from an array of chemical sensors broadly tuned to different chemical groups, similar to the human nose. When a sample is presented to the array, as each sensor is different, its response to that complex odour is unique, which can be learnt with a pattern recognition algorithm. These sensors are normally set into one or more gas chambers that are fed by a pneumatic system, which handles the introduction to and removal of samples from the sensors. The raw signals from the gas sensor array are then processed using both electronic hardware and software to extract the important features of the data. The sensory pathway from the nose to the brain handles the olfactory data in a similar way. There is an element of learning in both machine and biology, by which a neural network familiarises itself with common patterns of

responses from similar samples. Electronic nose systems can combine these elements to distinguish between different classes of samples with distinctive patterns, in a similar way to that employed by the human olfactory system.

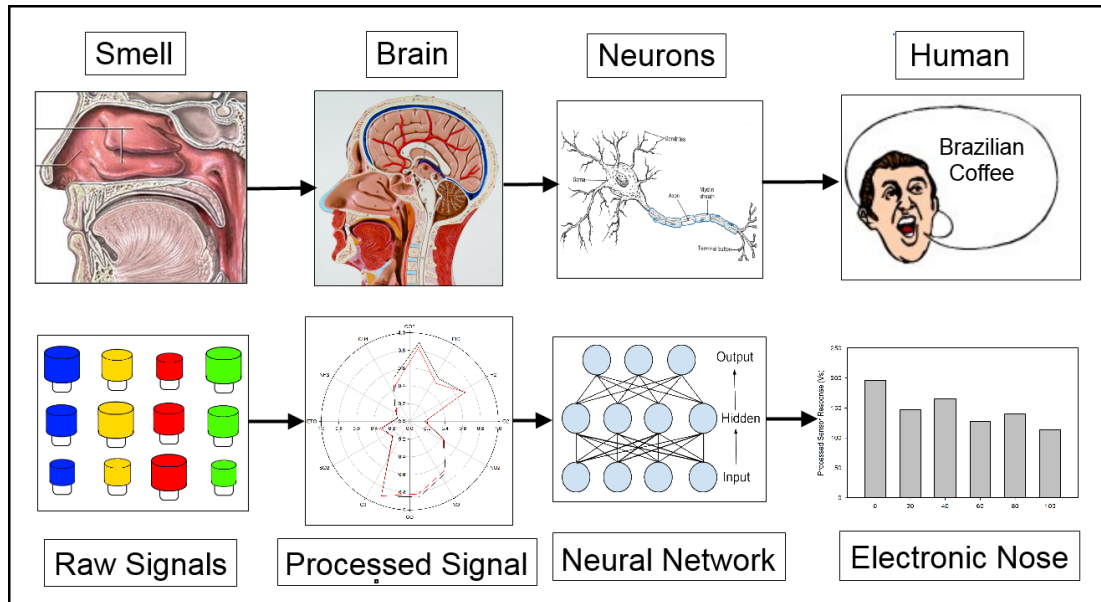


Figure 2.5: Comparison between the human and electronic nose

2.2.1. Sensor Technologies

This section describes a variety of sensors that are currently commercially-available and have the potential to be used in an electronic nose. Some of the technologies included are not currently employed by such instruments, but have the potential to be included in sensing arrays and take a role in providing targeted distinction for lower GI diseases.

2.2.1.1. Metal Oxide Sensors

The most common method for measuring target gases makes use of inorganic Metal Oxides (MOX) such as aluminium oxide or zinc oxide for electro-resistive detection of gases and volatiles. These materials have a porous outer layer that oxygen and water vapour will chemically bond to in ambient air, which in turn allows target gases to bond onto the surface of the sensor (75). A band gap diagram showing the specific electron energies for

the bonded and un-bonded states of some common MOX sensor materials and Hydrogen Sulphide (H_2S) is shown in Figure 2.6 (76). In this case, the energies of H_2S electrons are shown as bounded lines below the H_2S label on the top of the diagram. The solid line bands for the metal oxide compounds (underneath the other three top labels) are filled energy levels and the dashed lines are unfilled. Energy must be given to the H_2S electrons (equivalent to a vertical move upwards on the diagram) in order for bonding to occur. This shows that bonding of H_2S is more likely on copper as compared with aluminium and chromium oxides, as the unfilled energy level bands for this metal are vertically closer to those occupied by the gases electrons in their natural state. This means that less energy is required for bonding to copper than is needed for bonding to the other two materials.

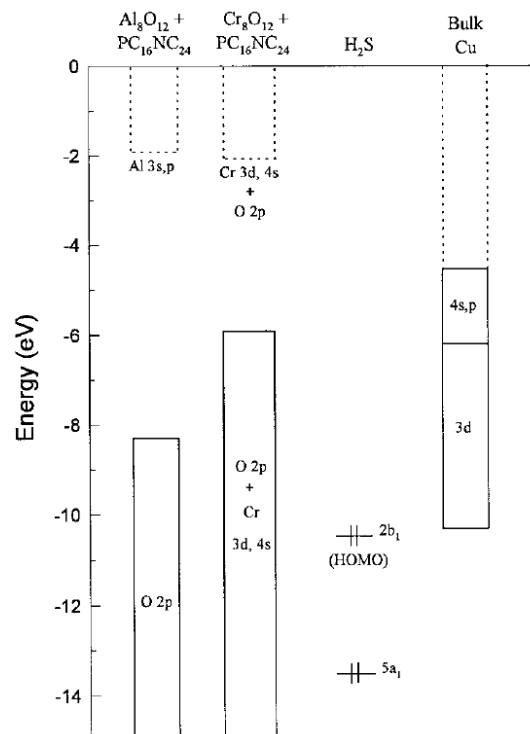


Figure 2.6: Band gap energy diagram for Al_8O_{12} , Cr_8O_{12} and Cu with H_2S (76)

The addition of the extra chemicals effectively dopes the semiconductor, and either increases or decreases the overall resistance of the sensor by a small amount depending on

the target gas. Figures 2.7 and 2.8 show two structural implementations of MOX sensors, with the former being the more widely-available thick film method and the latter a thin-film method deposited on a planar substrate.

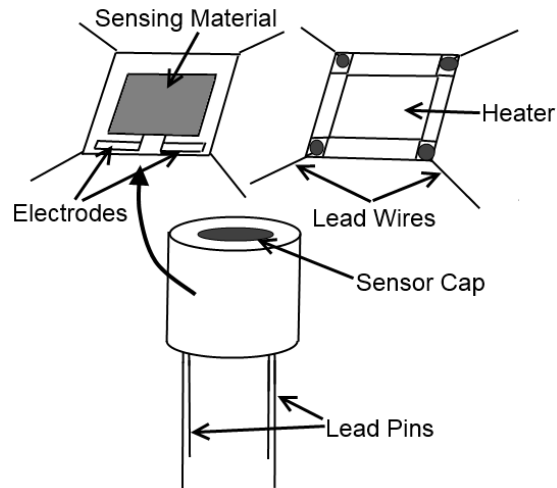


Figure 2.7: Structural diagram of a thick film metal oxide gas sensor

Careful measurement of the sensor resistance allows for monitoring of the gas species that have become bonded to the sensor (as shown in Figure 2.8). Some selectivity can be achieved by introducing filters, changing the sensing materials and increasing heater temperature, but this is a broad-range technique which is not currently truly selective. However, an array of different sensors used in parallel can provide a measure for detailed changes in the composition of a sample, with no indication of the species responsible. (77) These sensors must also be heated to very high temperatures (usually over 200 °C) to increase conductivity of the sensing material and decrease the time for bonding and separation to occur with sensitive chemicals. Regardless of high temperature purging after each sample, the response of these sensors will end up drifting long-term due to some species becoming irreversibly bonded to the surface, and to the active sites becoming redistributed within the semiconductors as part of the relaxation process of the material (78). Despite these disadvantages, this technique produces extremely sensitive devices

with ranges as low as 10-100 parts per billion (ppb) and so is widespread within current commercial electronic noses. (79)

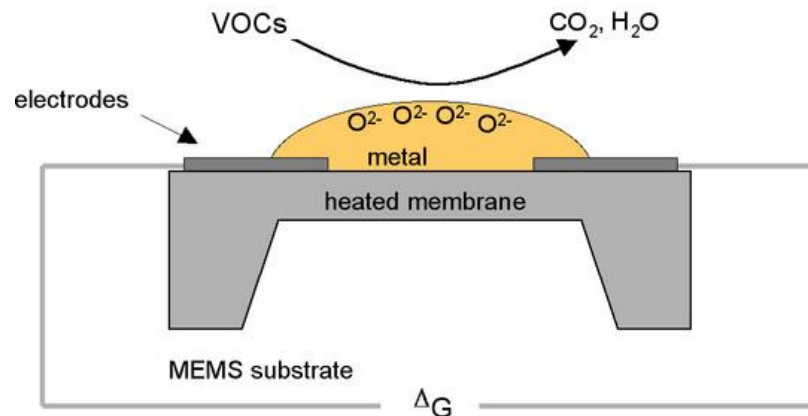


Figure 2.8: Structural diagram of a thin film metal oxide gas sensor (80)

2.2.1.2. Electrochemical Cells

Electrochemical sensors were first used in the 1950's in order to monitor oxygen levels, but have since been expanded to target a wide range of gases. The most common application for these sensors continues to be environmental monitoring for oxygen and toxic gases (81). Their operation is based on a pair of electrodes named the 'working' and 'counter' electrodes with a constant potential difference between them. A particular target gas, specified by the level of voltage difference, will react with these electrodes within a suitable medium of electrolyte to create an electrical current. This current can then be measured by introducing a resistive load onto the end of the sensor circuit. The potential difference is kept constant by the introduction of a third, reference electrode in order to maintain the same sensitivity over a long period of time (81). The addition of a suitable gas permeable membrane on the sensor chamber's gas entrance can prevent the electrolyte from leaking out, prevent water vapour from entering the chamber, control which gases are being introduced to the electrodes and limit their concentrations. While the current signal output of these sensors is not ideal and their sensitivity has traditionally been lower

than other technologies, the newest generation of electrochemical sensors have sensitivities in the ppm (parts per million) range and can be reliably used over long periods of time (over two years) at room temperature. This makes them easier and less costly to run compared with other technologies. (82) The overall structure of electro-chemical sensors is illustrated in Figure 2.9.

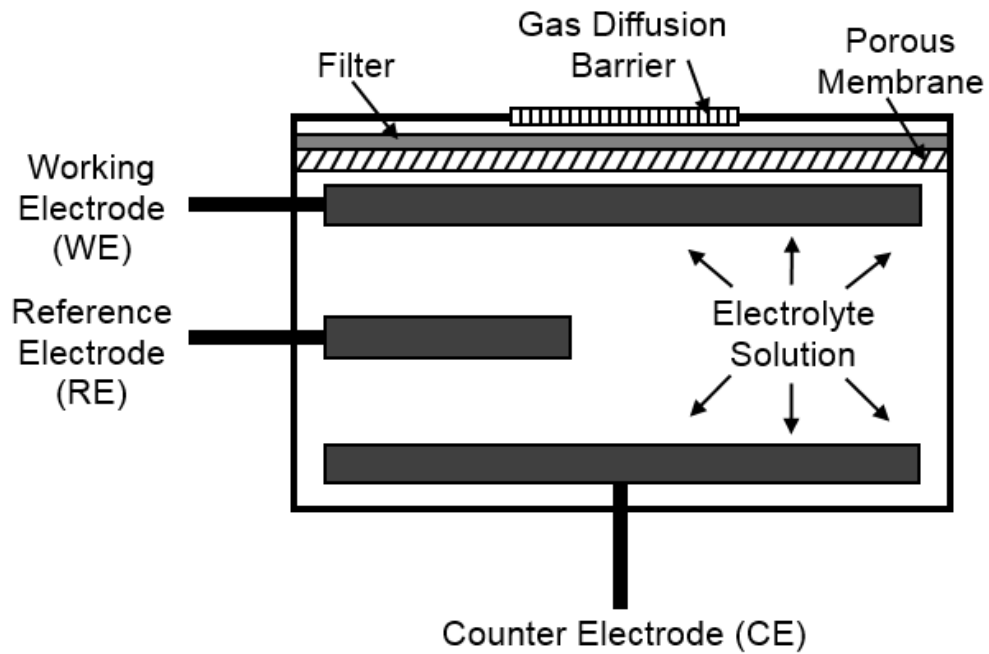


Figure 2.9: Internal structure of a modern electrochemical gas sensor (83)

2.2.1.3. Non-Dispersive Infrared Sensors

Optical methods such as non-dispersive infrared (NDIR) sensing can also be used to measure target gases by Beer's Law, relying upon the ability of gaseous molecules to absorb a specific wavelength of light when it is passed through them in an open chamber (84). Typically, these sensors consist of an optical chamber that contains gases to be measured, and a pair of different detectors that are tuned to different wavelengths. One of these is tuned for detection of the target gas, while the other is used as a baseline level for calculation of the gas concentration in the chamber. The operation of an NDIR sensing

chamber is shown in Figure 2.10, which incorporates an infrared (IR) source on one end that flashes to send light into it, with a filter that only allows the target and baseline wavelengths through. Two IR detectors at the other end of the chambers monitor the levels of IR light sent through, and the level of absorbance by the sample is found by calculating the difference between these readings. Sensors which employ this technique are very cost effective and reliable, as there are no chemical components which can be altered in the system and failure is only dependant on the lamp and circuit operation. However, the sensitivity of these sensors is highly compromised by the path length of IR light within them, and so small commercial sensors do not have a comparative sensitivity to the other techniques described in this section. Also, the pre-requisite for target gases of these sensors is a reasonable level of IR-frequency light at a specific, measurable wavelength that is significantly different to that of water. Therefore, this technology is severely limited in the range of chemicals it can detect effectively, which include CO₂ and CH₄. (85)

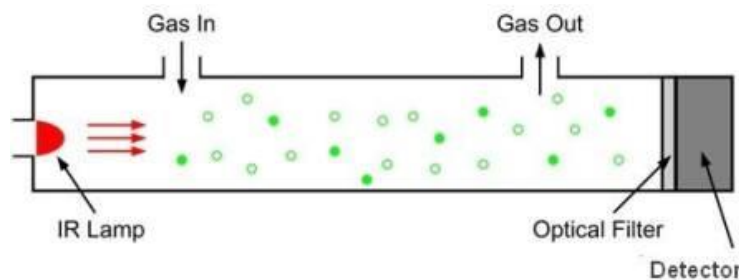


Figure 2.10: Sensing chamber of a Non-Dispersive Infrared gas sensor (86)

2.2.1.4. Pellistor Sensors

One final technique which utilises the electro-resistive properties of materials is the Pellistor, which is used to detect the presence of combustible gases. It is comprised of an alumina detector that is loaded with combustion catalyst (normally an unreactive metal, such as platinum or iridium), and a thin platinum wire used to heat the sensor up to around

500 °C (illustrated in Figure 2.11). In the presence of any combustible gases, this environment will cause combustion on the surface of the detector. The heat released by this combustion is transferred to the alumina, which will cause a small change in its electrical resistance that is converted to a voltage difference by a Wheatstone bridge arrangement of resistors (circuit diagram shown in Figure 2.12).

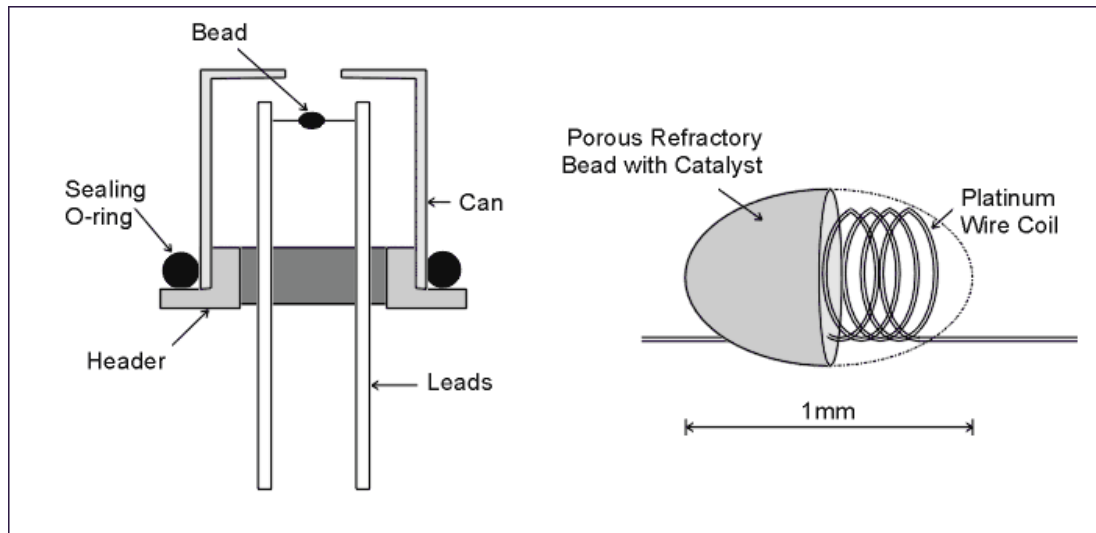


Figure 2.11: Pellistor catalytic gas sensor internal structure (87)

While pellistors are a very reliable method for detecting levels of combustible gases on their own with a sensitivity within the ppm range, this can be inhibited or poisoned permanently by some of the other target gases known to be present in human secretions and excretions (such as H₂S). This method can also only be used for detecting combustible gases such as H₂ and CH₄.

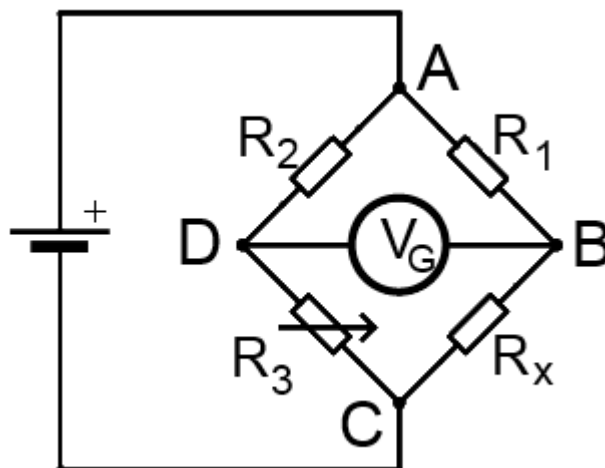


Figure 2.12: Wheatstone bridge circuit for pellistor sensor

2.2.1.5. Conductive Polymers

The electro-resistive capability of some Conducting Polymers can also be employed to detect target gases within a sample. There are not many conductive polymer sensors that are commercially-available as individual packages, but they are used in a number of different commercial electronic nose instruments (described in Section 2.2.4). The principle of detection is almost identical to that described for metal oxide semiconductor above, with the nitrile, sulphile, or other groups within the polymers being used as the active site for bonding rather than that of oxide groups (88). Unfortunately, devices which use this technology also suffer from the same drawbacks of low selectivity and long-term drift as metal oxides, and are less developed and widely-used due to their more recent discovery. (89)

2.2.2. Ion Mobility Spectrometry

Another technology that could be used to detect the chemical composition of gases and volatile mixes is Ion Mobility Spectrometry (IMS) (90). It is not an electronic nose technology in that a single detector is used rather than an array of sensors, but the

separation achieved by the technique allows for similar statistical methods to be applied and for it to be employed in similar application areas. In order to be detected, the molecules within a sample must first be ionised using one of a variety of methods. These include corona discharge using high electric fields, photo-ionisation at atmospheric pressure, electron bombardment by electrospray ionisation and that by a radiation source. The technique achieves separation based on a physical characteristic of all charge particles known as mobility, which is a function of their relative mass and charge ratio.

2.2.2.1. Drift Tube Ion Mobility Spectrometry

The established and most widely-used form of ion mobility spectrometry makes use of a drift tube that is under a constant voltage gradient along its length, in order to pull groups of ions with separate mobilities across this region at different speeds (91). An example of the structure and response pattern produced by one such instrument can be seen in Figure 2.13. The ionised species are first placed in a reaction region, where some chemical bonding can occur, in order to halt and contain the ions to be analysed. At an established baseline time, an ion shutter separating the reaction and drift regions (shown as a vertical dotted line in Figure 2.13) opens and all ions begin moving towards the detector shown on the far right of the diagram. The ions will move along the drift region at different velocities, resulting in large groups or “swarms” of ions separating from each other based on their mobility coefficient through the region. The mobility coefficient is calculated using Equation 2.1 for a constant electric field. The term v_d denotes the drift velocity in m/s through a 1-dimensional axis of space (calculated by distance from the shutter to the detector divided by drift time), and E is the electric field strength in V/m.

$$K = v_d/E \tag{2.1}$$

The detector will respond with total ionic counts over an established period of time after baseline (typical time of 10 ms shown in Figure 2.13), giving a single output that shows peaks from multiple different “swarms” of ions. Note that this form of IMS cannot fully discriminate between individual ions with the singular constant voltage gradient being used, as there are too many species with charge/mass ratios that result in very similar drift velocities.

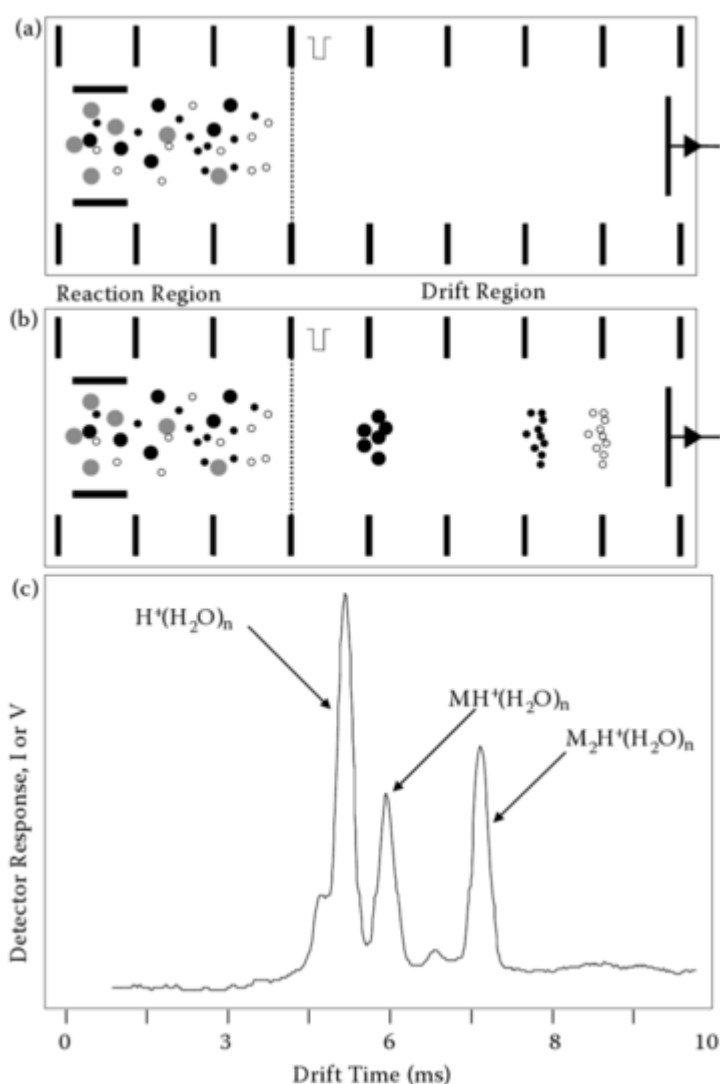


Figure 2.13: Diagram showing the operation of Ion Mobility Spectrometry by drift tube, (a) during the initial baseline halt state, (b) after opening the ion shutter, and (c) typical response (11)

2.2.2.2. *Field Asymmetric Ion Mobility Spectrometry*

Field Asymmetric Ion Mobility Spectrometry (FAIMS) is a more complex method of IMS that has been developed more recently to individualise the ions being analysed (92). It takes advantage of changes in mobility coefficient that some ionic species experience under a strong electric field, allowing for another metric by which ions may be separated. The mobility coefficient equation K is expanded to that shown in Equation 2.2, where N is a constant to describe the change in K under strong field conditions, and α is a function describing the relationship between field strength/ density ratio and ion mobility.

$$K\left(\frac{E}{N}\right) = K_0\left(1 + \alpha\left(\frac{E}{N}\right)\right) \quad (2.2)$$

As with the previous technique, ions are separated by both molecular mass and charge, by applying a high-voltage asymmetric waveform across two parallel plates shown in Figure 2.14. The waveform (shown at the top of the figure) contains sections where a weak negative voltage is applied for a long period of time, and others where a strong positive voltage is applied for a short period. These sections have the same integral value as each other, which maintains an equal mobility coefficient based on the simpler example described in Section 2.2.2.1, while inducing different coefficients in the two states as shown in Equation 2.2. The repeated switching between a high-level positive voltage and low-level negative voltage will cause the ions to exhibit trajectory changes which have two constituent parts: a transient oscillation dependent on its changing mobility coefficient, and a constant attraction to one of the plates according to its overall ionic charge. In order to capture more than a very small subset of ions over the course of measurement, a second “sawtooth” waveform of compensation voltage is applied across the plates (as shown at the bottom of Figure 2.14). At any particular point in the waveform, the compensation voltage applied will negate the constant attraction offset for one small set of ions of a

particular mobility, which will pass through the plates to the detector beyond. The detection method is designed to further separate the negative and positive ions being analysed by using a pair of electrometers, one with a positive bias and the other with a negative. By sweeping the duty cycle of the compensation voltage between preset minimum and maximum values for each asymmetric waveform, a pair of 3-dimensional matrices can be built up with a comprehensive separation of the ions based on charge and mass.

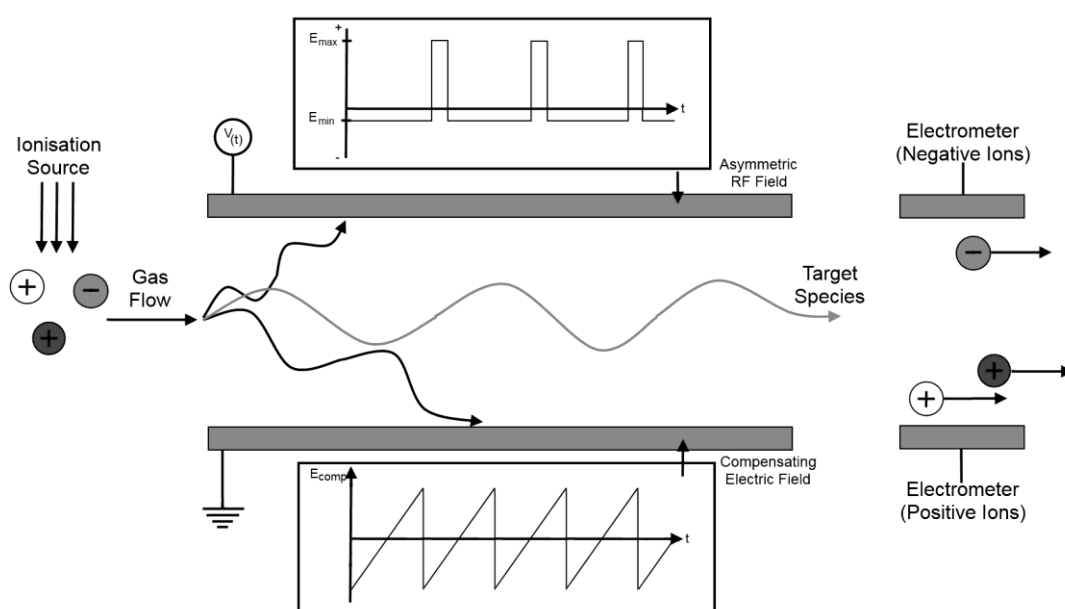


Figure 2.14: Illustration of the operation of a Field Asymmetric Ion Mobility Spectrometer

(93)

2.2.3. Electronic Nose Statistical Methods

The statistical techniques used for post-processing of electronic nose data generally follow a similar pattern based on the non-specific multivariate nature of the information being used. The process involves extracting a number of features from the response data of each sensor (or sections of data in the case of IMS), and performing some multivariate analysis on them to form a classification or regression for identification of the separation of

different sample groups. The steps included in this process will be described in the sections below.

2.2.3.1. Feature Extraction

The majority of multivariate techniques use individual features extracted directly from the sensor response, rather than assigning a score to the fit of full responses to a derived function (94). A list of parameters taken from sensor responses in a large range of electronic nose studies is shown in Table 2.6. A number of different categories are constituent to this list, including those measuring: some form of maximum response, the difference between two separate samples, an integral of some or the entire response signal, the differential gradient within a response, and the time taken to reach a fraction of the maximum response. Note that the descriptions of some of the features in Table 2.6 directly reference other features in order to provide a succinct explanation. The features towards the bottom of the list are commonly used in many different studies, while a small number of investigations have expanded to a much wider range of specific features to optimise separation (95, 96).

Parameter	Description
Baseline	$\sum_{T=\text{gasOn}-4s}^{\text{gasOn}}$ (sensor value)
Final response	Sensor value (averaged over 5 s) at gasOff - baseline
30/90 s on/off response	Sensor value (averaged over 5 s) 30/90 s after gasOn/Off - baseline
Maximum response	Max(sensor value) - baseline
Min/max derivative	Min/max difference between two samples during measurement
On/off derivative	(Sensor value 10 s after gasOn/Off - baseline) /10
Plateau derivative	(Response - 90 s on response)/30
Derivative	$\sum_{T=\text{gasOn}}^{\text{gasOff}}$ (sensor value - baseline)
Off integral	$\sum_{T=\text{gasOff}}^{\text{gasOff}+119s}$ (sensor value - baseline)
Short on/off interval	$\sum_{T=\text{gasOn}/\text{gasOff}}^{\text{gasOn}/\text{gasOff}+9s}$ (sensor value - baseline)
Response/on integral	Response/on integral
T0-90%	Time from gasOn for sensor value to reach baseline + 0.9 x response
T0-60%	Time from gasOn for sensor value to reach baseline + 0.6 x response
T100-10%	Time from gasOff for sensor value to reach baseline + 0.1 x response
T100-40%	Time from gasOff for sensor value to reach baseline + 0.4 x response
Responses of special time	Response value of special time in the whole response curve
Time of special responses	Time of special response value in the whole response curve
Area	Area values of sensor response curve and time axis surrounded
Integral	$I = \int_a^b x(t)dt$
Derivative	$D' = \frac{dx(t)}{dt}$
Difference	$x(t_j) - x(t_i)$
Second Derivative	$D' = \frac{d^2x(t)}{d^2t}$

Table 2.6: List of features extracted directly from sensor responses in electronic nose studies (94)

In addition, there are also a number of curve fitting parameters that can be used as a feature to help classify electronic nose data, a common list of which is shown in Table 2.7. These are used by comparing either the total or partial sensor response to one of the equations listed, and calculating a standard deviation metric for the difference between them. Table includes a number of functions with polynomial, exponential and trigonometric components in them, with most of these being written explicitly in the

description. The Lorentzian and Double-sigmoid models are much more complex techniques involving multiple parameters with individual physical meanings, which are combined to give a more comprehensive method for fitting to curve profiles commonly seen in sensor responses. The full set of equations for both of these models, as well as the explicit description of their parameters, is presented in a study by Carmel et al (97).

Model	Description
Third-order polynomial function	$Y = A_0 + A_1x + A_2x^2 + A_3x^3$
Single-exponential function	$Y = A(1 - \exp(-\frac{x}{T}))$
Double-exponential function	$Y = A_0 + A_1 \exp(-\frac{x}{T_1}) + A_2 \exp(-\frac{x}{T_2})$
ARX model	$y(t) = a_1y(t-1) + a_2y(t-2) + bx(t-1)$
Lorentzian model	Parameters detailed in (24REF27)
Double-sigmoid model	Parameters detailed in (24REF27)
Sigmoid function	$f(k, \theta) = \theta_1 \left(\frac{1}{1+e^{\theta_2(\theta_3-k)}} \right) \left(1 - \frac{1}{1+e^{\theta_4(\theta_5-k)}} \right)$
Fractional function	$Y = \frac{x}{Ax + B}$
Arctangent function	$Y = A * \arctan(\frac{x}{B})$
Hyperbolic tangent function	$Y = A * \tanh(\frac{x}{B})$

Table 2.7: List of features extracted from curve fitting parameters in electronic nose (E-nose) studies (94)

Finally, a number of studies have transformed the domain of the responses in order to compact or simplify the data before taking individual features afterwards (94). These have included transforms using Wavelet or Fourier coefficients, to be used both in conjunction with the other techniques described above or as a blanket data compression technique before extracting all features from a dataset (98, 99).

2.2.3.2. Classification Methods

Once features have been extracted from the raw sensor responses, a classification method must be performed on the extracted values to separate distinct groups of samples. In order to prove the statistical relevance of the classification results, it must be subsequently validated by an independent technique (100). A flow diagram of the processes used for

sample classification in studies investigating analysis of breath is shown in Table 2.8. The stage immediately following the raw sensor values (shown on the second row of the diagram) is a pre-processing and dimension reduction step, which incorporates the feature extraction techniques described in Section 2.2.3.1. The majority of the studies use principle component analysis (PCA) and/or some form of variable selection for reducing the number of dimensions analysed, which involves taking individual features and comparing them against one another to see separation gradients between classes (100). A smaller proportion of studies did not reduce variables and used all raw sensor values for classification, while an even smaller minority used a partial least squares regression technique (PLS) (101).

The next stage in the process is the actual classification step used to separate groups of samples based on the variables presented from the previous step. The most commonly-employed classification method by a large margin is linear discriminant analysis (LDA) in the review of breath studies (100). LDA is a technique that orders features based on their ability to minimise spread within disease groups and maximise the separation between them, and applies an individual factor to each proportional to their success. All proportioned features are then added together to form a discriminant function for each inter-group separation metric. The general equation for discriminant function $g(x)$ is illustrated below in Equation 2.3, where w_i and x_i are respectively the weights and values of the 'ith' extracted feature (ranging from 1 to d), and w_0 is a constant threshold weight. A number of other methods were used for classification in much smaller numbers, such as logistic regression, neural networks, support vector machines and random forest.

$$g(x) = w_0 + \sum_{i=1}^d w_i x_i \quad (2.3)$$

The final step included in many methods is a validation using either a repeated removal of single samples from the training set (“Leave-one-out” in Table 2.8), or an external validation using a model of the separation that was developed during a training phase of the analysis (100). Internal validation using a form of “leave-one-out” technique was by far the most commonly-used technique, with a much smaller proportion using an external model. There are also a surprising number of studies that have not reported any validation of classification results, which is represented by the “In set validation” block in Table 2.8.

Pre-Processing Techniques	Classification Techniques	Validation Techniques
PCA	Neural Network	Training phase model (external) validation
Variable Selection + PCA	Logistic Regression	In-set validation
Partial Least Squares (PLS)	Linear Discriminant Analysis	Leave-one-out
	Support Vector Machine	
	Random Forest	

Table 2.8: Classification methods used in electronic nose studies (100)

A systematic review and comparison was made for all combinations of these techniques to determine their relative performance in group separation in breath analysis studies (100). This resulted in an inconclusive order for success in group distinction due to the large number of contributing factors that come into play, but it was found that the combination of PCA variable selection with LDA classification was a highly successful strategy. It was also reported that internal validation is essential to estimate the performance of the classification technique, and that external validation also improves the estimation of the true diagnostic value. Whatever the form of validation, appropriate metrics for the success of distinction is based on the sensitivity and specificity of a technique to one particular target group against controls. The first of these is a measure of the proportion of the target group samples that were correctly distinguished by the technique (the “True Positives”),

while the second gives the proportion of control samples that are correctly distinguished (the “True Negatives”).

2.2.4. Commercial Electronic Noses

The range of electronic noses commercially available in the current market is shown in Table 2.9. This list does not include a large number of models that have been developed in the academic sector as they have not currently been released into the wider market. It can be seen that typically the electronic noses currently available have an array of between 10 and 40 sensors, with the vast majority including electro-resistive sensors such as metal oxides and conductive polymers (102). This is likely due to the relative ease of electronically interfacing directly with such sensors, their potential to be manufactured in miniature sizes, and their relatively high sensitivity to ppb-levels of target gases and volatiles (which have only recently been achieved by some other methods). The movement towards smaller and more portable form factors is also highlighted, with some notable exceptions from manufacturers looking to maintain a higher level of sensitivity and versatility (AlphaMOS and Lenmartz). There are some examples included that deviate from the overall trends described above, which use techniques such as ion mobility spectrometry, mass spectrometry and gas chromatography to achieve separation and distinction with only a single detector.

Electronic Nose Model	Manufacturer	Sensors Included	Format (Portability)
Bloodhound 307	Roboscientific Ltd.	12 conductive polymers	Desktop (portable)
Cyranose C320	Sensigent	32 conductive polymers	Handheld (portable)
Fox 2000	Alpha MOS	6 metal oxides	Desktop (stationary)
Fox 3000	Alpha MOS	12 metal oxides	Desktop (stationary)
Fox 4000	Alpha MOS	18 metal oxides	Desktop (stationary)
JPL Enose	NASA	16 conductive polymers	Handheld (portable)
E-Nose Mk3	E-Nose Pty. Ltd	6 metal oxides	Desktop (portable)
Moses II	Lenmartz Electronics	8 metal oxides, 8 quartz microbalances, 4 amperometrics	Desktop (stationary)
PEN 3	Airsense Analytical	10 metal oxides	Desktop (portable)
Znose	Electronic Sensor Technology	1 surface acoustic wave (w/ gas chromatography)	Desktop (portable)
Aeonose	The eNose Company	5 metal oxides	Handheld (portable)
VSens	VaporSens	8 Chemiresistors	Desktop (portable)
Lonestar	Owlstone Ltd.	field asymmetric ion mobility spectrometer	Desktop (portable)
MMS-1000	1 st Detect	mass spectrometer	Desktop (portable)

Table 2.9: List of commercially-available electronic noses on the market (102)

2.2.5. Gas Chromatography – Mass Spectrometry

Gas Chromatography (GC) is a method to separate the constituent molecules within gas and volatile mixtures according to their molecular weight and polarity (103). This is done using long, thin columns with a retentive coating along the inside wall, which only gives gases passing through it a reduced amount of mobility (relating to polarity and weight). These columns are subjected to a controlled temperature increase which slowly allows chemical species with lower and lower mobility to pass through, where the end detector will respond to produce a chromatograph in terms of molecular count and time. The injectors of these instruments have the option of splitting the flow of the sample to only allow a certain proportion of the collected sample into the column (along with an inert carrier gas such as Helium). This has the effect of increasing peak sharpness, while decreasing sensitivity to lower concentrations of analyte.

This technology can be combined with mass spectrometry, resulting in a powerful set of tools for determining the exact chemical compounds that are found within a gas/volatile mixture. Mass spectrometers operate by first ionising and breaking apart the molecules into constituent ion species, and then accelerating them using a potential difference into a right angle bend (as shown in Figure 2.15). An electromagnetic field is applied over this bend, which curves the paths of the species directly in relation to their molecular weight. By performing a controlled sweep of electromagnetic field strength while the species is coming into the chamber, the full quantitative spectrum of their molecular masses can be detected. Under total vacuum and a highly controlled temperature and environment, the proportions and levels of species masses within these spectra are almost completely unique to individual chemical compounds. Large libraries of compounds and their resulting mass spectra (such as the National Institute of Standards and Technology (NIST) library) have been built up and sold commercially by analytical chemistry companies. This makes it possible to identify the exact gases and volatile compounds that make up a sample, especially when this data is supported by the positions of the GC peaks (103).

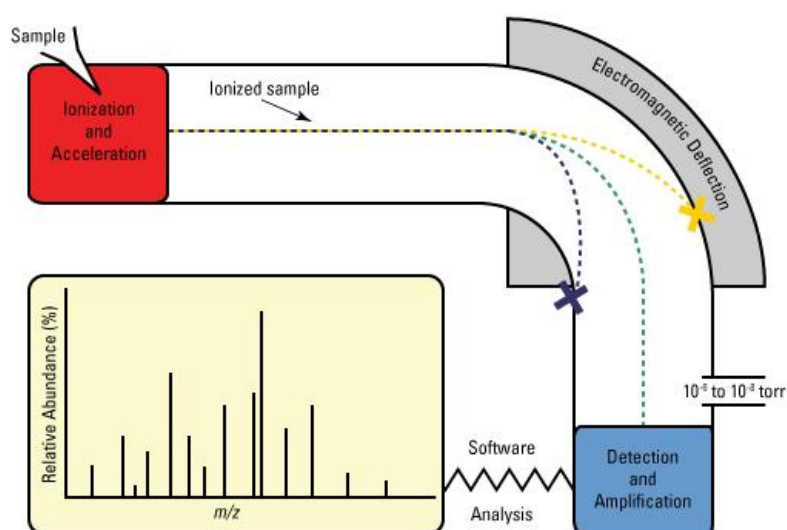


Figure 2.15: Illustration showing the operation of a mass spectrometer (104)

2.3. Review of Analytical Disease Detection by Gases and Volatiles

The links between the aromas given off by patients and disease has been reported by medical practitioners for a long period of time. This dates back even to Hippocrates, known as the father of modern medicine, who wrote that burning the sputum of a patient and smelling the resulting fumes could aid in discovering the source of their maladies (105). The great importance of extracorporeal information such as patient odours was detailed in a review by Fitzgerald and Tierney (106), to aid modern medical practitioners in using techniques for diagnosis often overlooked. Other studies have documented the power of evaluating 'effluvia' (the odour of a patient) in helping diagnosis of physiological (107), infectious and non-infectious diseases (108), as well as ingestion of drugs and chemicals (109).

Many metabolic bi-products are present in all biological waste media, such as exhaled air, sweat, urine and faeces (110). The exact mechanisms behind the generation of particular chemical groups are extremely varied and are affected by a broad spectrum of diet- and disease-related factors. A complex interaction of colonic cells, human gut microflora and invading pathogens produces the variety of gases and volatiles within the lower GI tract (111, 112). This group has previously hypothesised that the resultant products of this process could be measured in urine – so called urine metabolomics (113, 114), and later found evidence to support this (115, 116). A potential reason for this is the ability of digestive disease to alter the permeability of the GI area affected (117). This study aims to support current evidence showing that the volatile and gas groups within a patient's urine can be used as a bio-signature, which contains information regarding the disease state (118).

Initially once physicians had classified aromas as a diagnostic tool, the utility of biological olfaction systems for detecting diseases was investigated before the invention of electronic

methods of gas recognition. The basis for this thinking began with studies employing the use of dogs in detecting disease, due to their much more acute sense of smell (102). There have been a large number of studies highlighting the ability in canines to discriminate patients of prostate, breast, ovary and lung cancers from healthy individuals (119, 120, 121). They describe how urine and breath samples would contain some aromatic quality that showed their disease, and that the trained canines could detect the slight difference in odour. The results of these studies, amongst many others in and outside this field or research that have drawn similar conclusions, have led to the question of what particular chemical constituents cause this difference in sample aroma. A large number of studies are included in this section, and a full list of these is shown in Table 2.10.

The sampling techniques employed by the studies included in the table had similar traits that were identified to mitigate some confounding analysis factors. One study by Silva et al. took samples of morning urine after overnight fasting and stored at -80°C in order to limit the effects of diet on their volatile content. After thawing of analysis, aliquots of 4 mL were placed in an 8 mL glass vial for analysis as this ratio of liquid to headspace volume was found to be optimal for release of gases and volatiles. Polar compound extraction was also maximised by normalising the sample pH into the range of 1-2 and ensuring that salt had been added to saturation. The samples were incubated at 50°C in order to generate headspace for analysis (122). In another study by Di Natale et al., dipstick tests were performed on collection of patient urine giving information on pH, glucose, and protein levels to give an indication of the spread within the groups. Headspace was generated in sealed vials by incubation at 30°C for 30 minutes in this case (123). Finally, Khalid et al. also took morning urine prior to any other medical examination, in order to remove the effect of diet and environmental factors. Aliquots of 0.75 mL were made on collection before

storage at -20°C in sealed vials until analysis, and de-frosted at 60°C for 50 minutes of headspace development (124).

The methods that are generally employed for sample acquisition and processing stages shown in Figure 2.16. In this diagram, as well as in the subsequent chapters of this thesis, “injection” is taken to mean injection of a sample into a machine by any delivery mechanism either by syringe or by opening of sample flow channels. Similarly, “incubation” refers to the development of headspace from a liquid sample (urine or otherwise) by heating and/or agitation over a preset period of time. “Autosampler” is taken to mean any automated system that is used to prepare and inject a sample into a machine, and typically includes a motor-driven arm with a gas syringe on the end for sample transfer.

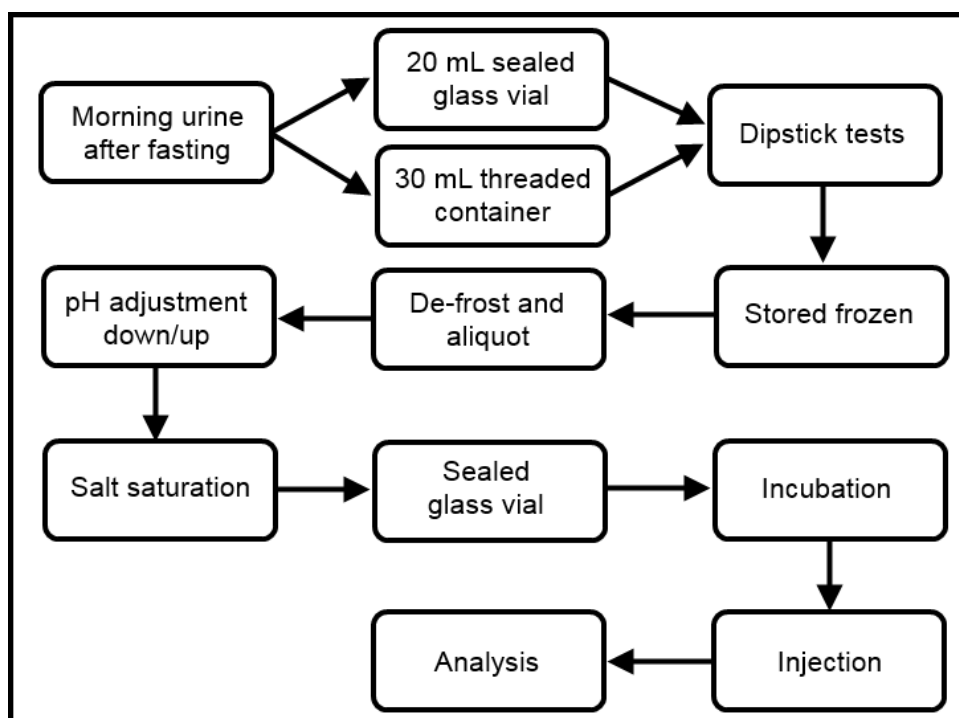


Figure 2.16: Diagram of methods for sample acquisition and processing

Despite the multitude of studies in the area, distinction of samples by gas and volatile content biological media carries an inherent sensitivity to environmental factors when

sampling and analysing. These include contamination by staff or patients physically taking the sample, the environment surrounding the collection, storage and assay of the sample, as well as cross-contamination between multiple samples during joint storage (particularly when still in the liquid phase). Many of these issues are addressed in studies looking to optimise the process of solid phase microextraction (SPME) for sample pre-concentration (125, 126).

Study	Diseases	Sample Media	Distinction Method	Sensing Technology
Pickel et al. 2004	skin cancer	skin contact	canine olfaction	canine olfaction
Willis et al. 2004	bladder cancer	urine	canine olfaction	canine olfaction
McCulloch et al. 2006	lung + breast cancer	breath	canine olfaction	canine olfaction
Horvath et al. 2010	ovarian cancer	tissue + blood	canine olfaction	canine olfaction
Gordon et al. 2008	breast + prostate cancer	urine	canine olfaction	canine olfaction
Cornu et al. 2011	prostate cancer	urine	canine olfaction	canine olfaction
Sonoda et al. 2011	colorectal cancer	breath + stool	canine olfaction	canine olfaction
Ondrula et al. 1993	colorectal cancer	breath	GC-MS	GC-MS
Phillips et al. 2003	lung cancer	breath	GC-MS	GC-MS
Hanson et al. 1997	lung infection	breath	GC-MS	GC-MS
di Natale et al. 1999	renal dysfunction	urine	electronic nose	quartz microbalance
Aathithan et al. 2001	renal infection	urine	electronic nose	conductive polymer
Peng et al. 2010	lung, breast, colorectal + prostate cancer	breath	electronic nose	electro-resistive
Altomare et al. 2013	colorectal cancer	breath	GC-MS	GC-MS
Silva et al. 2011	leukaemia, lymphoma + colorectal cancer	urine	GC-MS	GC-MS
Pavlou et al. 2002	urinary tract infection	agar culture	electronic nose	conductive polymer
Pavlou et al. 2000	gastro-oesophageal bacteria	broth culture	electronic nose	conductive polymer
Dutta et al. 2002	bacteria	saline solution	electronic nose	conductive polymer
Gardner et al. 2000	variety of pathogens	culture + breath	electronic nose	metal oxide
Kateb et al. 2009	brain cancer	chicken heart + liver tissue	electronic nose	conductive polymer
Machado et al. 2005	lung cancer	breath	electronic nose	conductive polymer
Asimakopoulos et al. 2014	prostate cancer	urine	electronic nose	metal oxide
McEntegart et al. 2000	urinary tract infection	urine	electronic nose	metal oxide + quartz microbalance

Table 2.10: List of studies investigating olfactory response for detection of biological diseases and

2.3.1. Biomarkers discovered using Gas Chromatography

The invention of Gas Chromatograph technologies in the field of analytical chemistry presented a range of valuable tools in discovering the biochemical indicators, or biomarkers, of many different diseases and conditions. In particular, Gas Chromatograph/Mass Spectrometer (GC-MS) instruments were of significant importance due to the selectivity in their unique response to individual species.

A large number of investigations into disease biomarkers have found that instead of a single indicator, a complex mixture of compounds from both breath and urine samples contributed to their unique aroma. These have included a study by Hanson and Steinberger (127) to detect respiratory infections in breath, as well as investigations using urine samples such as Turner and Magan's look into the indicators of renal dysfunction and failure (123), and another by Aathithan et al into bacteriuria (128). GC-MS instruments have also recently been shown to distinguish a range of different types of cancer by analysing the volatile compounds present in patient breath (129). Other recent studies have demonstrated the ability of GC-MS to separate CRC patients specifically from controls using both breath (130) and urine (131) as the chosen biological medium.

While GC-based systems are a useful tool in early analytical studies to discover chemical composition and could work well as a central analysis device for some clinical applications, it would not be feasible in a point-of-care scenario within a primary healthcare centre. In order for a technology to be widely accepted in this context, it must be able to ensure effective diagnosis while maintaining a fast working speed with a minimal cost, and finally to be operated by unskilled end users (102). The current diagnostic methods involve a many-staged process of building up a metabolic profile for the patient (132), which takes more time than many patients have from a prognostic perspective. GC-based systems are extremely expensive both in initial and running costs, and require highly trained personnel

to maintain and run effectively (133). Therefore, many have investigated the use of quicker, cheaper and more robust analytical methods, such as electronic nose technology, to detect differences in complex chemical output using Electronic Aroma Signature Patterns (134).

2.3.2. Studies using Commercial Electronic Noses

Many studies have been undertaken to investigate the suitability of electronic nose technology in aiding the diagnosis of a wide variety of infectious and non-infectious diseases. These use commercial systems with various sensor technologies to measure the gas and volatile contents of either human breath or the headspace of bodily fluid samples. The aim of these studies was not to find any specific biomarkers, but to separate diseased and healthy individuals into distinct groups with a complex difference in chemical makeup (102).

The Bloodhound BH-114 electronic nose, containing 14 conductive polymer sensors, was used by one group (135) to successfully categorise all but one patient samples into four distinct groups: uninfected urine as well as that infected with three different types of bacteria (*E. Coli*, *Proteus* and *Staphylococcus*). This system has also been shown to detect the presence of the gastro-oesophageal bacteria *Helicobacter pylori* by Pavlou et al (136). Another electronic nose based on conductive polymer sensors, the Cyranose, was used by Dutta et al (137) to classify six different kinds of bacteria which can lead to eye infections. After investigating a number of data analysis techniques, the samples were successfully classified at an accuracy of 96% by use of a series of non-linear methods. Another group (138) has also employed this device to distinguish lung cancer, a non-infectious disease, from breath samples of patients and healthy volunteers by PCA. They achieved this by initially running a training phase whereby 60 samples from separate individuals (14 diseased, 45 healthy) were run through to form the boundaries of the two classes.

Afterwards, when another similar group of samples (14 diseased, 62 healthy) were run through the system as unknowns for classification, the system was shown to have a 71.4% sensitivity and 91.9% specificity.

Gardner et al (139) produced an early study using the metal oxide semiconductor based Fox 2000 system to differentiate between two types of bacterial cultures by sampling the headspace of the culture containers. The Fox was able to classify the majority of the 360 samples correctly within their own distinct groups using linear discrimination analysis (LDA), with an accuracy of 80 - 90%. Fox electronic noses continued to be employed to investigate classification of diseased individuals, with Arasaradnam et al (140) using the Fox 4000 to classify healthy samples and those with inflammatory bowel disease and diabetes. This resulted in a separation accuracy of 97% using PCA and LDA techniques for sample classification.

The JPL ENose, a system comprising of 16 conductive polymer sensors, was used by Kateb et al (141) to distinguish between the odours of different body tissues and cell cultures, with an aim to use it for differentiating between cancerous tumour and healthy tissue during surgery. While the results only showed separation accuracies of 19% and 22% for tissues and cultures respectively, the authors indicated that as the JPL ENose was developed for air monitoring it may not be suitable for diagnosis. They deduced that using a system developed specifically to detect changes in gases and volatiles which are known to come from the body could improve separation results drastically.

The zNose is an example of a commercial system developed and published in 2000 (142) which combines separation of gas and volatile mixtures by fast GC column with distinction using a single surface acoustic wave (SAW) sensor technology. It has been employed to

detect E.Coli, Salmonella and mycobacteria by volatile organic compounds (VOCs) to date (143, 144).

More recently, there have been many advances in the field of disease detection by electronic nose via biological media. Commercial electronic noses based on metal oxides and conducting polymers have been shown in recent studies to detect lung cancers from healthy controls (145). Urine headspace has also been shown to be a suitable medium to measure by electronic nose for distinguishing prostate cancer (146). Some instruments using ampero-metric sensors have also been employed to measure gas and volatile products in other biomedical applications, such as the discrimination of bacteria (147). Faecal samples from CRC patients and healthy controls have recently been run through an electronic nose in previous work, with 85% sensitivity and 87% specificity being achieved for distinction of full cancer along with a reduced success in discriminating advanced adenomatous ulcers (a condition which leads to a near-100% lifetime risk of developing CRC) (67). Another group has been developing a GC/electronic nose instrument for the detection of volatiles and gases to distinguish human disease using a capillary column and a single metal oxide sensor. The group originally focussed on distinction of inflammatory bowel disease using faecal samples (148). This method has been expanded to achieve distinction of prostate and bladder cancers from healthy and diseased controls using urine samples in significant pilot studies (125, 126). However, there have been no current studies that combine the cross-sensitivities of multiple sensors with GC separation to distinguish between gastro-intestinal disease states using urine samples.

2.4. Conclusions

A systematic review has been conducted on a number of areas surrounding the background of this investigation. First of all, the clinical situation was explained for each of the key lower GI diseases included in this study, including the relative prevalence contributing

factors, the pathological features normally seen and the current diagnostic methods. It was found that prevalence is highly biased towards the least severe disease IBS, and that those with a higher associated mortality rate (such as IBD and CRC) have some internal pathologies that are highly distinctive. However, many of the techniques required to formulate a definitive diagnosis are very invasive for patients and costly to health centres, and the outward pathological features that can be reported by the patient are virtually indistinguishable between diseases. The current non-invasive diagnostic methods available can aid in informing physicians on how to proceed, but do not definitively show sensitivity or specificity that is sufficient to use as a full screening or triage tool.

The sensing technologies and statistical methods which are currently available for use in electronic nose technology were then reviewed, explaining their basic principles of operation. An investigation was also conducted to find the list of electronic nose instruments that are currently available on the market. This showed that a large range of different sensors were available that could be appropriate for use in electronic noses, with some current advancements in technologies such as electro-chemical cells making them more suitable than they have been previously. However, the majority of instruments that are currently manufactured only include electro-resistive sensor arrays, meaning that it would be beneficial to experimentally compare these technologies within the application. Statistical methods being used in studies that analyse breath (a popular biological medium) with electronic nose technologies was also reviewed, showing popularity and success with techniques such as PCA, LDA and "leave-one-out" internal validation.

A review investigation of the literature of disease detection using gas phase sample analysis was also conducted, showing the initial study into canine ability to detect biomarkers of cancers and other diseases using their sense of smell. This shifted to the distinction of biomarkers for various diseases and infections using gas chromatography/mass

spectrometry, showing a good level of distinction but poor compatibility for point-of-care applications in primary healthcare. Finally, a review of studies employing electronic nose instruments was included, showing that a large body of research has been done with both commercial instruments and bespoke sensor arrays. There have been a handful of reviews comparing these individual studies from an indirect standpoint, but it would be beneficial to make a direct comparison between a range of different technologies using similar experimental techniques and conditions.

2.5. References

- 1) Anderson, S.H.C., Davies, G., Dalton H.R., Irritable Bowel Syndrome. Key Topics in Gastroenterology. Oxford : BIOS Scientific Publishers Ltd., 1999.
- 2) Ponder, A., Long, M.D., A clinical review of recent findings in the epidemiology of inflammatory bowel disease. 2013, J Clin Epidemiol 5, 237-247.
- 3) Canavan, C., West, J., Card, T., The epidemiology of irritable bowel syndrome. 2014, J Clin Epidemiol 6, 71-80.
- 4) Siegel, R., DeSantis, C., Jemal, A., Colorectal Cancer Statistics, 2014. 2014, CA Cancer J Clin 64, 104-117.
- 5) Hungin, A.P., Chang, L., Locke, G.R., Dennis, E.H., Barghout, V., Irritable bowel syndrome in the United States: prevalence, characteristics, and referral. 2000, Gut 46(1), 78-82.
- 6) Keaton, K.W., O'Donnell, L.J., Braddon, F.E., Mountford, R.A., Hugher, A.O., Cripps, P.J., Symptoms of irritable bowel syndrome in a British urban community: consultants and nonconsulters. 1992, Gastroenterology 102(6), 1962-1967.
- 7) Jones, R., Lydeard, S., Irritable bowel syndrome in the general population. 1992, BMJ 304(6819), 87-90.

- 8) Andrews, E.B., Eaton, S.C., Hollis, K.A., Hopkins, J.S., Ameen, V., Hamm, L.R., Cook, S.F., Tennis, P., Mangel, A.W., Prevalence and demographics of irritable bowel syndrome: results from a large web-based survey. 2005, *Aliment Pharmacol Ther* 22, 935-942.
- 9) Lovell, R.M., Ford, A.C., Effect of gender on prevalence of irritable bowel syndrome in the community: systematic review and meta-analysis. 2012, *Am J Gastroenterol* 107(7). 991-1000.
- 10) Maxwell, P.R., Mendall, M.A., Kumar, D., Irritable bowel syndrome. 1997, *Lancet* 350(9092), 1691-1695.
- 11) Marmot, M., Allen, J., Bell, R., Bloomer, E., Goldblatt, P., Consortium for the European Review of Social Determinants of Health and the Health Divide. WHO European review of social determinants of health and the health divide. 2012, *Lancet* 380(9846), 1011-1029.
- 12) Grodzinsky, E., Hallert, C., Faresjö, T., Bergfors, E., Faresjö, A.O., Could gastrointestinal disorders differ in two close but divergent social environments? 2012, *Int J Health Geogr.* 11:5.
- 13) Locke, G.R., Zinsmeister, A.R., Talley, N.J., Fett, S.L., Melton L.J., Familial association in adults with gastrointestinal disorders. 2000, *Mayo Clin Proc* 75(9), 907-912.
- 14) Spiller, R., Aziz, Q., Creed, F., Emmanuel, A., Houghton, L., Hungin, P., Jones, R., Kumar, D., Rubin, G., Trudgill, N., Whorwell. P., Guidelines on the irritable bowel syndrome: mechanisms and practical management. 2007, *Gut* 56, 1770-1798.
- 15) Vanner, S.J., Depew, W.T., Paterson, W.G., DaCosta, L.R., Groll, A.G., Simon, J.B., Djurfeldt, M., Predictive value of the Rome criteria for diagnosing the irritable bowel syndrome. 1999, *Am J Gastroenterol* 94, 2912-2917.

- 16) Vandvik, P.O., Wilhelmsen, I., Ihlebaek, C., Farup, P.G., Comorbidity of irritable bowel syndrome in general practice: a striking feature with clinical implications. 2004, *Aliment Pharmacol Ther* 20, 1195-1203.
- 17) Longstreth, G.F., Drossman, D.A., Current Approach to the Diagnosis of Irritable Bowel Syndrome. International Foundation for Functional Gastrointestinal Disorders, IBS (163), 2009.
- 18) Wedlake, L., A'Hern, R., Russell, D., Thomas, K., Walters, J.R.F., Andreyev, H.J.N., Systematic review: the prevalence of idiopathic bile acid malabsorption as diagnosed by SeHCAT scanning in patients with diarrhoea-predominant irritable bowel syndrome. 2009, *Aliment Pharm Ther* 30, 707-717.
- 19) Tontini, G.E., Vecchi, M., Pastorelli, L., Neurath, M.F., Neumann, H., Differential diagnosis in inflammatory bowel disease colitis: State of the art and future perspectives. 2015, *World J Gastroenterol* 21(1), 21-46.
- 20) Molodecky, N.A., Soon, I.S., Rabi, D.M., Ghali, W.A., Ferris, M., Chernoff, G., Benchimol, E.I., Panaccione, R., Ghosh, S., Barkema, H.W., Kaplan, G.G., Increasing incidence and prevalence of the inflammatory bowel diseases with time, based on systematic review. 2012, *Gastroenterology* 142, 46-54.
- 21) Ng, S.C., Bernstein, C.N., Vatn, M.H., Lakatos, P.L., Loftus, E.V., Tysk, C., O'Morain, C., Colombel, J.F., Geographical variability and environmental risk factors in inflammatory bowel disease. 2013, *Gut* 62, 630-649.
- 22) Pinsk, V., Lemberg, D.A., Grewal, K., Barker, C.C., Schreiber, R.A., Jacobson, K., Inflammatory bowel disease in the South Asian pediatric population of British Columbia. 2007, *Am J Gastroenterol* 102, 1077-1083.
- 23) Katz, S., Pardi, D.S., Inflammatory bowel disease of the elderly: frequently asked questions (FAQs). 2011, *Am J Gastroenterol* 106, 1889-1897.

- 24) Ananthakrishnan, A.N., Binion, D.G., Treatment of ulcerative colitis in the elderly. 2009, *Dig Dis* 27(3), 327-334.
- 25) Baron, S., Turck, D., Leplat, C., Merle, V., Gower-Rousseau, C., Marti, R., Yzet, T., Lerebours, E., Dupas, J-L., Cortot, A., Colombel, J-F., Environmental risk factors in paediatric inflammatory bowel diseases: a population based case control study. 2005, *Gut* 54, 357-363.
- 26) Calkins, B.M., A meta-analysis of the role of smoking in inflammatory bowel disease. 1989, *Dig Dis Sci* 34, 1841-1854.
- 27) Magro, F., Langner, C., Driessen, A., Ensari, A., Geboes, K., Mantzaris, G.J., Villanacci, V., Becheanu, G., Borralho Nunes, P., Cathomas, G., Fries, W., Jouret-Mourin, A., Mescoli, C., de Petris, G., Rubio, C.A., Shepherd, N.A., Vieth, M., Eliakim, R., European consensus on the histopathology of inflammatory bowel disease. 2013, *J Crohns Colitis* 7, 827-851.
- 28) Sanders, D.S., The differential diagnosis of Crohn's disease and ulcerative colitis. 1998, *Baillieres Clin Gastroenterol* 12, 19-33.
- 29) Koukoulis, G.K., Ke, Y., Henley, J.D., Cummings, O.W., Detection of pyloric metaplasia may improve the biopsy diagnosis of Crohn's ileitis. 2002, *J Clin Gastroenterol* 34, 141-143.
- 30) Dignass, A., Eliakim, R., Magro, F., Maaser, C., Chowers, Y., Geboes, K., Mantzaris, G., Reinisch, W., Colombel, J.F., Vermeire, S., Travis, S., Lindsay, J.O., Van Assche, G., Second European evidence-based consensus on the diagnosis and management of ulcerative colitis part 1: definitions and diagnosis. 2012, *J Crohns Colitis* 6, 965-990.
- 31) Aghazadeh, R., Zali, M.R., Bahari, A., Amin K., Ghahghaie, F., Firouzi, F., Inflammatory bowel disease in Iran: a review of 457 cases. 2005, *J Gastroenterol Hepatol* 20, 1691-1695.

- 32) Targownik, L.E., Bernstein, C.N., Nugent, Z., Leslie, W.D., Inflammatory bowel disease has a small effect on bone mineral density and risk for osteoporosis. 2013, *Clin Gastroenterol Hepatol* 11, 278-285.
- 33) Panes, J., Bouhnik, Y., Reinisch, W., Stoker, J., Taylor, S.A., Baumgart, D.C., Danese, S., Halligan, S., Marincek, B., Matos, C., Peyrin-Biroulet, L., Rimola, J., Rogler, G., van Assche, G., Ardizzone, S., Ba-Ssalamah, A., Bali, M.A., Bellini, D., Biancone, L., Castiglione, F., Ehehalt, R., Grassi, R., Kucharzik, T., Maccioni, F., Maconi, G., Magro, F., Martín-Comín, J., Morana, G., Pendsé, D., Sebastian, S., Signore, A., Tolan, D., Tielbeek, J.A., Weishaupt, D., Wiarda, B., Laghi, A., Imaging techniques for assessment of inflammatory bowel disease: joint ECCO and ESGAR evidence-based consensus guidelines. 2013, *J Crohns Colitis* 7, 556-585.
- 34) Magro F, Langner C, Driessen A, Ensari A, Geboes K, Mantzaris GJ, Villanacci V, Becheanu G, Borralho Nunes P, Cathomas G, Fries W, Jouret-Mourin A, Mescoli C, de Petris G, Rubio CA, Shepherd NA, Vieth M, Eliakim R. European consensus on the histopathology of inflammatory bowel disease. 2013, *J Crohns Colitis* 7, 827-851.
- 35) Annese, V., Daperno, M., Rutter, M.D., Amiot, A., Bossuyt, P., East, J., Ferrante, M., Götz, M., Katsanos, K.H., Kießlich, R., Ordás, I., Repici, A., Rosa, B., Sebastian, S., Kucharzik, T., Eliakim, R., European Crohn's and Colitis Organisation. European evidence based consensus for endoscopy in inflammatory bowel disease. 2013, *J Crohns Colitis* 7, 982-1018.
- 36) Bourraille, A., Ignjatovic, A., Aabakken, L., Loftus, E.V., Eliakim, R., Pennazio, M., Bouhnik, Y., Seidman, E., Keuchel, M., Albert, J.G, Ardizzone, S., Bar-Meir, S., Bisschops, R., Despott, E.J., Fortun, P.F., Heuschkel, R., Kammermeier, J., Leighton, J.A., Mantzaris, G.J., Moussata, D., Lo, S., Paulsen, V., Panés, J., Radford-Smith, G., Reinisch, W., Rondonotti, E., Sanders, D.S., Swoger, J.M., Yamamoto, H., Travis, S.,

- Colombel, J.F., Van Gossum, A., Role of small-bowel endoscopy in the management of patients with inflammatory bowel disease: an international OMED-ECCO consensus. 2009, *Endoscopy* 41, 618-637.
- 37) Van Assche, G., Dignass, A., Panes, J., Beaugerie, L., Karagiannis, J., Allez, M., Ochsenkühn, T., Orchard, T., Rogler, G., Louis, E., European evidence-based Consensus on the diagnosis and management of Crohn's disease: Definitions and diagnosis. 2010, *J Crohns Colitis* 4, 7-27.
- 38) Vavricka, S.R., Spigaglia, S.M., Rogler, G., Pittet, V., Michetti, P., Felley, C., Mottet, C., Braegger, C.P., Rogler, D., Straumann, A., Bauerfeind, P., Fried, M., Schoepfer, A.M., Systematic evaluation of risk factors for diagnostic delay in inflammatory bowel disease. 2012, *Inflamm Bowel Dis* 18(3), 495-505.
- 39) Ghosh, N., Premchand, P., A UK cost of care model for inflammatory bowel disease. 2015, *Frontline Gastroenterology* 0, 1-6.
- 40) Siegel, R., Naishadham, D., Jemal, A. Cancer statistics, 2012. *CA Cancer J Clin.* 62, 10-29.
- 41) Ferlay, J., Parkin, D.M., Steliarova-Foucher, E. Estimates of cancer incidence and mortality in Europe in 2008. 2010 *Eur. J. Cancer.* 46, 765-81.
- 42) Haggar, F.A., Boushey, R.P., Colorectal Cancer Epidemiology: Incidence, Mortality, Survival, and Risk Factors. 2009, *Clin Col Rect Surg* 22(4), 191-197.
- 43) Boyle, P., Langman, J.S., ABC of colorectal cancer: Epidemiology. 2000, *BMJ* 321(7264), 805-808.
- 44) Wilmink, A.B.M., Overview of the epidemiology of colorectal cancer. 1997 *Dis Colon Rectum* 40(4), 483-493.
- 45) Boyle, P., Ferlay, J., Mortality and survival in breast and colorectal cancer. 2005, *Nat Clin Pract Oncol* 2(9), 424-425.

- 46) Janout, V., Kollarova, H., Epidemiology of colorectal cancer. 2001, Biomed Pap Med Fac Univ Palacku Olomouc Czech Repub 145, 5-10.
- 47) Ries, L.A.G., Melbert, D., Prapcho, M., SEER cancer statistics review, 1975-2005. 2008, Bethesda, MD.
- 48) O'Connell, J.B., Maggard, M.A., Livingstone, E.H., Yo C.K., Colorectal cancer in the young. 2004, Am Surg 2003(69), 866-872.
- 49) De Jong, A.E., Morreau, H., Nagengast, F.M., Prevalence of adenomas among young individuals at average risk for colorectal cancer. 2005, Am J Gastroenterol 100(1), 139-143.
- 50) Jackson-Thompson, J., Ahmed, F., German, R.R., Lai, S.M., Friedman, C., Descriptive epidemiology of colorectal cancer in the United States, 1998-2001. 2006, Cancer 107(5, Suppl), 1103-1111.
- 51) Skibber, J., Minsky, B., Hoff, P., Cancer of the colon and rectum, DeVita, V.T., Hellmann, S., Rosenberg, S.A., Cancer: principles & practice of oncology. 6th ed. Philadelphia: Lippincott Williams & Wilkins, 2001, 1216-1271.
- 52) Willett, W.C., Diet and cancer: an evolving picture. 2005, JAMA 293(2), 233-234.
- 53) Larsson, S.C., Wolk, A., Meat consumption and risk of colorectal cancer: a meta-analysis of prospective studies. 2006, Int J Cancer 119(11), 2657-2664.
- 54) National Institutes of Health. What You Need To Know About Cancer of the Colon and Rectum. Bethesda, MD, U.S. Department of Health and Human Services & National Institutes of Health, 2006.
- 55) Zisman, A.L., Nickolov, A., Brand, R.E., Gorchow, A., Roy, H.K., Associations between the age at diagnosis and location of colorectal cancer and the use of alcohol and tobacco: implications for screening. 2006, Arch Intern Med 166(6), 629-634.

- 56) Botteri, E., Iodice, S., Raimondi, S., Maisonneuve, P., Lowenfels, A.B., Cigarette smoking and adenomatous polyps: a meta-analysis. 2008, *Gastroenterology* 134(2), 388-395.
- 57) Jemal, A., Thun, M.J., Ries, L.A., Annual report to the nation on the status of cancer, 1975-2005, featuring trends in lung cancer, tobacco use, and tobacco control. 2008, *J Natl Cancer Inst* 100(23), 1672-1694.
- 58) Jemal, A., Clegg, L.X., Ward, E., Annual report to the nation on the status of cancer, 1975-2001, with a special feature regarding survival. 2004, *Cancer* 101(1), 3-27.
- 59) Astin, M., Griffin, T., Neal, R.D., Rose, P., Hamilton, W., The diagnostic value to symptoms for colorectal cancer in primary care: a systemic review. 2001, *Br J Gen Pract*, 231-243.
- 60) Barraclough, K., The predictive value of cancer symptoms in primary care. 2010, *Br J Gen Pract* 60(578), 639-640.
- 61) Kato, H., Sakamoto, T., Otsuka, H., Yamada, R., Watanabe, K., Endoscopic Diagnosis and Treatment for Colorectal Cancer, Ettarh, R., *Colorectal Cancer – From Prevention to Patient Care*. 2012, Intech Open.
- 62) Kim, E.C., Lance, P., Colorectal polyps and their relationship to cancer. 1997, *Gastroenterol Clin North Am* 26, 1-17.
- 63) Morson, B.C., Dawson, I.M.P., *Gastrointestinal pathology*. Oxford: Blackwell Scientific, 1972.
- 64) Schlemper, R.J., Hirata, I., Dixon, M.F., The macroscopic classification of early neoplasia of the digestive tract. 2002, *Endoscopy* 34, 163-168.
- 65) Pox, C.P., Altenhofen, L., Brenner, H., Theilmeier, A., von Stillfried, D., Schmiegel, W., Efficacy of a Nationwide Screening Colonoscopy Program for Colorectal Cancer. 2012, *Gastroenterology* 142, 1460-1467.

- 66) Sonnenberg, A., Delco, F., Inadomi, J.M., Cost-Effectiveness of Colonoscopy in Screening for Colorectal Cancer. 2000, *Ann Intern Med* 133, 573-584.
- 67) De Meij, T.G., Ben Larbi, I., van der Schee, M.P., Lentferink, Y.E., Paff, T., Terhaar Sive Droste, J.S., Mulder, C.J., van Bodegraven, A.A., de Boer, N.K. Electronic nose can discriminate colorectal carcinoma and advanced adenomas by fecal volatile biomarker analysis: proof of principle study. 2014, *Int. J. Cancer*. 134, 1132-1138.
- 68) Hirai, H.W., Tsoi, K.K.F., Chan, J.Y.C., Wong, S.H., Ching, J.Y.L., Wong, M.C.S., Wu, J.C.Y., Chan, F.K.L., Sung, J.J.Y., Ng, S.C., Systematic review with meta-analysis: faecal occult blood tests show lower colorectal cancer detection rates in the proximal colon in colonoscopy-verified diagnostic studies. 2016, *Aliment Pharmacol Ther* 43, 755-764.
- 69) Cubiella, J., Salve, M., Diaz-Ondina, M., Vega, P., Alves, M.T., Iglesias, F., Sanchez, E., Macia, P., Blanco, I., Bujanda, L., Fernandez-Seara, J., Diagnostic accuracy of the faecal immunochemical test for colorectal cancer in symptomatic patients: comparison with NICE and SIGN referral criteria. 2014, *Col Dis* 16, 273-282.
- 70) Imperiale, T.F., Ransohoff, D.F., Itzkowitz, S.H., Levin, T.R., Lavin, P., Lidgard, G.P., Ahlquist, D.A., Berger, B.M., Multitarget Stool DNA Testing for Colorectal-Cancer Screening. 2014, *N Engl J Med* 370, 1287-1297.
- 71) Mitchell, E., McDonald, S., Campbell, N.C., Weller, D., Macleod, U., Influences on pre-hospital delay in the diagnosis of colorectal cancer: a systematic review. 2008, *Br J Cancer* 98, 60-70.
- 72) Esteva, M., Leiva, A., Ramos, M., Pita-Fernández, S., González-Luján, L., Casamitjana, M., Sánchez, M.A., Pérttega-Díaz, S., Ruiz, A., Gonzalez-Santamaría, P., Martín-Rabadán, M., Costa-Alcaraz, A.M., Espí, A., Macià, F., Segura, J.M., Lafita, S., Arnal-Monreal, F., Amengual, I., Boscá-Watts, M.M., Manzano, H.,

- Magallón, R., Factors related with symptom duration until diagnosis and treatment of symptomatic colorectal cancer. 2013, BMC Cancer 13(87).
- 73) Ahmed, S., Leis, A., Fields, A., Chandra-Kanthan, S., Haider, K., Alvi, R., Reeder, B., Pahma, P., Survival Impact of Surgical Resection of Primary Tumor in Patients With Stage IV Colorectal Cancer: Results From a Large Population-Based Cohort Study. 2014, Cancer 120(5), 683-691.
- 74) Persaud, K., Dodd, G.H. Analysis of discrimination mechanisms of the mammalian olfactory system using a model nose. 1982, Nature. 299, 352-355
- 75) Boettern, L. How Oxygen, Electrochemical Toxic, and Metal Oxide Semiconductor Sensors Work. Biosystems, 2000. AN2000-1.
- 76) Rodriguez, J.A., Charturvedi, S., Kuhn, M., Hrbek, J., Reaction of H₂S and S₂ with Metal/Oxide Surfaces: Band-Gap Size and Chemical Reactivity. 1998, J Phys Chem B 102, 5511-5519.
- 77) AppliedSensor GmbH. Metal Oxide Semiconductor (MOS) Sensors. AppliedSensor GmbH, 2008.
- 78) S. Di Carlo, M. Falasconi. Drift Correction Methods for Gas Chemical Sensors in Artificial Olfaction Systems: Techniques and Challenges. Wang, W., Advances in Chemical Sensors. Intech, 2012.
- 79) Yamazoe, N., Sakai, G., Shimano, K., Oxide Semiconductor Gas Sensors. 2003, Catalysis Surveys from Asia, 63-75.
- 80) "AppliedSensor GmbH – Chemical gas sensors to detect contaminants", Biotechnology and Life Sciences in Baden-Wurttemberg, 6th March 2014, <http://www.bio-pro.de/magazin/thema/04546/index.html?lang=en&artikelid=/artikel/04606/index.html>

- 81) E2V Technologies (UK) Limited, E2V Electrochemical and Pellistor Gas Sensor Evaluation Kit User Guide. E2V Technologies (UK) Limited, 2010.
- 82) Narayanan, S.R., Valdez, T.I., Chun, W., Design and Operation of an Electrochemical Methanol Concentration Sensor for Direct Methanol Fuel Cell Systems. 2000, *Electrochem Solid-State Lett*, 117-120.
- 83) Technical Specification: SO₂-B4 Sulphur Dioxide Sensor – 4 Electrode, Ref. SO₂B4/AUG14, Alphasense Ltd. 2014
- 84) Gibson, D., MacGregor, C., A Novel Solid State Non-Dispersive Infrared CO₂ Gas Sensor Compatible with Wireless and Portable Deployment. 2013, *Sensors* 13, 7079-7103.
- 85) Meléndez, J., de Castro, A.J., López, F., Meneses, J., Spectrally selective gas cell for electrooptical infrared compact multigas sensor. 1995, *Sensors and Actuators A: Physical*, 417–421
- 86) “How does an NDIR CO₂ Sensor Work?”, CO₂Meter.com Blogs, 6th March 2014, <http://www.co2meter.com/blogs/news/6010192-how-does-an-ndir-co2-sensor-work>
- 87) “Pellistors”, City Technology Ltd., 15th May 2015, https://www.citytech.com/loader/frame_loader.asp?page=https://www.citytech.com/technology/pellistors.asp
- 88) Bai, H., Shi, G., Gas Sensors Based on Conducting Polymers. 2007, *Sensors* 7, 267-307.
- 89) Miasik, J.J., Hooper, A., Tofield, B.C., Conducting polymer gas sensors. 1986, *J Chem Soc, Faraday Trans. 1*, 1117-1126.
- 90) Wohltjen, H., Mechanism of operation and design considerations for surface acoustic wave device vapour sensors. 1984, *Sensors and Actuators* 5(4), 307–325.

- 91) Eiceman, G.A., Karpas, Z., Hill, H.H. Introduction to Ion Mobility Spectrometry. Ion Mobility Spectrometry, Third Edition. CRC Press, Taylor & Francis Group LLC, 2014.
- 92) Buryakov, I.A., Krylov, E.V., Nazarov, E.G., Rasulev, U.K., A new method of separation of multi-atomic ions by mobility at atmospheric pressure using a high-frequency amplitude-asymmetric strong electric field. 1993, Int J Mass Spec Ion Proc 128, 143-148.
- 93) Kolakowskia, B.M., Mester, Z., Review of applications of high-field asymmetric waveform ion mobility spectrometry (FAIMS) and differential mobility spectrometry (DMS). 2007, Analyst 132, 842-864
- 94) Yan, J., Guo, X., Duan, S., Jia, P., Wang, L., Peng, C., Zhang, S., Electronic Nose Feature Extraction Methods: A Review. 2015, Sensors 15, 27804-27831.
- 95) Eklov, T., Martensson, P., Lundstrom, I., Enhanced selectivity of MOSFET gas sensor by systematical analysis of transient parameters. 1997, Anal Chim Acta 353, 291-300.
- 96) Zou, X., Zhao, J., Wu, S., Huang, X., Vinegar Classification Based on Feature Extraction and Selection from Tin Oxide Gas Sensor Array Data. 2003, Sensors 3, 101-109.
- 97) Carmel, L., Levy, S., Lancet, D., Harel, D., A feature extraction method for chemical sensors in electronic noses. 2003, Sens Act B Chem 93, 67-76.
- 98) Distantea, C., Leo, M., Sicilianoa, P., Persaud, K., On the study of feature extraction methods for an electronic nose. 2002, Sens Act B Chem 87, 274-288.
- 99) Yan, J., Tian, F., He. Q., Shen, Y., Xu, S., Feng, J., Chaibou, K., Feature Extraction from Sensor Data for Detection of Wound Pathogen Based on Electronic Nose. 2012, Sens Mater 24, 57-73.

- 100) Leopold, J.H., Bos, L.D.J., Sterk, P.J., Schultz, M.J., Fens, N., Horvath, I., Bikov, A., Montuschi, P., Di Natale, C., Yates, D.H., Abu-Hanna, A., Comparison of classification methods in breath analysis by electronic nose. 2015, *J Breath Res* 9, 046002.
- 101) Bastien, P., Vinzi, V.E., Tenehaus, M., PLS generalised linear regression. 2005, *Comput Stat Data An* 48, 17-46.
- 102) Wilson, A.D., Baietto, M., Applications and advances in electronic-nose technologies developed for biomedical applications. 2011, *Sensors* 11, 1105-1176.
- 103) Karasek, F.W. and Clement, R.E. Basic gas chromatography-mass spectrometry: Principles and techniques. New York : Elsevier Science, 1988.
- 104) Thermo Fisher Scientific Inc. Overview of Mass Spectrometry. Thermo Scientific: Pierce Protein Biology Products. Thermo Fisher Scientific Inc. 06/06/2013, <http://www.piercenet.com/browse.cfm?fldID=33C6C4ED-4B0D-49FA-ABD2-23BCB0FADEC0>.
- 105) Adams, F., Hippocratic writings: Aphorisms IV, V. 1994, The Internet Classic Archive, pp. 1-10.
- 106) Fitzgerald, F.T. Tierney, L.M., Jr., The bedside Sherlock Holmes. 1982, *West J Med*, 169-175.
- 107) Daughaday, W.H. The adenohipophysis., Williams R.H., Saunders, W.B., Textbook of Endocrinology. Philadelphia, 1968, 27-84.
- 108) Liddell, K., Smell as a diagnostic marker. 1976, *Postgrad Med J*, 136-138.
- 109) Schiffman, S.S., Williams, C.M., Science of odor as a potential health issue. 2005, *J Environ Qual*, 129-138.
- 110) Buszewski, B., Keszy, M., Ligor, T., Amann, A. Human exhaled air analytics: biomarkers of disease. 2007, *Biomed Chromatogr* 21, 533-66.

- 111) Garner, C.E., Smith, S., de Lacy Costello, B., White, P., Spencer, R., Probert, C.S., Ratcliffe, N.M. Volatile organic compounds from feces and their potential for diagnosis of gastrointestinal disease. 2007, *FASEB J* 21, 1675-88.
- 112) Probert, C.S., Ahmed, I., Khalid, T., Johnson, E., Smith, S., Ratcliffe, N. Volatile organic compounds as diagnostic biomarkers in gastrointestinal and liver disease. 2009, *J Gastroenterol Liver Dis* 18, 337-43.
- 113) Arasaradnam, R.P., Pharaoh, M.W., Williams, G.J., Nwokolo, C.U., Bardhan, K.D., Kumar, S. Colonic fermentation--more than meets the nose. 2009, *Med Hypotheses* 73, 753-6.
- 114) Arasaradnam, R.P., Quraishi, N., Kyrou, I., Nwokolo, C.U., Joseph, M., Kumar, S., Bardhan, K.D., Covington, J.A. Insights into 'Fermentonomics': Evaluation of volatile organic compounds (VOCs) in human disease using an Electronic 'e' Nose. 2011, *J Med Eng Technol* 35, 87-91.
- 115) Arasaradnam, R.P., Ouaret, N., Thomas, M.G., Gold, P., Quraishi, M.N., Nwokolo, C.U., Bardhan, K.D., Covington, J.A. Evaluation of gut bacterial populations using an electronic e-nose and field asymmetric ion mobility spectrometry: further insights into 'fermentonomics'. 2012, *J Med Eng Technol* 36, 333-7.
- 116) Covington, J.A., Westenbrink, E.W., Ouaret, N., Harbord, R., Bailey, C., O'Connell, N., Cullis, J., Williams, N., Nwokolo, C.U., Bardhan, K.D., Arasaradnam, R.P. Application of a novel tool for diagnosing bile acid diarrhoea. 2013, *Sensors (Basel)* 13, 11899-912.
- 117) Arasaradnam, R.P., Bardhan, K.D. *Bioactive foods and Extracts – Cancer treatment and prevention*. Taylor Francis, New York 2010.
- 118) Arasaradnam, R.P., Covington, J.A., Harmston, C., Nwokolo, C.U. Review article: next generation diagnostic modalities in gastroenterology--gas phase volatile compound biomarker detection. 2014, *Aliment Pharmacol Ther* 39, 780-9.

- 119) Lippi, G., Cervellin, G. Canine olfactory detection of cancer versus laboratory testing: myth or opportunity? 2012, *Clin Chem Lab Med* 50, 435-9.
- 120) Sonoda, H., Kohnoe, S., Yamazato, T., Satoh, Y., Morizono, G., Shikata, K., Morita, M., Watanabe, A., Morita, M., Kakeji, Y., Inoue, F., Maehara, Y. Colorectal cancer screening with odour material by canine scent detection. 2011, *Gut* 60, 814-9.
- 121) Arasaradnam, R.P., Nwokolo, C.U., Bardhan, K.D., Covington, J.A. Electronic nose versus canine nose: clash of the titans. 2011, *Gut* 60, 1768.
- 122) Silva, C.L., Passos, M., Câmara, J.S. Investigation of urinary volatile organic metabolites as potential cancer biomarkers by solid-phase microextraction in combination with gas chromatography-mass spectrometry. 2011, *Br J Cancer* 105, 1894-904.
- 123) Hanson, C.W., Steinberger, H.A., The use of a novel electronic nose to diagnose the presence of intrapulmonary infection. 1998 *Crit Car Med* 26(1), 21-143
- 124) Khalid, T., White, P., de Lacy Costello, B., Persad, R., Ewen, R., Johnsons, E., Probert, C.S., Ratcliffe, N., A Pilot Study Combining a GC-Sensor Device with a Statistical Model for the Identification of Bladder Cancer from Urine Headspace. 2013, *PLOS One* 8 (7) e69602.
- 125) Alpendurada, M. de F., Solid-phase microextraction: a promising technique for sample preparation in environmental analysis. 2000, *J Chromatogr. A* 889 (1-2), 3-14.
- 126) Blount, B.C., Kobelski, R.J., McElprang, D.O., Ashley, D.L., Morrow, J.C., Chambers, D.M., Cardinali, F.L., Quantification of 31 volatile organic compounds in whole blood using solid-phase microextraction and gas chromatography-mass spectrometry. 2006, *J Chromatogr. B* 832 (2), 292-301

- 127) Di Natale, C., Mantini, A., Macagnano, A., Antuzzi, D., Paolesse, R., D'Amico A.,
Electronic nose analysis of urine samples containing blood. 1999, *Physiol Meas*
20(4), 377-384.
- 128) Aathithan, S., Plant, J.C., Chaundry, A.N., French, G.L., Diagnosis of bacteriuria by
detection of volatile organic compounds in urine using an automated headspace
analyzer with multiple conducting polymer sensors. 2001, *J Clin Microbiol* 39(7),
2590–2593.
- 129) Peng, G., Hakim, M., Broza, Y.Y., Billan, S., Abdah-Bortnyak, R., Kuten, A., Tisch, U.,
Haick, H. Detection of lung, breast, colorectal, and prostate cancers from exhaled
breath using a single array of nanosensors. 2010, *Br J Cancer* 103, 542-51.
- 130) Altomare, D.F., Di Lena, M., Porcelli, F., Trizio, L., Travaglio, E., Tutino, M.,
Dragonieri, S., Memeo, V., de Gennaro, G. Exhaled volatile organic compounds
identify patients with colorectal cancer. 2013, *Br J Surg* 100(1), 144-50.
- 131) Jellum, E., Stokke, O. and Eldjam, L., Application of gas chromatography, mass
spectrometry and computer methods in clinical biochemistry. 1973, *Anal Chem*
46(7), 1099-1166.
- 132) D'Amico, A., Di Natale, C., Paolesse, R., Macagnano, A., Martinelli, E., Pennazza,
G., Santonico, M., Bernabei, M., Roscioni, C., Galluccio, G., Bono, R., Finazzi Agro,
E., Rullo, S., Olfactory systems for medical applications. 2008, *Sens Actuat B:
Chem* 130(1), pp. 458-465.
- 133) Roscioni, C., De Ritis, G., On the possibilities to using odors as a diagnostic test of
disease. 1968, *Ann 1st Carlo Forlanini* 28(4), 457-461.
- 134) Wilson, A.D., Lester, D.G. and Oberle, C.S., Development of conductive polymer
analysis for the rapid detection and identification of phytopathogenic microbes.
2004, *Phytopathology* 94(5), 419-431.

- 135) Pavlou, A.K., Magan, N., McNulty, C., Jones, J., Sharp, D., Brown, J., Turner, A.P.,
Use of an electronic nose system for diagnoses of urinary tract infections. 2002,
Biosens Bioelectron 17(10), 893-899.
- 136) Pavlou, A.K., Magan, N., Sharp, D., Brown, J., Barr, H., Turner, A.P., An intelligent
rapid odour recognition model in discrimination of *Helicobacter pylori* and other
gastroesophageal isolates in vitro. 2000, Biosens Bioelectron 15(7-8), 333-342.
- 137) Dutta, R., Hines, E.L., Gardner, J.W., Boilot, P., Bacteria classification using
Cyrano 320 electronic nose. 2002, BioMed Eng OnLine 1, 1-4.
- 138) Gardner, J.W., Shin, H.W., Hines, E.L., An electronic nose system to diagnose
illness. 2000, Sens Actuat B: Chem 70(1-3), 19-24.
- 139) Arasaradnam, R.P., Quraishi, N., Kyrou, I., Nwokolo, C.U., Joseph, M., Kumar, S.,
Bardhan, K.D., Covington, J.A., Insights into 'fermentonomics': evaluation of
volatile organic compounds (VOCs) in human disease using an electronic 'e-nose'.
2011, J Med Eng & Tech 35, 87-91.
- 140) Kateb, B., Ryan, M.A., Homer, M.L., Lara, L.M., Yin, Y., Higa, K., Chen, M.Y., Sniffing
out cancer using the JPL electronic nose: A pilot study of a novel approach to
detection and differentiation of brain cancer. 2009, NeuroImage 47(Suppl 2) T5-T9.
- 141) Staples, E.J., The zNose™, A New Electronic Nose Using Acoustic Technology.
2000, J Acoust Soc Am. 2aEA4.
- 142) Berna. Z., Webb, C.C., Erickson, M.C., Electronic nose and fast GC for detection of
volatiles from *Escherichia Coli* O157:H7, *Escherichia Coli* and *Salmonella* in lettuce.
2013, International Society for Horticultural Science 10, e17660.
- 143) McNerney, R., Mallard, K., Okolo, P.I., Turner, C., Production of volatile organic
compound by mycobacteria. 2012, FEMS Microbiol Lett 328, 150-156.
- 144) Machado, R.F., Laskowski, D., Deffenderfer, O., Burch, T., Zheng, S., Mazzone, P.J.,
Mekhail, T., Jennings, C., Stoller, J.K., Pyle, J., Duncan, J., Dweik, R.A., Erzurum,

- S.C. Detection of lung cancer by sensor array analyses of exhaled breath. 2005, *Am J Respir Crit Care Med* 171, 1286-1291.
- 145) Asimakopoulos, A.D., Del Fabbro, D., Miano, R., Santonico, M., Capuano, R., Pennazza, G., D'Amico, A., Finazzi-Agro, E. Prostate cancer diagnosis through electronic nose in the urine headspace setting: a pilot study. 2014, *Prostate Cancer P D* 17, 206-211.
- 146) McEntegart, C.M., Penrose, W.R., Strathmann, S., Stetter, J.R. Detection and discrimination of coliform bacteria with gas sensor arrays. 2000, *Sens Actuat B: Chem* 70, 170-176.
- 147) Garner, C.E., Smith, S., de Lacy Costello, B., White, P., Spencer, R., Probert, C.S., Ratcliffe, N.M. Volatile organic compounds from feces and their potential for diagnosis of gastrointestinal disease. 2007, *FASEB J.* 21, 1675-88.
- 148) Aggio, R.B.M., de Lacy Costello, B., White, P., Khalid, T., Ratcliffe, N., Persad, R., Probert, C.S.J., The use of a gas chromatography-sensor system combined with advanced statistical methods, towards the diagnosis of urological malignancies. 2016, *J Breath Res.* 10 (1) e017106.

3. Volatile Content of Urine Samples by Gas Chromatography – Mass Spectrometry

3.1. Scope and Disease States Studied

While electronic nose systems are able to quickly and effectively identify groups of samples based on the levels of their responder chemicals (and complex mixtures thereof), they cannot give any more insight into the exact chemical composition. There is a large degree of cross-sensitivity between sensors for many common gases and volatiles, including those that are contained in all samples such as water vapour (1). Therefore, further investigation into the specific chemical components present in urine headspace samples was run in parallel to the electronic nose studies. In this case, the analysis was performed with gas chromatograph and mass spectrometry (GC/MS).

A large number of different disease states have been investigated by GC/MS analysis in order to correctly differentiate between the chemicals present in all urine and those unique to particular diseases. They are all conditions affecting the lower gastro-intestinal area that have similarities in symptoms, and are listed in Table 3.1. The table also specifies pre-concentration techniques that were used in samples of different disease groups to intensify the response of the instrument to chemicals in a particular molecular weight range. The technologies used for pre-concentration include In-Tube Extraction (ITEX) and Solid Phase Microextraction, both of which will be introduced in more detail in Section 3.2.1.

Disease Group	Pre-concentration Techniques
Colorectal Cancer (CRC)	ITEX + SPME
Irritable Bowel Syndrome (IBS)	ITEX + SPME
Volunteer (V)	ITEX + SPME
Coeliac Disease (CO)	ITEX + SPME
Inflammatory Bowel Disease (IBD)	ITEX
Colorectal Polyps (PS)	ITEX
Non-Alcoholic Fatty Liver Disease (NAFLD)	SPME

Table 3.1: List of disease groups analysed by GC-MS and pre-concentration techniques

employed

3.2. Methods and Materials

3.2.1. Instrument and Pre-concentration Method

The instrument used in these studies was a Scion SQ GC/MS system manufactured by Bruker, and was fitted with an RXI-624Sil MS capillary column (length 20 m, ID 0.18 mm, df 1.0 μ m) and used analytical grade (99.999%) helium as a carrier gas. In addition, the GC-MS was equipped with a CombiPAL autosampler that is currently capable of holding, sequential incubating and injecting up to 32 samples. Initially, a 2.5 mL gas syringe was fitted to the autosampler head to directly inject a known volume of gas into the machine. After direct gas injection gave insignificant sample concentration (described below) the autosampler was then fitted with a CTC ITEX-2 option for pre-concentrating by trapping into a 60/40 combination of Tenax GR (80/100 mesh) and CarboSieve S III (60/80 mesh). This combination is effective at trapping low-mid molecular weight volatiles and gases, while retaining some larger chain hydrocarbons. This same autosampler was also improved later by attaching a SPME pre-concentration fibre composed of poly-dimethylsiloxane (PDMS) of thickness 100 μ m and length 1 cm in place of the ITEX-2. This SPME pre-concentrator must be exposed to the volatile headspace for absorption to take place, and provides improved retention at the mid-high molecular weight range of volatiles to give insight into a wider variety of potential urine biomarkers. The pre-concentration and autosampler method was dictated by CombiPAL Cycle Composer software (version 1.6.0, CombiPAL) and the GC/MS system was controlled using MS Workstation System Control software (version 8, Bruker).

All non-functional materials that come into contact with the samples via the fittings and components in the system are glass, stainless steel, brass, aluminium, or polytetrafluoroethylene (PTFE), and the whole system was fully pre-conditioned beforehand. This allows for a negligible effect on the samples by most system artefacts or contamination.

3.2.2. Experimental Method

Urine samples used in the GC/MS had been collected by medical staff at the University Hospital of Coventry and Warwickshire (UHCW) using 30 mL sterilised polypropylene screw top containers, and stored frozen at -80 °C within walk-in freezers. Storage time within these freezers ranged between 0 – 2 years before selection for analysis.

Transfer of samples from hospital freezers to a -20 °C laboratory freezer occurred within a 1-hour period, an analysis took place within 1 week of transfer to this secondary storage location. They were thawed at a temperature of 5°C overnight before 5mL aliquots were transferred into 10mL glass vials, which were then sealed using aluminium crimp tops fitted with PTFE septa. This allowed an equal ratio of headspace volume and liquid sample volume (both 5 mL), which was consistent with techniques used in other studies in Section 2.3. The internal diameter of the vials was 15 mm, giving an area of sample/air interface of approximately 47.1 mm². The samples were aliquoted using a Gilson Pipetman P D-10mL pipette with individual sterilised polypropylene disposable tips.

All experimental methods involved headspace generation by individual sample incubation using an on-board heated incubator included in the CombiPAL autosampler. Liquid and headspace samples were transported around the system by the autosampler arm, which includes a 24 ga syringe-style end with one of the two pre-concentration methods fitted. The ITEX experimental method had vials kept at a temperature of 50°C for a period of 5

minutes in order to release the dissolved volatiles and gases, before being trapped in the ITEX-loaded syringe by extracting (and subsequently replacing) 500 μL of vial headspace a total of 15 times. The syringe was sent to the injector and the ITEX trap was heated to 250°C for 5 minutes, causing the sample to be released into the front injector port to the column upon syringe injection. The SPME method begins with the syringe puncturing the vial septa and exposing the absorbent fibre to the headspace for 5 minutes after initial incubation at 50°C . The turgid fibre is then retracted before insertion into the front injector port, where it is exposed and heated to 250°C for 5 minutes in order to release the headspace sample for analysis. Blank vials filled with laboratory air were run in between each sample vial in order to identify and eliminate peaks that were products of the laboratory environment or the system itself.

After each sample injection occurred the GC column was held at a temperature of 50°C for a period of 1 minute, before being heated at a steady ramp rate of 20°C per minute to a maximum of 280°C and finally held for another 2.5 minutes. The analytes contained in the headspace sample were thus separated from each other within the retentive column in terms of their molecular mass and electrostatic polarity, and sent to the Mass Spectrometer individually in separate time windows. The molecules were then bombarded with electrons, which caused them to break apart and form a group of ions that are characteristic of each individual species. The final detector analysed these ions to form a spectrum of different ion masses that came out of the column at each 50ms timeframe throughout the sample run.

3.2.3. Data Analysis Method

The data produced by the GC/MS control software for each sample is in the form of a chromatogram displaying Total Ion Count (TIC) over the entire run, with a linked mass spectrum showing the relative intensity of ion masses detected with each measurement.

These can be navigated and studied within the software, and TIC peaks cross-compared to previously-established reference standards found in the 2011 National Institute of Standards and NIST Library. The comparison involves giving a score to each reference based on the degree of success its spectrum has in forward- and reverse-fitting the spectrum found in the actual sample. This provides some insight into the chemicals that are candidates for producing each peak found in a sample run through the GC/MS system. Each chromatogram was manually studied to find peaks that were found to be present in urine headspace samples while not appearing in air blanks run before and after each sample. For each peak found in this way, a report file in XPS format was produced giving the mass spectrum for the peak as well as that of the top 3 scoring chemicals from the NIST database. The TIC peaks of each sample were ordered into similar time windows, marked by the disease group that the patient fell into. Particular bands of peaks were chosen as significant based on either having an overall incidence of 30% or higher in all urine samples, or on having an incidence of 30% or higher in at least one group along with deviations of at least 10% between one group and the full test population. The rates for the disease groups that were 10% lower and 10% higher than that of the full sample set were indicated by colour code (red for low, green for high). These peaks of significance were investigated further, with the top 3 scorers for each given a rating based on its score and tallied in a full list of all candidate chemicals for each peak timeframe. This analysis was proposed to clarify the identity of the constituents of urine headspace in an environment where a large degree of individual sample variation can be found.

3.3. Results

3.3.1. System Artefact Peaks

There are a number of peaks present in all samples and blanks, which can be attributed to artefacts of the actual column and system. The retention times, maximum ion count and mass spectra of these peaks described below are all common to every sample and blank

run through this instrument, and so can be eliminated from consideration when investigating the volatile contents of urine headspace. Figures 3.1 and 3.2 illustrate the output of typical blank samples run after urine samples that did not contain a high enough concentration of any volatiles to produce any saturation, using ITEX and SPME pre-concentration techniques. These highlight the artefact peaks without confusing them for any genuine peaks produced by a sample.

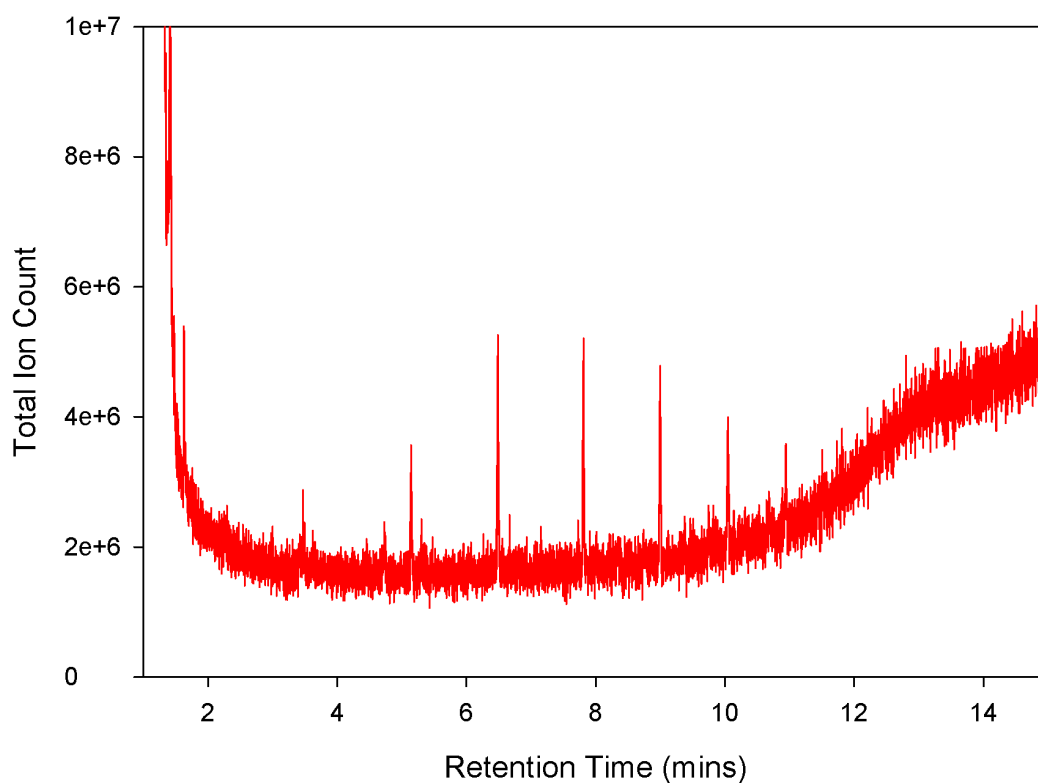


Figure 3.1: Example of chromatogram of a blank air sample run with ITEX pre-concentration

The two different methods produce a variation in relative scale of these artefact peaks, but they can be seen to have identical retention times. This can be a measure of the relative success that the pre-concentration techniques have at absorbing compounds of various molecular masses. It can be seen that ITEX has a better compound retention at the lower mass ranges, while the SPME fibre's retention is greatest at medium-large compounds and

then sharply trails off. There is a regular time gap between the peaks, indicating that their molecular masses will increase incrementally and giving clues to their origin as differently-sized fragments of the same regular matrix structure.

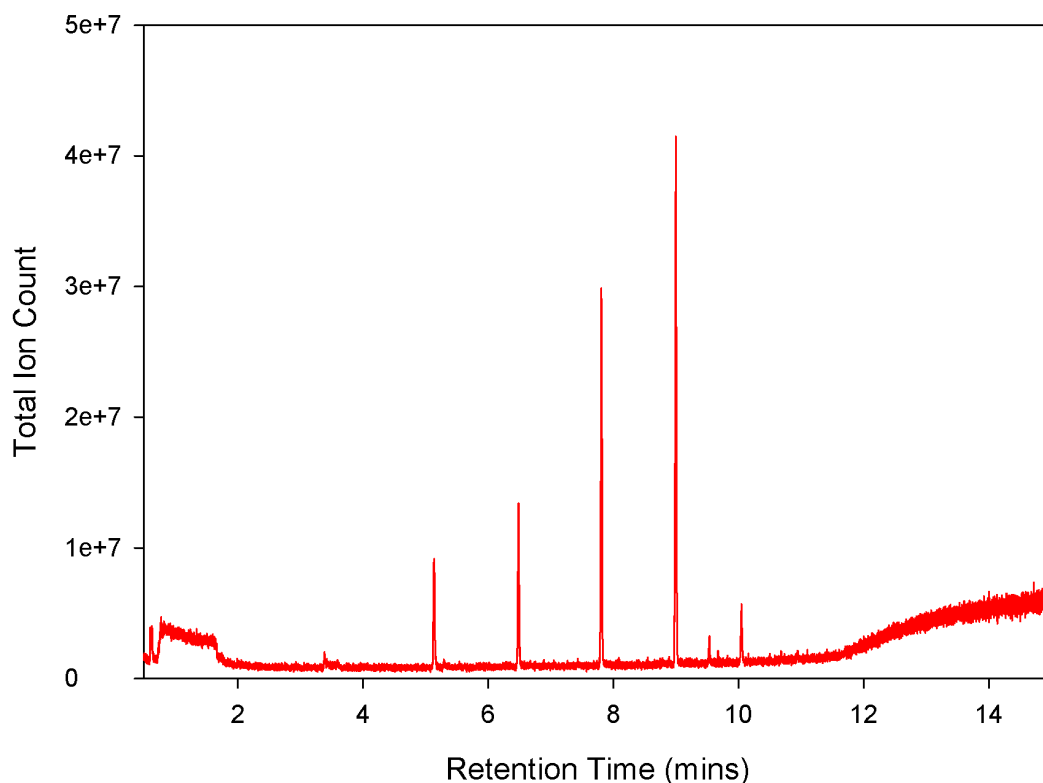


Figure 3.2: Example of chromatogram of a blank air sample run with SPME pre-concentration

The earliest peak to be observed in these chromatographs, which can be attributed to system artefacts, is at approximately 3.39 minutes (Figure 3.3). The mass spectra of peaks found in this region have relatively low molecular mass ranges compared with the others found at later retention times. NIST library cross-referencing yields the most common likely candidate compound to be Dimethyl-Silanediol, which contains a combination of carbon, silicon and alcohol groups.

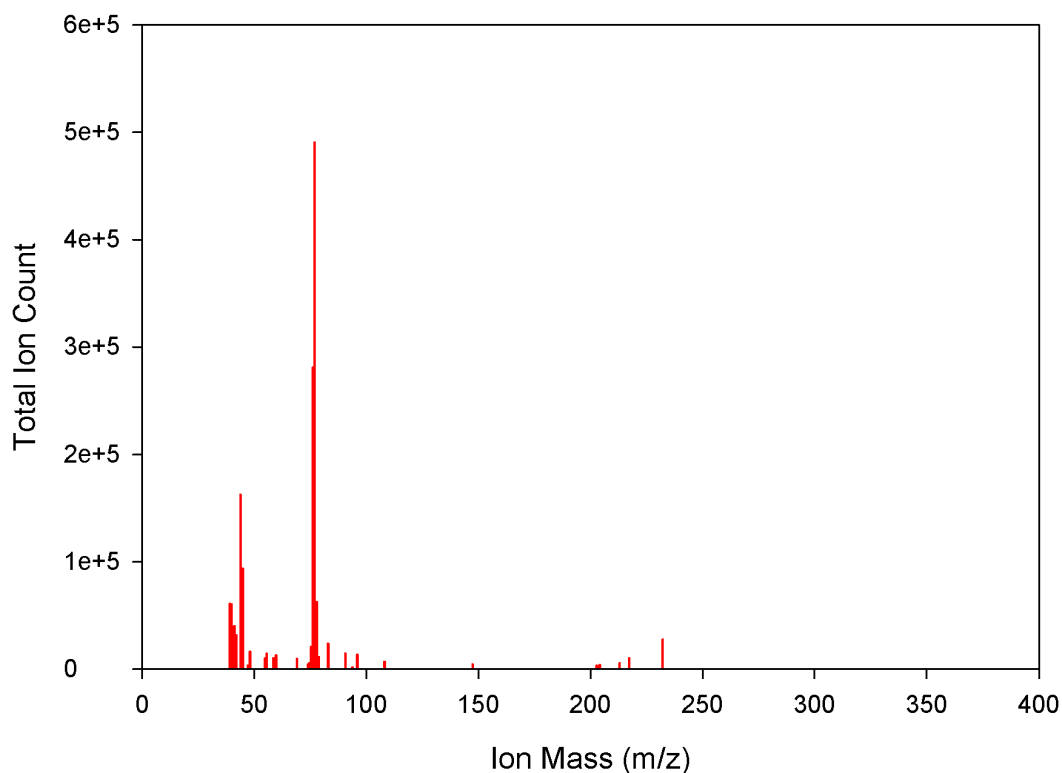


Figure 3.3: Example of the mass spectrum of an artefact peak found at 3.39 minutes

The next artefact peak is produced at approximately 5.14 minutes and has a mass spectrum with much more prominent peaks at relative masses above 200 (Figure 3.4). Cross-referencing with the NIST library reveals the most likely candidate compound to be Octamethyl-Cyclotetrasiloxane. The molecule has a circular central structure of silicon and oxygen atoms, with outstretching methyl groups surrounding it. This reveals a greater wealth of information on the internal structure of the column, as the siloxane group could help to retain other molecules from within a larger matrix. The previous silanediol compound found at 3.34 minutes could represent fragments of the cyclic siloxane group found within these molecules that have broken off to form stable alcohol groups.

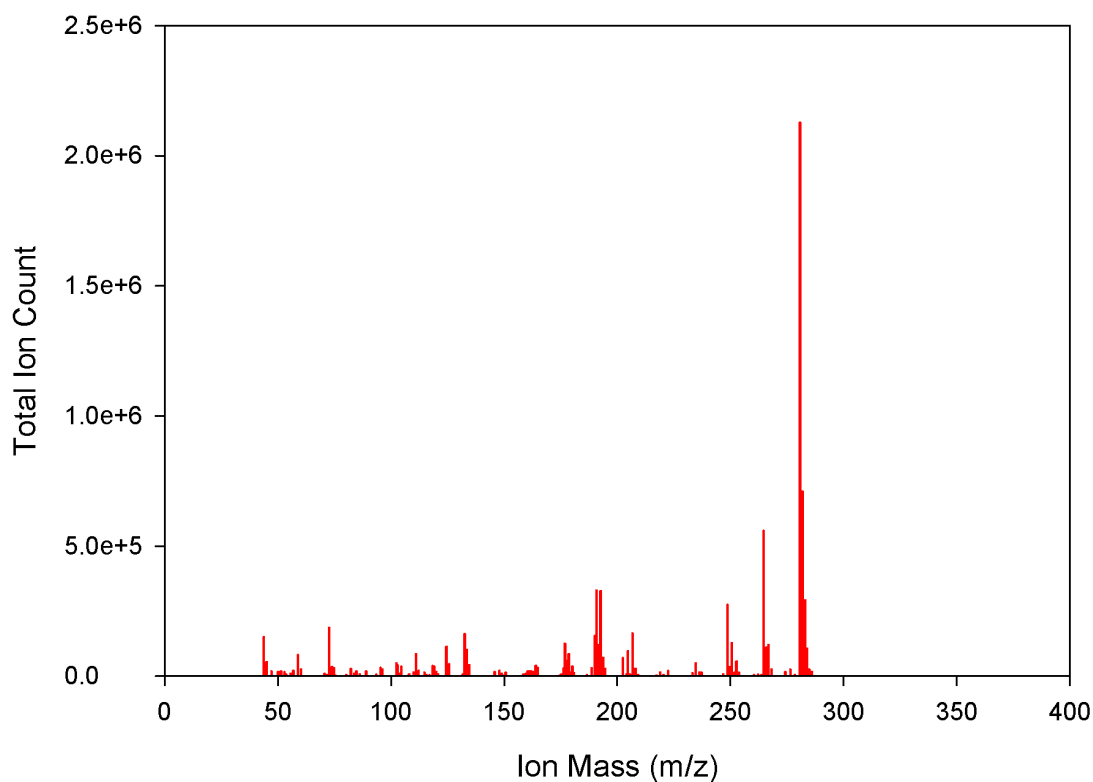


Figure 3.4: Example of the mass spectrum of an artefact peak found at 5.14 minutes

The remainder of the mass spectra for these artefact peaks can be found in Appendix 1, and show similar patterns and candidate molecules to those described in this section, but with sequentially increasing molecular masses.

3.3.2. Sample Variation

The data gathered from the urine headspace samples on the GC-MS incorporates many barriers to an even interpretation and comparison, not least of which was a large degree of variation in the relative dilutions of samples due to particular patients' water intake. This did not seem to affect any specific compound singly, but made it very difficult to find many

common peaks with a high degree of confidence.

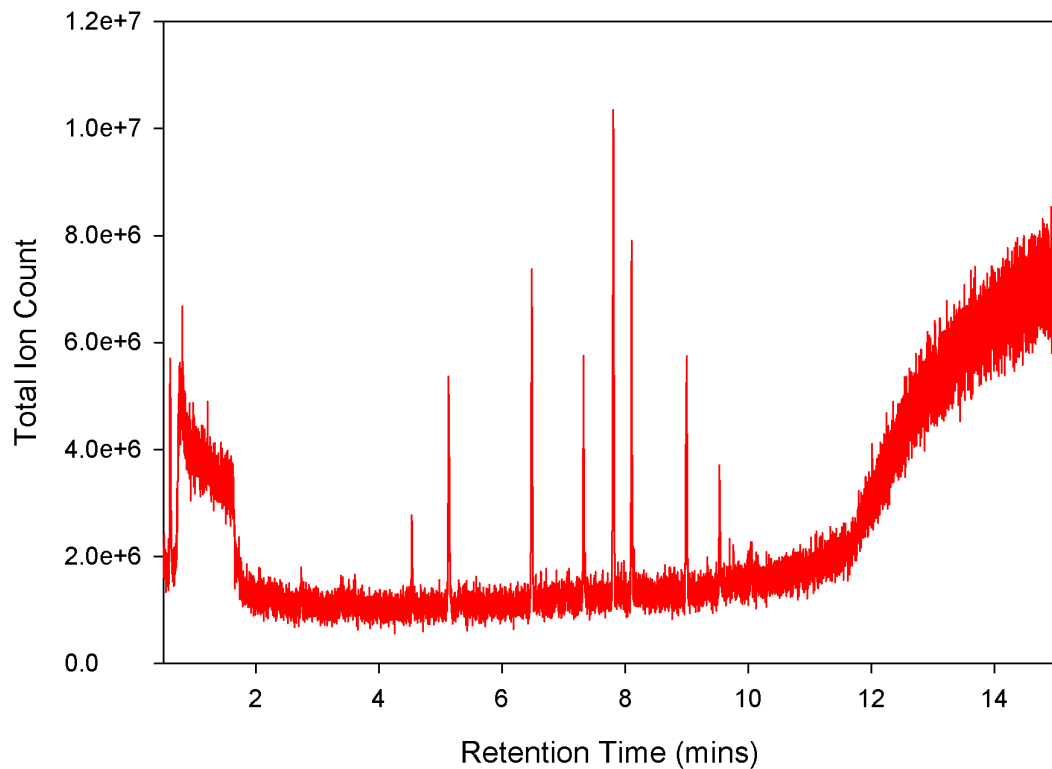


Figure 3.5: Example chromatogram of a typical urine sample

To demonstrate the effect described above, Figure 3.5 shows the chromatogram produced by a typical urine sample with a reasonable dilution level for analysis. In addition to the peaks associated with system artefacts, there are several other distinctive peaks, for example at the 4.5, 7.2, 8.0 and 9.5 minute marks. Figure 3.6 shows, by contrast, a sample with very few distinctive peaks aside from that at 9.5 minutes. This is caused by an excess of water being expelled in the patient's urine, making for heavily diluted samples to be captured and stored for analysis. The delicacy of the liquid phase storage medium for volatile compounds and the limited volume collected for analysis made it infeasible to attempt to decrease the dilution of these samples by evaporating or otherwise removing water from the urine, without mitigating risk of losing volatile content.

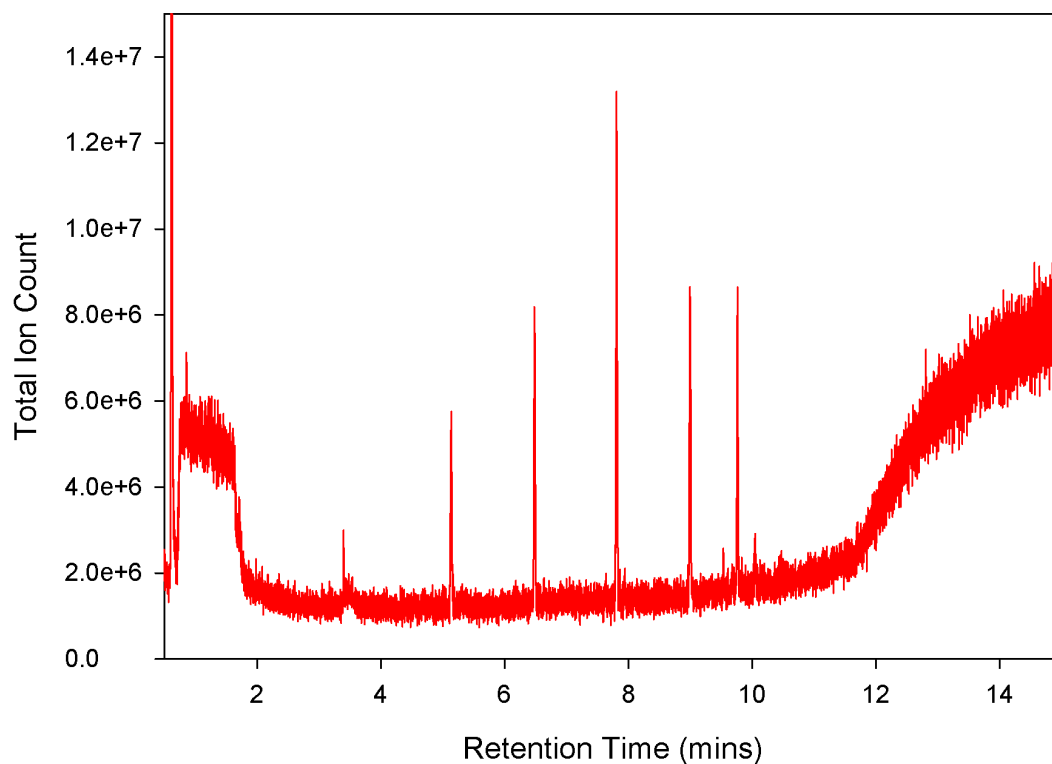


Figure 3.6: Example chromatogram of a heavily-diluted urine sample

In addition, particular constituents of the recent diet of some patients caused large sets of unique peaks to be produced in their samples. Figure 3.7 is one example of this, where peaks such as limonene and levomenthol have come out of one sample due to the proposed consumption of fruit teas. Large peaks such as these have the potential to saturate the detector and mask other peaks that were actually produced by the patients' metabolomic processes.

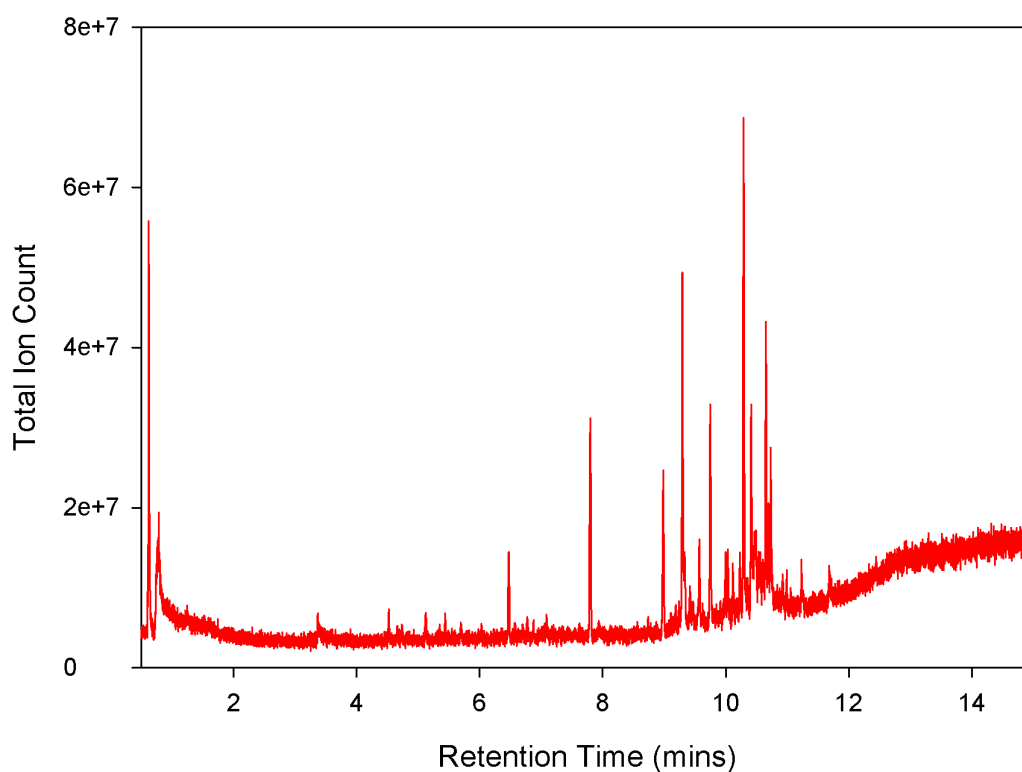


Figure 3.7: Example chromatogram of a urine sample with unique dietary peaks

These complications in the sample preparation have not allowed for any quantitative analysis of peaks found from the urine headspace samples. Therefore, chromatogram peaks have simply been measured and compared using their percentage of incidence found within samples of each disease group, and significant “common” peaks described below are labelled as such because of their high incidence levels in the sample set as a whole.

3.3.3. Common Urine Peaks

There have been several common peaks found in the urine samples as a whole, and most of these show a significant degree of variation between disease groups to indicate some potential links between changes in metabolomic processes and the various disease states. In addition, the ITEX and SPME pre-concentration techniques yielded differences in retention levels across the range of molecular masses picked up by the GC-MS. This causes

some common peaks of both techniques to overlap each-other, while others are found exclusively using a particular pre-concentration method.

The retention times for common chromatogram peaks are detailed in Table 3.2, along with the top candidate chemicals as found by NIST classification. The table also includes the incidence rate for peaks within each of the individual disease groups and the full group of all urine samples. There was a wide range of variation in incidence rates within the group of peaks analysed, which resulted in higher levels of confidence in some chemical classifications as compared to others. The earliest peak to be prominently found in most urine samples using ITEX pre-concentration was measured at approximately 1.74 minutes, and is extremely consistent throughout all disease groups in its high percentage of incidence. These can be found in Table 3.2 where it shows incidence levels of 90-100% in nearly all groups, with a slightly decreased level in polyps patients only. By contrast, another peak that occurred with a reasonable incidence was found at a retention time of 2.83 minutes. However, examples of this set of peaks were much less likely to be found in any particular sample, as by the percentages of incidence between 0% and 30% shown in Table 3.2. The NIST classification tallying put forward two molecules that have the potential to have caused these peaks, but this result was much less clear than for the previous peak due to the large number of other compounds that were also classified in single cases at this retention time. This lack of clarity in classification may have been partly caused by the small GC peak size as compared to the background sample noise, which caused the system artefact noise to be wrongly identified as relatively important within the mass spectra of these peaks and used in the classification.

Volatile Content of Urine Samples by Gas Chromatography – Mass Spectrometry

SPME Pre-Concentration		4.54	4.67	4.75	5.31	
Peak Time (minutes):						
Top Three Candidate Chemicals	3-Pentanone, 2,4-dimethyl-		1,3,5,7-Cyclooctatetraene	Cyclopropane, isothiocyanato-	Oxime-, methoxy-phenyl-	
	4-Heptanone		Benzeethanamine, N-[(4-hydroxy)hydrocinnamoyl]- Styrene	Allyl Isothiocyanate	4-Ethylbenzoic acid, 2-butyl ester 4-Ethylbenzoic acid, cyclopentyl ester	
	Rates of Incidence within Sample Sets	FULL: 66.7% CRC: 65.0% IBS: 75.4% V: 64.8% CO: 39.5% CLD: 61.5%	64.7% 65.0% 42.1% 78.9% 63.2% 30.8%	19.8% 10.0% 31.6% 14.1% 26.3% 3.8%	63.1% 43.3% 56.1% 78.9% 52.6% 61.5%	
	SPME Pre-Concentration					
	Peak Time (minutes):		1.74	2.83	2.95	4.56
	Top Three Candidate Chemicals	Acetone		Propane, 2-(ethoxyloxy)-	2-Pentanone	4-Heptanone
1,2,4,5-Tetroxane, 3,3,6,6-tetramethyl-Diazene, dimethyl-			2-Pentanone	2-Butanone, 3-methyl- 3-Aminopyrrolidine	3-Pentanone, 2,4-dimethyl- 1-Hydroxy-2-pentanone	
Rates of Incidence within Sample Sets		FULL: 92.8% CRC: 90.3% PS: 69.2% IBD: 100.0% IBS: 98.7% CO: 100.0% V: 87.8%	20.4% 17.5% 7.7% 0.0% 31.2% 29.2% 17.1%	10.0% 16.5% 46.2% 0.0% 0.0% 0.0% 12.2%	65.6% 56.3% 30.8% 81.0% 71.4% 87.5% 68.3%	

Table 3.2: List of top three tallied NIST classifications for chromatogram peaks (chosen candidates in bold) and rates of incidence (low in red, normal in black, high in green)

SPME Pre-Concentration		7.95	9.53	9.76
Peak Time (minutes):	Carvone			
Top Three Candidate Chemicals		Ethanone, 1,1'-(1,4-phenylene)bis-	Ethanone, 1,1'-(1,3-phenylene)bis-	Phenol, 2,4-bis(1,1-dimethylethyl)-
Rates of Incidence within Sample Sets	FULL	42.5%	28.2%	91.7%
	CRC	36.7%	20.0%	90.0%
	IBS	49.1%	35.1%	82.5%
	V	35.2%	16.9%	98.6%
	CO	36.8%	28.9%	60.5%
	CLD	50.0%	50.0%	96.2%
SPME Pre-Concentration				
Peak Time (minutes):		4.7	5.3	5.37
Top Three Candidate Chemicals		Benzeneethanamine, N-[(4-hydroxy)hydrocinnamoyl]-	Oxime-, methoxy-phenyl-	1,3-Propanediamine
Rates of Incidence within Sample Sets	FULL	67.0%	22.6%	20.4%
	CRC	81.6%	17.5%	9.7%
	PS	0.0%	0.0%	23.1%
	IBD	9.5%	23.8%	42.9%
	IBS	71.4%	23.4%	24.7%
	CO	87.5%	58.3%	66.7%
	V	61.0%	19.5%	0.0%

Table 3.2: List of top three candidate NIST classifications for chromatogram peaks (chosen candidates in bold) and rates of incidence (low in red, normal in black, high in green)

Examples of the mass spectra relating to some of the peaks are described in Sections 3.3.3.1 – 3.3.3.4, in order to highlight the main features of the data. Mass spectra for the remainder of the common peaks found in urine headspace by both ITEX and SPME pre-concentration techniques can be found in Appendix 1.

3.3.3.1. ITEX Pre-concentrated Peak at 1.74 Minutes

Figure 3.8 displays a typical mass spectrum associated with the GC peaks produced at 1.74 minutes, which had major components at relative masses of 44 and 58 and tended to have very little variation between samples. This consistency, along with the high incidence rate within all samples (as shown in Table 3.2), provides a high confidence level in the classification of these peaks as Acetone.

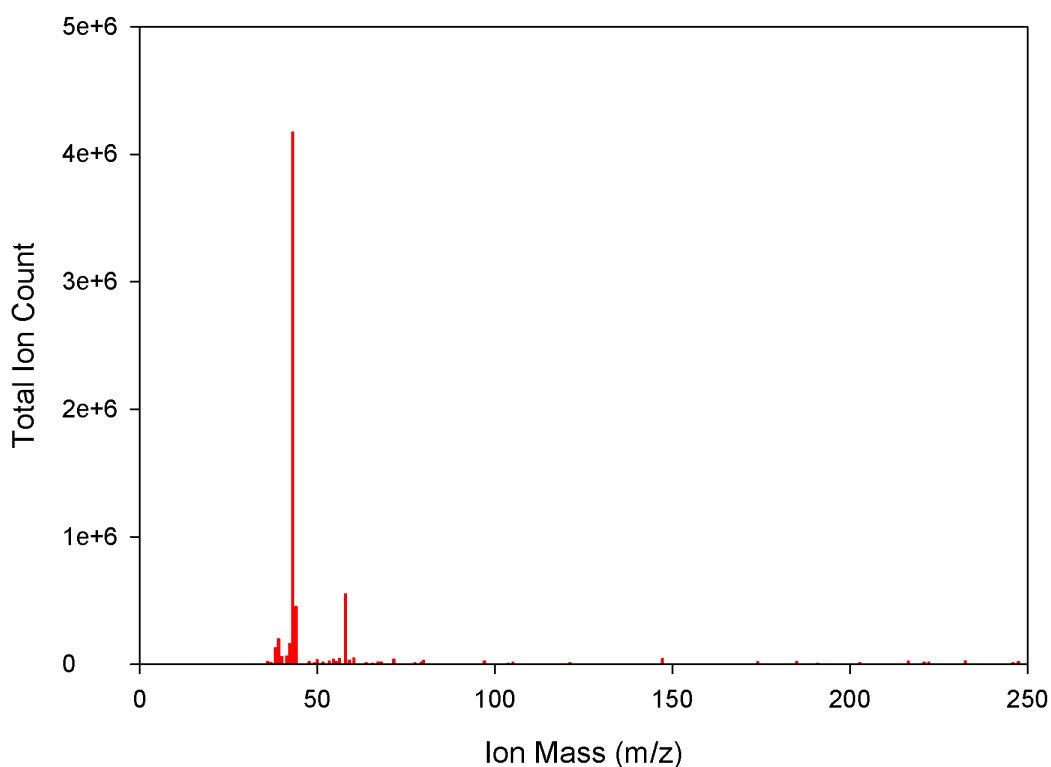


Figure 3.8: Example mass spectrum of an ITEX peak found at 1.74 minutes

3.3.3.2. ITEX Pre-concentrated Peak at 4.56 Minutes

Classification by NIST library produced reasonably conclusive results on the identity of the molecule causing these peaks, with 4-Heptanone and 2,4-dimethyl-3-pentanone both giving high tallies (as seen in Table 3.2). These molecules have very similar groups to each other and an identical molecular weight, which makes it very difficult to distinguish between them. The typical mass spectrum shown in Figure 3.9 shows high ion counts at

relative masses of 43, 71 and 114, which are consistent spectra produced by both of these candidate chemicals.

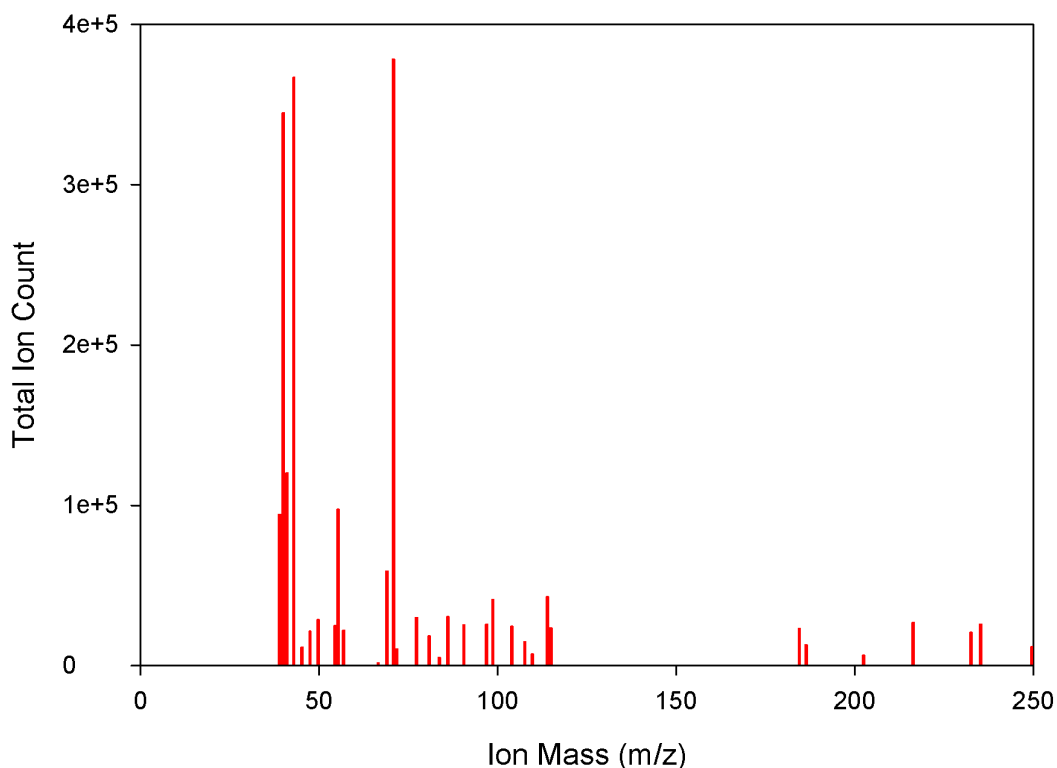


Figure 3.9: Example mass spectrum of an ITEX peak found at 4.56 minutes

3.3.3.3. SPME Pre-concentrated Peak at 4.54 Minutes

The mass spectra associated with these peaks are consistent with those found using ITEX pre-concentration, with components found at relative masses of 43, 71 and 114 (illustrated by Figure 3.10). Cross-referencing with NIST library entries has yielded similar candidate molecules in 2,4-dimethyl-3-Pentanone and 4-Heptanone, adding confidence to their potential as causes for these peaks. These results correlate very well with those shown in Section 3.3.3.4, which also classify peaks in the region of 4.55 minutes as being produced by these molecules.

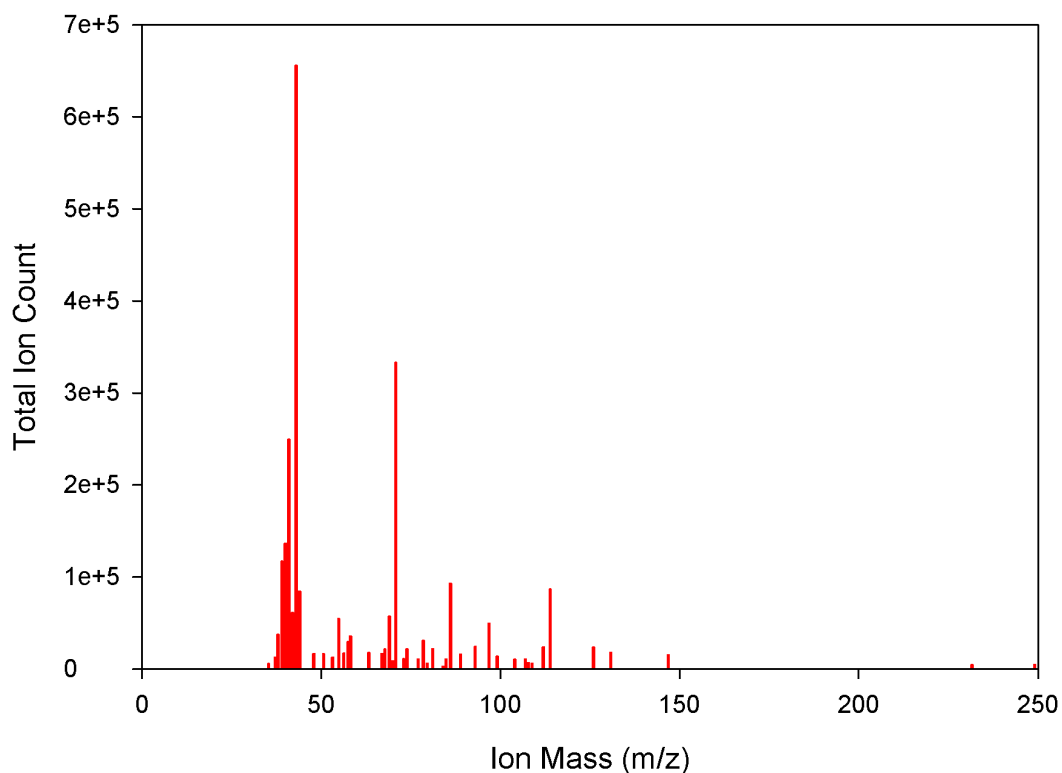


Figure 3.10: Example mass spectrum of a SPME peak found at 4.54 minutes

3.3.3.4. SPME Pre-concentrated Peak at 9.76 Minutes

There is very good agreement between mass spectra associated with these peaks, an example of which is shown in Figure 3.11. The major spectrum component for these is found at a relative mass of 191, with other components appearing at many regular points including 57, 74, 105, 128, et cetera. This correlates well with the large degree of allyl and phenyl fragmentation that could be seen in all of the top three NIST classification candidates, which are all of type dimethylethyl-Phenol. These only vary from each other in the relative positions of the branching ethyl and methyl groups, and constitute the overwhelming majority of classifications.

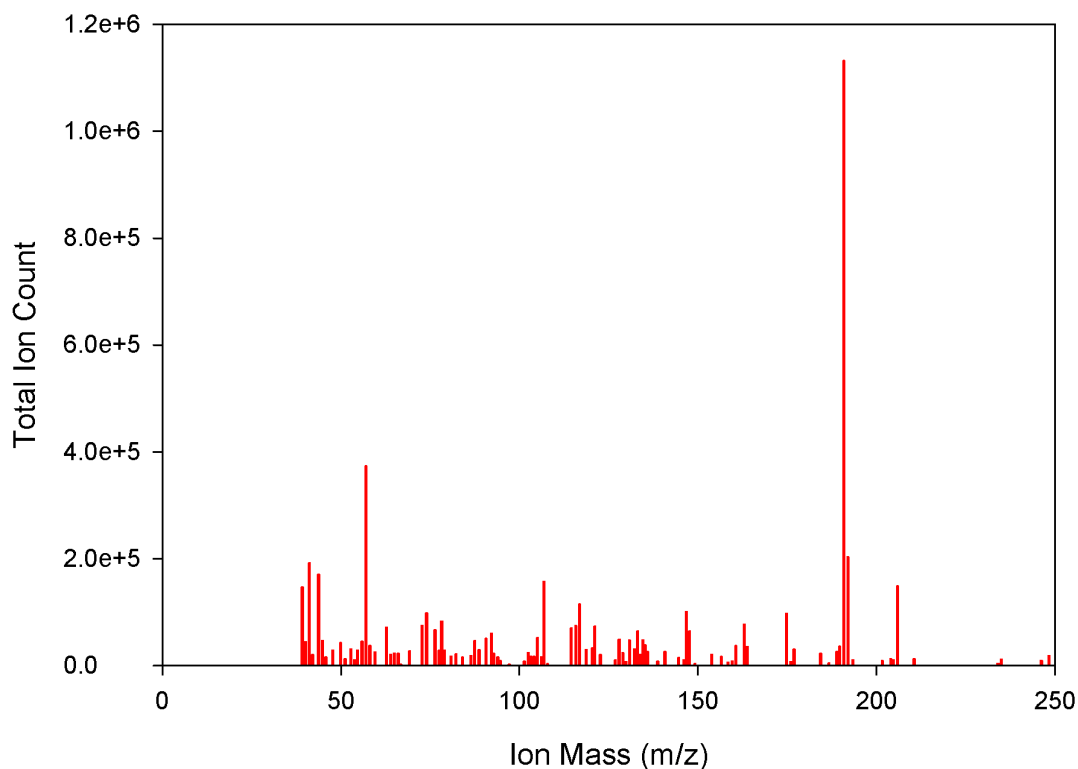


Figure 3.11: Example mass spectrum of a SPME peak found at 9.76 minutes

3.3.3.5. Unclassified Peaks

There were a large number of GC peaks found by this method that did not give any distinct classification upon cross-referencing with the standard mass spectra in the NIST library. These peaks were generally presented at very low overall ion counts, and so had a significant level of system noise introduced to their spectra. In many cases, this lack of clarity was exacerbated by an overall incidence rate of 30% or lower in all urine samples. This resulted in very little coherence in the NIST classifications, presenting no significant leaders in potential candidate molecules. The top suggested candidates had a distinct lack of coherence in terms of molecular structure, usually in addition to a molecular weight that was inconsistent with the area of the chromatogram at which they had presented. These unclassified peaks, their level of incidence for each disease group and their top three candidate molecules are listed in Appendix 1.

3.4. Discussion and Conclusions

3.4.1. Metabolic and Dietary Links

A full list of the potential compounds found with reasonable confidence by these two combined GC-MS techniques is summarised in Table 3.3. There have been a number of studies that have used gas chromatography-mass spectrometry techniques to analyse the volatile contents of human urine in the past. Studies by Wahl et al (2) and Mills et al (3) both support the findings of many of the volatile organic compounds classified in this work, employing cryogenic and SPME methods for pre-concentration, respectively. Table 3.3 details the cases where these studies have identified similar if not identical compounds (marked in green if present), including a range of ketone, aromatic and sulphide compounds. The investigation by Mills et al. concludes that a large range of metabolic products are transferred to urine and may be released into volatile headspace for analysis, and that a GC-MS system with a PDMS-based SPME fibre is suitable to profile volatile compounds in investigations relating to metabolic disturbances.

Volatile Compound	Wahl et al.	Mills et al.
Acetone		
2-Pentanone		
4-Heptanone		
1,3,5,7-Cyclooctatetraene		
Allyl Isothiocyanate		
Oxime-, methoxy-phenyl-		
1,3-Propanediamine		
Carvone		
Ethanone, 1,1'-(1,4-phenylene)bis		
Phenol, 2,4-bis(1,1-dimethylethyl)-		

Table 3.3: List of candidate volatiles found in this study and their presence in the results of

Wahl et al. (2) and Mills et al. (3), with presence indicated by shading cells green

A number of the volatiles identified by this investigation have been found to contribute to the metabolic processes within the lower gastro-intestinal tract by previous studies. Acetone has been shown to contribute to pH regulation within the mammalian system, and

also to have the potential to be used as an additional fuel to aid metabolic processes in the liver (4). Higher levels of acetone have been found to be produced under fasting conditions or if the subject has diabetes. Other studies have shown that acetone may also be produced by oxidation of fatty acids by gut bacteria, and have thus been linked to glucose levels in the blood (5).

2-Pentanone has been found to occur naturally within fruits, vegetables and fermented foods, and has also been found to increase within faeces after the consumption of symbiotic foods such as yoghurts and honey (6). It has also been found, along with 4-heptanone and 2,4-bis(1,1-dimethylethyl)-phenol, in previous GC-MS based studies as a common urinary volatile metabolite. Of these 3 compounds, 4-heptanone was found more exclusively within the samples of healthy control groups over those of leukaemia, colorectal and lymphoma cancer patients in this study (7). The presence of 4-heptanone in human urine has also been shown to be caused by the oxidation of 2-ethylhexanoic acid by many plasticisers including di-(2-ethylhexyl)-phthalate (8). 1,3,5,7-Cyclooctatetraene has not been noted in studies investigating the products of metabolic processes, but has been found in fermented wheat germ after 40 days of germination at room temperature (9). This provides a potential connection with the metabolic products being absorbed in the gut. Allyl isothiocyanate is a commonly-known constituent chemical of cruciferous vegetables, and is generally added to food products as a flavour additive and preservative (10). However, it has also been found to inhibit the growth of many strains of harmful intestinal bacteria, thus affecting the gut population and potentially preventing inflammatory intestinal disease (11). Myxobacteria such as *Sorangium cellulosum*, which is found in the gut and in human faeces, have been observed producing methoxy-phenyl-oxime heavily (12). The compound itself has also been identified in the volatile content of IBS patients in a recent study on the subject (13). Polyamines such as 1,3-propanediamine

have been found to be essential components for many bacterial processes (14), and have also been detected within the human gut in previous studies (15). Carvone is well known as a food additive and natural product in mint, but has also been shown to inhibit the growth of fungal and bacterial microbes (16).

Compounds with phenyl and ethanone groups have been found in both human faeces and urine (17), in addition to being linked to breast cancer specifically through breath sample volatiles in a 2006 study (18). However, the specific molecule 1,1'-(1,4-phenylene)bis-Ethanone is not mentioned specifically in literature. 2,4-bis(1,1-dimethylethyl)-Phenol has been mentioned in a long list of volatile and heavier phenols discovered in palm (19), seed (20) and olive oils (21) by GC-MS, which have also been observed to be excreted in human urine (22). In addition, these compounds have also been linked to interactions between gut bacteria metabolism and host physiology (23), giving potential for a connection between gut pathology and the presence of oils in the host's diet leading to these phenols being found in the urine.

3.4.2. Disease Incidence of Common Peaks

Table 3.4 displays a list of all disease states represented in the urine samples analysed by GC-MS, with the compounds that had an abnormal incidence level in each group. There is a large variety of inferences that could be made on the diet or the gut microflora population of members of each group. However, a series of more thorough metabolomic investigations is required to separate the contributing sources of each compound from the complex inter-dependant relationship between diet and gut bacteria. For example, the low incidence of 2-Pentanone in Inflammatory Bowel and Coeliac Disease patients could be caused by the avoidance of probiotic foods in their diet, but this link cannot be made confidently without greater knowledge of the patients diet and background. Therefore, the

observed abnormalities in incidence rate of these candidate compounds can only be listed in this study.

Colorectal Cancer	
High Incidence	Low Incidence
1,3,5,7-Cyclooctatetraene	Oxime-, methoxy-phenyl- 1,3-Propanediamine
Irritable Bowel Syndrome	
High Incidence	Low Incidence
Isothiocyanate	
1,3,5,7-Cyclooctatetraene	
Phenol, 2,4-bis(1,1-dimethylethyl)-	
Inflammatory Bowel Disease	
High Incidence	Low Incidence
1,3-Propanediamine	Phenol, 2,4-bis(1,1-dimethylethyl)-
4-Heptanone	1,3,5,7-Cyclooctatetraene
	2-Pentanone
Healthy Volunteers	
High Incidence	Low Incidence
Oxime-, methoxy-phenyl-	Ethanone, 1,1'-(1,4-phenylene)bis
	1,3,5,7-Cyclooctatetraene
	1,3-Propanediamine
Colorectal Polyps	
High Incidence	Low Incidence
	Phenol, 2,4-bis(1,1-dimethylethyl)-
	Oxime-, methoxy-phenyl-
	1,3,5,7-Cyclooctatetraene
	4-Heptanone
	Acetone
Coeliac Disease	
High Incidence	Low Incidence
1,3-Propanediamine	Phenol, 2,4-bis(1,1-dimethylethyl)-
Oxime-, methoxy-phenyl-	2-Pentanone
1,3,5,7-Cyclooctatetraene	

Table 3.4: Compounds found at abnormal rates of incidence within samples of each disease group

3.4.3. Conclusions and Future Work

This investigation has resulted in a total of 294 urine samples from subjects in 6 different disease states being run through the Bruker Scion SQ GC-MS system, with either an ITEX or SPME pre-concentration method for greater yield of constituent chemicals. A variety of

consistent GC peaks were found between the majority samples, some of whose incidence rates that varied significantly between different disease groups. The mass spectrum from each one of these peaks was cross-referenced with standards from the NIST library and the top three classifications for consistent sets were tallied. This methodology has yielded a total of 10 likely candidate constituent chemicals of urine volatile content. Each of these compounds has been previously shown to have links with common components of the modern diet and/or gut bacteria populations. While greater detail can be seen in the changes in incidence rates between disease groups, there is little that can be inferred solely from this data without further experimentation.

However, in general the investigation could not extend far beyond an indication that volatile groups are present in urine headspace and that these seem to have some element of commonality between large numbers of samples. Only a small number of chemicals were identified by this work, and their low and inconsistent incident rates make them unreliable as biomarkers for any disease state. A high variation in colour saturation of urine samples was observed during the course of the study, which could be due to large differences in patient water excretion causing dilution to be inconsistent throughout the set.

Individual experiments should ideally be performed for each candidate compound, which control dietary and other environmental variables in order to properly ascertain the sources of these incidence rates in reference to disease. A great deal of support can also be added to these findings by running chemical standards of each likely candidate through the same GC-MS system to ensure that they are indeed presented at the same retention time. Finally, full quantitative analysis could not be completed on these samples because of the wide variation in the pH, salt concentration, and water dilution level of the urine samples. These three factors will confound the quantity of any volatiles contained within

Volatile Content of Urine Samples by Gas Chromatography – Mass Spectrometry

the urine sufficiently to limit this study to only qualitative analysis. However, a further study where the samples are saturated with salt and neutralised in pH so as to remove the effect of the first two environmental variables. This will allow some measure of quantitative analysis to be completed while the rate of diffusion of volatiles into the sample headspace will at least have been made constant.

3.5. References

- 1) Wilson, A.D., Baietto, M., Applications and Advances in Electronic-Nose Technologies. 2009, *Sensors* 9, 5099-5148.
- 2) Wahl, H.G., Hoffman, A., Luft, D., Liebich, H.M., Analysis of volatile organic compounds in human urine by headspace gas chromatography–mass spectrometry with a multipurpose sampler. 1999, *Journal of Chromatography A* 847(1-2), 117-125.
- 3) Mills, G.A., Walker, V., Headspace solid-phase microextraction profiling of volatile compounds in urine: application to metabolic investigations. 2001, *Journal of Chromatography B: Biomedical Sciences and Applications* 753(2), 259-268.
- 4) Kalapos, M.P., On the mammalian acetone metabolism: from chemistry to clinical implications. 2003, *Biochimica et Biophysica Acta – General Subjects* 1621(2), 122-139.
- 5) Galassetti, P.R., Novak, B., Rose-Gottron, C., Cooper, D.M., Meinardi, S., Newcomb, R., Zaldivar, F., Blake, D.R., Breath ethanol and acetone as indicators of serum glucose levels: an initial report. 2005, *Diabetes Technol Ther* 7(1), 115-123.
- 6) Vitali, B., Ndagijimana, M., Cruciani, F., Carnevali, P., Candela, M., Guerzoni, M.E., Brigidi, P., Impact of a Synbiotic Food on the Gut Microbial Ecology and Metabolic Profiles. 2010, *BMC Microbiology* 10(4), 10.1186/1471-2180-10-4.
- 7) Rizzello, C.G., Nionelli, L., Coda, R., De Angelis, M., Gobbetti, M., Effect of sourdough fermentation on stabilisation, and chemical and nutritional characteristics of wheat germ. 2010, *Food Chemistry* 119, 1079-1089.
- 8) Walker, V., Mills, G.A., Urine 4-heptanone: a β -oxidation product of 2-ethylhexanoic acid from plasticisers. 2001, *Clinica Chimica Acta* 306(1-2), 51-61.
- 9) Silva, C.L., Passos, M., Camara, J.S., Investigation of urinary organic metabolites as potential cancer biomarkers by solid-phase microextraction in combination with

- gas chromatography-mass spectrometry. 2011, *British Journal of Cancer* 105, 1894-1904.
- 10) Jiao, D., Ho, C.T., Foiles, P., Chung, F.L., Identification and quantification of the N-acetylcysteine conjugate of allyl isothiocyanate in human urine after ingestion of mustard. 1994, *Cancer Epidemiology, Biomarkers & Prevention* 3, 487-492.
- 11) Kim, M.G., Lee, H.S., Growth-inhibiting activities of phenethyl isothiocyanate and its derivatives against intestinal bacteria. 2009, *Journal of Food Science* 74(8), 467-471.
- 12) Xu, F., Tao, W., Sun, J., Identification of volatile compounds released by myxobacteria *Sorangium cellulosum* AHB103-1. 2011, *African Journal of Microbiology Research* 5(4), 353-358.
- 13) Ahmed, I., Greenwood, R., de Lacy Costello, B., Ratcliffe, N., Probert, C., An investigation of Fecal Volatile Organic Metabolites in Irritable Bowel Syndrome. 2013, *PLOS ONE* 8(3), e58204.
- 14) Lee, J., Sperandio, V., Frantz, D.E., Longgood, J., Camilli, A., Phillips, M.A., Michael, A.J., An Alternative Polyamine Biosynthetic Pathway Is Widespread in Bacteria and Essential for Biofilm Formation in *Vibrio cholera*. 2009 *J Bio Chem* 284(15), 9899-9907.
- 15) Murray, K.E., Shaw, K.J., Adams, R.F., Conway, P.L., Presence of N-acyl and acetoxy derivatives of putrescine and cadaverine in the human gut. 1993, *Gut* 34, 489-493.
- 16) Jay, J.M., Rivers, G.M., Antimicrobial activity of some food flavouring compounds. 1984, *J Food Safety* 6(2), 129-139.
- 17) Sato, H., Hirose, T., Kimura, T., Moriyama, Y., Nakashima, Y., Analysis of Malodorous Volatile Substances of Human Waste: Feces and Urine. 2001, *J Health Sci* 47(5), 483-490.

- 18) Phillips, M., Cataneo, R.N., Ditkoff, B.A., Fisher, P., Greenberg, J., Gunawardena, R., Kwon, C.S., Tietje, O., Wong, C., Prediction of breast cancer using volatile biomarkers in the breath. 2006, *Breast Cancer Res Tr* 99 (1), 19-21.
- 19) Sabrina, D.T., Gandahi, A.W., Hanafi, M.M., Mahmud, T.M.M., Nor Azwady, A.A., Oil palm empty-fruit bunch application effects on the earthworm population and phenol contents under field conditions. 2012, *Afr J Biotechnol* 11(19), 4396-4406.
- 20) Kumar, N.N., Ramakrishnaiah, H., Krishna, V., Deepalakshmi, A.P., GC-MS analysis and antimicrobial activity of seed oil of *Broussonetia Papyrifera* (L.) vent. 2015, *Int J Pharm Sci Res* 6(9), 3954-3960.
- 21) Tuck, K.L., Hayball, P.J., Major phenolic compounds in olive oil: metabolism and health effects. 2002, *J Nutr Biochem* 13(11), 636-644.
- 22) Caruso, D., Visioli, F., Patelli, R., Galli, C., Galli, G., Urinary excretion of olive oil phenols and their metabolites in humans. 2001, *Metabolism* 50(12), 1426-1428.
- 23) Nicholson, J.K., Holmes, E., Kinross, J., Burcelin, R., Gibson, G., Jia, W., Pettersson, S., Host-Gut Microbiota Metabolic Interactions. 2012, *Science* 336 (6086), 1262-1267.

4. Commercial Electronic Noses for Detection of Colorectal Cancer

4.1. Scope and Objectives

It was decided to begin comparative investigation of electronic nose technologies in detecting chemical changes between urine samples of healthy and diseased individuals using devices that are well-established and currently available commercially. Commercial electronic noses have already been shown to be able to detect odour changes for a wide range of applications, including food monitoring (1, 2) and explosives detection (3, 4). There were two commercial electronic nose technologies available for study - the AlphaMOS Fox 4000 (France) electronic nose and the Owlstone Lonestar (UK) Field Asymmetric Ion Mobility Spectrometer (FAIMS).

It was proposed that urine samples should be used as the test biological media due to an increased patient acceptability rate compared to use of stool samples (5), as well as better storage stability when compared to breath samples (6). The test cohort included known patients of CRC as well as controls that encompass both individuals known to be healthy, and those known to be suffering from a non-inflammatory lower gastro-intestinal disease such as IBS. This provided a test criteria that illustrates the ability of the commercial instruments to distinguish CRC from disease states that are either non-symptomatic, or those that seem similar in symptoms without further evidence.

4.2. Fox 4000 Electronic Nose

4.2.1. Methods and Materials

The Fox 4000 system (7) comprises a fully integrated CombiPAL HS-100 auto-sampler with 2.5 mL gas syringe. The air supply for the Fox 4000 is provided by a Parker Balston HPZA-7000 Zero Air Generator, with a gas purity requirement of <0.05 ppm concentration of total

hydrocarbons and capable of supplying multiple machines with a total flow rate capacity of up to 7 L/min.

The electronic nose is composed of an array of 18 electro-resistive metal oxide gas sensors with sensitivities in the parts-per-million to parts-per-billion range. Five of the first sensors have been doped in P-type and as such have an excess of electron charge carriers that are transferred to a target chemical. This interaction manifests itself as an increase in electrical resistance. The metal oxide semiconductor sensors that are constructed from platinum and titanium oxides give them an N-type response to sensitive chemicals by having a detriment of electron charge carriers. These were taken from targets and reduce the resistance of the sensors. These sensors are housed in a total of three chambers that are connected on the sample flow path in series with each-other. A time offset in their response to samples is present, which is compensated for and removed by the post-processing algorithm. A description of the names and types of each sensor in the Fox 4000 are included in Table 4.1.

Classes	Name	Doping Type
Chromium – Titanium based	LY2/LG	N
	LY2/G	P
	LY2/AA	P
	LY2/GH	P
	LY2/gCTI	P
	LY2/gCT	P
Titanium based	T30/1	N
	T70/2	N
	T40/2	N
	T40/1	N
	TA/2	N
Platinum based	PA/2	N
	P30/1	N
	P40/2	N
	P30/2	N
	P10/1	N
	P10/2	N
	P40/1	N

Table 4.1: List and description of sensors included in the Fox 4000 electronic nose (7)

The auto-sampler allowed for the carriage of two racks of samples, as well as incubation of up to 6 samples and injection into a port at the top of the machine using the installed Hamilton Gastight 1200 μ L gas syringe. The specific sensors in the Fox 4000 were chosen in order to detect the presence of a wide range of gases and volatile compounds, making it a versatile overall system. The raw output of voltage changes across these sensors is processed by hardware housed within the machine, before being transferred via serial communication to the custom-made AlphaSoft program (AlphaMOS v12.36) on a desktop PC and saved into grouped data files. This data can then be viewed from the PC software, or exported into a text format that can be analysed by separate data analysis package. This same program also allows the user to control most of the variables involved in the process of sample preparation and injection through the instrument, including temperatures

Commercial Electronic Noses for Detection of Colorectal Cancer

(sample and sensor chamber), flow rates and the timing for incubation, injection and sensor detection. A photo of the machine is shown in Figure 4.1.

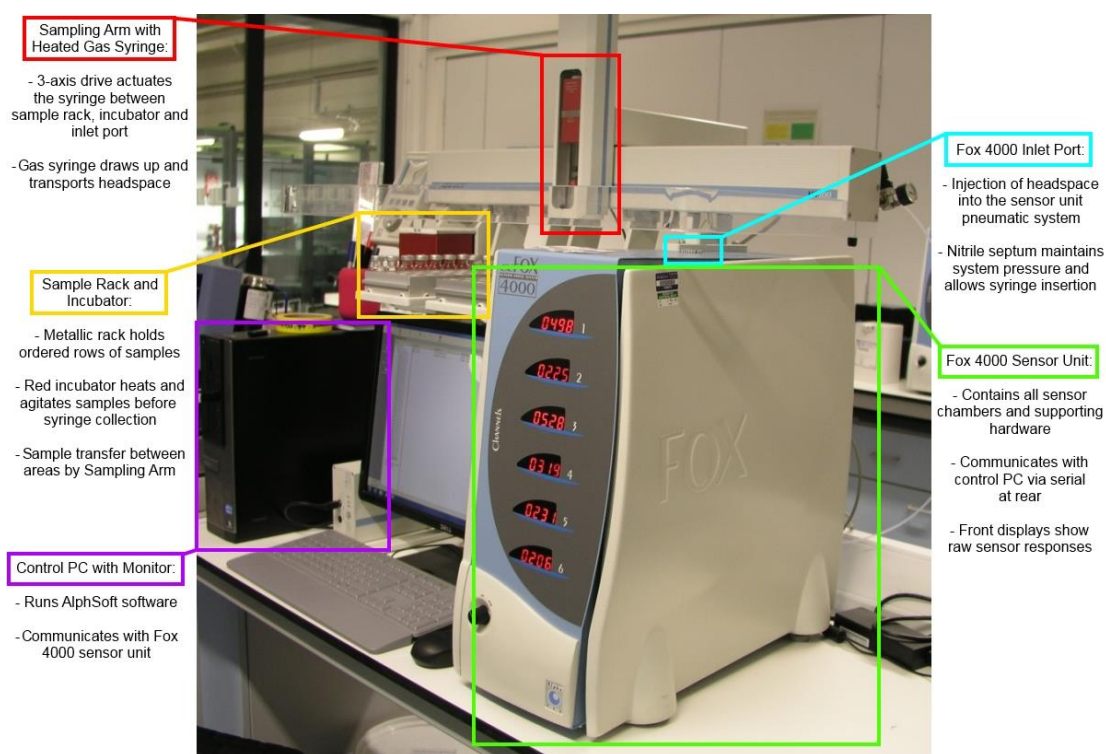


Figure 4.1: Photograph of the Fox 4000 in the laboratory

4.2.2. Urine Samples

Urine samples from pre-diagnosed patients of CRC and IBD were recruited from those being treated at the University Hospital of Coventry and Warwickshire. A total of 93 patient samples were collected, with 38 patients with CRC, 36 with IBS, and 19 volunteers recruited from healthy staff members. The CRC patients were characterised as such by a “gold standard” of positive colonoscopy discovery of carcinomas with a diameter of over 8 mm, while IBS patients were characterised by diagnosis from a display of confirmed symptoms without any detectable pathology, inflammatory or otherwise. Healthy volunteers were only characterised by their lack of diagnosis for any digestive diseases. Suitable ethical approval has been agreed on for samples of this nature, with the Ethical Approval Number

09/H1211/38. The demographics of the samples for the Fox 4000 study are shown in Table 4.2. Once collected, these urine samples were stored under similar conditions to those detailed in Section 3.2.2.

	CRC	IBS	Controls
Number	38	36	19
Mean Age	70	48	41
Male %	70	11	70
Mean BMI	27	28	24
Current Smokers	6.7%	10%	6.7%
Alcohol - average units per week	7.3	2	9.2

Table 4.2: Patient demographics for urine sample cohort run through the Fox 4000

4.2.3. Experimental Methods

4.2.3.1. Method Development

Some initial comparative tests were conducted by previous students in order to find reasonable values for some of the controllable variables on the Fox 4000. The sample temperature on the Fox 4000 was varied from 40 °C at intervals of 10 °C, up to a maximum of 90 °C in one study using volunteer urine samples, showing a shift in Discriminant Function results with increasing sample temperature. Overall group variability increased with temperature as well; it was hypothesised that this was due to a higher number of volatile compounds being released. However, the humidity levels of the samples also increased with temperature. As the prerogative of this study was to limit variation within groups while trying to maximise inter-group changes, a lower overall temperature of 40-50 °C was chosen. The optimisations of other variables were investigated in similar studies, resulting in a decided sample volume of 5mL, injection volume of 1000uL, and incubation time of 5 minutes. Please see Figure 4.1 for description of the Fox 4000 setup.

4.2.3.2. Proposed Method

Chemical standards were used to verify sensor performance at regular intervals throughout the lifetime of the Fox 4000. An example of this verification for benchmarking sensitivity to three volatile solutions can be seen in Section 4.2.5. Samples were made by taking reagent grade acetone, 1-propanol and iso-propanol and dissolving them each in a separate volume of water, to the respective concentrations of 0.1%, 0.1% and 0.05%. 1 mL aliquots of these solutions were transferred into a total of 10 glass vials of 10 mL internal volume, with 3 each of acetone and iso-propanol and 4 of 1-propanol.

These were crimp sealed with septum lid for use in the Fox 4000, and loaded into the first 10 positions in the HS-100 autosampler rack. A particular diagnostic method was used to run these samples through the Fox 4000, though its execution in terms of machine conditions is very similar to the method described for the urine samples as detailed later in this section. Each sample was individually heated for 5 minutes at 40 °C in order to produce sufficient headspace (similar to the FAIMS method). 1 mL of this headspace was extracted and introduced to the sensor array at a flow rate of 150 mL/min for 180 seconds. The corresponding responses were measured and sent to the AlphaSoft software on PC. Purge cycles, where sensors are heated to 150 °C in the presence of clean dry air, were also run after each headspace sample as part of the instrument's standard autosampling routine for returning the sensor output to baseline.

Urine samples were initially thawed overnight at 5 °C in a laboratory refrigeration unit, and then divided into separate 5 mL aliquots for analysis in each of the instruments employed in this study. One 5 mL aliquot was pipetted into a 10 mL glass vial and sealed with a crimp lid for analysis using the Fox 4000. These aliquots were arranged in groups of 20 onto sampling racks for use with the HS-100 autosampler, including examples of all disease groups dispersed randomly in each group in order to prevent a false classification based on

sensor drift during the course of the study. Each group of samples was also run for 3 repeats through the system in order to collect the maximum amount of volatile information. The method used within the Fox 4000 for each sample was identical to that described above for the reference samples.

Figure 4.2 illustrates an example of the raw sensor output of the Fox 4000 sensors upon introduction to a urine sample, in terms of the change in resistance over the baseline. The negative initial peaks from the N-type devices and the positive from the P-types can be seen, as well as the overall trend back to original resistance values after the sample has been washed away. These response measurements are where the features are extracted for combining to form the discriminant functions of a Linear Discriminant Analysis (LDA) plot. It can be seen that the response level of the sensors varies a great deal, even in proportion to their baseline resistance values. This shows a variety of different sensitivities to the gaseous and volatile groups present in the urine headspace samples. The level of response to the samples gives an indication of the suitability of each sensor to distinguishing between disease groups, but is not necessarily definitive as even a minute response from a particular sensor may be a distinctive feature for a group of samples.

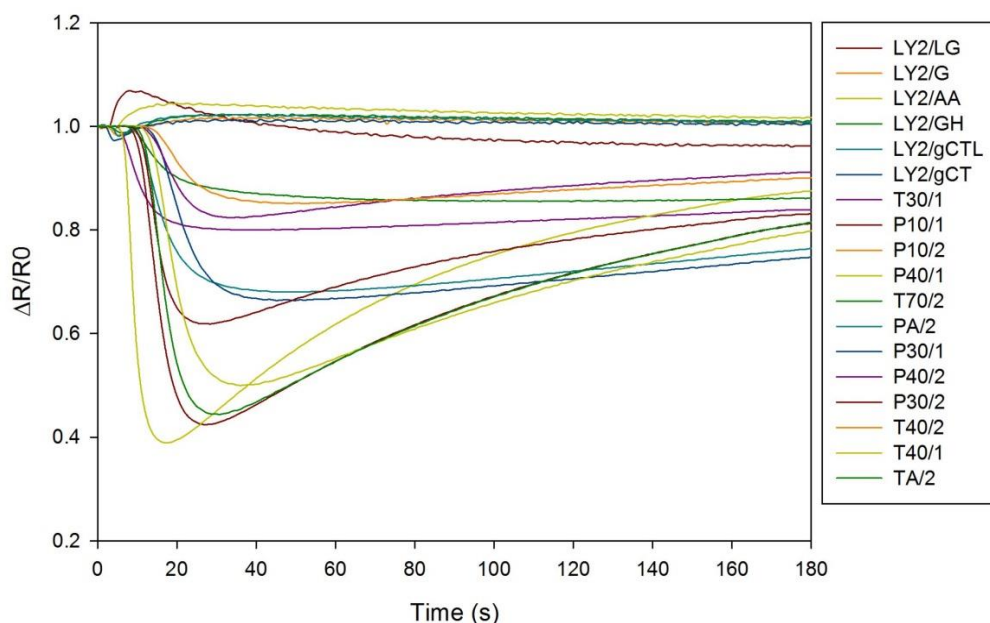


Figure 4.2: Raw sensor output data from a urine headspace sample

4.2.4. Statistical Methods

For the electronic nose analysis, the raw data was extracted using Alphasoft and exported as tab delimited text files for processing, to be analysed in Multisens Analyzer (JLM Innovations, Germany). The reference data was analysed using a classification technique named Principle Component Analysis, which takes a number of features from the sensor outputs and uses them as individual components for separation. Any particular feature that can be extracted from an individual sensor output could be used as a component, such as the maximum value or area underneath the curve.

The urine data was classified using a more complex method named Linear Discriminant Analysis, a technique which actively aims to increase clustering of distinct groups rather than passively presenting data. Features are also extracted from sensor outputs in this method. The first of these used in this example was “Sig-base3” or the maximum deviation of the signal to the baseline in the response curve, averaged over three values. It is described in Equation 4.1, where x is the response and the baseline is assumed to be the

values taken at the earliest point i . The maximum area underneath the sensor output curve (“AreaMax”) is also extracted as used for separation, and is described in Equation 4.2 with x once again being the response over the whole of the curve (point i from 1 to i_{max}). The final feature used is the time taken t for the response x to reach maximum and then decay to half of that value (“T50”) shown in Equation 4.3.

$$Sig - Base3(x) = \left(\frac{\sum_{max-1}^{max+1} x}{3} - \frac{\sum_{i=1}^3 x}{3} \right) \quad (4.1)$$

$$AreaMax(x) = \sum_{i=1}^{i_{max}} x_i \quad (4.2)$$

$$T50(x) = t\left(\frac{x_{max}}{2}\right), \text{ where } t > t_{x_{max}} \quad (4.3)$$

Each of these features was ranked in terms of their ability to maximise separation between distinct disease groups and minimise spread within them. They were each multiplied by a unique conversion factor proportional to their scores in the above ranking, and then a number of the converted features were combined to create (n-1) discriminant functions (where n is the number of disease groups). The classification was then drawn up as a (n-1)-dimensional graph, with the ‘x’ and ‘y’-value of each sample being their scores for the two discriminant functions. The summing function for features to create a discriminant function “g(x)” is shown in Equation 4.4, where w_0 is an initial offset, x_i is the ‘ith’ feature used in the function, ‘ w_i ’ is its loading factor (as determined by its importance in separation of different groups) and ‘d’ is the total number of features used in the function.

$$g(x) = w_0 + \sum_{i=1}^d w_i x_i \quad (4.4)$$

A 3-group LDA classification was made for all of the disease groups in this study, including CRC, IBS and healthy volunteers. A 2-group classification was also made for the CRC and IBS samples as this gives a reasonable reflection of a situation presented in the clinical setting, with individual patients coming in complaining of similar symptoms.

Individual samples were then removed from the actively-clustered ‘training set’ and re-introduced as unknowns to test their distinction as CRC samples against the negative controls of IBS. This second classification was achieved by passively executing the same discriminant function calculations on them. These individual unknowns were then re-classified using a (n-1) K-nearest neighbour (KNN) method, which assigns the unknown a group based on the groups of the three known samples that are closest to it. This re-classification method was repeated for every individual sample in the study, with subsequent re-introduction as a known in the “training set”. The sensitivity and specificity were then calculated for this technique, by first comparing the re-classified disease group assigned to the introduced unknown to the original group to which it actually belongs. This comparison would yield a result for each individual sample as a “true positive” (TP), “false positive” (FP), “false negative” (FN) or “true negative” (TN) depending on its actual class and the one that it had been re-assigned to as an unknown. The numbers of each of these markers were tallied, with the totals being used to calculate sensitivity and specificity of the LDA classification to CRC detection using Equations 4.5 and 4.6 below.

$$Sensitivity = \frac{TP}{TP + FN} \quad (4.5)$$

$$Specificity = \frac{TN}{TN + FP} \quad (4.6)$$

4.2.5. Volatile Sample Results

The results of the volatile reference data are shown below, with graphs showing PCA scores of the 1 mL acetone, 1-propanol and iso-propanol samples. Subsets of these samples were analysed that were run through the Fox 4000 on the 8th May 2013 (black), the 4th April 2014 (red), and the 23rd April 2015 (green), with approximately 1 year time periods between them. The average sensor responses to each of the volatiles at each year-point was calculated and arranged into polar plots, which show their ability to produce unique response upon introduction of different volatile groups. Also, the variations between the plots on these graphs can give an indication on how the sensors have drifted over the course of the 2-year time period. Figure 4.3 shows a degree of drift from all of the sensor response to acetone, with some extreme examples such as T30/1 and T70/2. Both of these examples show a particularly heavy drift between 2014 and 2015. Many other sensors, such as P10/1, PA/2 and P30/1, seem to have drifted away from their 2013 levels after the first year, before later returning to these original baselines.

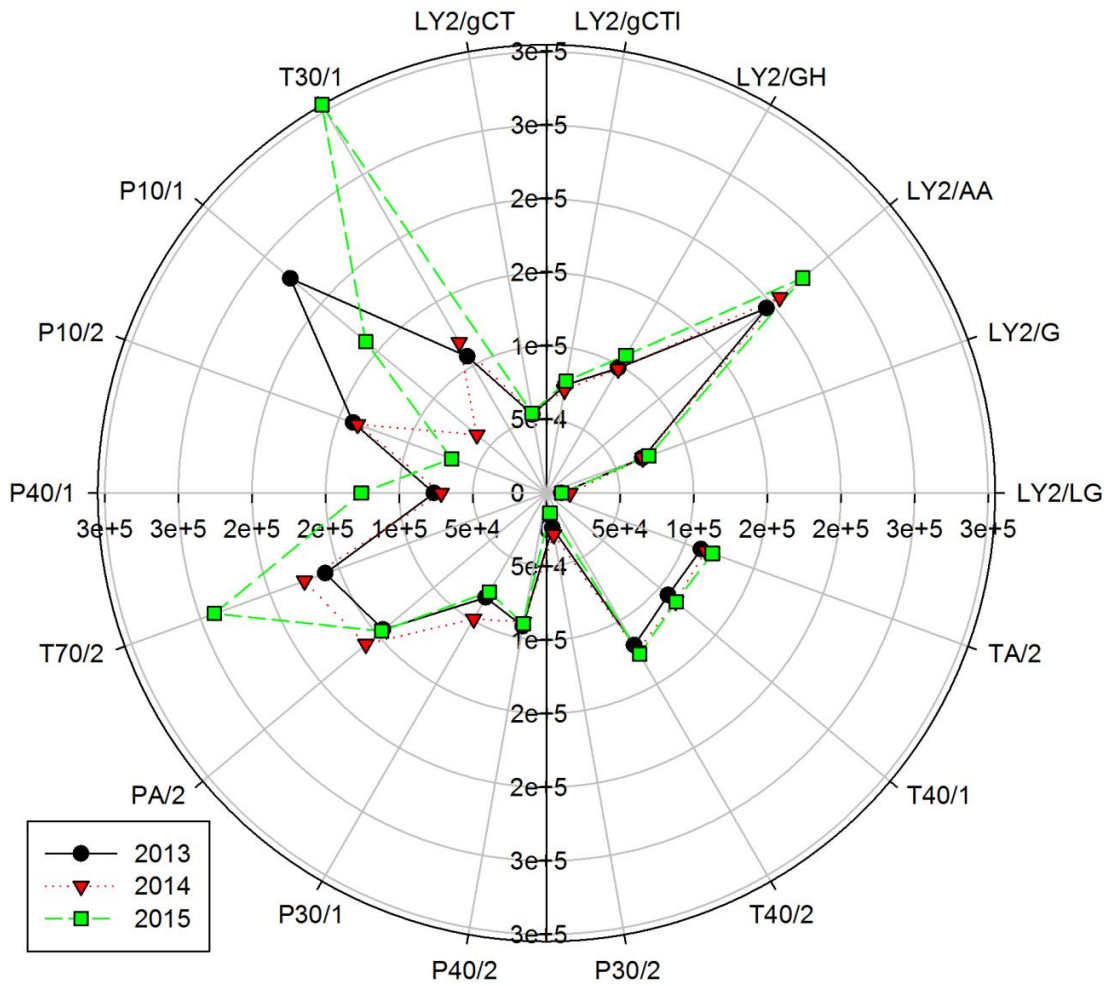


Figure 4.3: Average sensor responses to acetone between 4th May 2013 and 23rd April 2015

Figure 4.4 shows the average sensor response data to isopropanol across the same time period, with a reasonably different response profile to that shown in Figure 4.4. However, the sensors present a very similar set of drifts year-to-year to the above, with variation that looks to be proportional to response magnitude. Once again, T30/1 and T70/2 have changes in response which are uni-directional and extreme, while other sensors seem to have shifted back and forth over the course of the 2-year period.

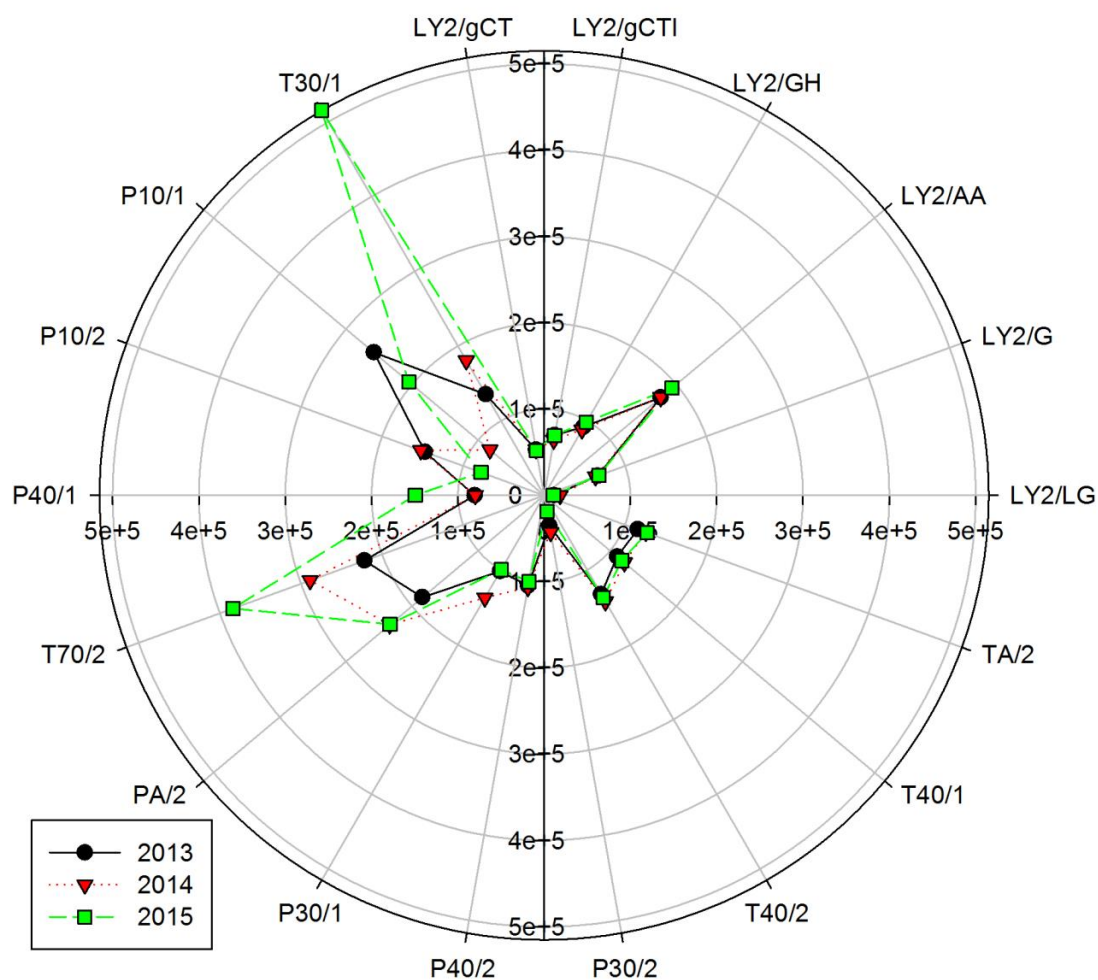


Figure 4.4: Average sensor responses to isopropanol between 4th May 2013 and 23rd April 2015

Finally, the average responses of the sensors to 1-propanol from 2013 to 2015 are displayed on the polar plot in Figure 4.5. The levels shown in this figure are very similar to those shown in Figure 4.4 for isopropanol, with only very subtle differences that can be seen in sensors such as T70/2 and P40/2. This is to be expected, as the two chemicals in question have an identical composition with a variation found in their molecular structure. Once again, similar trends can be seen to those described above for Figures 4.4 and 4.5. These findings add empirical evidence to the premise that different volatiles and gases will produce unique response patterns from the sensors. However, support is also given to the

fact that the sensors have drifted in a significant manner over the course of a 3-year period. This highlights the need for accurate baseline readings with standard samples at regular intervals in order for any parallels to be made between samples across any month-year scale time period.

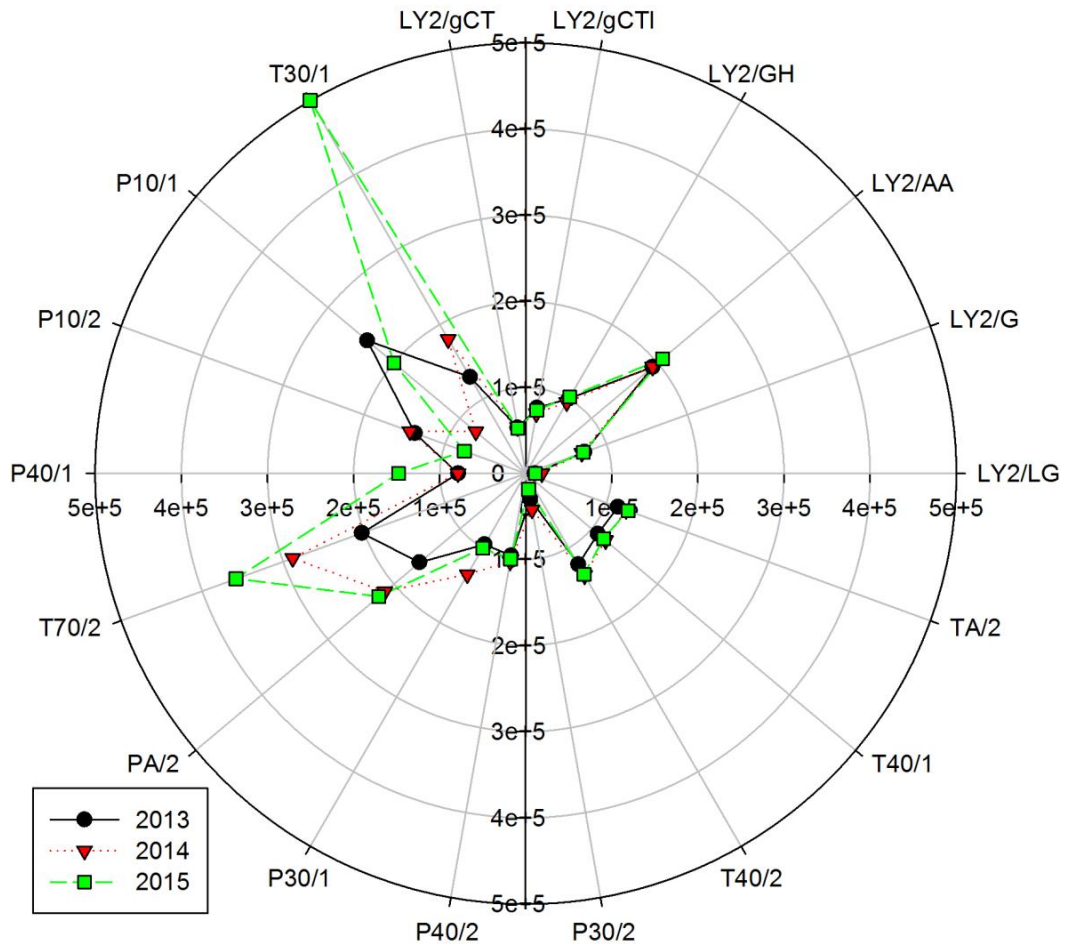


Figure 4.5: Average sensor responses to 1-propanol between 4th May 2013 and 23rd April 2015

4.2.6. Urine Sample Results

The full 3-group LDA plot for these samples on the Fox 4000 is shown in Figure 4.6, with CRC samples shown as black circles, IBS as red triangles and volunteers as green squares. A total of 30 features were used for this classification, which is significantly less than the

samples included in the relevant disease groups in order to maintain some statistical viability. The groups in this plot are not very well-defined, with some degree of clustering but with a large amount of overlap in the space occupied by more than one disease state. The poor definition of distinct groups is characterised in the centre of this plot, where there are many outliers that are located very near to several other samples from different disease groups. This large spread within groups could be expected in the volunteer samples, as it has been noted in previous studies by this research group that the variation in the healthy state is actually much wider than in any disease (8). This wide variation in sample output is also an expected quality in the IBS samples, as the disease itself is merely a collection of symptoms relating to abnormal function of the gastro-intestinal tract with no known underlying linked root cause. The classifications of samples in this disease group have not been isolated to a single type of IBS, such as constipation-based (IBS-C), diarrhoea-based (IBS-D) and alternating (IBS-A) symptoms. The wide variety in response characteristics from CRC samples is most unexpected in the classification in Figure 4.6, and extends far into the central areas of the two other disease groups with very little distinction from them. However, all three disease states do occupy a mildly discriminate location within the LDA plot.

The loadings of individual features in the overall discriminant functions for this LDA classification were analysed to gain insight into which of the sensors were most instrumental in separating the three disease groups from each-other. The highest contributor to this separation by far was the "T50" time of the P-type device LY2/G, which was multiplied by factors of 37.4 and 7.63 higher than the nearest runner-up in contributing to separation on Discriminant Function 1 and 2, respectively. This sensor is sensitive to almost all volatile compounds, indicating that the total concentration of chemicals is higher in some disease states than others. The next largest contributors to LDA

separation were the “Sig-base3” features of LY2/AA, LY/gCT, T40/1 and TA/2, which include a pair of both P-type and N-type devices each. Most of these had a slightly greater contribution to Discriminant Function 2, but were all instrumental in achieving a form of separation in this classification. Features that did not contribute in any meaningful way to separation included the “T50” values for all of the other sensors in the array aside from P10/2, P30/1 and TA/2, and so these were removed from the classification in order to optimise the number of features included. A number of “AMax” values were also omitted from the scores in the classification, including those from LY2/G, LY2/AA, LY2/GH, LY2/gCTI, LY2/gCT, P10/1, P40/1, T70/2, PA/2, and P40/2. This list consists of a variety of both P- and N-type sensors.

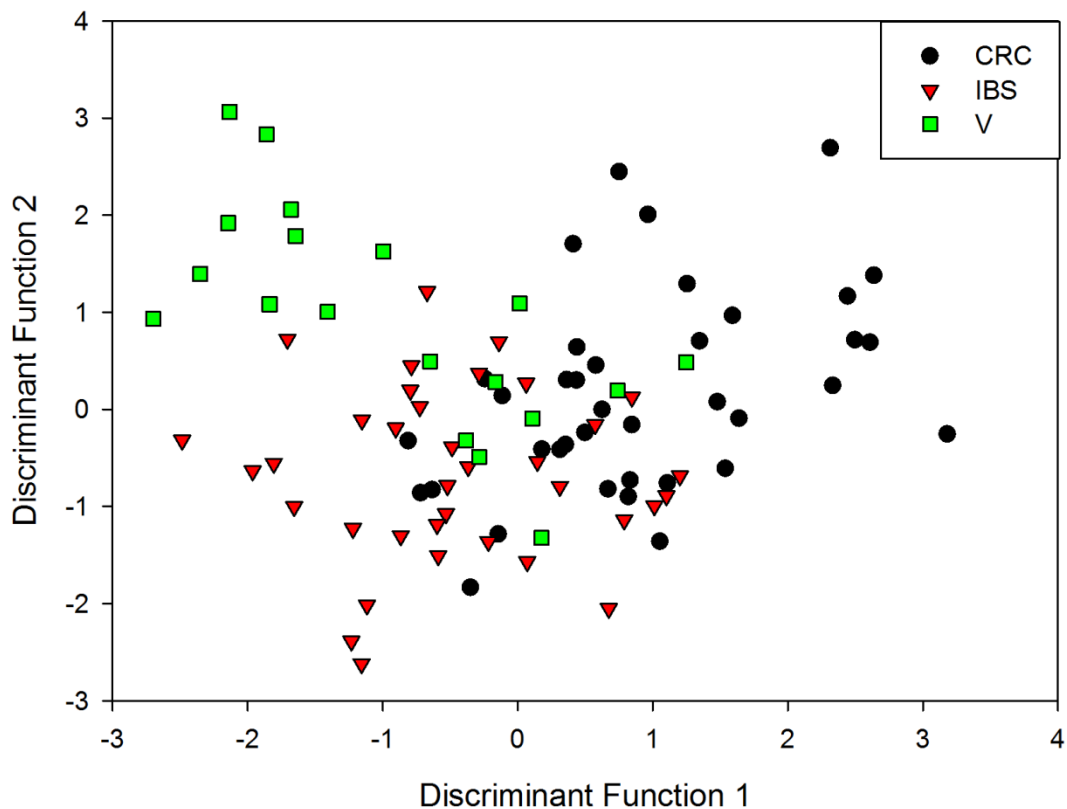


Figure 4.6: LDA plot of CRC against IBS and volunteer samples run through the Fox 4000

Figure 4.7 shows a 2-group LDA classification using only the IBS and CRC samples run through the Fox 4000, illustrated as a box plot showing the quartiles and outlier samples are located for each group on a single discriminant function. This was used as a major contributing factor in deciding the performance of this electronic nose in suitability for application, as this accurately reflects a clinical decision that must be made on patients entering with similar symptoms. A poor level of distinction can be seen on this Figure for this classification as well, with the outliers of both groups overlapping into the median values of each-other, and a large number of CRC samples extending along the entire 2-dimensional region occupied by the IBS samples. Similar to the previous classification shown in Figure 4.6 there is an unexpectedly wide variation in the response to CRC samples in this study. The variation in CRC is significantly larger than that shown by the IBS samples, which would already be expected to be substantial due to the issues in its clinical classification described above.

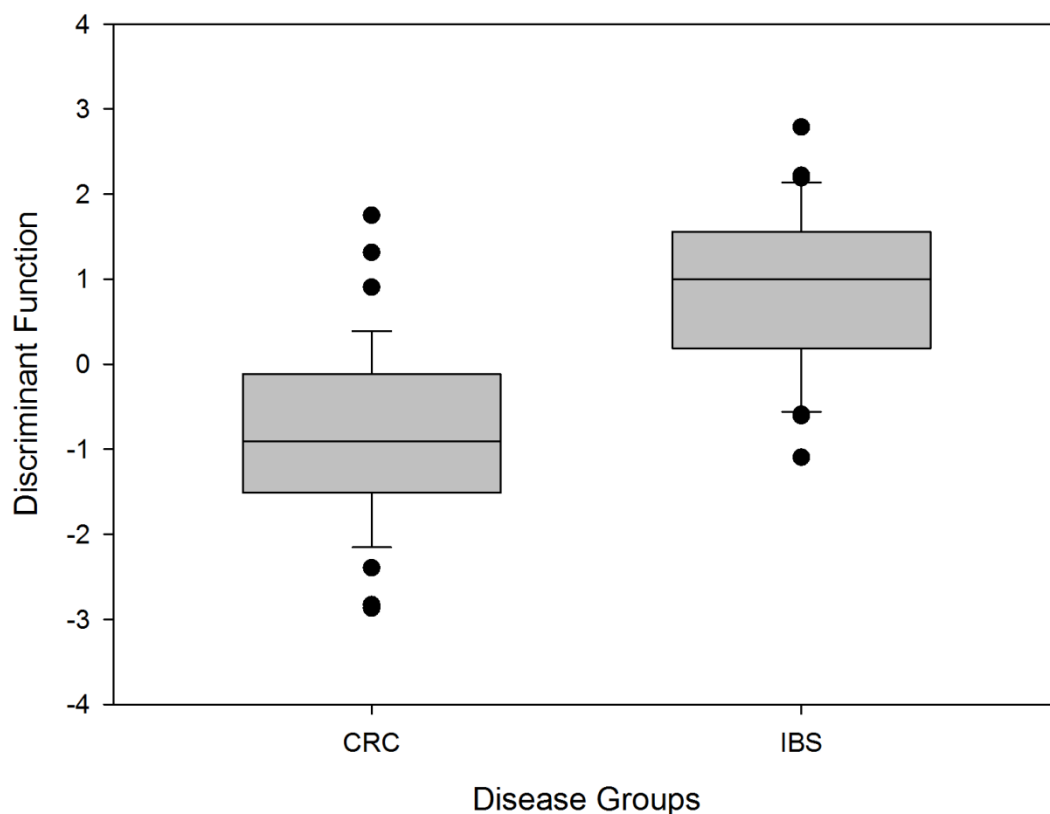


Figure 4.7: LDA plot of CRC against IBS samples run through the Fox 4000

The poor degree of separation and clustering of the disease states in the 2-group classification is reflected in the sensitivity and specificity to CRC against IBS determined by re-classification of samples into this same classification. The re-classifications and calculations were undertaken in the manner described above in Section 4.2.4. The overall sensitivity to CRC was found to be 54.1% with an associated specificity of 48.6%, which is shown to be particularly poor from the proximity of these levels to the 50% seen by random chance events. Previous studies have shown a better degree of separation between similar groups when the sample size in each class was smaller, such as one 2013 study conducted by this research group of CRC, volunteer and ulcerative colitis samples (9). However, the performance of these sensors in separation of urine samples in these two groups is clearly not very significant when the sample sizes are scaled up further.

The poor re-classification success rate described above is associated with the average response of each sensor to a CRC and IBS sample and the difference between these, as is illustrated as a polar plot in Figure 4.8. It can be seen that the average peak response is very similar from all sensors to a sample belonging to either of these disease groups. The only significant change that can be seen on Figure 4.8 is from P30/1, which must have been highly variant within groups as well due its lack of inclusion in the most significant contributing features in group distinction described above.

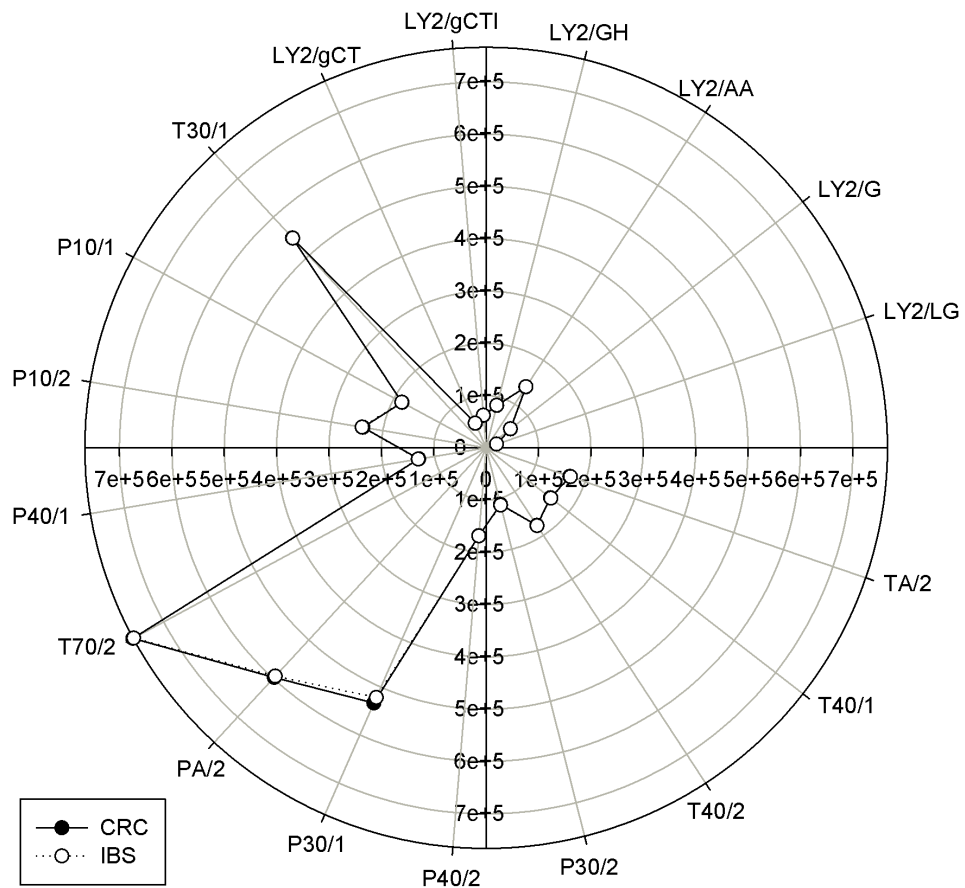


Figure 4.8: Polar plot of average response from each sensor to CRC and IBS samples

The low success rate for re-classification could be attributed to a lack of focus on the response to biologically-produced gases and volatiles in sensor sensitivities within the Fox

4000. This electronic nose has been designed for versatility in detection of volatiles present in a wide variety of different applications (7), and the design has not been tailored to maximise distinction of biological media. The results in Section 4.2.5 also show experimental proof of long-term drift of the sensors, which could be associated with degradation in their sensitivity to particular gases and volatiles. This set of samples was run through the Fox 4000 in October and November of 2013, which is very early on in the timescale of the data shown in Section 4.2.5. However, the Fox 4000 had been in operation since 2011, and so there would likely have been previous degradation of sensors.

Degradation of the urine samples must also be considered as a potential cause for the lack of distinction between the three disease states. The samples used in this investigation were collected over the course of a number of years, which could introduce a variation in degradation level within disease groups even at a storage temperature of -80°C . However, due to the slow rate of collection for these urine samples from a lack of donor patients, it was necessary to use the samples that were available for these investigations.

4.3. Owlstone Lonestar FAIMS

4.3.1. Methods and Materials

The FAIMS system incorporated an Owlstone Lonestar detection unit, as well as an ATLAS sampling unit and mass flow control (MFC) unit in order to accurately control the sample preparation variables (pictured in Figure 4.9). The air supply for all of these is from the same Zero Air Generator as described in Section 4.2.1. The Lonestar itself has a radioactive Ni-63 source, which bombards sample gases so that they can be ionised and sent into the detection chamber (10). The detection plates run sweeps of voltage intensity and take readings, which are then arranged into a single, 52,224-point 3-dimensional matrix from within a Labview-based software program. These matrix files are also saved onto the in-

built computer housed in the Lonestar, where they can be exported into usable formats for analysis. Similar to the Fox 4000, users can also control a wide variety of parameters using the software such as split and make-up flow ratios, as well as temperatures of the sample chamber and transfer lines. Figure 4.9 shows a labelled photograph of the FAIMS system, with brief descriptions of the units involved and what their functions are. The FAIMS method development and urine-based diagnostic investigations were completed in conjunction with other members of the FAMISHED research groups, as acknowledged in the resulting paper published in PLOS ONE (11).

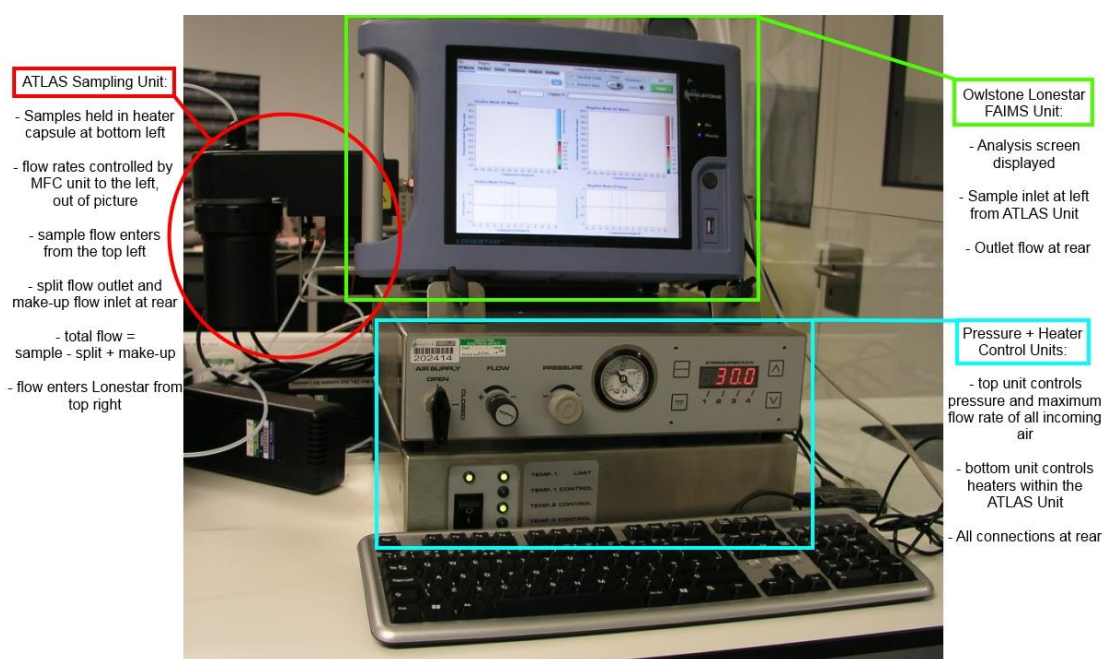


Figure 4.9: Labelled photograph of the Owlstone Lonestar setup in the laboratory

4.3.2. Urine Samples

The cohort of samples used for characterising the Lonestar only included a total of 83 known CRC patients and 50 healthy volunteer controls, the majority of which are separate from those used in the Fox study. This variation in sample populations, along with the difference in time between the executions of these two studies, means that they must be considered as separate investigations for the purposes of comparison. These samples were

collected under the same ethical approval as mentioned in Section 4.2.2. The demographics of the samples for the Lonestar urine samples are in Table 4.3. Frozen storage methods for these samples are similar to those described in Section 3.2.2.

	CRC	Controls
Number	83	50
Mean Age	68	47
Male %	64	42
Mean BMI	27	26
Current Smokers	6%	1.5%
Alcohol – average units per week	5.3	3.8

Table 4.3: Patient demographics for urine sample cohort run through the Owlstone

Lonestar FAIMS

4.3.3. Experimental Methods

4.3.3.1. Method Development

Similar initial studies were done with the Lonestar to determine experimental method variables, with optimal values for sample incubation coming in line with what was found for the Fox 4000. In addition, a short investigation was performed to discover the minimum split ratio between sample air flow and that of make-up air, as there had been previous issues with system contamination when the full 2L/min required for the IMS unit was sent over the sample. This resulted in an optimal sample air flow of 500 mL/min, incorporating a 3:1 split between sample and make-up. Please see Figure 4.9 for description of the Lonestar setup.

4.3.3.2. Proposed Method

A similar 5 mL aliquot to that described in Section 4.2.3.2 was transferred into a 22 mL glass vial by pipette for analysis in the Lonestar FAIMS (Owlstone) and placed in the ATLAS sampling system attached to the instrument. The sample was then heated to 40 °C for a period of 5 minutes to produce a reasonable headspace of volatiles. This headspace was

extracted, mixed with a make-up flow of clean air at a ratio of 1:3, and run through a Lonestar FAIMS using an attached ATLAS sampling unit (see Figure 4.9). The headspace of each sample was used to produce three full matrices of FAIMS data from the instrument, and blanks of clean, dry air were run both before and after each urine sample to ensure that the baseline response was returned.

The raw output of the Lonestar comes in the form of a pair of 3-dimensional matrices that originate from the output of the positive and negative terminals of the ion mobility spectrometer. Figure 4.10 shows an example of the positive terminal array matrix produced by introduction of a CRC patient urine sample. Initial sample introduction yields the results shown in the lower half of the Figure, without any real separation of the ions. As the level of dispersion field increases, however, different distinctive groups of gases and volatiles are separated into individual “plumes” based on their mobility (a characteristic determined by their charge and mass). Each of the urine samples will have a set of three matrices that were taken from consecutive runs of measurement directly after each-other. It was found that the 2nd of these matrices produced the greatest separation of classes in the subsequent classification plots, and so must provide the largest amount of relevant information for distinction of CRC patients from controls.

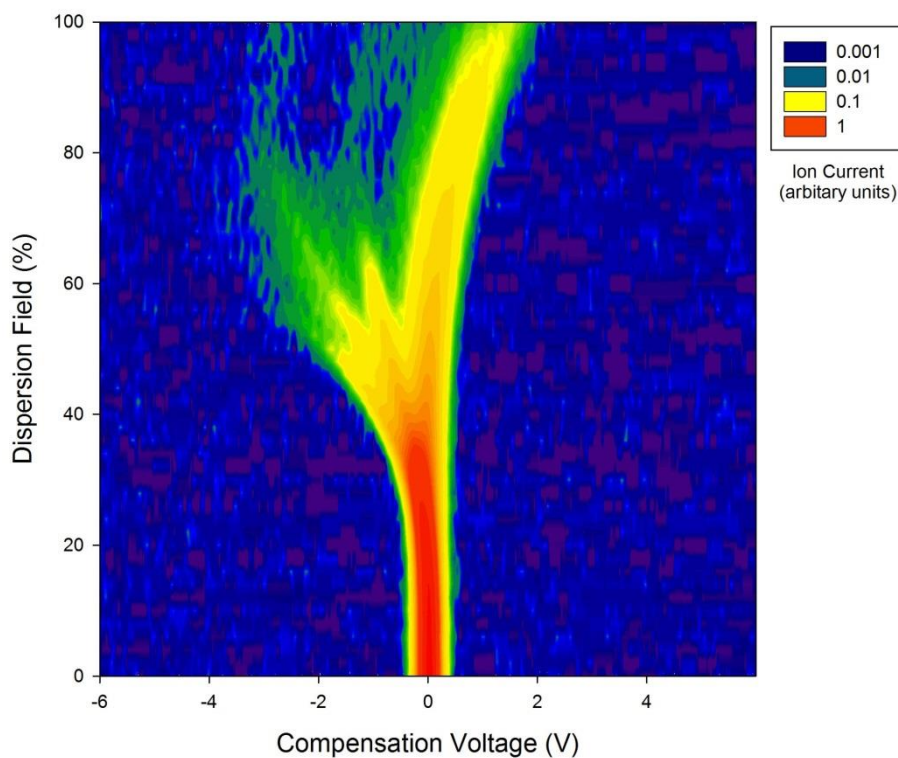


Figure 4.10: Raw data from the Lonestar FAIMS for a colorectal cancer patient

4.3.4. Statistical Methods

FAIMS data was processed in a custom LabVIEW program (Ver 2012, National Instruments, USA) using a method named Fisher Discriminant Analysis (FDA; a pre-classified linear technique). The positive and negative ion matrices for each scan were concatenated and joined to make a single 52,224 element array to be used in the analysis algorithm. These were then transformed using a Daubechies D4 wavelet in order to compress the information from the original large array into a more useable format. Features in the resulting transformed array, which was now suitable for discrimination, were then identified. For each feature, the class scatter $(\sum\sigma_i)^2$ and the between class scatter: $(\sigma_\mu)^2/(\sum\sigma_i)^2$, were calculated and then thresholds set to identify variables for analysis. (σ_i : the standard deviation of the dimension in question within the class i , and σ_μ was the standard deviation of the means of the dimension under test between classes). These were used as the input to an FDA algorithm.

Different thresholds were then set for within class scatter and between class scatter and the variables that were within these thresholds were then used for data processing by FDA. In order to determine the sensitivity and specificity of the method to detecting CRC samples, one sample was removed from the original set, the remaining samples were re-analysed, and then this single sample was re-introduced as an unknown. Re-classification was attempted based on the FDA weights using a K-Nearest-Neighbour routine. The actual calculation of sensitivity and specificity was completed using Equations 4.5 and 4.6 shown above, similar to the method used in the Fox 4000 study. This exploration identified groups of common variables in the parameter space where re-classification exceeded that which would be expected from random re-classification (three standard deviations from the mean). The most successful variables for re-classification were used in the resulting proposed classification in Section 4.3.5. For more details on the analysis, please see the original publication by Covington et al that used this technique (8).

4.3.5. Urine Sample Results

The 2-group FDA classification of CRC patients against healthy controls is illustrated in Figure 4.11, with the CRC samples in brown and the controls in green. There is a small degree of overlap between the two groups included, with some scatter seen in the healthy control samples coming into the region that the CRC class occupies in particular. However, overall there is a reasonable degree of clustering in both the disease and healthy state, and they generally occupy different areas of the discriminant function.

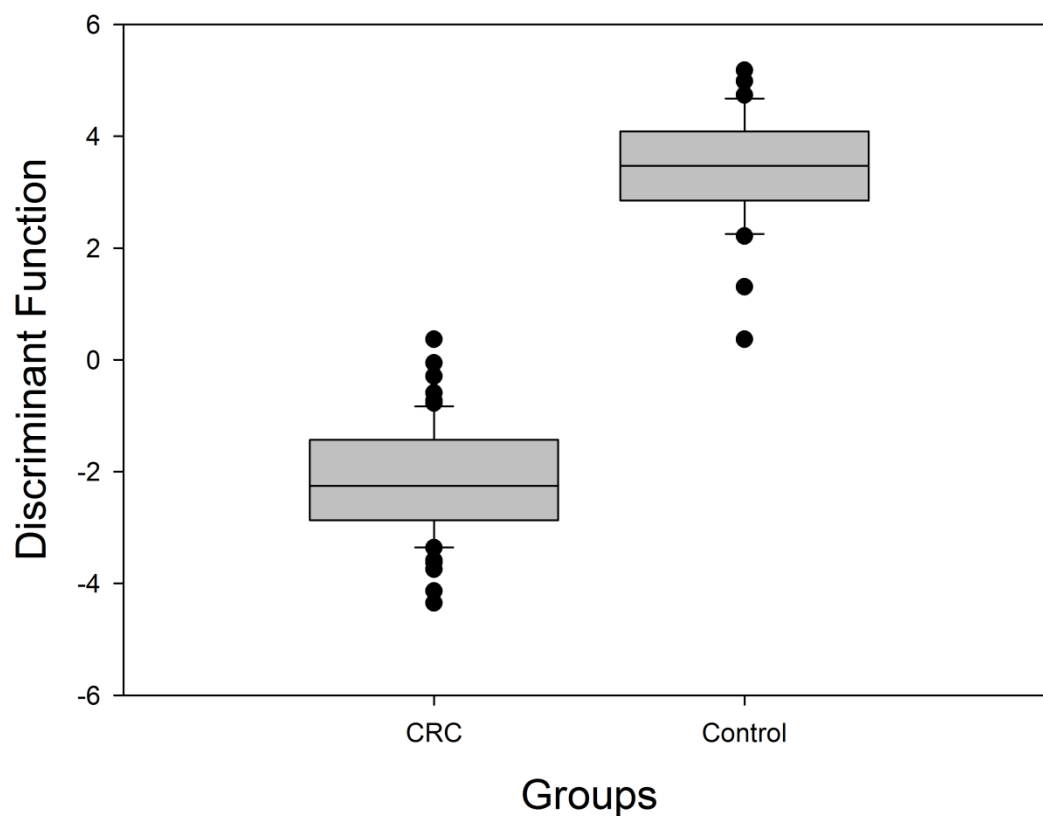


Figure 4.11: FDA plot of CRC against healthy control samples run through the Lonestar

The positive results of the FDA classification seen in Figure 4.11 are reflected in the success of re-classification of introduced unknowns from both groups using the KNN method. The overall sensitivity and specificity of the Lonestar method for distinguishing CRC urine samples from healthy controls were 88% and 60%, respectively. The lower level of specificity is somewhat expected by the fact that the control samples had some wide outliers compared to those for CRC, and it has been previously shown by this research group that the range of urine volatile output in healthy samples has a wider variety than that of any disease group (8). However, these results show that the FAIMS method for distinguishing CRC from healthy controls is very effective. A full direct comparison cannot be made between this study and that using the Fox 4000 due to the lack of IBS controls.

Future studies with this technology must include a disease control (ideally IBS) that has more clinical relevance for patients coming in complaining of similar symptoms.

4.4. Conclusions and Further Work

A total of 93 urine samples from patients of CRC and IBS, as well as healthy individuals, were successfully run through the Fox 4000 commercial electronic nose instrument. A number of reference samples of volatile solutions were also run through the Fox 4000 in repeated batches over the course of two years. These reference sample runs showed that a degree of long-term drift in response of sensors was experienced by the instrument over the two-year collection period, potentially leading to degradation in sensitivity to some/all gaseous and volatile chemicals.

Resulting 2-group and 3-group LDA classifications produced from the disease urine sample data show lack of clear distinction between the scores for the different groups, with a large degree of overlap and spread. A high variation in controls and IBS was shown as expected, but a much higher variation in response to CRC samples was not expected from these results. This led to very poor performance of the LDA plot to re-classify samples that were taken out from the LDA 'training set' and introduced again as unknowns. The sensitivity and specificity of distinguishing CRC samples against IBS controls were a very poor 54% and 48%, respectively.

Another study involving the Owlstone Lonestar commercial FAIMS instrument was also completed, using a total of 83 CRC and 50 healthy volunteer urine samples (11). A 2-group FDA classification was produced from the response data to the urine samples, which showed very impressive distinction between the groups with very little overlap. Re-classification using a similar KNN technique to the Fox 4000 study yielded a sensitivity and specificity of 88% and 60% for distinguishing CRC from healthy controls.

This investigation highlights a need for new technology with more directed sensitivities to biologically-produced gases and volatiles in order to better distinguish between biological disease states. There is a large portion of the population of commercially-available gas sensor technologies that have not been included in electronic nose systems at present, with much more potential for tailoring the sensors to the clinical application than is included in the Fox 4000. Other forms of gas-phase separation techniques may also be used to improve distinction of disease groups (such as chromatography) provided they are robust and repeatable enough to be used with urine headspace samples.

The number of samples included in this study is still relatively small compared to the populations of CRC or IBS sufferers in the UK (12) (13), and so there is a requirement to include greater numbers of samples for all disease states in future studies. The use of samples from ideal control groups for comparison (such as IBS patients or healthy volunteers) was limited during this investigation due to the precious nature of the samples. Care was needed to ensure that sufficient urine samples were available for all studies within the research group, but this situation resulted in an inability to directly compare the Owlstone Lonestar FAIMS to the other technologies included here. Therefore, additional investigation is required on the Lonestar FAIMS instrument to include samples from IBS patients or another disease group in order to show the success of CRC distinction against a control group that will be seen in clinic. There must be a continuing effort to ensure that sample collection dates are within 12 months of each-other in order to maintain stability of the urine volatile and gas content, despite the difficulty in collection numbers within that timescale.

4.5. References

- 1) Berna, A., Metal Oxide Sensors for Electronic Noses and Their Application to Food Analysis. 2010, *Sensors* 10, 3882-3910.

- 2) Kolakowski, B.M., D'Agostino, P.A., Chenier, C., Mester, Z., Analysis of Chemical Warfare Agents in Food Products by Atmospheric Pressure Ionization-High Field Asymmetric Waveform Ion Mobility Spectrometry-Mass Spectrometry. 2007, Anal Chem 79, 8257-8265.
- 3) Yinon, J., Detection of Explosives by Electronic Noses. 2003, Anal Chem, 99-105.
- 4) Eiceman, G.A., Krylov, E.V., Krylova, N.S., Nazarov, E.G., Miller, R.A., Separation of Ions from Explosives in Differential Mobility Spectrometry by Vapor-Modifies Drift Gas. 2004, Anal Chem 76, 4937-4944.
- 5) Probert, C.S., Ahmed, I., Khalid, T., Johnson, E., Smith, S., Ratcliffe, N., Volatile organic compounds as diagnostic biomarkers in gastrointestinal and liver disease. 2009, J Gastroinestin Liver Dis. 18, 337-343.
- 6) Peng, G., Hakim, M., Broza, Y.Y., Billan, S., Abdah-Bortnyak, R., Kuten, A., Tisch, U., Haick, H., Detection of lung, breast, colorectal, and prostate cancers from exhaled breath using a single array of nanosensors. 2010, Br J Cancer. 103, 542-551.
- 7) AlphaM.O.S. SA. Operating Manual: FOX 2000 – FOX 3000 – FOX 4000 Electronic Nose. Daurat : AlphaM.O.S. SA, 1996
- 8) Covington, J.A., Westenbrink, E.W., Ouaret, N., Harbord, R., Bailey, C., O'Connell, N., Cullis, J., Williams, N., Nwokolo, C.U., Bardhan, K.D., Arasaradnam, R.P., Application of a novel tool for diagnosing bile acid diarrhoea. 2013, Sensors (Basel). 13, 11899-912.
- 9) Westenbrink, E.W., Arasaradnam, R.P., O'Connell, N., Bailey, C., Nwokolo, C., Bardhan, K.D., Covington, J.A., Towards the non-invasive detection of colorectal cancer: the role of electronic noses (E-nose) and Field Asymmetric Ion Mobility Spectroscopy (FAIMS). DDW 2013, Orlando.

- 10) "Lonestar User Manuals", Owlstone Support Website (Owlstone Nanotech), 31st Jan 2016, <http://support.owlstonenanotech.com/forums/20205836-9-Lonestar-User-Manuals-Being-Updated>.
- 11) Arasaradnam, R.P., McFarlane, M., Ryan-Fisher, C., Westenbrink, E.W., Hodges, P., Thomas, M.G., Chambers, S., O'Connell, N., Bailey, C., Harmston, C., Nwokolo, C.U., Bardhan, K.D., Covington, J.A., Detection of Colorectal Cancer (CRC) by Urinary Volatile Organic Compound Analysis. 2014, PLOS ONE 9, E108750.
- 12) Ferlay, J., Parkin, D.M., Steliarova-Foucher, E., Estimates of cancer incidence and mortality in Europe in 2008. 2010 Eur. J. Cancer. 46, 765-81.
- 13) S.H.C. Anderson, G. Davies, H.R. Dalton., Irritable Bowel Syndrome. Key Topics in Gastroenterology. Oxford : BIOS Scientific Publishers Ltd., 1999.

5. Development and Construction of the WOLF 4.1 Desktop Electronic Nose

5.1. Requirements and Objectives

The commercial instruments that have been tested in previous chapters highlight the effectiveness of both systems that use metal oxide/conductive polymer sensors in an array, and those that employ ion mobility spectrometry in distinguishing between groups of urine headspace samples. However, these techniques do not detect the full range of potential urine headspace content effectively, as ion mobility spectrometry is insensitive to low molecular weight gases and electro-resistive sensors do not have a sufficiently unique response to different sizes of molecule. Therefore, a more complete comparison of techniques must include an instrument that incorporates other technologies into its sensing element, which are able to differentiate between varying molecular weight chemicals more effectively. The sensors should be able to detect changes in chemical concentration at a resolution in the range of ppm or even ppb in order to compare reasonably to the instruments already included. It is also a major priority for this system to be sensitive to as large a range of gases and volatiles that are known to be regulated biologically as possible, and so included sensors had a variety of target gases between them.

There is an absence of commercially available electronic noses that include sensors that are not electro-resistive but have both a comparable resolution and appropriate resilience to the temperature and humidity of the urine headspace. There was also an opportunity to tailor some design aspects of current systems to the clinical environment, most notably in simplifying the interface for users and incorporating more into a single physical enclosure to save space. It was concluded that a new system would be developed and built as a test

platform so that other sensing techniques may be included in the comparison for the medical diagnostic application.

5.2. System Overview

The control system for the instrument being constructed, denoted the “WOLF 4.1”, incorporates many parts of other desktop electronic noses such as the Fox 4000 (as described in Chapter 4), with the majority of these elements housed within a single chassis. Figure 5.1 shows a diagram of the components in the flow path of the instrument, including many that are external to the chassis for executing a repeatable sampling method. There are a number of sensors and actuators listed in the flow diagram on the bottom half of Figure 5.1 that are either housed in the single gas chamber for introduction to the sample, or are incorporated into the air flow lines. These are each attached to some form of signal processing circuitry, including analogue-digital converters (ADC) or operation amplifiers, whose outputs will be read by a pair of data acquisition boards from National Instruments. These boards communicate with a built-in single board PC, which has a Windows XP operating system and National Instruments software installed for central control of the system. This instrument was built as a test platform for the electro-chemical and optical sensors housed inside, and so has a simple and flexible design to maximise the range of gaseous samples that can be introduced.

The airflow system within the WOLF 4.1 was designed to allow significant control over the samples being introduced into the machine, while maintaining versatility so that a variety of introduction techniques could be used. It can be seen in Figure 5.1 that a very straightforward method is used to send incoming gas/volatile mix samples directly through to the sensor chamber once it is entering the machine, while more complex introduction is implemented externally. The variables being controlled by the system are the pressure and flow rate of incoming air into the instrument, and the time for which the samples are

introduced to the sensors. Incoming air pressure and flow are controlled externally to the WOLF 4.1 instrument, using a manual pressure regulator and flow controller (green in the diagram). The actual flow rate is determined by the AWM 3300V flow meter described in Section 5.3.2. The flow meter is located after the chamber in order to minimise the effect on the samples before being observed by the gas sensor array. An electronic valve at the inlet to the instrument controls the sampling time of the system, and is coloured in yellow on Figure 5.1.

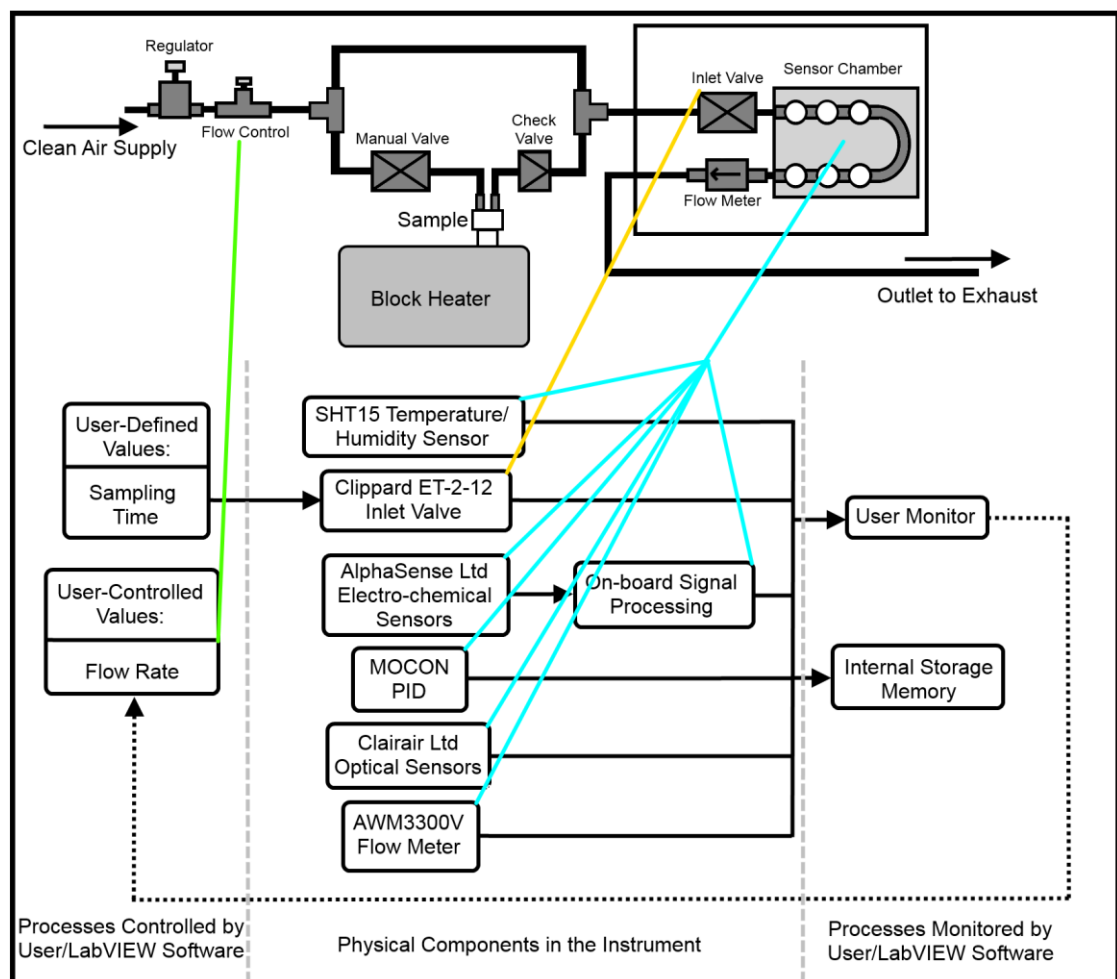


Figure 5.1: System block diagram for the WOLF 4.1 electronic nose

The basis for the control and measurement algorithm is also shown in a flow diagram on the bottom half of Figure 5.1, with indication on which sections are implemented in

Development and Construction of the WOLF 4.1 Desktop Electronic Nose

hardware and which are dictated by the user or control software. The responses of the sensors (coloured in teal on the flow diagram) were sent through sensor drive and signal processing circuitry which implement the algorithm shown by Figure 5.1 as described in Section 5.3.3.

A program has been developed in LabVIEW for this application that implements the sampling control algorithm and processes the incoming sensor data further for storage in text files. The front panel of the program (shown in Figure 5.2) allows users to change testing variables such as the duration of sample tests, sample repeats and purge times afterwards. The program also allows users to monitor the raw sensor outputs and environmental factors both during and between experiments to ensure operation within acceptable limits, as seen in the centre and right side of Figure 5.2.

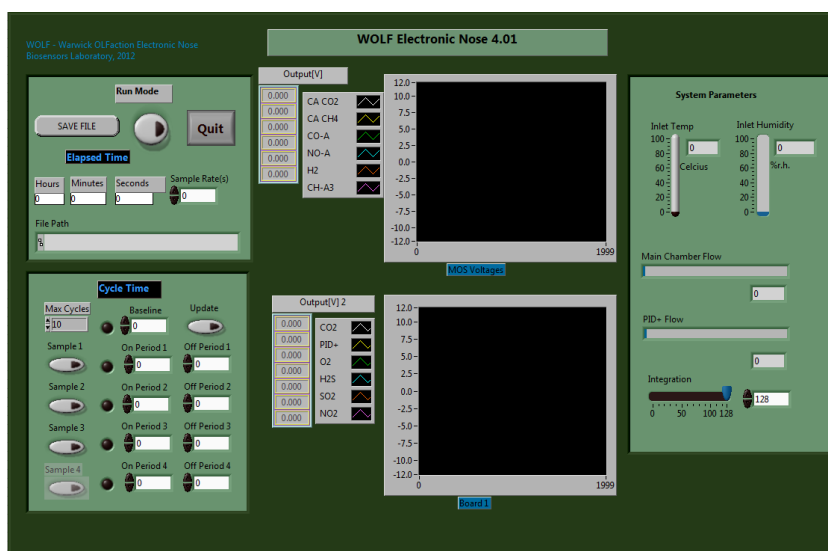


Figure 5.2: Front End of the LabVIEW control software for the WOLF 4.1

5.3. Sensor Technology

The basis of this new instrument is the chemical sensor array; the decisions as to what should be included are integral to optimising how effective it may be at detecting diseases.

Optical sensors are limited in the range of chemicals that can be detected (1) and do not overlap with electro-chemical cells in sensitivity. Therefore, these two types of device were combined together in order to maximise the cross-sensitivity and detection range of the overall system.

5.3.1. Gas Sensor Array

The gas sensing element consists of an array of 13 sensors, which employ a range of different sensing techniques. This total includes 8 amperometric electro-chemical sensors (Alphasense Ltd.), two NDIR optical devices (Clairair Ltd.) and a single photo-ionisation detector (Mocon). This group includes almost the entire range of electro-chemical sensors that were commercially available from Alphasense at the time of construction, in order to test a sufficient range using this sensing technique. These sensors are each constructed within a cylindrical package that includes all the physical components required for the detection method. While each of these sensors is designed to target a single gas at competitive sensitivities when compared with metal oxides (detailed in Table 5.1 with gas sensitivities shown from AlphaSense reports (2)), they are also capable of detecting a large variety of different gas and volatile compounds. This set of sensors has been chosen to combine the detection of a number of specific gases believed to be medically significant (such as CO₂ and methane), while also having a broad range of overlapping cross-sensitivities. The PID-tech Plus photo-ionisation detector made by Baseline-MOCON has been included in the array to give an indication as to the total quantity of gas and volatile molecules passing through the chamber during a sample run. In this manner, the WOLF 4.1 system attempts to maximise the amount of information collected on the bio-signature of an individual, thereby making it more applicable to the characterisation and distinction of disease states.

Manufacturer (Sensing Technique)	Gas Sensor (target gas)	Sensitivity Range
Alphasense Ltd. (Electro-chemical Cell)	CO-BX (Carbon Monoxide)	2,000 ppm
	H2S-B1 (Hydrogen Sulfide)	200 ppm
	NH3-B1 (Ammonia)	50 ppm
	O3-B4 (Ozone)	0.1 ppm
	SO2-BF (Sulfur Dioxide)	100 ppm
	NO2-B1 (Nitrogen Dioxide)	20 ppm
	NO-B1 (Nitric Oxide)	250 ppm
	ETO-B1 (Ethylene Oxide)	100 ppm
	O2-A2 (Oxygen)	15 - 25%
	CO-BX (Carbon Monoxide)	2,000 ppm
H2S-B1 (Hydrogen Sulfide)	200 ppm	
Clairair Ltd. (Non-Dispersive Infrared Optical)	Cirius 1 (Methane)	0 – 5%
	Cirius 3 (Carbon Dioxide)	0 – 10%
MOCON (Photo-ionisation Detector)	10.6 eV piD-TECH Plus (Black)	2,000 ppm

Table 5.1: List of sensor manufacturers, mechanisms, and target gases included in the

array

5.3.2. Environmental Sensing

There are a number of monitors for environmental factors within the machine that affect the response of the sensors. Two such factors are the temperature and humidity of the sample chamber, for which the electro-chemical sensors will have some response to. The SHT15 sensor from Sensirion (pictured in Figure 5.3) (3) measures both of these conditions in a small surface-mount package.

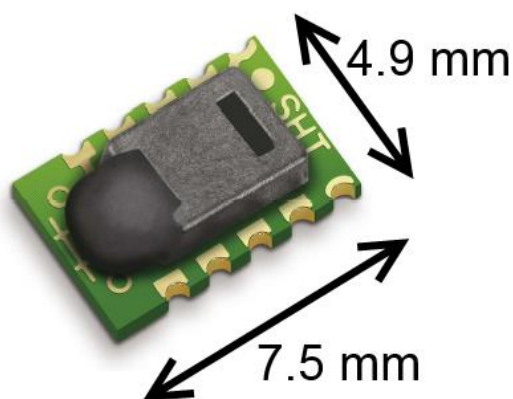


Figure 5.3: 3-Dimensional diagram of the SHT15 temperature/humidity sensor (3)

Flow rate through the machine was monitored by an AWM3300V mass flow meter from Honeywell (4). The unit includes an electronic transduction module that reads flow rates from the inlet (P_1) to the outlet (P_2) in the range of 0 – 1000 ml/min.

5.3.3. Sensor Drive

The electronic interface between the sensor array and the control PC is included in the printed circuit boards (PCBs) in the WOLF 4.1, and comprise a variety of sub-systems described below. Each single sensor is plugged into an individual PCB that contains control electronics for converting the raw detection response into an analogue voltage signal so that it can be easily integrated into the data acquisition architecture. For the electro-chemical sensors this is accomplished by commercial Individual Sensor Boards (ISBs) produced by Alphasense (5).

These control boards maintain the potential between the working and counter electrodes, the biasing on a reference electrode to induce reduction/oxidation of the target, and measuring current for conversion of the ampero-metric signal into analogue voltage. Most of this is achieved using the circuit design shown in Figure 5.4, which has no biasing included (6). The current supply that drives the actual cell reaction in this circuit is

operational amplifier (op amp) IC2, which also has its inverting input attached to the reference electrode to ensure output potential is always high. The JFET Q1 will enter a high impedance state to “enable” the sensor, after which the circuit will strive for the working electrode to reach the potential of the reference electrode. Finally, IC1 is a sensing op amp that converts the working electrode current to a voltage signal using an appropriate R_{load} . Some of the sensors included in the array (such as NO-B1) include a bias voltage applied to the control op amp ground, in order to tune the sensitivity of the cell to other ranges of chemicals. The ISBs are also dual-channel with an auxiliary electrode on the sensors, which is exposed to environmental effects such as temperature change but not to any analytes (5).

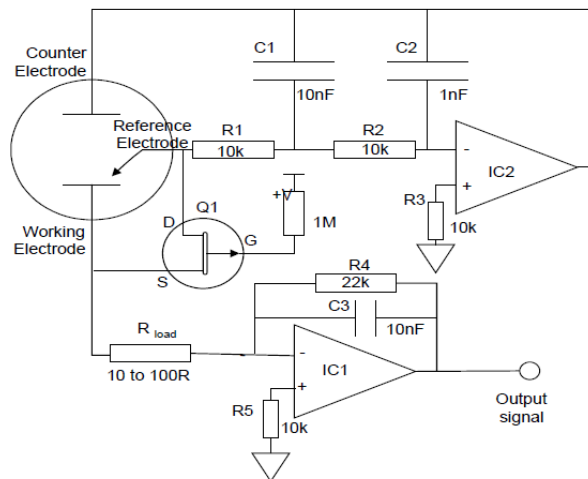


Figure 5.4: Potentiostatic circuit for driving an electro-chemical sensor (6)

The Clairair optical sensors are also controlled using a commercially-produced PCB called Cirius X, which has an on-board temperature/pressure monitor and drive for the infrared sources (7). The Mocon photo-ionisation detector includes a circuit for converting to analogue voltage within the physical cylindrical package, so that in-house constructed break-out PCB was all that was required (8). The above control measures remove the effects of environmental effects that the detectors are sensitive to, thus allowing for ppm-

and ppb-level resolution to be possible. The actual detection principles for all of the sensors included in the WOLF 4.1 are detailed in Chapter 2.

A single voltage input channel is used for processing the response of each individual sensor aside from the AlphaSense devices, which required dual channels. These were used for the working and auxiliary outputs of a single sensor, and were given appropriately-tuned gain resistors in matching pairs for each channel.

5.4. Final Construction

All of the components of the WOLF 4.1 are housed in an H2 Classic Silent PC case from NZXT. The interior structure of the system is illustrated in Figure 5.5, with the sensor housing chamber shown at the bottom and the data acquisition (DAQ) interfacial PCBs and in-built Windows PC above. The circuit boards were fastened to the PC using structural aluminium bars that spanned along the interior sides of the case, as seen in Figure 5.5. The sensor chamber and flow meter were fastened to the grille on the bottom of the case, with valves and external connectors fastened to the Peripheral Component Interconnect (PCI) slot in the back of the case as is usual for desktop PC connection. The power supplies from Tracopower were housed at the front of the machine, where a pair of large circulation fans aid in thermal energy management.

Development and Construction of the WOLF 4.1 Desktop Electronic Nose



Figure 5.5: Photograph of the interior of the WOLF 4.1

Once the WOLF 4.1 was fully constructed, it was connected to an external monitor, keyboard and mouse and setup in the laboratory where there was an external air and power supply. Figure 5.6 shows photographs of the exterior of the system and user interface for the LabVIEW software as configured for laboratory use.

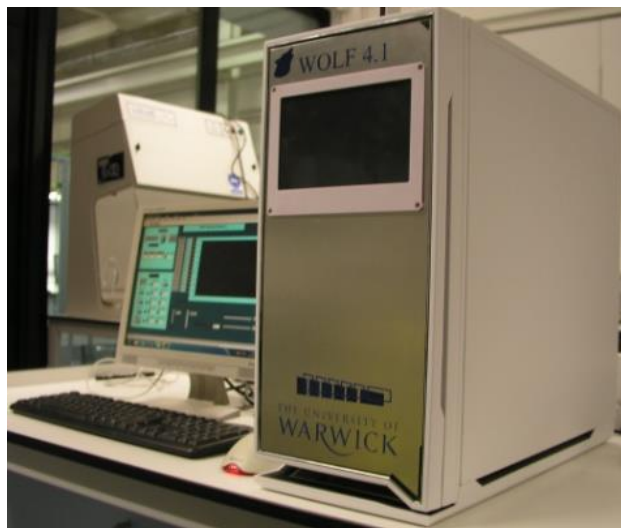


Figure 5.6: Photograph of the user interface and exterior of the WOLF 4.1

5.5. Experimental Testing of WOLF 4.1 with Single-Volatile Samples

5.5.1. Introduction

The electro-chemical and optical sensors included in the array of the WOLF 4.1 were designed to detect specific target gases, and chosen based on the links between their targets and biological output media. Therefore, a reasonable level of confidence was already present in the ability of the sensors to detect the trapped gaseous content of urine. However, there was very little known regarding the sensitivities of any of the sensors to volatile groups. Sensors using NDIR techniques are unlikely to detect any chemicals outside of their absorption range due to the selectivity of the technology (1). However, there was potential seen in the electro-chemical sensors to detect a wide range of volatiles that could react in the electrical bias conditions setup by the sensors (2). Therefore, initial testing was conducted on the WOLF 4.1 with a variety of different short-chain organic compounds, which were dissolved in aqueous solution at a range of concentrations on the ppm scale. This would verify that a distinction can be made between the disease groups, and thus allow development of an experimental method before utilising patient urine samples.

5.5.2. Methods and Materials

An experimental method was setup for the WOLF 4.1 by use of a Dri-Block® DB-2D (Techne) heater to allow the release of headspace from samples based on aqueous solutions. A flow of clean dry air supplied by the Zero Air Generator described in Section 4.2.1 was regulated and then split into two channels, one of which was sent into the sample with a valve to cut off flow in between sample runs. A check valve was included in the sample channel before re-joining with the other “make-up” flow path, which prevents a sudden increase in air pressure and flow rate upon introduction of a sample to minimise the effect on sensor response. A custom heating block was machined to hold 30 mL universal sample

containers, and fitted into the heater before being brought to a temperature of 40 ± 0.1 °C. Sample aliquots held in 30 mL universal sample containers (in conjunction with standard containers used in the medical field) with customised caps that included bulkhead fittings to allow air flow.

Initially, a variety of different short-chain organic compounds with different functional groups (such as ketone, ester, alcohol and aromatic) were dissolved in aqueous solution at a range of concentrations on the ppm scale. The full list of these compounds is given in Table 5.2. These were used to determine the cross-sensitivities of the WOLF 4.1 sensors to these chemical standards.

The standards were produced by first taking a 250 mL capped glass container and pipetting 100 mL of de-ionised water into it using a Gilson Pipetman D10mL pipette and sterile PTFE disposable tips. An appropriate volume of a particular volatile (usually in the range of 20 – 100 μ L) was added to the water using a Glison Pipetman D200 pipette, followed by sealing and inverting the mixture for approximately 5 minutes to allow dissolution to occur. A 5 mL sample of the resulting solution was then transferred by D10mL pipette to the 30 mL universal container. The solutions began the headspace production stage immediately after this, with no gap for volatile content to escape. It should be noted, however, that the concentrations in ppm discussed in Section 5.5.3 are all in terms of volume in water. Therefore, these results can be used to determine sensitivity of the WOLF 4.1 sensors but cannot be used to directly compare against other instruments tested using single volatile samples made from other methods, such as in Section 6.6.3.

The 5 mL samples were heated to 40 ± 0.1 °C for 5 minutes in order to build up headspace and then introduced into the WOLF 4.1. The sample headspace was sent into the instrument for 5 minutes at a total flow rate of 300 mL/min with a sample flow rate of 150

mL/min. The incoming air to the machine was regulated to 0.2 bar to avoid damage to the internal components. The relative humidity and any volatiles introduced by the sample were then purged from the pneumatic system using clean air for another 10 minutes at a flow rate of 300 mL/min. This process was repeated three times for each sample. The sequence of solution concentrations tested was randomised to mitigate the chances that a long-term response drift would allow for fabrication of response change with increasing concentration.

Chemical Group	Ketone	Alkyl Ester	Primary Alcohol	Secondary Alcohol	Aromatic
Compound Included	Acetone	Ethyl Acetate	Propan-1-ol	Propan-2-ol	Toluene

Table 5.2: Volatile groups tested in aqueous solution to determine WOLF sensor sensitivities

5.5.3. Results and Discussion

The results of the initial experiments with aqueous solutions of individual volatile compounds revealed various relationships between sensor responses and concentration. However, the presence of each individual compound evoked responses from a different set of sensors within the array, which will be described in detail in the following sections. The responses were corrected by the baseline values, and averaged over the full introduction period in order to add clarity to the patterns presented below. Some of the sensor responses varied at a much larger scale than others, and so two graphs are shown for each volatile type: one that shows the full sensor array response and highlights the high variance sensors, and another that only includes the low variance sensors. This allows for clearer examination of all sensor responses, regardless of their relative scale. Individual sensors are labelled using their manufactured target gas; their part numbers can be found in the list shown in Chapter 6.

5.5.3.1. Acetone Sample Results

The average responses of the all sensors in the array to the acetone samples at concentrations of 0 – 100 ppm are shown in Figure 5.7. The response changes in this graph are dominated by that of the photo-ionisation detector (PID), which also looks to be decreasing with increasing concentration. This is reasonable as the PID sensor is a fairly accurate measure of the total volatile content of the sample. Other sensor responses are relatively smaller, and so are not clear on this diagram.

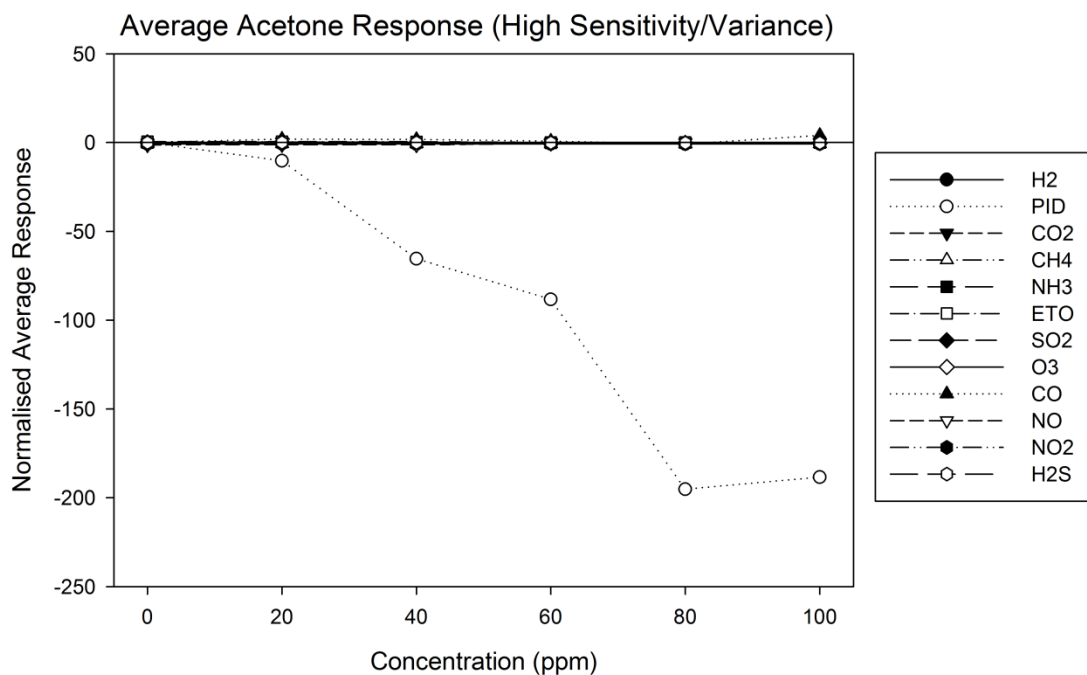


Figure 5.7: High variance average sensor response to acetone

Figure 5.8 shows the low variance responses to acetone at a 0 – 100 ppm concentration range within the sensor array. There seems to be a negative gradient in the responses of sensors such as ammonia (NH₃), ozone (O₃) and ethylene oxide (ETO), whereas many of the other sensors do not look to be responding more to increasing concentration. A number of sensors have sharp offsets between 0 and 20 ppm, which is likely due to an

increase in environmental humidity in the samples as the 0 ppm baseline sample used dry air.

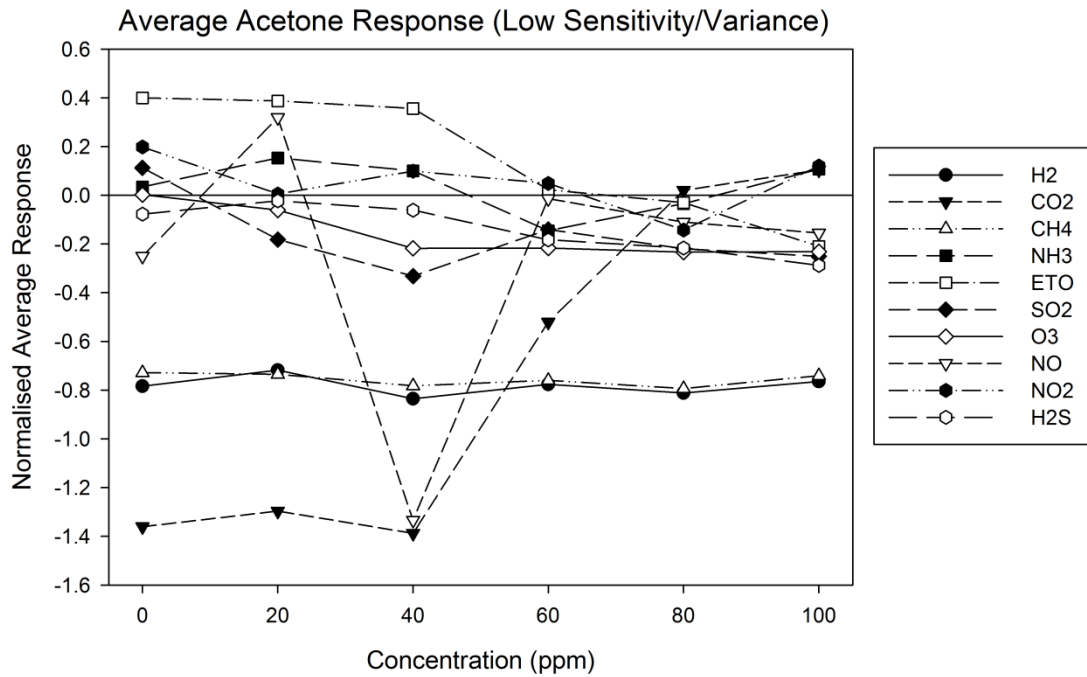


Figure 5.8: Low variance average sensor response to acetone

5.5.3.2. Ethyl Acetate Sample Results

The full sensor array response to ethyl acetate samples in concentrations of 0 – 100 ppm is shown in Figure 5.9, which highlights the large response change in the PID sensor to this volatile as well. Some variation can be seen in the remainder of the sensors, but there is little clarity at this scale.

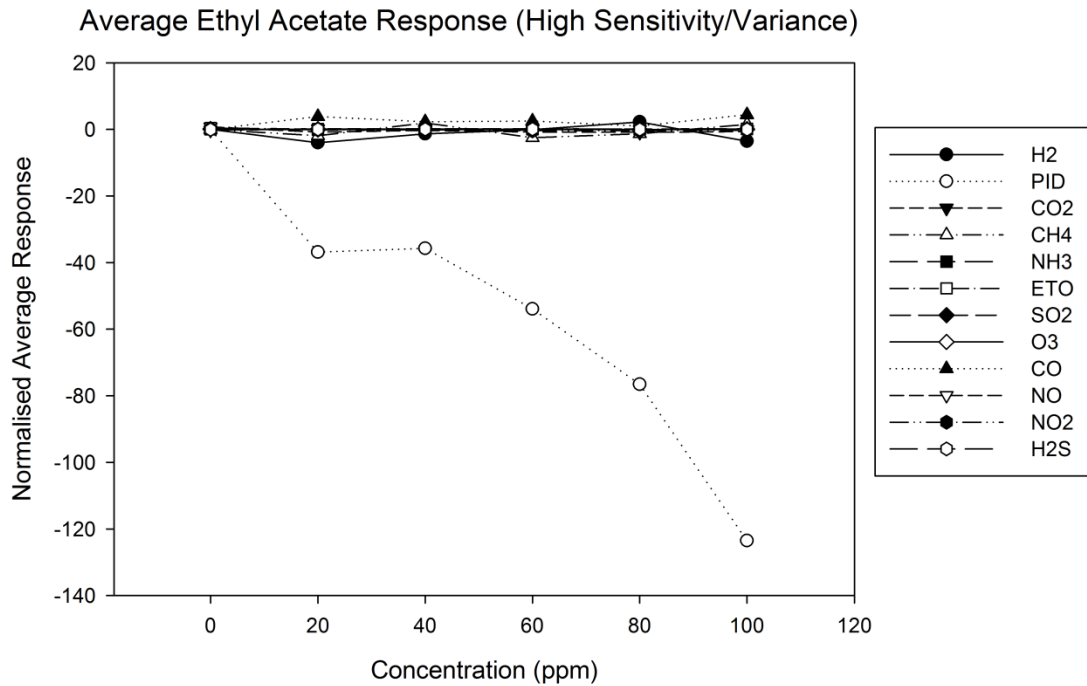


Figure 5.9: High variance average sensor response to ethyl acetate

Figure 5.10 shows the smaller-scale response changes in a subset of the sensors on the WOLF 4.1 when introduced to samples of ethyl acetate at concentrations of 0 – 100 ppm. There are a number of higher variance sensors, such as carbon monoxide (CO), methane (CH4) and hydrogen sulphide (H2S), which do not show any relationship between concentration of sample and response. This could be due to an increasing humidity level within the machine, as samples were not run in order of increasing concentration to avoid the false identification of a relationship. These partially mask the small but proportional response of the nitrogen dioxide (NO2) sensor. There also seems to be some response to ethyl acetate from the carbon dioxide (CO2) sensor. There do not seem to be many other sensors that respond well to this ester. Again, many of the sensor responses have sharp gradients between 0 and 20 ppm samples, most likely due to the change in humidity.

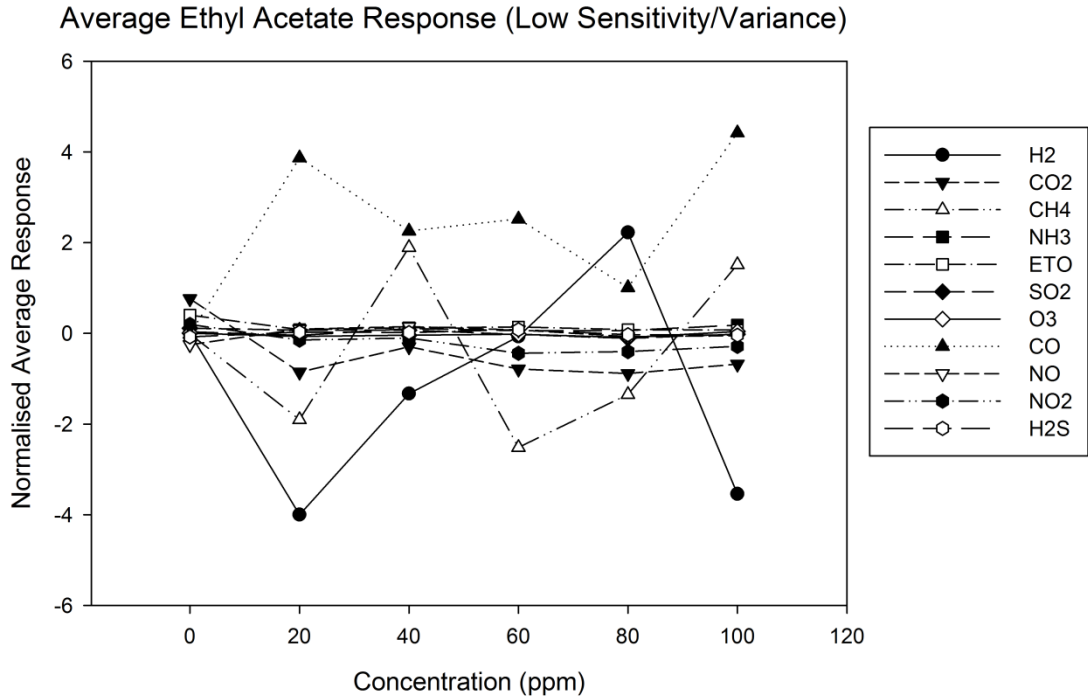


Figure 5.10: Low variance average sensor response to ethyl acetate

5.5.3.3. Propan-1-ol Sample Results

The baseline-corrected full array response to samples with concentrations of propan-1-ol from 0 to 100 ppm is shown in Figure 5.11, and includes a very high variance response from the CO sensor. This does look to be proportional with concentration rate, but this could also be the product of increasing humidity within the system, as a similar trend is seen in the CO₂ sensor as shown in Figure 5.12. Little else can be seen in the graph in Figure 5.11 aside from the branching of sensor response from 0 to 20 ppm, which is again likely to be a product of humidity inclusion.

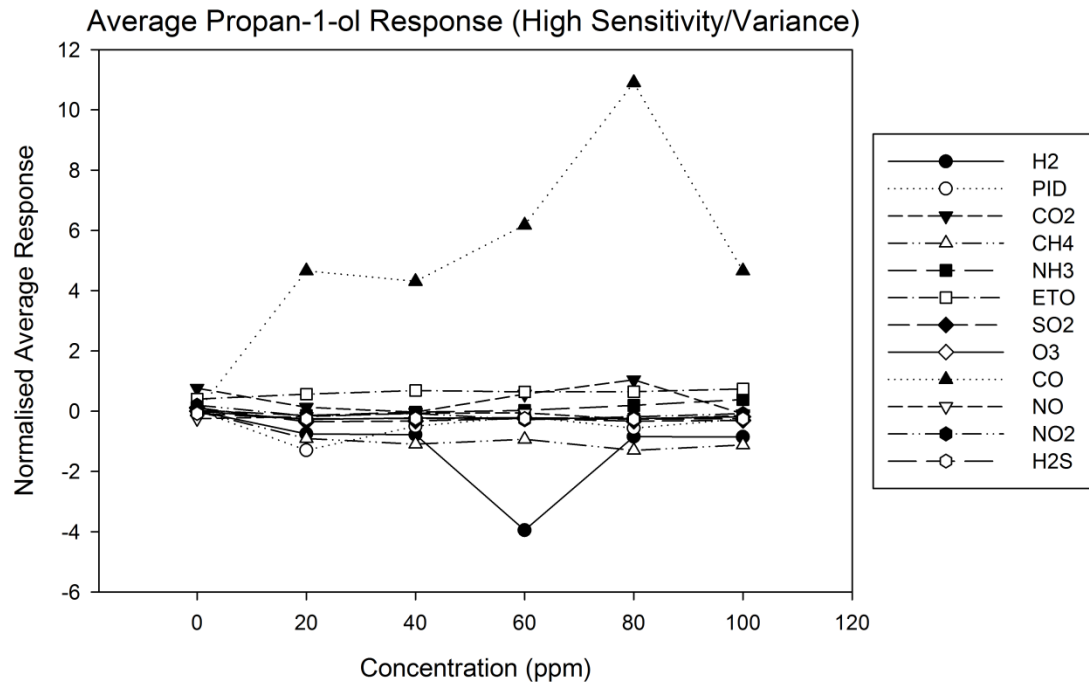


Figure 5.11: High variance average sensor response to propan-1-ol

There is a clearer picture of sensor sensitivity to propan-1-ol concentration in the low variance sensor subset shown in Figure 5.12. As mentioned above, the CO2 sensor looks to be responding proportionally to volatile concentration but with a sharp drop between 80 and 100 ppm. This feature, as well as the similarity between the response patterns of CO2 and CO, indicates that they could both be a symptom of a confounding humidity factor. There does look to be a large group of sensors whose response is varying in relation to the concentration of propan-1-ol present, including ETO, NH3, NO2 and CH4. The PID sensor also looks to have a proportional response, but with a heavy offset introduced between 0 and 10 ppm concentrations.

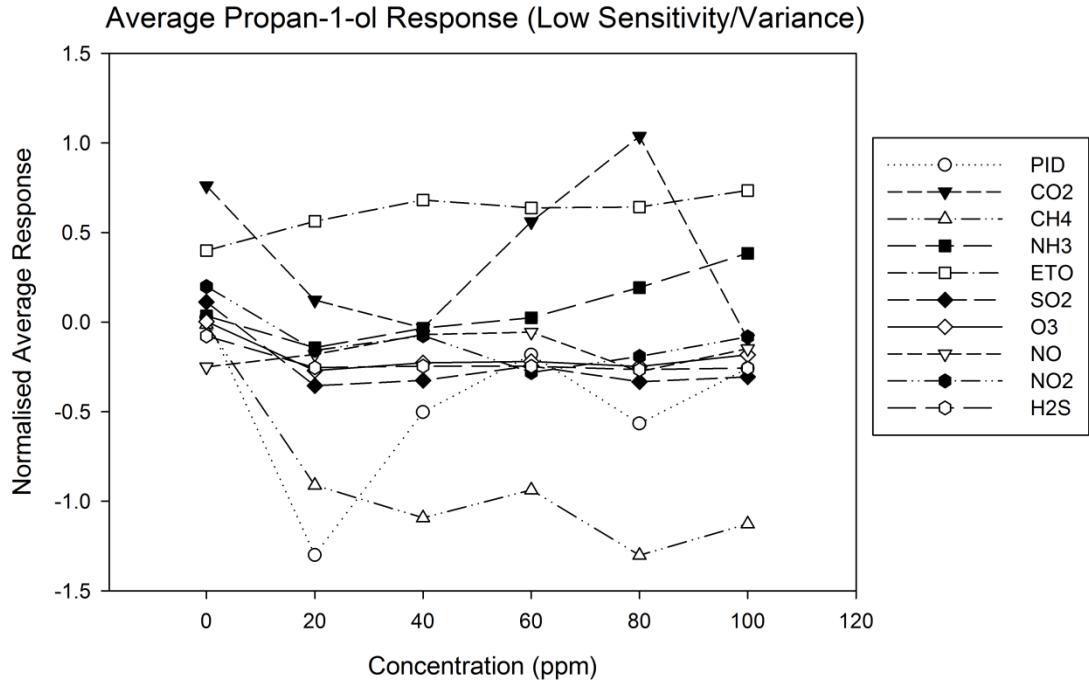


Figure 5.12: Low variance average sensor response to propan-1-ol

5.5.3.4. Propan-2-ol Sample Results

Figure 5.13 shows the baseline-corrected responses of all sensors in the array to increasing concentrations of propan-2-ol, within the range of 0 – 100 ppm. At the smaller scale some sensors appear to be increasing in response with concentration, but this isn't clear due to a very high variance and erratic response from the CO sensor. There is also a non-proportional response from the H2 sensor, which is removed from the low variance subset for this set of results.

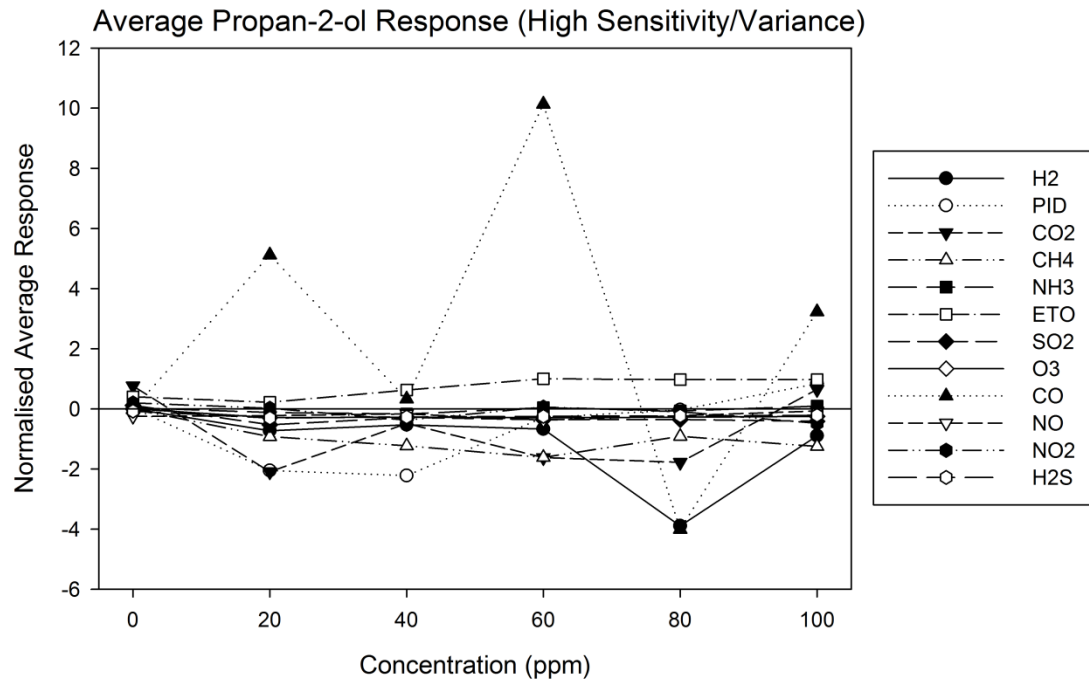


Figure 5.13: High variance average sensor response to propan-2-ol

The low variance response subset of sensors for propan-2-ol samples in the 0 – 100 ppm concentration range is shown in Figure 5.14. The sensors whose average responses look to be changing in relation to the propan-2-ol concentration include ETO, CH4, and to a lesser extent SO2, NH3 and H2S. All of the sensors once again seem to be heavily affected by humidity levels, as shown by the large offset seen between 0 and 20 ppm.

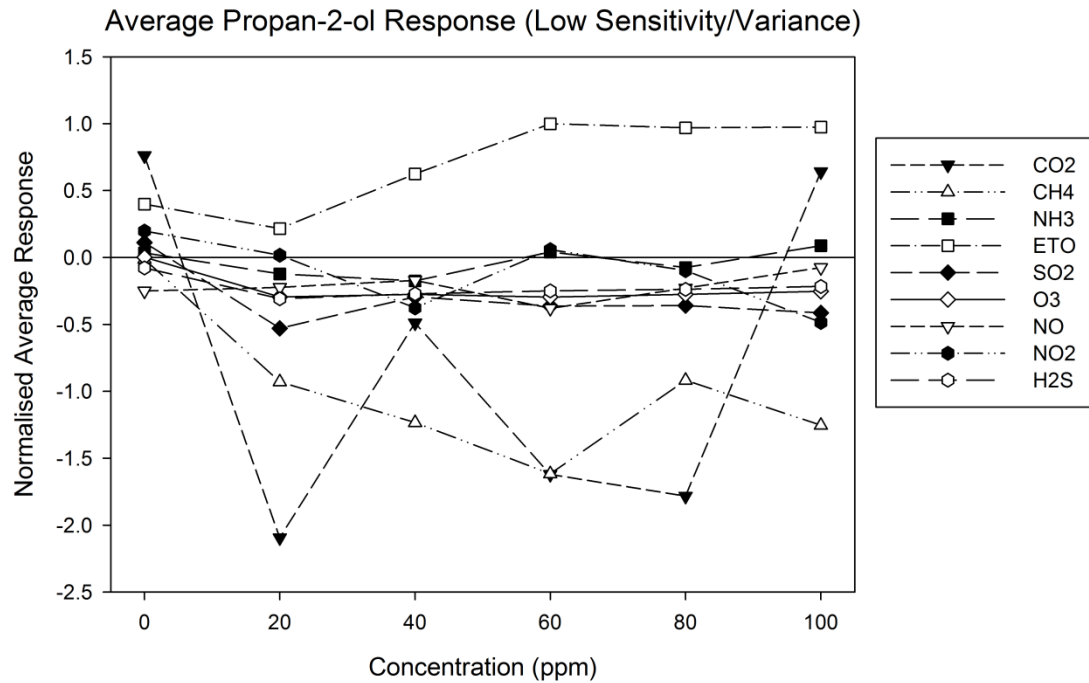


Figure 5.14: Low variance average sensor response to propan-2-ol

5.5.3.5. Toluene Sample Results

Figure 5.15 shows the responses of the full array of WOLF 4.1 sensors to toluene samples with a concentration varying between 0 and 100 ppm. This graph is dominated by the large response changes seen from the O3 sensor, which includes an initial offset between 0 and 20 ppm (likely caused by differences in environmental humidity) and then a steep decreasing level of response with increasing toluene concentrations. There appear to be relationships between concentration and the response of the CO, CO2 and H2 sensors that are consistent throughout the full range of concentration. A proportional change in response of the PID sensor to the levels of toluene in the samples until the 100 ppm concentration is reached, whereby the response sharply returns to baseline level.

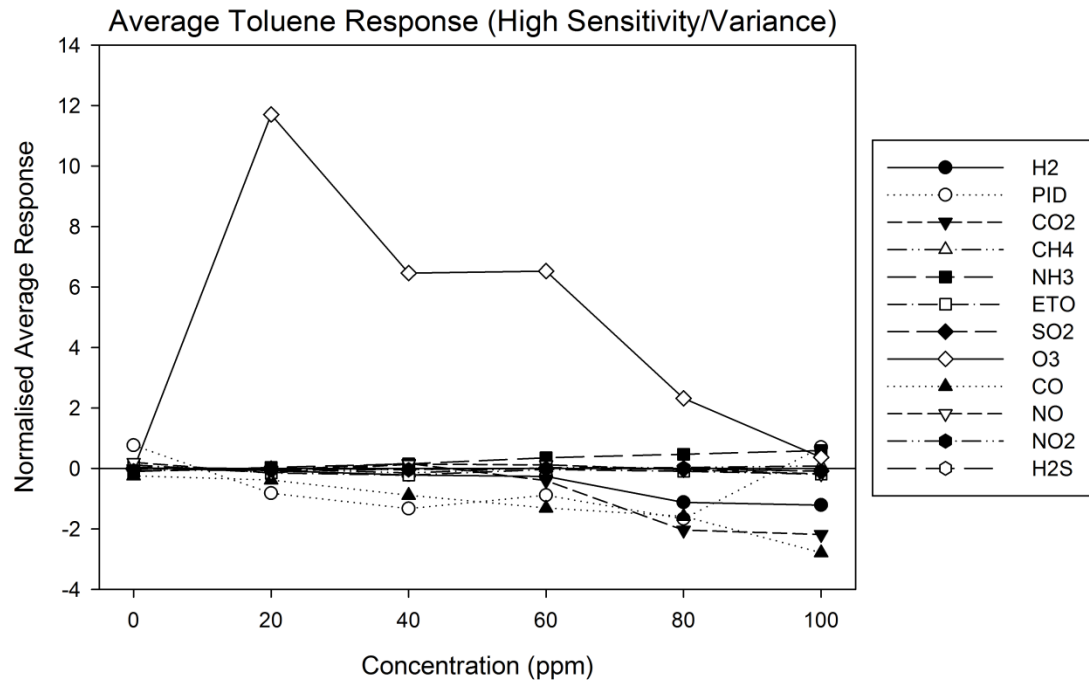


Figure 5.15: High variance average sensor response to toluene

The low variance subset of sensors for toluene samples are shown in Figure 5.16, with many of the previously-discussed responses removed in order to clarify some of those with very gradual consistent gradients. The sensor that looks most promising in terms of proportional response to toluene concentration is NH3, with no other discernible correlation with any other sensors in this array for this volatile.

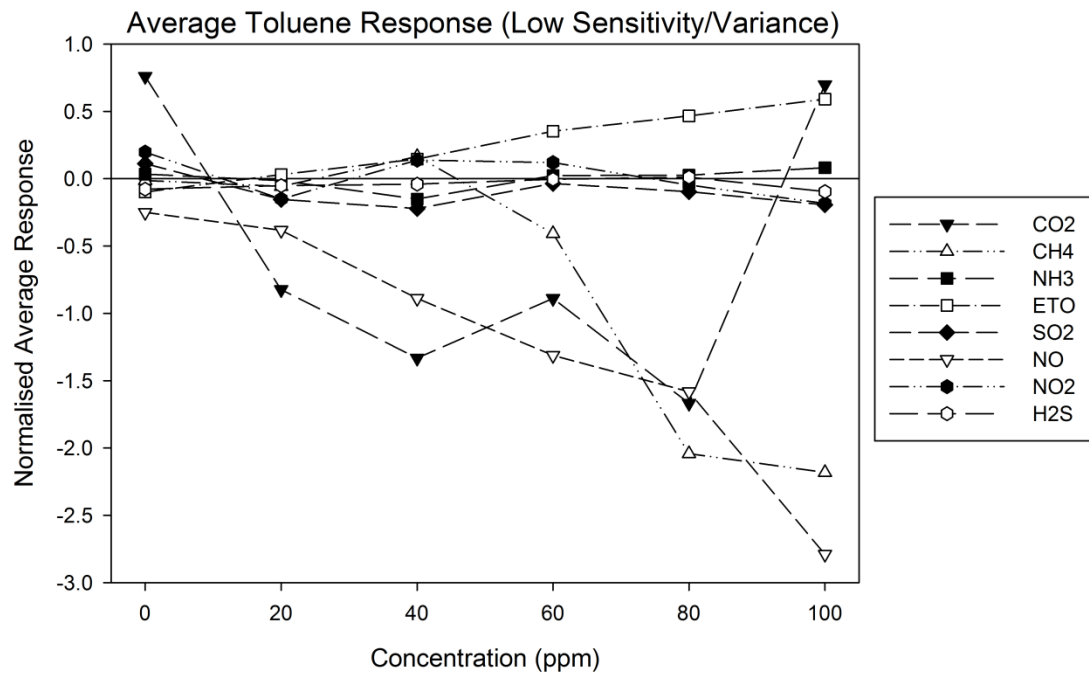


Figure 5.16: Low variance average sensor response to toluene

5.6. Conclusions

An electronic nose instrument was successfully designed and constructed, using an array of 13 gas sensors based on electro-chemical, infrared optical and photo-ionisation technologies. These sensors are recent releases from manufacturers and have not yet been included into other electronic nose instruments. Therefore, this new instrument represents a group of technologies that have not been compared experimentally within this forum until now. All sub-systems included in the WOLF 4.1 are controlled using a built-in single-board PC with installed LabVIEW 2013 software. The control and sensor data is processed using a pair of data acquisition units from National Instruments Ltd and electronic hardware that was designed in-house. The airflow system through the instrument is simple and flexible, to maximise its ability to adapt to the experimental method required. It was constructed as a test platform to qualify the new sensors included, with extra additions required before it could enter into clinical use.

The initial experiments using single volatile aqueous solutions has shown a reasonable degree of cross-sensitivity from the electro-chemical and optical sensors to ppm-level concentrations, with correlations being presented from slightly different subsets for each volatile. This gives further confirmation of a likely response change due to the chemicals released from urine headspace, and potentially a degree of separation between disease states. However, there was also a large confounding factor of environmental humidity variation and retention within these results. Manifestations of this humidity issue include a disproportionate initial offset between 0 and 20 ppm concentrations in all cases, and some high variance noise within the responses of many sensors. This made the relative responses of the sensors difficult to interpret within this dataset. Some variation in the humidity of samples is representative of what will be experienced by the system when urine headspace samples are introduced, greater care is needed to control humidity in future experimentation. The results of these experiments was one of the events which led to the development of the humidity and volatile testing rig used to verify the sensitivity of sensors in the WOLF 3.1 instrument, as described in Section 6.4. While this rig produces volatile standards with concentrations more directly relevant to sensor sensitivity, they cannot be compared directly to the results in this chapter.

This initial testing also allowed for individual tuning of sensor response gains before the introduction of urine samples and the development of an experimental method for headspace samples from 5 mL aqueous solutions, in order to maximise the potential for successful distinction in subsequent experimentation. Some of the sensors (such as NH₃ for example) had responses that were consistently small in scale relative to other sensors, but showed a sensitivity to many volatiles that was magnified using a higher gain.

Parallel experimental testing to that conducted with the commercial electronic noses (Chapter 4) was needed to compare the utility of the sensor technologies included in them. This work is completed in Chapter 7.

5.7. References

- 1) Meléndez, J., de Castro, A.J., López, F., Meneses, J., Spectrally selective gas cell for electrooptical infrared compact multigas sensor. *Sensors and Actuators A: Physical*, 1995. 417–421.
- 2) Alphasense Ltd., AAN 109-02: Interfering gases, Issue 13. Alphasense Ltd.
- 3) Sensirion AG. Datasheet SHT1x (SHT10, SHT11, SHT15): Humidity and Temperature Sensor IC. Sensirion AG, 2011.
- 4) Honeywell, AWM3000 Series Microbridge Mass Airflow Sensors. Honeywell, 2002.
- 5) Alphasense Ltd. AAN 085-2217: Alphasense 4-Electrode Individual Sensor Board (ISB) User Manual. Alphasense Ltd., 2015.
- 6) Alphasense Ltd., AAN-105-03: Designing a potentiostatic circuit. Alphasense Ltd, 2009.
- 7) Clairair Ltd., Cirius X: OEM 4-20mA Transmitter for NDIR Gas Sensors. Clairair Ltd., 2009.
- 8) Baseline-MOCON Inc., piD-TECH plus Photoionization Sensor, D024.9. Baseline-MOCON Ltd.

6. Development and Construction of the WOLF 3.1 GC/E-Nose Instrument

6.1. Requirements and Objectives

This project has so far included a number of different commercial electronic nose instruments and the development of a new e-nose, incorporating a wide variety of different sensing technologies into the comparative study. There has also been experimentation with a GC-MS instrument, which has provided a degree of insight into the actual chemical composition of the gas and volatile headspace of urine. The GC-MS achieves this by combining the chromatographic separation of headspace components, followed by identification by the mass spectrometer. It was therefore proposed that a more efficient distinction of samples may be achieved using a combination of a gas chromatograph element to separate out gas/volatile components in the temporal range with a sensor array to separate them by the combination of sensor sensitivities.

The sensors to be used for the array in this new instrument must include a good diversity in order to capture and distinguish the largest number of potential chemical groups. They must also hold a very small internal volume in order to be effective after the chromatograph element. This is due to the very low flow rates that are possible through gas chromatograph columns, causing the separation of the chemical components to be lost if they are allowed to re-combine while travelling slowly through a large volume (1). The gas chromatograph column must be able to effectively separate chemicals in the gas and volatile range, in order to provide some temporal distinction between the contents of urine headspace. It must also have a moderate degree of polarity, in order to affect both polar and non-polar compounds.

The control system around these two elements also has a large number of requirements in order to maintain the environmental conditions necessary for effective separation and detection. The temperature and humidity of the sensors should be closely monitored, as their response will be highly affected by these two factors (2). In addition, the inlet pressure and temperature of a gas chromatograph column dictates the flow rate and degree of separation through it at any given point (3). Thus the separation of chemicals through the chromatograph element must be monitored indirectly through measurement of both temperature and pressure, and the careful control of one of these. It has been decided to employ “temperature-controlled separation”, by keeping the inlet pressure constant while the temperature is varied through a tightly-controlled system in order to avoid varying the flow rate past the sensors and causing their responses to be affected (4). Flow rate through the system must also be carefully controlled, while the pressure must be maintained at a level to allow chromatography separation to occur. There must finally be a method by which the headspace samples can be introduced to the separation and sensing elements, and then switched to a supply of background air supply.

6.2. System Overview

The sensing and GC elements required an overarching control system to provide a suitable sampling method and to maintain optimal environmental conditions for separation and detection. A summary of the control method is shown in Figure 6.1, with a combined diagram of airflow and block diagram of sensors/transducers and control algorithms. The airflow system is shown in the top left corner, with blue lines pointing to locations of the components listed in the control algorithm below. The weightings and offsets applied to the comparators in this diagram have not been included for clarity, but were developed individually by empirical testing of each control loop. The temperature and humidity of the gas sensors affect their baseline response levels and subsequent sensitivity to chemicals

(2), and so were carefully monitored with changes limited throughout sample introduction. The separation from the GC column is dependent on the pressure and temperature experienced through its interior (3), and so were also carefully controlled in order to achieve a reasonable distinction.

6.2.1. Airflow Sub-system

The initial input of clean, dry air came in from the Supply Port and traveled through an MFC before splitting between make-up and sample flow (as shown in Figure 6.1). The make-up air passed into a second MFC, while the sample flow exited the machine at the Sample Outlet Port at a calculated flow rate equal to the value of the first MFC (total flow) minus that of the second (make-up flow). Thus the flow rate through a sample could be controlled while minimising the chance of any humidity or volatiles reaching the internal components of an MFC. This path flows across a volatile or headspace sample that is external to the instrument, picking up the released gases and volatiles before returning into the instrument at the Sample Inlet Port. The Sample Introduction Valve controlled the entry of headspace volume into the instrument, and the timeframe that it is open was tuned to balance a low temporal resolution of the GC separation with high sensor response levels. Any sample introduced into the system mixes with any make-up air flow in a linear mixing chamber (represented by a T-piece in Figure 6.1), and then entered the GC column to be separated according to molecular weight and polarity. Finally, the separated compounds passed through the sensor chambers before being expelled out of the Exhaust Outlet Port. The flow rate of air and sample headspace through the instrument was controlled in an open-circuit manner from the system perspective. This is due to the close circuit loop embedded in the MFCs themselves, but the system makes regular checks that the output voltage of the MFCs is within range and similar to demand. Valves were used to attenuate the flow rate through the MFCs to a proportional point between the minimum and

maximum flow rates, in this case 0 to 300 ml/min. The device would then read back the actual flow value that was being achieved and convert this back to another 0 to 5 V signal.

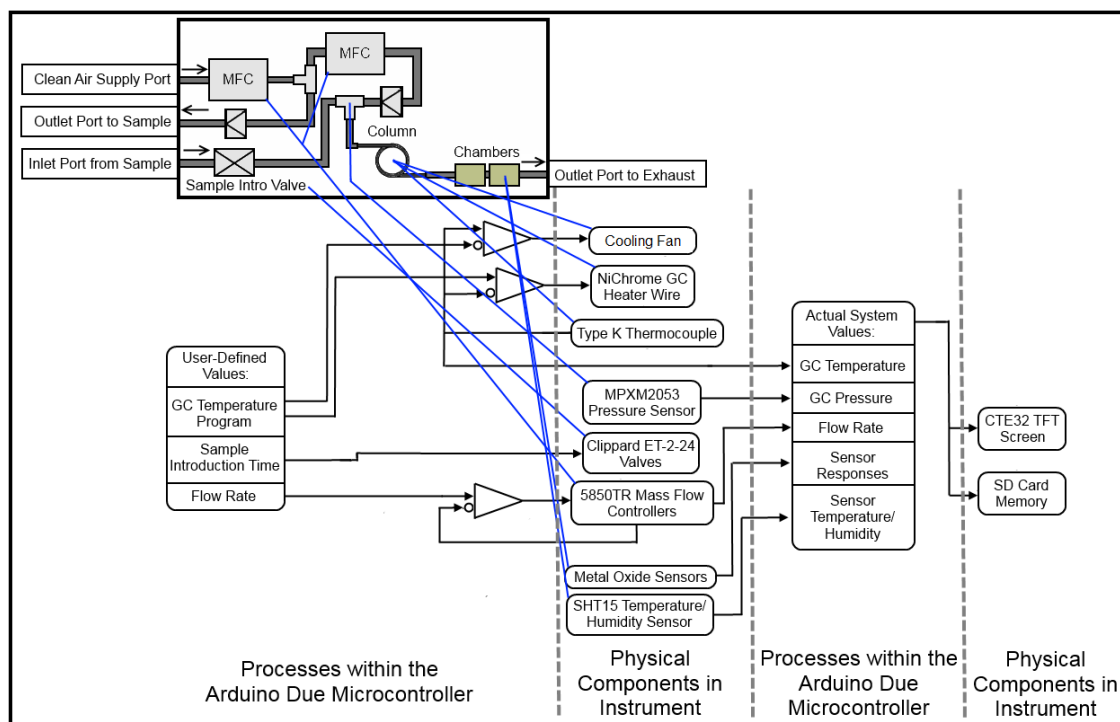


Figure 6.1: Illustration of the airflow system layout and the control algorithm used for the

WOLF 3.1

6.2.2. Chromatography Sub-system

The control of gas chromatography is a fine balance of pressure and temperature that pushes molecules through the column. A constant pressure of 1 bar was found to give the best results alongside careful control of the temperature to help accelerate differently-sized molecules through to the sensors. This is known as “temperature-controlled separation”, and should avoid an increasing flow rate past the sensors affecting their response. This is achieved using the opposing action of a length of Nickel-Chromium wire to heat the column, and a fan to cool it by drawing room-temperature air across it. Finally, a method for introducing a sample of urine headspace was developed to allow enough volume into the instrument to be measured by the sensors without limiting the temporal

resolution of the GC column. This was achieved by creating a difference in flow rate between the two MFCs and opening the sample introduction valve, which forced the remaining flow to pass through the sample and back into the instrument for analysis.

Throughout the course of sample analysis, the temperature of the GC column was also very carefully controlled according to the temperature program stored in the GC method array. The measurement of the actual temperature of the column and the update of the setpoint for heating it was updated every 200 ms, in order to be able to form a very responsive control loop around these variables. A pair of offsets was then applied to this value based on the measured temperature values taken by the thermocouple circuit. They incorporate both proportional and integral elements into the control loop, with maxima and minima chosen based on the values that provided the most stable output with optimisation of response time and overshoot/instability, taken from a large number of trials in adjusting these values. The resulting precision of this control loop was approximately 2 – 3 °C when running the temperature programs being used in Sections 6.6.3.2 and 7.2.2.2, which featured time periods when temperature was constant and other when it rose by approximately 0.13 °C per second.

The feedback loop for temperature control required two main physical elements, the heating element by which to enact the control onto the column from the processor, and a sensor to feed the actual temperature information back. The assembly of these two with the GC column formed a cohesive temperature management system, as shown in Figure 6.2 with a length of column and heater wire (depicted as a single coil of tubing) wrapped around a large metal pipe. This large thermal mass was used to better distribute the heat from the Nickel-Chromium (NiCr) wire across the whole of the column area. However, in order to secure these components to the rest of the case additions would have to be made to this design.

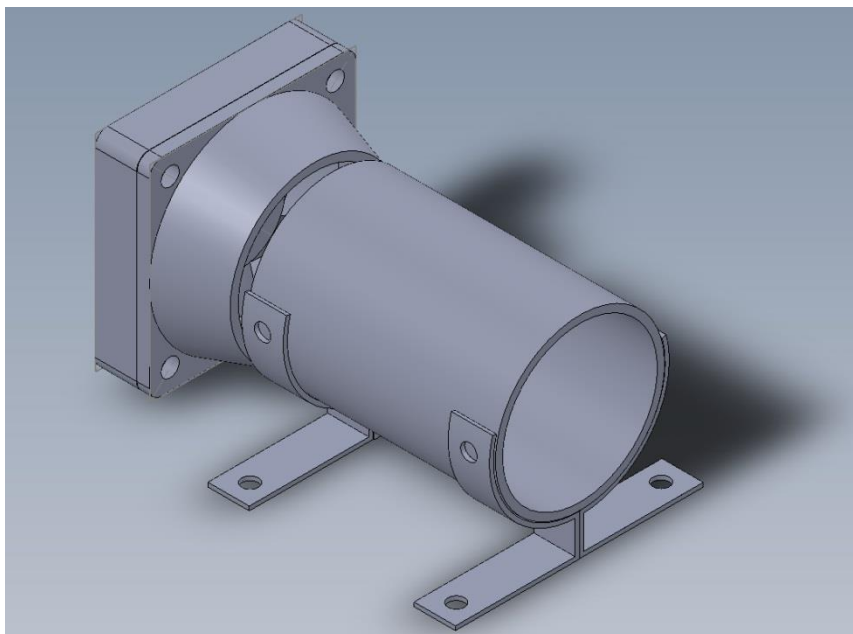


Figure 6.2: Model of the GC temperature control assembly in the WOLF 3.1 (NiCr wire and thermocouple wrapped around hollow bar)

Another form of temperature control actuation was created by the addition of a Multicomp MC36260 5 V fan with a DC brushless motor, also seen in Figure 6.2 located at the edge of the GC system's thermal mass. The fan was lined up with the internal diameter of a hollow steel bar which formed the thermal mass, so that it could effectively pull cool air through it while pushing heat out of vents in the WOLF 3.1 case. This action was particularly useful when cooling down the whole assembly more quickly following analysis (5).

The temperature sensing element comes in the form of a type K thermocouple in a long wire form factor (6). This thermocouple has a maximum temperature of 320 °C, meaning that it will not be damaged by overheating the NiCr wire.

6.2.3. Micropacked Column

The GC element that was used in the instrument was a 1 m long HayeSep R micropacked column with a 100/120 mesh and a 1.00 mm internal diameter (7). This column is made for

Development and Construction of the WOLF 3.1 GC/E-Nose Instrument

separating out gases and light volatiles with organic chemical groups, with a mild degree of polarity on the Hayesep R material and the mesh and length providing reasonable separation for C1 – C6 organic compounds. An example chromatogram of the separation of C1 – C3 compounds that can be achieved with this column with helium carrier gas in a full size GC instrument is illustrated in Figure 6.3. It has a rated temperature range up to 250 °C, and an outside diameter of 1/16” that allows for easy connection to standard Swagelok compression fittings. The recommended inlet pressure rating for this column is 30-45 psi, or approximately 2 – 3 bar (8).

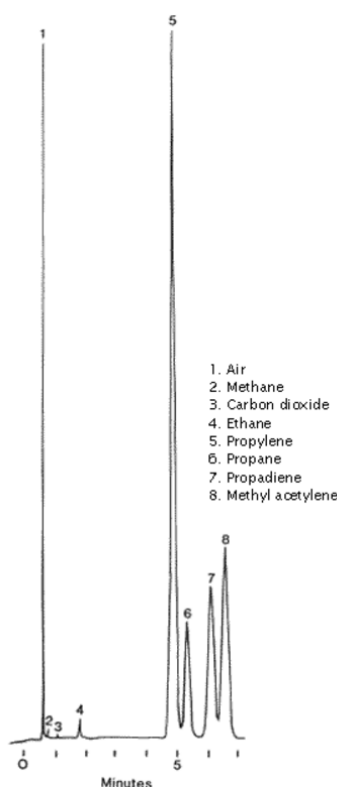


Figure 6.3: Chromatogram of HAYESEP R micropacked column separation of MAPP gases (9)

6.2.4. User Interface

The entire user interface for the WOLF 3.1 is operated using a 3.2” touchscreen (10). This GUI divides all potential activity on the instrument into three levels of control: basic running of samples based on the default method, development of the method by changing

timing and heating variables, and testing the base electronic circuitry and IC for fault diagnosis and resolution. Analysis can be run continuously by an unskilled user, while the higher levels allow for method development, maintenance and troubleshooting to be performed by those with more technical experience. This allows for easier introduction into the clinical setting, where everyday users may not be very experienced.

6.3. Sensor Technology

Sensors that have an extremely small form factor were required for this instrument in order to minimise dead volume within the gas sensor array. This is to maintain a good degree of the separation of chemicals coming from the GC column outlet even at the low flow rates produced. The only sensors that were deemed compact enough for this application were micro-hotplate metal oxide sensors, which are already currently produced by a small number of commercial manufacturers. These have separated heater and sensitive layers that are independent of the sensor itself, so that the sensitive layers can be brought to the correct temperature for performance without adversely affecting the response by electrical interference. The small form factor also allows for very rapid and low power heating and response times from this type of sensor. The full range of sensors included in the array on the WOLF 3.1 is shown in Table 6.1.

Manufacturer	Gas Sensor (target gas)	Sensitivity Range
SGX Sensortech	MiCS-2614 (Ozone)	10 - 1,000 ppm
	MiCS- 4514 (Nitrogen Dioxide)	0.05 - 5 ppm
	MiCS- 4514 (Carbon Monoxide)	1 - 1,000 ppm
	MiCS-5914 (Ammonia)	0.1 - 100 ppm
AppliedSensors GmbH	AS-MLV-P (VOCs)	0.1 - 100 ppm

Table 6.1: List of sensor manufacturers, mechanisms, and target gases included in the array

6.3.1. E2V MICS Sensors

The manufacturers SGX Sensortech (previously E2V Sensors) produce a range of low cost (sub £10 each) micro-hotplate gas sensors in the MICS range (11) that have a very small form factor of just 7.5 x 5.0 mm as shown in Figure 6.4. The sensor design consists of one basic N-type and P-type sensing layer, with specific sensitivities of these materials being harnessed by individual sensors employing different filters on the inlet of the physical casings. The range of sensors chosen to be used in this new instrument include the MICS-4514, 5914 and 2614 variants; the first of these contains one N-type and one P-type sensor that employ the same filter, and the others are single sensor packages. These three devices represent a single N-type and three versions of the P-type material with separate filters attached, giving manufacturer-tested sensitivities to carbon monoxide, nitrogen dioxide, ammonia and ozone, respectively. These will have sensitivities to many compounds that are known to be biologically-produced (12), duplicating some of those included in the previous WOLF 4.1 instrument, and shows a good overview of the variety of this sensor range for comparative test.

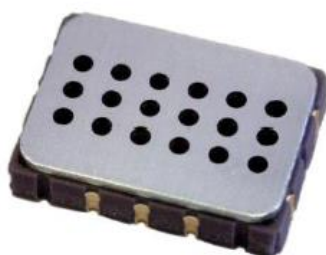


Figure 6.4: SGX Sensortech MICS sensor body (11)

The electronic control requirements for these sensors are reasonably straightforward, with a DC voltage supply used to provide adequate heating and power to the sensitive layer. An example of these circuits is displayed in Figure 6.5, for the dual sensor MICS-4514 in this

case. The voltage across the load resistors RLOAD_RED and RLOAD_OX can provide a simple bridge method for high resolution analogue measurement of the sensor resistance changes. These load resistors must have a value that is low enough to maximise sensitivity of the circuit to the sensor changes, while not going past a minimum value that could overload the voltage measurement equipment. The minimum acceptable resistance for RLOAD of all of the MICS sensors is provided on their datasheets as $820\ \Omega$ (11), and in order to avoid overloading the load resistance used in the measurement circuitry was $1\ \text{k}\Omega$.

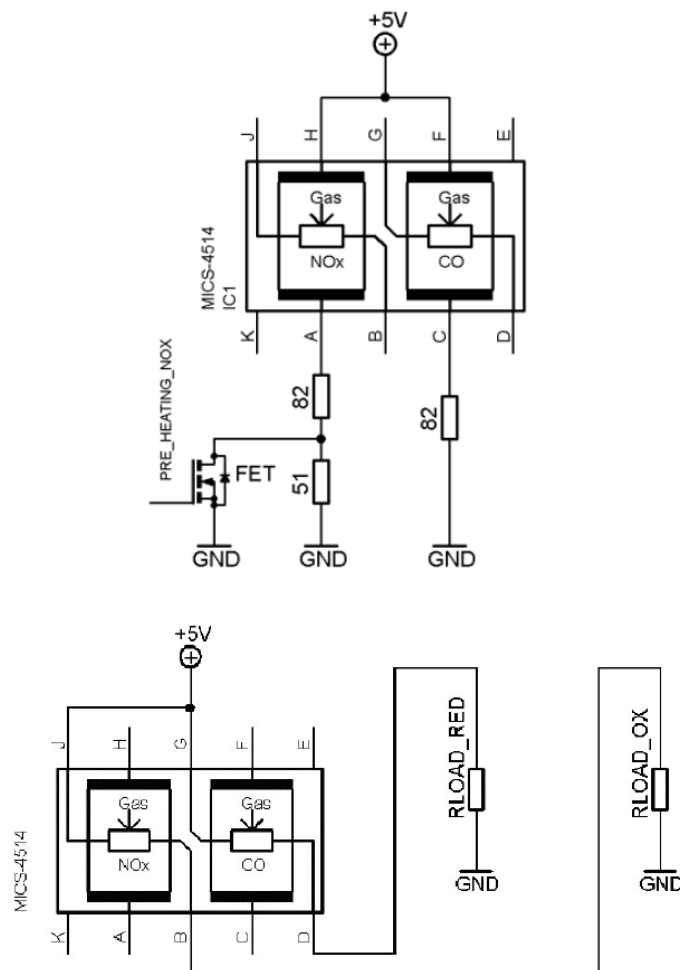


Figure 6.5: Typical MICS sensor heating and measurement circuits (11)

6.3.2. AppliedSensors AS_MLV_P Sensors

Another sensor that was chosen for use in the instrument was the AS-MLV-P from AppliedSensors GmbH (13). It was developed specifically to detect volatile organic compounds and is a much higher-end product in terms of quality and precision. A P-type sensing material is housed on a larger PCB in a 9.0 mm diameter canister-style package, with a total PCB area of 13.2 x 17.5 mm. This size (shown in Figure 6.6) is larger than the previously-described MICS sensors, but with a consistently low dead volume within the canister.



Figure 6.6: Appliedsensor AS-MLV-P sensor body (13)

The circuit board layout in Figure 6.7 displays the very small actual sensor size of approximately 2 mm², and the pinout locations of each of the sensing and heater pins allowing for surface mount and through-hole connection to the board. These simple dimensions will make the interface for a chamber to hold these sensors uncomplicated to produce. The electrical connections for this sensor are similar to those shown in Figure 6.5 for the MICS sensor, aside from the much higher sensing resistance of the AS-MLV-P requiring a larger value for the RLOAD resistor (611 k Ω was used in place of 1 k Ω).

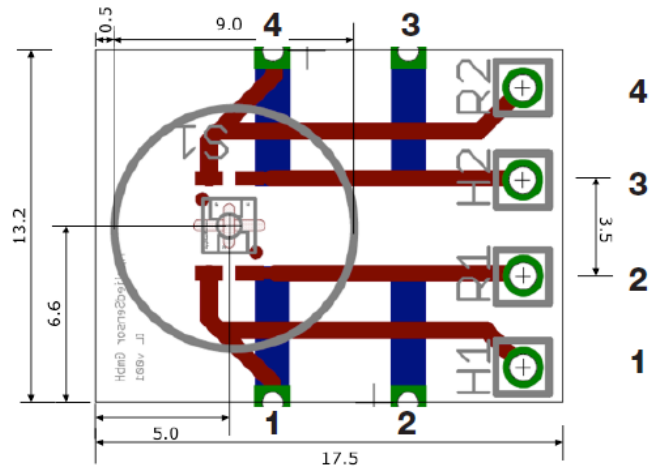


Figure 6.7: Appliedsensor AS-MLV-P sensor circuit layout (13)

6.3.2.1. Sensor Chambers

The sensor chambers developed for this instrument were required to fully house the sensors within a sealed flow path where samples could be introduced to them and then pass by and flush away. Due to the complicated and low resolution accuracy that would be required to machine such low volume chambers for these small form factor sensors, it was decided to print them on a highly accurate 3D-printing platform. Models of the desired chambers were developed on 3D computer-aided design (CAD) studio Solidworks (Dassault Systemes Solidworks Corp). The model for the chamber holding the four MICS sensors is illustrated in Figure 6.8. The chambers were designed to hold a PCB, with two sensors each soldered to them, on either side and fastened together using long 2.5 mm diameter screws. Figure 6.8 shows deeper square depressions made to house physical bodies of the MICS sensors, with shallow 10 mm diameter circular depressions around them to hold N-Buna rubber O-rings used to seal around the outside of the sensors.

When the ends of this chamber are threaded and attached to pneumatic fittings, this assembly would be able to expose the open sensing holes in the sensors to any gases travelling through the 3 mm diameter flow channel in the centre of the chamber. The total

volume of the flow channel and sensor interiors in the chamber is approximately 0.42 mL, which is a volume that should completely pass through to the outlet in 1.26 seconds at 20 ml/min chamber flow rate.

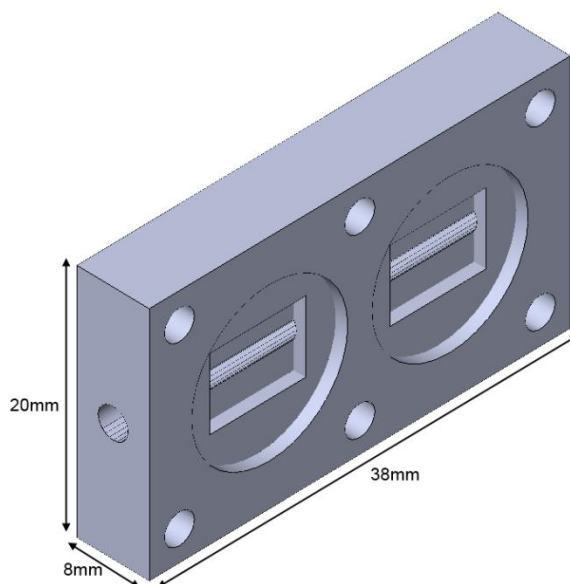


Figure 6.8: Scaled Solidworks model of the MICS sensor chamber

Chambers were designed for both MICS and AS-MLV-P sensors, and were subsequently made into prototypes by Envisiontec Micro DSP printer. The Micro DSP had a sufficient build volume to fully actualise these small chambers, and provided an impressive resolution of 50 μm (14) which minimised the chance of inaccuracies to cause issues with fitting or sealing. This printer employs a light projection technique to cure a liquid epoxy into complex shapes of hard, inflexible material. Due to the high Young's modulus of the resulting E-shell © epoxy produced from the curing process, the chambers were reasonably fragile and prone to breaking if handled incorrectly. The material could also degrade in temperatures over 180 °C, creating a potent odour that could over-saturate sensors. However, these temperatures were not experienced by the chambers within the proposed environment during any of the experimentation undertaken, and the advantage in

producing these complex shapes and features at such resolution and speed outweighed these drawbacks.

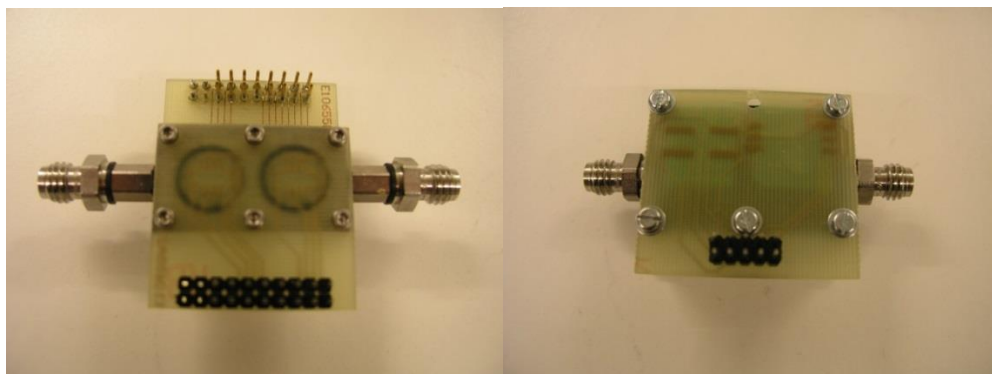


Figure 6.9: Photographs of fully assembled sensor chambers for the WOLF 3.1

The final prototypes of the 3D-printed chambers were attached to simple breakout PCBs for the appropriate sensors to connect them to a measurement board via ribbon cable, and sealed using O-rings and M2.5 nuts and bolts. The ends of the chambers' central flow channels were threaded and attached to 1/8th inch Swagelok fittings for connection to the wider airflow system. Figure 6.9 shows examples of the final chambers with fitted PCBs and fittings, which were used to test the sensitivities of the sensors and later implemented into the full instrument design.

6.3.3. Environmental Monitoring

The environment within the instrument was monitored by measuring the temperature, humidity and pressure at specific key points within the gas flow path through the instrument. The first of the devices used to monitor environmental conditions in the sensor chambers was the SHT15 temperature and humidity sensors from Sensirion (Sensirion AG, Switzerland) (shown in Section 5.3.2). This is a compact surface-mount sensor that can stably measure humidity and temperature down to a resolution of 0.05 % relative humidity and 0.01 °C respectively.

The other environmental monitoring sensor used in the instrument is a MPXM2053GS on-board pressure sensor from Freescale Semiconductor. This surface-mount sensor can measure the relative pressure at a range of 0 to 50 kPa from the top nozzle and outputs a proportional analogue voltage signal between 0 and 40 mV (15). This was used to monitor the pressure in the gas flow lines before the gas chromatography element, as the flow rate and degree of separation through it will be determined chiefly by the temperature of the column and the pressure difference across it.

6.4. Full Assembly

Once the models were created for each individual component, they were added and duplicated in a full assembly Solidworks model to represent the sum total of parts in the whole system. These were arranged in a physical configuration that held them efficiently within a cuboid volume with dimensions that would be preferred for a case, but with sufficient space between components such that pneumatic and electrical connections could be fit in between them. Using this volume as a rough reference, a number of different candidate cases were found that would most likely house the whole system within them with some extra margin to mitigate risk. The final decision for the chosen case involved consideration of the cost, availability and suitability of the options. This concluded with a brushed aluminium enclosure made by Nobsound and normally used for high definition audio equipment, with external dimensions of 221.5 x 150 x 311 mm.

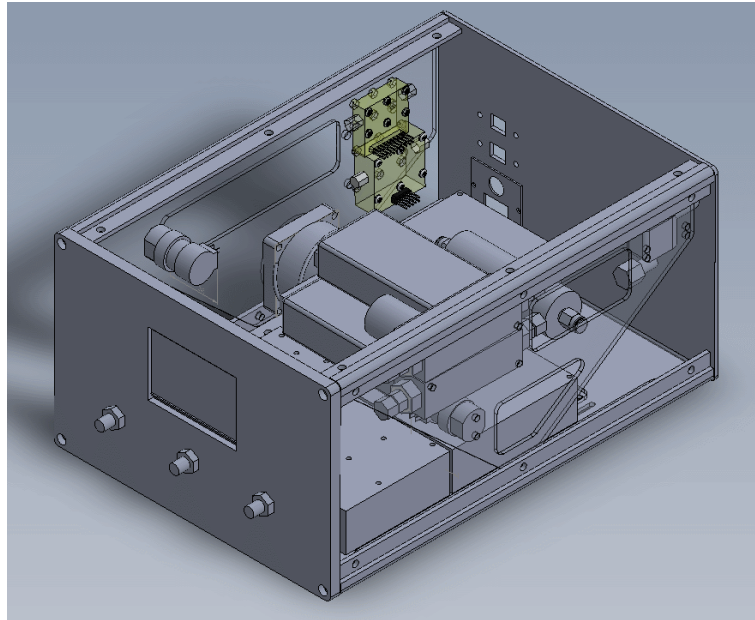


Figure 6.10: Full assembly Solidworks model for the WOLF 3.1 system

This enclosure was found to have more than ample volume to fit all of the required components, and was composed of panels on all sides that could be individually removed to easily perform maintenance and modifications on the instrument. Solidworks models were made of all of the required panels and fastening pieces of the enclosure, and were included in the full assembly of the whole system. The internal components were then placed inside the enclosure such that they could all be fit and fastened to its bottom or side panels, to ensure that this case was indeed suitable for housing the full system. The final assembly drawing is shown above in Figure 6.10, and also includes holes cut into the final enclosure to house the external USB sockets, power connections, bulkhead Swagelok fittings and the CTE32 touchscreen. The side and top panel models of the enclosure have been removed in order to better view the internal assembly of the system.

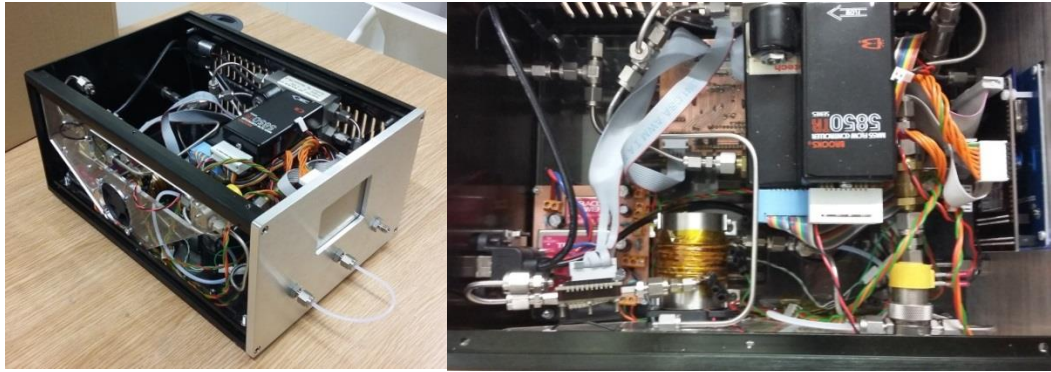


Figure 6.11: Final implementation of the WOLF 3.1 with exposed interior

Figure 6.11 shows the implementation of the full system based on the design detailed in the Solidworks full assembly model. The pneumatic and electrical connections have been fitted here, but the mixing chamber was omitted due to air pressure testing underway at the time. The overall positions of components are very similar to those proposed in the model, due to the acrylic structural plates being designed directly from it and the suitable amount of space left for internal connections. This also minimised the amount of re-prototyping that was required during construction and testing, thus drastically reducing the final build time for the instrument. The final construction also provides a large amount of space in the rear of the assembly, in order to fit the necessary pneumatic components and fittings required for an internally pumped system. These additions would be essential for use in locations without access to an external air supply, such as primary health centres. Figure 6.12 illustrates the final implementation of the instrument in operation with the full set of enclosure panels fitted.



Figure 6.12: Final implementation of the WOLF 3.1 in operation

6.5. Development and Construction of a Humidity Generator for the Sensor Testing Rig

6.5.1. Requirements and Objectives

New electronic nose instruments have been developed to discriminate between different disease states based on the gaseous emissions from urine samples. The sensors used in these instruments were designed to detect gases, and so the sensitivity of each sensor to many common gases was generally tested explicitly by the commercial manufacturers (16). However, volatiles are much less widely tested by sensor manufacturing companies. Therefore, the sensitivities of these sensors have to be tested in-house to ensure their suitability to the application before being tested with urine samples. This testing must be undertaken using a controlled method in order to ensure the accuracy and repeatability of these experiments. The instruments must be tested with a variety of volatiles with different active molecular groups, at a range of concentrations and humidity levels. The ranges of volatile concentration and relative humidities must be representative of levels seen from the headspace of urine samples (after heating). Individual sets of conditions within the two ranges must be maintained for minute-to-hour time periods with a reasonable resolution

Development and Construction of the WOLF 3.1 GC/E-Nose Instrument

and repeatability. The test system must ideally be automated in order to maximise its repeatability and add convenience of testing without constant monitoring.

There are many factors relevant in the production of accurate and repeatable volatile concentrations from stable standard samples that would make it very difficult and time-consuming to develop a test system completely. Therefore, it was decided to purchase a commercial volatile testing rig to be used for this purpose. Owlstone Inc. produces the OVG-4 high accuracy calibration gas generator, which uses permeation tubes to create highly accurate volatile concentration samples (17). A cased testing rig system named the GEN-SYS is also produced by Owlstone, which can provide 24 V DC power, clean air supply and RS-485 communications to up to three modular rack units (such as the OVG-4) that fit inside it (17). There is also a humidity unit available from Owlstone, but in order to minimise costs it was decided to develop an in-house built humidity generation unit to operate alongside the OGV-4 in one of the modular slots in the GEN-SYS testing rig. This module must be able to accurately and repeatably produce air flows of relative humidity concentrations from 0 to 90%, and at flow rates of up to 200 – 300 mL/min in order to provide most commercial electronic nose instruments their required conditions for samples. The commercially-produced modules compatible with the GEN-SYS use RS-485 communication, controlled externally from a laptop PC for automated testing. The developed humidity unit must be contained in a modular rack case identical to the units produced by Owlstone, along with the same 24 V power supply, rear compressed air supply, and RS-485 communication capabilities. The GEN-SYS also includes a water bubbler that is held in a holster on the side of the rig, which the developed unit must be able to use for generating air at the humidity levels stated above.

6.5.2. Control and Measurement System for Humidity Unit

The purpose of the pneumatics system is to provide a single airflow output with a range of humidities. A bottle was provided with the OVG unit to be used to bubble air through a volume of water for humidifying the output. The bottle contains two ports attached to a modified lid that connect using Swagelok, including an inlet with an internal bubbler attached to push the airflow underneath the water line. Therefore, external fittings should be included in the design to push some flow through the bottle. A number of internal environmental conditions must also be monitored in order to have an effective picture of the effects of different actuation. The chief factor to be measured is humidity, but other conditions such as temperature and internal pressure are also helpful in order to understand what is occurring within the machine. Finally, information on all of the measurement and actuation states of the components should be communicated to both the user and external devices, such as the control PC for the OVG rig. Each of these operations is done by one of the electronic circuits present within the humidity generator.

All of the processes of actuation, measurement and communication must have the possibility to be undertaken simultaneously, and managed effectively by the system. It was proposed that the simplest way of keeping track of all of these operations is for them to be controlled by a single central processing unit. Some internal memory was required as well, in order to store a number of internal variables for control functionality, and to send some of these back through RS485 communication.

The proposed system design is shown in Figure 6.13, including the flowpath diagram on the top half linking to a representation of the control and measurement algorithm on the bottom half. The flow paths diverging from the clean air supply are each controlled by one Brooks 5850TR mass flow controller (MFC – coloured green). There is also an extra in-line valve in place just before the MFCs and just before the final outlet, in order to halt any

Development and Construction of the WOLF 3.1 GC/E-Nose Instrument

forward or back-pressure in the system when flow rate is zero through either/both of the paths (coloured yellow). One of these controlled flow paths passes through an outlet port, through the bubbler to add water vapour to the air, and back in through the inlet port on the bottom face of the diagram. Both of these flow paths, one that has been humidified and one that hasn't, meet within a mixing chamber and the humidity is measured (coloured teal). This measured humid air path is then sent to the final machine outlet port, to be combined with outlets from the other units to provide external systems with testing standards.

The user inputs to the humidity system are a pair of set-point values to aim for, in the form of total flow rate and relative humidity of air through the final outlet port ("to Analyser" in Figure 6.13). Resolution of these set-points is currently 1 mL/min and 1 %RH, respectively. A calculation is made to convert these into a proposed flow rate for the dry and humid flow paths. Closed loop control of total flow rate against the user-defined set-point is maintained by measurement of the calculated sum of the rates through both of the MFCs. Meanwhile, humidity is controlled by measuring at the end of the mixing chamber by an appropriate sensor with the value set by the user. The 5850TR MFC has an accuracy of ± 3.00 mL/min and a repeatability of ± 0.75 mL/min, which are both within a suitable range for reasonably accurate operation (18).

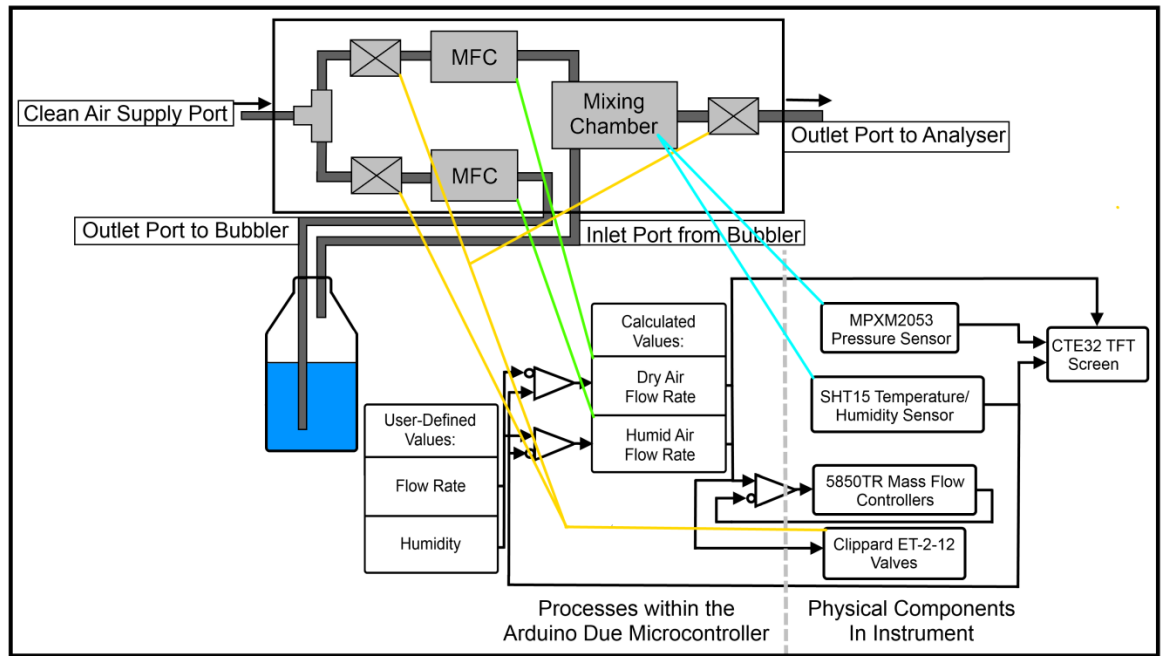


Figure 6.13: Diagram of the airflow pathways and control algorithm of the humidity rig control system

There are a number of environmental conditions that need to be monitored on the humidity rig so that the user can ensure that the system is operating normally. The most relevant of these is humidity – it is important to have a measurement device that is independent of the airflow system to ensure that the output air from the rig has the correct concentration of water vapour. Internal air temperature is also a relevant environmental metric, as this could be a factor affecting the response of the sensors that the rig is testing. Both of these conditions are measured by the same element, the SHT15 temperature/humidity sensor from Sensirion shown in Section 5.3.2 (19). The SHT15 has a maximum resolution of 0.4 %RH, accuracy of ± 2.0 %RH and repeatability of ± 0.1 %RH, which is reasonable for measurement in the humidity control loop considering variations in urine sample humidity (as described in detail in Section 7.1.3).

Another useful environmental condition to monitor is internal pressure in the air lines, as this can help determine whether there is a change in the flow path such as a leak (constituting a drop in pressure) or blockage (which could manifest as a rise or drop in pressure). The pressure in the mixing chamber of the rig is measured by the Freescale MPXM2053GS 0 – 50 kPa pressure sensor (15). The pressure values do not require a large amount of accuracy (similar to temperature), as it is not part of the control algorithm but is helpful to the user to ensure the rig's safe operation. The algorithms for the control processes operating within the humidity unit (shown in Figure 6.13) were translated in to 'C' or Arduino 'C++' languages and programmed onto the Arduino Due's SAM3X chip.

6.5.3. Assembly and Integration

The choice of components and design of the overall structure by Solidworks modelling was followed by the final physical assembly of the humidity unit in the machined enclosure, and integration with the overall testing rig.

The assembled unit was put in place as shown in Figure 6.14. All connections to the overall rig come in from the rear of the unit (17). The inlet and outlet of a water bubbler is connected to the bottom two Swagelok connectors on the front panel of the humidity unit, with the top bulkhead used to connect the final output of the unit onto the wider testing rig pneumatic connection.



Figure 6.14: Photograph of the assembled full testing rig

The RS-485 communications socket at the rear of the testing rig is connected to an adaptor to convert the signal format to USB and sent to the external control PC. This interacts with the units in the testing rig using software developed in LabVIEW 2014 by James Covington, which is built around a core program designed to communicate with Eurotherm 3216 temperature controllers and supplied by Owlstone (17). The fully integrated software allows a user to either manually control actuation of the volatile and humidity generation units, or define an automated test where volatile concentrations and humidity levels will be sent to the device under test at accurately controlled time periods. A number of indicators for flow rates, temperature and humidity of the units and output are shown on the front screen, and are taken from value sent to the PC via RS-485 communication.

6.6. Experimental Testing of GC/E-Nose WOLF 3.1 with Single Volatile Samples

6.6.1. Introduction

The LDA urine distinction results from the WOLF 4.1 shown in Section 8.2.4 indicated that an electronic nose-based diagnostic solution could be possible. However, the sensitivity and specificity levels produced by sensor array alone did not compare favourably against current clinical techniques. A new system was proposed that could offer improved capability for volatile/gas distinction over the previously-tested instruments by employing a gas chromatography (GC) pre-separation method. This technology uses a tubed column filled with a chemically-retentive matrix, which can effectively separate mixed gas phase chemicals according to molecular weight and polarity. Separation by GC has been found to be very effective in revealing unique features of the content of urine headspace in Chapter 3. The addition adds a temporal element to the response of each sensor to all gases or volatiles, and so a smaller number of sensors may be required to distinguish samples with different mixtures.

To this end a new GC/electronic nose instrument was developed in-house for the purpose of distinguishing between digestive disease groups - again by using the volatile content of urine headspace samples, and denoted the WOLF 3.1 (described in Chapter 7). As per the WOLF 4.1, this new system needed to be validated with known chemical standards in order to evaluate its performance in its designed application. The main reasons for this initial testing are: to check whether the sensors respond to samples of volatile chemicals with a range of functional groups in manners that are distinctive to one another, and to ensure that these groups are also retained effectively by the GC column to separate their responses from each-other within a reasonable timeframe for clinical diagnostic requirements.

Development and Construction of the WOLF 3.1 GC/E-Nose Instrument

The experiments to test for sensor response must be performed across a range of concentrations for each individual volatile, in order to determine the relationship between response level and amount of sample being introduced to the sensors. The effect of relative humidity of the sample supply being sent on the sensors must also be investigated, as the metal oxide sensors included in the WOLF 3.1 are known to be highly affected by environmental humidity (6, 7, 20 + 21). Therefore, the response of the sensors at each volatile concentration must also be tested at a range of relative humidity levels that includes what is seen from urine headspace samples as seen in previous commercial studies (Chapter 4). The relative humidity levels tested must also be comprehensive enough to gain sufficient understanding in the relationship between sensor response and environmental humidity.

The GC retention testing must include runs with a similar number and scope of volatiles as the response tests described in Section 5.5.2, and across a similar range of concentrations. The water content of the samples will be retained by the column similar to other sample constituents and will likely be introduced separately to the target volatiles, and so the relative humidity level will not factor greatly into the response of these tests. Therefore, an appropriate level of relative humidity will be chosen that is similar to that seen in a typical urine headspace sample, and be used across all tests in this section. This round of experimentation will also have the additional purpose of allowing for development of an appropriate machine method to be used on the WOLF 3.1 when running urine samples. Conditions to be determined by this method development include: the flow rate characteristics through the instrument, the baseline, sample introduction and purge times, and the GC temperature program to be used to effective separation of different volatile groups.

6.6.2. Materials and Methods

The WOLF 3.1 was used in all of the tests described in this section, without the GC column attached for the sensor sensitivity tests and in its final full construction for the GC retention testing. The pneumatic system for the WOLF 3.1 is shown in Figure 6.15, which includes the original compressed air inlet to the machine at the top left port, sample supply and inlet on the middle and bottom left, and the machine exhaust on the bottom right. The air supply entering the left inlet was provided by the same Zero Air Generator described in Section 4.2.1. The volatile testing rig being used to provide accurate volatile samples already feeds from a compressed air supply, and it was not possible for it and the WOLF 3.1 to communicate to each-other. Therefore, care had to be taken with all of these tests as to which of the machines was in full control of sample introduction and which was taking on a passive role for supply or measurement.

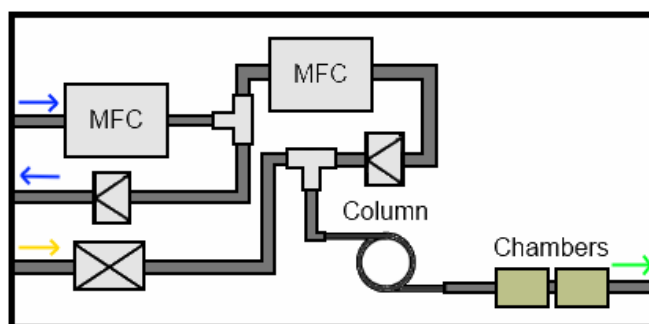


Figure 6.15: Schematic of the pneumatic system in the WOLF 3.1

The supply of volatile concentrations and humidity levels for testing the WOLF 3.1 were all given by the volatile testing rig. The central unit in the rig uses permeation tubes to supply an accurate concentration of a single volatile at a specified flow rate at its outlet (located in the centre of the unit and pictured with tubing connected to it), and was developed by Owlstone (22). The right-most unit uses an external bubbler that is normally connected to the bottom two ports on its front to provide air supply at a stable relative humidity and

Development and Construction of the WOLF 3.1 GC/E-Nose Instrument

specified flow rate to its outlet (located on the top port along the right side of its front face). The outlets of these two units were connected together using a 1/8" Swagelok 3-way connector and sent to the sample inlet of the WOLF 3.1 to provide sample supply.

The volatile testing rig was controlled by an external PC running the LabVIEW 2014 program based on a core developed by Owlstone (23), and expanded to fit this actual application in-house. This software allows a user to control the units in the testing rig manually from the front-end display pictured in Figure 6.16. There is also an option to set up a test sequence that may be run automatically without user input, from a separate tabular section of the program. The software controls the flow rates, humidity and calculated volatile concentration from the two units according to the test sequence previously setup, and then monitors and displays measured values in numerical and graph form.

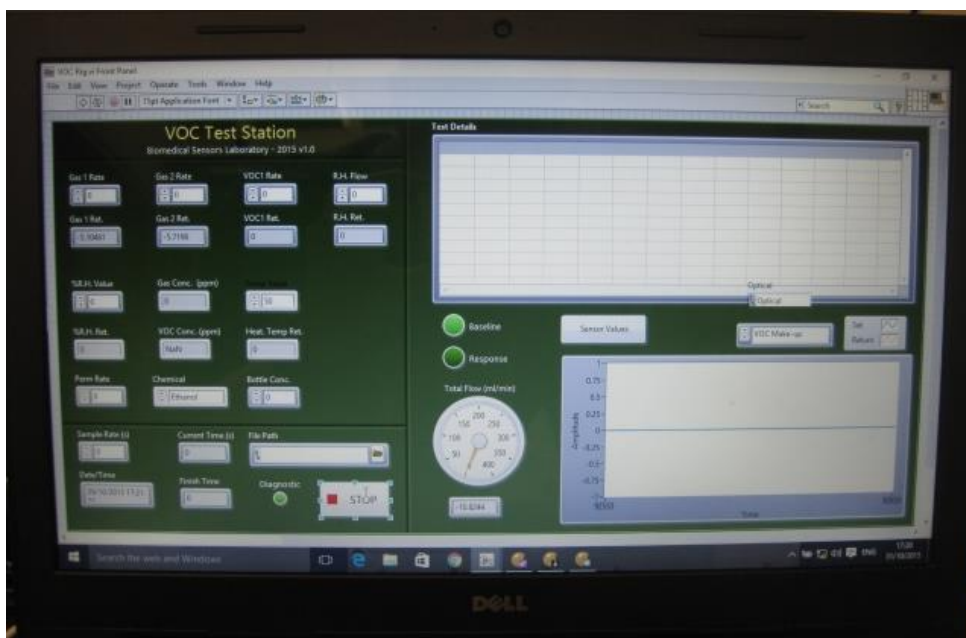


Figure 6.16: LabVIEW PC control front-end of the volatile testing rig

Single tests were executed, each at a specified volatile concentration and humidity, in order to ensure that timing was constant throughout testing and that any offset were not introduced between these runs. The volatile rig outlet was allowed to run straight to a laboratory exhaust port for a period of a few minutes before sample introduction to ensure that the specified concentration and humidity conditions had propagated to the end of the outlet tubing. In all tests the combined flow rate for the volatile test rig outlet and those in the WOLF 3.1 were all set to the same value, to prevent any back-up of pressure causing complications to the test or damage to the machines. Note that the concentrations of single volatile samples produced by this rig are in terms of volume in air, and so are the concentrations actually being experienced by the sensors. While this is an effective method for testing the sensitivity of the sensors, these results cannot be directly compared with responses of other instruments in this investigation to single volatile samples being made using another method (such as in Section 5.5.3).

6.6.2.1. Method Development

Initial method development was carried out with just the sensors being tested and then with GC retention tests. This was done to ensure that all relevant chemical information was being captured, distinction between different samples was represented and that the tests could be completed in a timeframe that would be clinically acceptable. For sensor sensitivity tests, a range of different flow rates were attempted in order to balance what was thought to be the resulting GC flow rate and the unsaturated response from the sensors. The general expectation of the resolution of sensors (6, 7, 20, 21) and the volatile concentrations present in urine headspace samples (24) led to the concentrations being chosen for test.

The GC retention test method contained a much larger set of condition variables that needed to be specified before full execution could be completed. The flow rate that could

Development and Construction of the WOLF 3.1 GC/E-Nose Instrument

be achieved through the GC was first required in order to continue with further testing. Once this was measured and set, an appropriate temperature program needed to be specified for detection of the target volatiles in a timeframe that was acceptable as compared to other electronic nose applications. Initially, programs that involved single constant temperatures including 60°C and 80°C were used. While these methods would have given very accurate measurement of response to gases and very light volatiles, the timescale required to provide this would be an hour or more with the current GC column. In addition, the larger volatile groups being sent through from some samples may remain retained in the column until a subsequent sample is introduced. However, when these single constant temperatures were increased to higher levels such as 120 – 160 °C, the level of temporal discrimination seen between different light volatiles was negligible.

Experimentation using a few initial urine samples determined that 100 seconds of introduction time gave a good level of response while maintaining some degree of separation. This was calculated by understanding the volumes between the headspace sample and the flow path to the GC column shuttered by the inlet valve. The tubing used in the WOLF 3.1 has an internal diameter of 1.59 mm, and the length from the sample headspace to the inlet valve in the experimental setup was approximately 250 mm. Adding in the internal volumes of the in-line fittings and the valve itself, this leaves a total volume from the sample to the inlet of 1.09 mL. The volume of headspace within the sample (12mL from the vial size minus the liquid sample volume) must be added to this total to make 13.09 mL of headspace that must be sent past into the GC column. This would take a total of approximately 39.3 seconds to reach past the GC column, and so the sample introduction time must be at least this time period to send the entire headspace volume through the GC column if total headspace volume transfer could be assumed. However, the sample outlet and inlet lines were adjacent at the top of the vial cap, leaving the possibility

of a flow path to be created across the top of the headspace volume without pulling in the volatile content closest to the liquid urine. This means that it could take considerably longer to remove the entire volatile headspace from the vial from turbulent flow, and so the introduction time was increased by a factor of approximately 2.5.

The next temperature methods used in development included an initial constant low temperature followed by a controlled rise up to a maximum, and finally a constant high temperature stage. Several variables were adjusted across a range of values, including initial and final temperatures, as well as the times to hold each and ramp between them. The reasonable ranges used for each of the variables were found by drawing upon technical resources from the GC column manufacture Restek (25), and from previous studies completed by Richard Sacks in the development of GC-based instruments and temperature control methods (26). The final proposed method detailed in Section 8.3.2.2 balances a significant level of discrimination between the different volatile groups under test, the potential to capture a wider molecular weight range of gases and volatiles, and an acceptable length of analysis time. It was also discovered through initial sample trials and further review of Richard Sacks studies that the sample introduction period must also be very carefully tuned in order to avoid overlap of volatile retention times through the GC and over-saturation of sensors. This was also tested at a range of values, before optimising volatile discrimination and clarity of response separation from urine samples using the proposed introduction time period.

6.6.2.2. Proposed Experimental Method

6.6.2.2.1. Sensor Sensitivity Testing Method

The WOLF 3.1 was used as a passive measurement unit in the sensor sensitivity tests. Sensor measurements started approximately two minutes before an automated test

Development and Construction of the WOLF 3.1 GC/E-Nose Instrument

sample introduction method began on the volatile test rig. These measurements continued throughout the volatile rig method and for a short while afterwards. These experiments were performed in a total time of 760 seconds, with instrument initial baseline set to 1 second and final purge time of 10 seconds. The compressed air supply inlet and the sample supply port on the instrument were closed with 1/8" Swagelok end pieces, and the sample inlet was connected to the outlets of the volatile and humidity supplies of the testing rig. The humidity levels were initially introduced to the WOLF 3.1 sensors to provide an initial baseline for 300 seconds, and then the volatile concentration was supplied for 150 seconds to establish a new stable response level. A final purge of 300 seconds was then executed by the volatile testing rig to remove the volatile from the sensor chambers. The total flow rate of air sent through to the WOLF 3.1 was 100 mL/minute.

A total of four volatile samples were used to determine sensor sensitivity including acetone, ethanol, toluene and valeraldehyde, which each have a different molecular weight, polarity and functional chemical group. Relative humidity levels of the background air of the samples were in the range of 0 – 20% with steps of 5%. The sample concentrations tested included steps of 10, 20, 50 and 100 ppm to capture a reasonable range of concentrations seen from urine headspace samples (22). For each of the test runs at a specified volatile concentration and relative humidity, the final stable response level seen at the end of the 150-second sample introduction period was taken from the test data for each sensor. These values were plotted on two sets of separate graphs, to determine the relationships of sensor response against the both the relative humidity and the specific volatile concentration supplied from the volatile rig.

6.6.2.2.2. GC Retention Testing Method

In the GC retention tests, the WOLF 3.1 was used to control the sample introduction to the GC and sensor elements, while the volatile testing rig was setup as a passive supply unit.

Development and Construction of the WOLF 3.1 GC/E-Nose Instrument

The rig was set to simply supply a specified humidity and volatile concentration level for a specified period of time. The compressed air supply inlet port on the instrument was connected to the laboratory air supply, while the sample supply port was kept closed with a 1/8" Swagelok end connector. The total test time for GC retention was 1500 seconds, and was set to emulate the actual clinical test time for urine samples. An initial baseline was set for the first 300 seconds, after which the sample was introduced to the inlet of the GC column for 100 seconds. A period of 980 seconds where only dry air was provided to the system then took place. This was done so that the introduced sample could travel through the column and be sent across the sensors. During 1080 seconds, which included the sample introduction and response periods, a temperature program was run on the GC with an initial temperature of 80 °C held for 120 seconds. The temperature was started on a controlled ramp for 780 seconds from 80 °C to a final temperature of 180 °C, which is then held for an additional 180 seconds. Once the response data had been gathered, a final purge of 300 seconds was instigated at 180 °C through the column and sensors in order to remove any leftover sample in the system. The flow rate sent through the GC column was 50 mL/minute at all points throughout the tests.

The same four volatile compounds were used in this test as in the sensor sensitivity testing in Section 8.3.3.2.1, at a range of concentrations covering 10 to 50 ppm. These were all introduced at a relative humidity of 5%, as this is similar to the level seen by the WOLF 4.1 study shown in Section 8.1 from urine headspace samples. The water vapour that causes the humidity levels in these samples will also be separated from the volatile portions, and so the relationship between the responses of volatiles at different humidity levels is not required for the full system. The resulting response traces were then plotted against measurement time in order to determine the regions of time where different volatiles were sent from the column outlet and introduced to the sensors.

6.6.3. Results and Discussion

6.6.3.1. Sensor Sensitivity Tests

A number of tests were completed with only the sensor array connected in the pneumatic system, in order to test their sensitivities to volatile groups without the GC element. A total of four volatile groups were used as standards, including acetone, ethanol, toluene and valeraldehyde (or pentanal). For each of the individual tests, a single volatile sample (at a specified relative humidity) was supplied from the testing rig described in Chapter 4. The background humidity was first supplied at the start of testing during the “Baseline” stage, with the actual volatile being introduced after 300 seconds at the “Sample” stage, which lasted a further 150 seconds. Finally the sample is removed and then a 300-second “Purge” occurs. This test method was repeated for sample concentrations of 10, 20, 50 and 100 ppm and relative humidities in the range of 0 – 20% in steps of 5%. These conditions were chosen by encompassing the range of relative humidities that could be produced from a urine headspace sample when heated up to 10 minutes, and a reasonable range of volatile concentrations that are well above the sensor resolutions, but lower than estimated saturation levels.

Each of these tests produced a text file with a column of response data from each sensor and a timestamp for each recorded value. The final resting level of the sensor response at the end of “Sample” (at 450 seconds) was taken from each sensor’s response at each humidity and concentration, and plotted as graphs showing the relationship of these values with the relative humidity across a single concentration. Separate graphs were also plotted showing the relationship between sensor response and volatile concentration across the full range of relative humidity. These results are shown in this section, with the response changes used to indicate the level of sensitivity of the sensors to both humidity and volatile concentrations.

Sensor response traces shown in the remainder of Section 6.6.3 all have associated colours as detailed in Table 6.2.

Sensor Name	CO	NH3	H2S	O3	AS-MLV-P
Response Colour	Black	Red	Green	Yellow	Blue

Table 6.2: Corresponding response colours for WOLF 3.1 sensors in Section 6.6.3

6.6.3.1.1. Acetone Sensor Test

Figure 6.17 shows the variation in sensor response to 10 ppm acetone concentrations at a range of relative humidity levels between 0 and 20%. A strong positive correlation between humidity and response level can be easily seen in many of the plots, particularly in the CO sensor with a minor variation seen in the O3 sensor. Very little change is seen in both the NH3 and H2S sensors, which could be potentially due to saturation of the sensor.

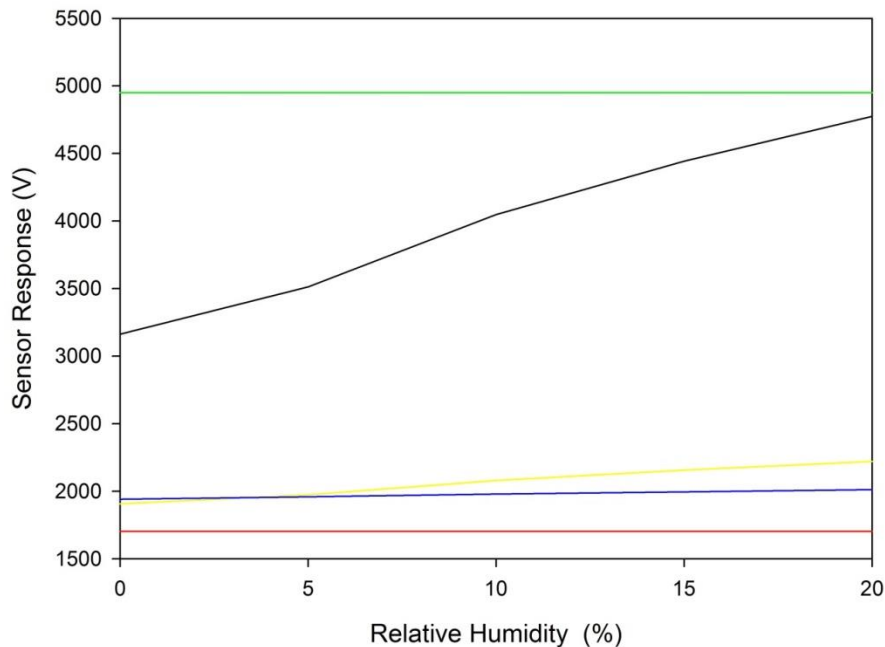


Figure 6.17: Graph of the relationship between sensor response and relative humidity at 10 ppm acetone concentration

Development and Construction of the WOLF 3.1 GC/E-Nose Instrument

The relationships between acetone concentration of samples and sensor response at relative humidity levels ranging from 0-20% inclusive are shown in Figure 6.18. There is a positive increase in responses from the CO, O₃ and AS-MLV-P sensors with increasing concentrations of acetones, with little to no change from the remaining devices throughout the full range. A number of variations in response can be seen with increasing humidity. In particular, the offset voltage of the CO and O₃ sensors can be seen to have a positive correlation with humidity, but the overall gradient of response change over concentration does not seem to change. The H₂S sensor seems to be overloaded in all of these examples of introduction to acetone.

Development and Construction of the WOLF 3.1 GC/E-Nose Instrument

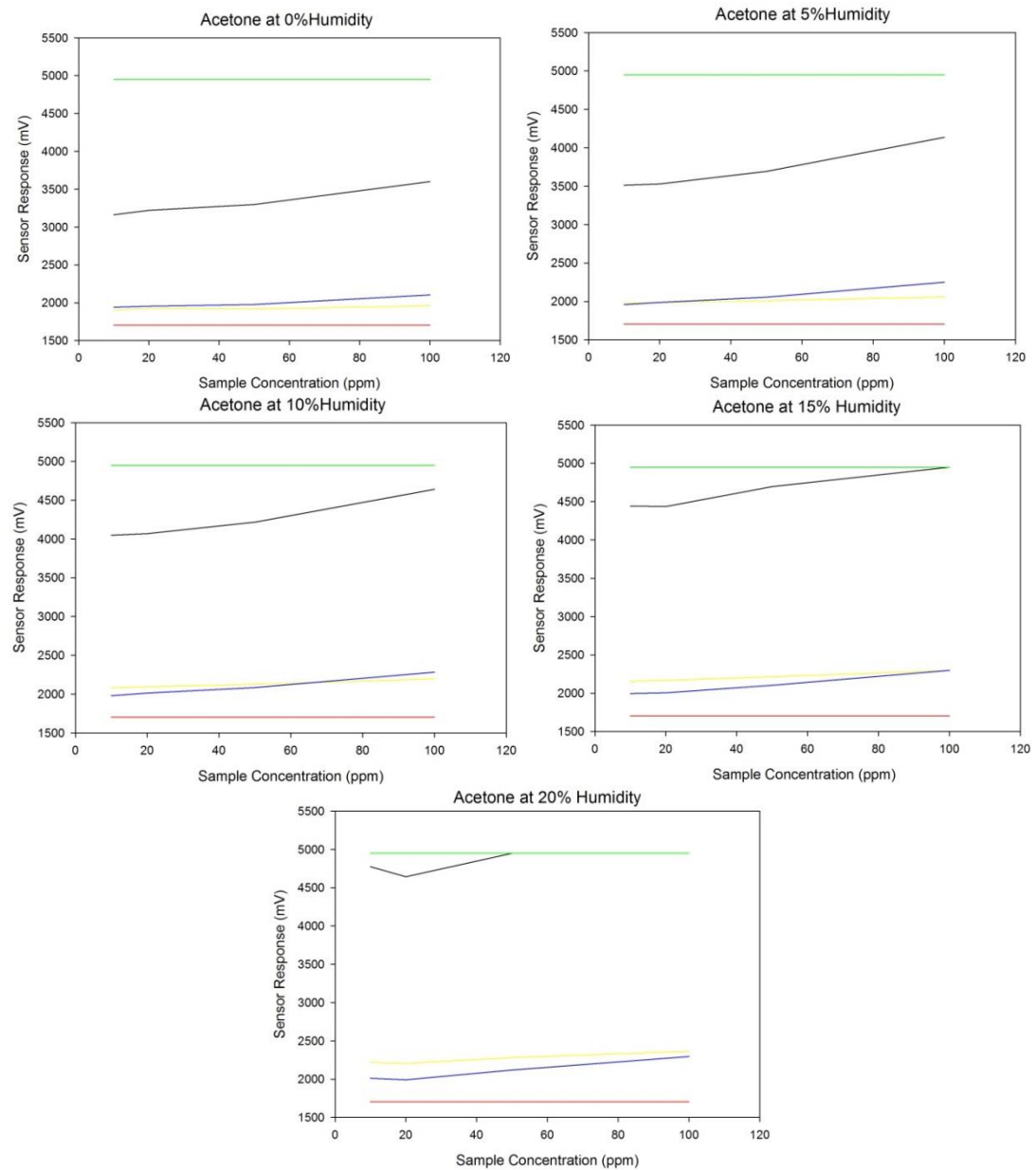


Figure 6.18: Graphs showing the relationship between sensor responses and 10 – 100 ppm concentrations of acetone at relative humidity levels of 0%, 5%, 10%, 15% and 20%

6.6.3.1.2. Ethanol Sensor Test

Figure 6.19 displays the response characteristics of the sensors with increasing sample concentration of ethanol, within the specified 0-20% humidity level range. It can be seen that the CO and NH₃ sensors only exhibit a very small or non-existent change in response with ethanol concentration within the 10 – 100 ppm range. However, the remaining

Development and Construction of the WOLF 3.1 GC/E-Nose Instrument

sensors show a strong positive correlation with ethanol concentration. The change in response of the H₂S sensor is particularly extreme at higher humidity levels, while being somewhat erratic at lower concentrations throughout the full humidity range.

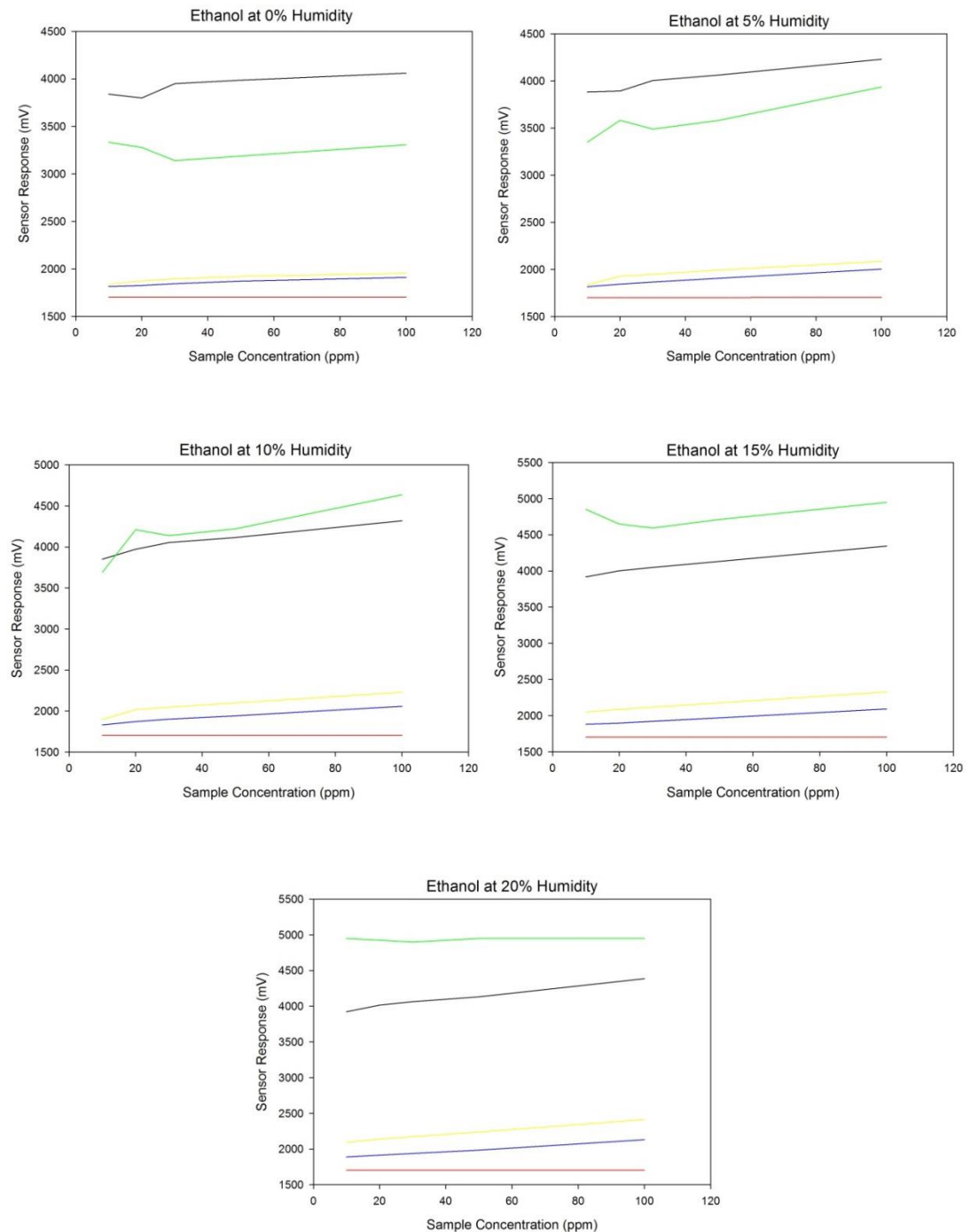


Figure 6.19: Graphs showing the relationship between sensor responses and 10 – 100 ppm concentrations of ethanol at relative humidity levels of 0%, 5%, 10%, 15% and 20%

6.6.3.1.3. Toluene Sensor Test

The response characteristics of the sensors after introduction to 10 – 100ppm concentrations of toluene are seen in Figure 6.20. The erroneous behaviour seen in the H2S and AS-MLV-P sensors is due to the order in which tests, at particular sample concentrations, were executed. These two sensors seem to have some hysteresis to their response to samples, as reflected by their increasing response to temporally consecutive tests. However, AS-MLV-P and CO sensors still show some positive correlation between toluene concentration and final body resistance.

Development and Construction of the WOLF 3.1 GC/E-Nose Instrument

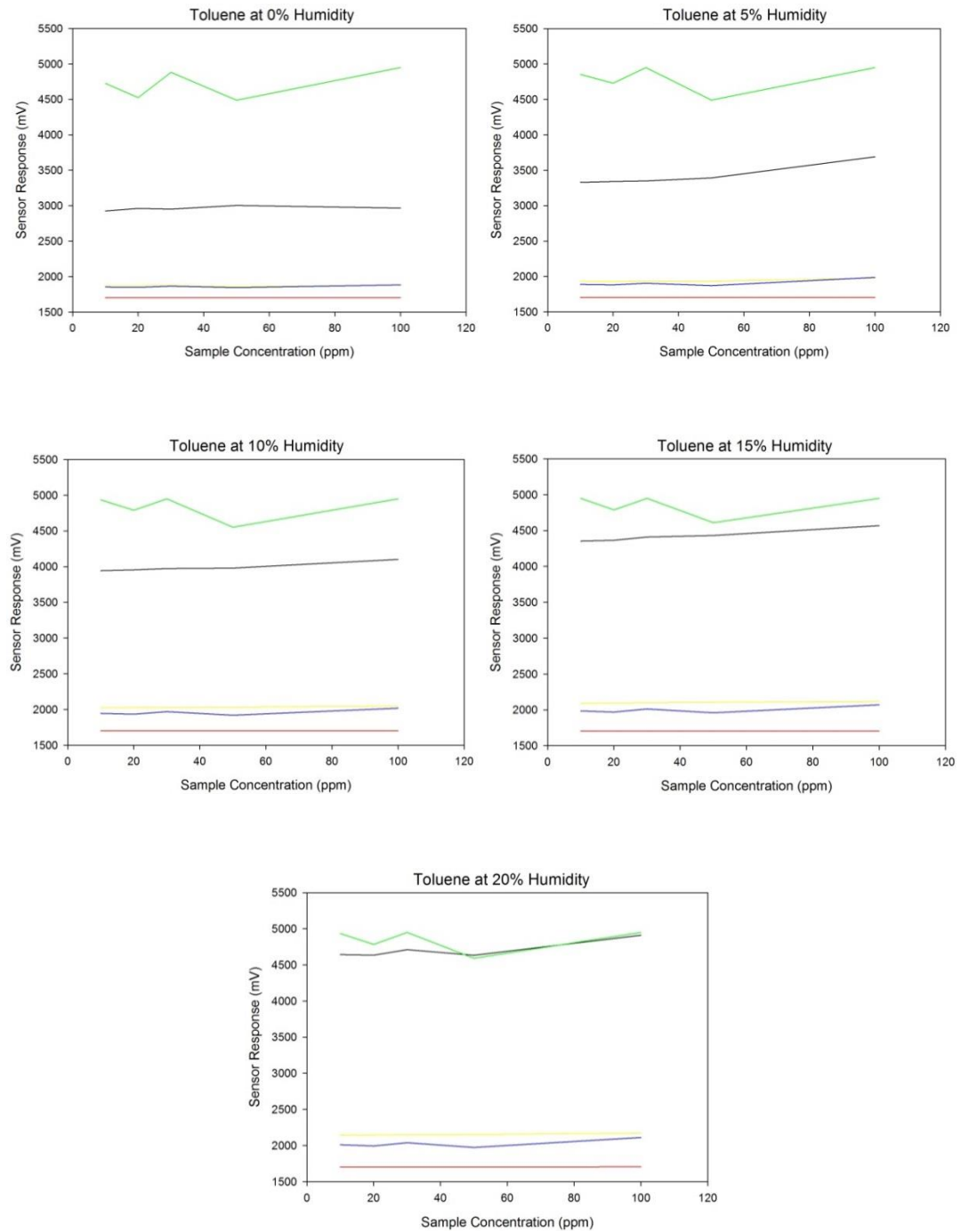


Figure 6.20: Graphs showing the relationship between sensor responses and 10 – 100 ppm concentrations of toluene at relative humidity levels of 0%, 5%, 10%, 15% and 20%

6.6.3.1.4. Valeraldehyde Sensor Test

Figure 6.21 illustrates the response of the sensors to concentrations of valeraldehyde in the range of 10 – 100 ppm at the relative humidity levels of 0 and 5%. Once again, it can be seen that there is a strong positive correlation between concentration and the final response voltage of the CO and AS-MLV-P sensors, with a weak relationship with the O₃ sensor. The H₂S sensor seems to be saturated by these concentrations and humidity levels at this flow rate, while the NH₃ sensor does not respond again.

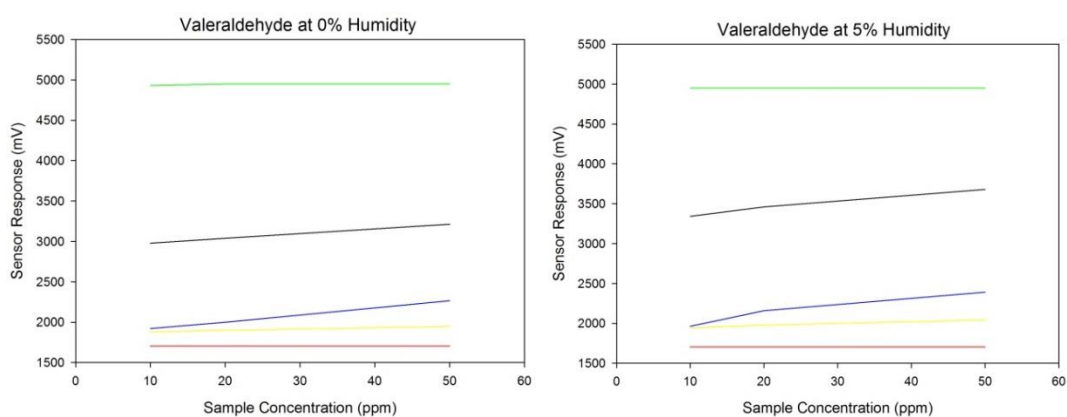


Figure 6.21: Graphs showing the relationship between sensor responses and 10 – 100 ppm concentrations of valeraldehyde, at relative humidity levels of 0% and 5%

6.6.3.2. GC Retention Tests

Once it had been proven that the micro hotplate metal oxide sensors proposed for the system would respond to a range of different volatiles, the GC element was added to introduce pre-separation. Prior to this, the GC had to be conditioned within the WOLF 3.1 system without the sensors attached in order to provide a smooth baseline to the responses to volatile samples. This process involved maintaining a heat of 100 °C for a period of 2 hours in order to remove any artefacts of the environment from the retentive elements of the column. The same volatiles were used in this set of experiments as the sensor-only tests shown in Section 6.6.3.1. The CO sensor response was found to be

constantly saturated at the maximum of 4950 mV throughout all GC tests, probably due to the low maximum flow rate through the GC of 50 mL/min at the pressure given at the mass flow controller outputs. Therefore, the response of this sensor was not included on the graphs for these tests.

6.6.3.2.1. Acetone GC Test

Acetone samples were first introduced to the system at concentrations of 10, 20 and 50 ppm and at a relative humidity of 5%, which is within the range seen in urine headspace (Section 6.6.2). The results of these experiments are shown in Figure 6.22, with the consecutive graphs corresponding to increasing concentration. The response to humidity and air elements can be seen at the 950-second mark of all of the graphs, which is common to all of the samples run through the WOLF 3.1. There is also an area of response from the H₂S, O₃ and AS-MLV-P sensors at approximately 1300 seconds, which increases across the three graphs as concentration of acetone increases. The sensor population that responds in this area and the positive correlation with acetone concentration in samples provides strong evidence that this is the response of the sensors to acetone.

Development and Construction of the WOLF 3.1 GC/E-Nose Instrument

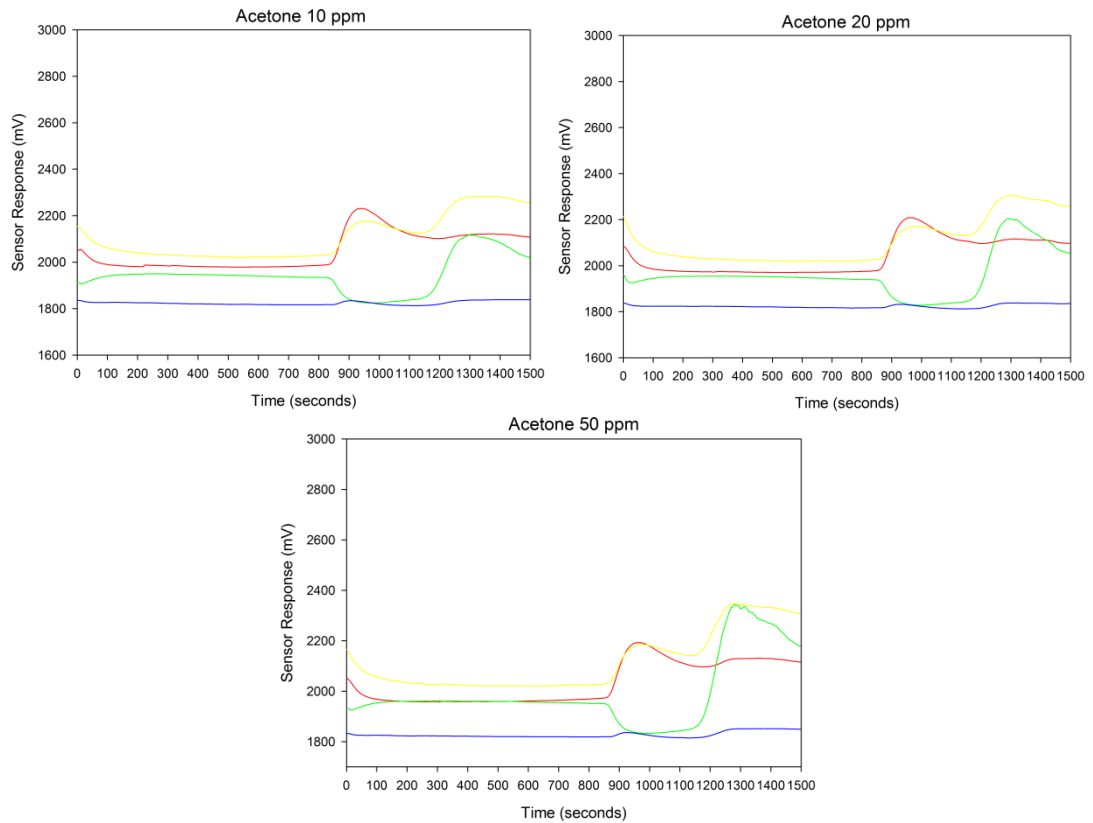


Figure 6.22: Graphs of WOLF 3.1 sensor response to acetone concentrations of 10 ppm, 20 ppm and 50 ppm at 5% relative humidity

6.6.3.2.2. Ethanol GC Test

Samples that included concentrations of ethanol of 10, 20 and 50 ppm were individually introduced to the system at 5% relative humidity in a similar manner to the acetone samples described above (Section 6.6.3.2.1). The results of these are illustrated in Figure 6.23, with increasing concentration of ethanol used in the samples in the same order as described previously. These show a similar response to air gases and humidity at 950 seconds. In addition, there is also a response pattern shown at a similar starting time period of 1300 seconds to the acetone results. This response is seen in the same three sensors as acetone as well, including the H₂S, O₃ and AS-MLV-P. While at lower concentrations this response pattern is frustratingly difficult to distinguish from the acetone samples, the 50 ppm samples yielded a wider dual response peak in the case of

Development and Construction of the WOLF 3.1 GC/E-Nose Instrument

this second volatile. This indicates that ethanol is not distinctive from acetone at concentrations of 20 ppm or lower, but may be distinguished at concentrations higher than this. This is supported by the fact that ethanol and acetone are similar molecules in terms of size and polarity, and have similar retention times in other GC-based methods (25).

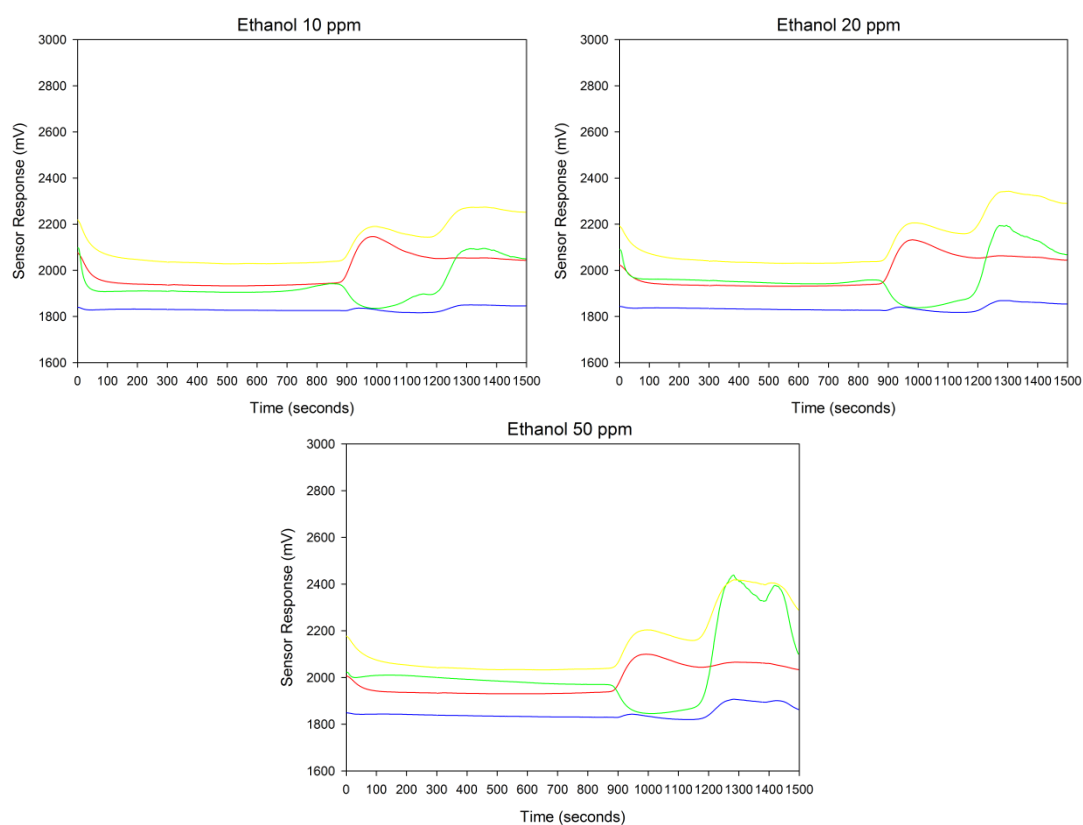


Figure 6.23: Graphs of WOLF 3.1 sensor response to ethanol concentrations of 10 ppm, 20 ppm and 50 ppm at 5% relative humidity

6.6.3.2.3. Toluene GC Test

Samples with concentrations of toluene of 10, 20 and 50 ppm were introduced into the system at a relative humidity of 5% in order to determine retention time of the GC column for the WOLF 3.1. The three graphs shown in Figure 6.24 illustrate the results of these experiments, with an increasing order of sample toluene concentration on consecutive graphs. There is a similar response of all sensors to the background air and humidity gases

Development and Construction of the WOLF 3.1 GC/E-Nose Instrument

at approximately 950 seconds. Another area of response begins at 1300 seconds as seen at all concentrations, with a gradual increase that ends beyond the 1500-second mark. This response is actually seen in all of the sensors, which is most visually apparent in the final graph corresponding to a sample concentration of 50 ppm. It is also seen that the peak response is reached on the H₂S and O₃ sensors before the end of the tests at the concentration at least, but that response is still increasing on the NH₃ and AS-MLV-P sensor lines. This provides evidence that it would be beneficial to increase GC pressure, accelerate the temperature increase in the GC method, or lengthen the time that the system is left at its final high temperature in order to capture more of this response data. These changes have been shown to increase the retention measurement range of other GC-based systems (27). While some adjustment is needed to the final GC method, this response pattern is different to that of acetone and ethanol sensors in terms of both sensor population and retention time. This means that distinction of toluene-like chemical groups from those similar to ethanol and acetone can be achieved with this system.

Development and Construction of the WOLF 3.1 GC/E-Nose Instrument

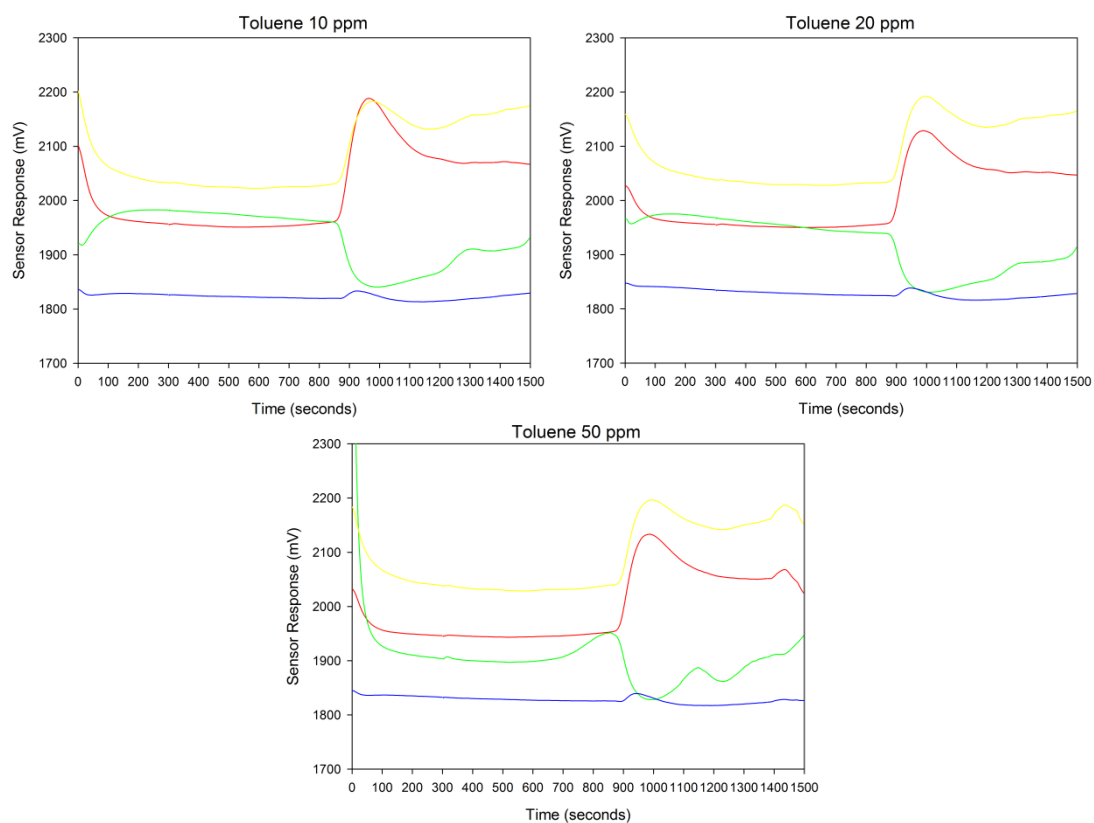


Figure 6.24: Graphs of WOLF 3.1 sensor response to toluene concentrations of 10 ppm, 20 ppm and 50 ppm at 5% relative humidity

6.6.3.2.4. Valeraldehyde GC Test

Valeraldehyde (or pentanal) samples were run through the instrument with concentrations of 10, 20 and 50 ppm and a relative humidity of 5%, similar to those of the other volatiles. Figure 6.25 shows a set of three graphs showing increasing concentrations of valeraldehyde on consecutive plots. Along with the response from humidity and air gases seen in all samples at 950 seconds, there is a general response shown across the full region of the graphs. This becomes more obvious when concentrations of 20 or 50 ppm are introduced the system, though is also somewhat apparent at 10 ppm. The region of response begins with a peak at approximately 325 seconds, and continues up in ramped fashion throughout the GC temperature method. These results give evidence to show that aldehydes such as valeraldehyde are not retained as effectively by the GC column as compared to other

Development and Construction of the WOLF 3.1 GC/E-Nose Instrument

chemical groups. The sensors responding to valeraldehyde in these tests include the O₃, NH₃ and AS-MLV-P sensors, with H₂S sensor response remaining relatively constant for the full range of concentrations. This data highlights a very distinctive response of the system to aldehyde groups, including peaks in particular areas of retention time from a unique group of sensors.

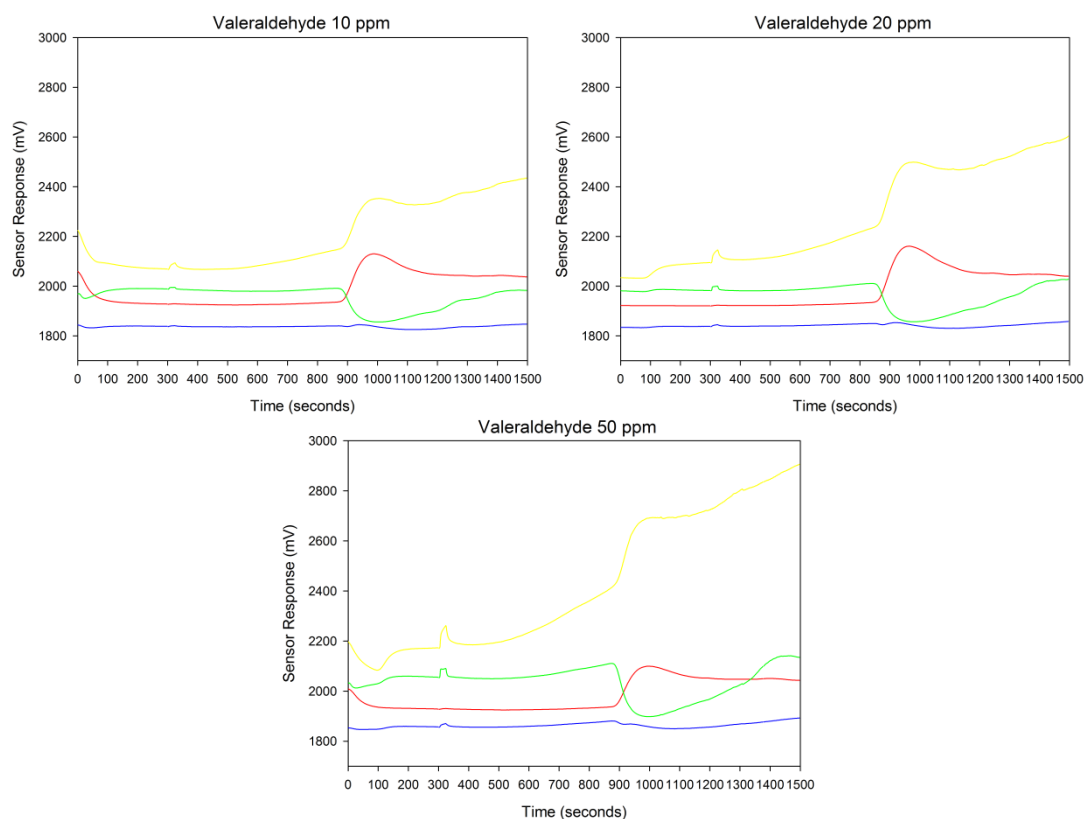


Figure 6.25: Graphs of WOLF 3.1 sensor response to valeraldehyde concentrations of 10 ppm, 20 ppm and 50 ppm at 5% relative humidity

6.7. Conclusions

A new instrument that incorporates a micro-packed gas chromatography column for separating gases and volatiles with an array of micro-hotplate metal oxide gas sensors was successfully designed and constructed. The sensors are held within 3D-printed chambers that were designed to seal their sensitive filter layer in the sample flow path while soldered

Development and Construction of the WOLF 3.1 GC/E-Nose Instrument

onto bespoke PCBs. The instrument is controlled by an application-driven C-based software program. The data processing electronic hardware and pneumatic system were also designed and assembled in-house.

A large body of testing has been completed on the WOLF 3.1 using four separate volatile compounds with different functional chemical groups. The scale of this experimentation includes the measurement of sensor response characteristics across a range of concentrations of each volatile, and a range of different relative humidity levels, both with and without the GC element providing temporal separation. This has provided a good degree of understanding the scales of response of the sensors and the level of retention that can be achieved by the GC column, and illustrated the ability of the instrument to distinguish between these volatile groups using these two factors as a metric. An experimental method for the analysis of gaseous samples with a constituent volatile and gas mix (including a representative humidity) has also been developed for the WOLF 3.1, which balances a timescale that allows sufficient chemical separation without becoming inappropriate for clinical triage use. These results are a direct measure the sensitivity of the sensors to volatiles of a particular concentration, but cannot be directly compared with the results of Section 5.5.

It has been noted that a more ideal solution could be achieved in terms of volatile separation and response with a method that would take a longer time. However, this was not pursued due to the impact on the sample analysis time that is already 25 minutes long. A substantial amount of further experimentation could be done with the volatile testing rig to better characterise the responses of the WOLF 3.1 on a much wider range of chemicals, in terms of molecular weight and functional group. Mixes of volatiles with known concentrations could also be run through the instrument to better understand the separation that can be achieved with the current method or others. However, this

Development and Construction of the WOLF 3.1 GC/E-Nose Instrument

constitutes a large body of work and could not be completed within the scope of this investigation.

This system represents a combination of separation and sensing elements that have not been used within commercially-available instruments as of yet. This will be helpful to add to comparative experimental results using other technologies, to understand its relative suitability to the clinical application of detecting colorectal cancer (covered in Chapter 7). The WOLF 3.1 was designed in a relatively portable form factor, to demonstrate its potential for use within a primary healthcare centre.

6.8. References

- 1) MSP Kofel, Gas Chromatography Troubleshooting and Reference Guide: Version 1.0. MSP Kofel, Aug 2005.
- 2) Wang, C., Yin, L., Zhang, L., Xiang, D., Gao, R., Metal Oxide Gas Sensors: Sensitivity and Influencing Factors. 2010, Sensors 10, 2088-2106.
- 3) Potkay, J.A., Lambertus, G.R., Sacks, R.D., Wise, K.D., A Low-Power Pressure- and Temperature-Programmable Micro Gas Chromatography Column. 2007, J Microelectromech Syst 16(5), 1071-1079.
- 4) Agah, M., Potkay, J.A., Lambertus, G., Sacks, R., Wise, K.D., High-Performance Temperature-Programmed Microfabricated Gas Chromatography Columns. 2005, J Microelectromech Syst 14(5), 1039-1050.
- 5) Premier Farnell Plc., Multicomp MC36260 DC Brushless Fan. Premier Farnell Plc., Dec 2011
- 6) Labfacility, IEC Mineral Insulated Thermocouples: Type 'K' & 'N' with threaded pot & tails, 310 stainless steel of Inconel Alloy 600 sheath. Labfacility.
- 7) Restek Corp., Packed & Micropacked Columns, GC Columns, 96-117. Restek Corp.
- 8) Restek Corp., Micropacked Columns (0.53 mm ID). Restek Corp., 2010.
- 9) Valco Instruments Co. Inc., HayeSep Chromatograms: MAPP gas – HayeSep R. Valco Instruments Co. Inc., 2014, http://www.vici.com/hayesep/hsr_c2.php, 28th Feb 2016.
- 10) SainLABS engineering, Quickstart Guide: 3.2" TFT LCD with SD and Touch for Arduino Mega with adjustable TFT shield. Sainsmart.com
- 11) SGX Sensortech, MiCS-4514 Datasheet: 0278 rev 15. SGX Sensortech, 2015.
- 12) Wilson, A.D., Baietto, M., Advances in Electronic-Nose Technologies Developed for Biomedical Application. 2011, Sensors 11, 1105-1176.
- 13) AppliedSensor GmbH, VOC Sensor: AS-MLV-P. AppliedSensor GmbH, Apr 2010.

Development and Construction of the WOLF 3.1 GC/E-Nose Instrument

- 14) EnvisionTEC Inc., Perfactory Micro DSP Series. EnvisionTEC Inc.
- 15) Freescale Semiconductor Inc., MPX2053 Series: 50 kPa On-Chip Temperature Compensated and Calibrated Silicon Pressure Sensors. Freescale Semiconductor Inc., Oct 2012.
- 16) Alphasense Ltd., AAN 109: Interfering Gases. Alphasense Ltd., Issue 12.
- 17) Owlstone Ltd., 90-0323-AAA: GEN-SYS User Manual. Owlstone Ltd., 2008.
- 18) Brooks Instrument, Installation and Operation Manual: Brooks Model 5850TR. Brooks Instrument, 2008.
- 19) Sensirion AG., Datasheet SHT1x (SHT10, SHT11, SHT15): Humidity and Temperature Sensor IC. Sensirion AG., 2011.
- 20) E2V Technologies (UK) Ltd., MiCS-2614 O3 Sensor, September 2009, Version 2, E2V Technologies Plc.
- 21) E2V Technologies (UK) Ltd., MiCS-5914 NH3 Sensor, September 2009, Version 1, E2V Technologies Plc.
- 22) Westenbrink, E., Arasaradnam, R.P., O'Connell, N., Bailey, C., Nwokolo, C., Bardhan, K.D., Covington, J.A., Development and application of a new electronic nose instrument for the detection of colorectal cancer. *Biosensors and Bioelectronics* 67, 733-8.
- 23) Restek Corporation, Micropacked Columns (0.53 mm ID), 2010, Restek Corporation.
- 24) Agah, M., Potkay, J.A., Lambertus, G., Sacks, R., Wise, K.D., High-Performance Temperature-Programmed Microfabricated Gas Chromatography Columns. *J. Microelectromech. Syst.* 14 (5), 1039-50.
- 25) Potkay, J.A., Lambertus, G.R., Sacks, R.D., Wise, K.D., A Low-Power Pressure- and Temperature-Programmable Micro Gas Chromatography Column. *J. Microelectromech. Syst.* 16 (5), 1071-9.

- 26) Curvers, J., Rijks, J., Cramers, C., Knauss, K., Larson, P., Temperature programmed retention indices: Calculation from isothermal data. Part 1: Theory. *J. High Res. Chrom.* 8 (9), 607-10.
- 27) Esfahani, S., Sagar, N.M., Kyrou, I., Mozdiak, E., O'Connell, N., Nwokolo, C., Bardhan, K.D., Arasaradnam, R.P., Covington, J.A., Variation in Gas and Volatile Compound Emission from Human Urine as It Ages, Measured by an Electronic Nose. *Biosensors* 6 (4), 10.3390.

7. Experimental Testing of WOLF 4.1 and WOLF 3.1

Two new electronic nose instruments were developed for the purpose of detecting colorectal cancer from the gaseous and volatile content of urine headspace samples. Both the WOLF 4.1 and WOLF 3.1 were fitted with state-of-the-art sensors, which have not been employed in commercial electronic noses to date. A significant amount of experimental testing was performed on these instruments to compare them with the commercial instruments included in this investigation. Descriptions of the methods used and the results found from these experimental studies are detailed in this chapter.

7.1. WOLF 4.1 Colorectal Cancer Distinction from Healthy and Diseased Controls

After gaining insight on how known volatile groups affected the response of the WOLF 4.1 sensors, testing of the machine's diagnostic capabilities on biological samples was undertaken using urine from patients of colorectal cancer and irritable bowel syndrome, along with healthy subjects.

7.1.1. Methods and Materials

Urine samples were collected from pre-diagnosed patients recruited at the University Hospital of Coventry and Warwickshire, including a total of 39 suffering from CRC and 35 from IBS. In addition, 18 additional healthy controls were tested (Ethical Approval Number: 09/H1211/38). Table 7.1 shows the demographics of each patient group. All cases of CRC (adenocarcinoma) were confirmed on colonoscopy and histology. The demographics do show a variation in some factors, including gender and age. However, these are indicative of the average demographics of patients found within the disease groups. For example, IBS sufferers are much more likely to be female, and CRC patients are only very rarely under

Experimental Testing of WOLF 4.1 and WOLF 3.1

the age of 60. All samples were collected alongside urine “dipstick” tests were conducted to rule out the presence of infection, diabetes or renal disease. Urine samples were stored frozen at -80 ± 0.1 °C within two hours of being collected, and then defrosted overnight at 5 ± 0.1 °C before experimental testing. These were run through an identical experimental method to the volatile solutions as described in Section 5.5.2, with 5 mL aliquots running with initial headspace build-up at 40 ± 0.1 °C for 5 minutes followed by another 5 minutes of sample introduction. Clean air was then run through the instrument directly after each sample introduction step for 10 minutes. This was also repeated three times per sample, again to ensure that a full profile of volatile and gaseous content of each was being measured.

	CRC	IBS	Controls
Number	39	35	18
Mean Age	70	48	41
Male %	70	11	70
Mean BMI	27	28	24
Current Smokers	6.7%	10%	6.7%
Alcohol - average units per week	7.3	2	9.2

Table 7.1: Patient demographics for urine sample cohort run through the WOLF 4.1

7.1.2. Statistical Analysis

Statistical analysis was undertaken using multivariate techniques common to electronic noses. First, features were extracted from the raw data based on the baseline-corrected voltage changes averaged over three points (Sig-Base3), the response integrals from the start of response to the maximum response (AreaMax) and the times for the sensor responses to return from maximum to 50% of that value (T50). The equations 4.1-4.3 were used to calculate these three features in respective order, as described in Section 4.2.4. The remainder of the statistical methods for processing the extracted features into an LDA plot and then qualifying it are also equivalent to those described in this section. This resulted in

an assessment based on sensitivity and specificity of Colorectal Cancer against the relevant controls.

7.1.3. Results and Discussion

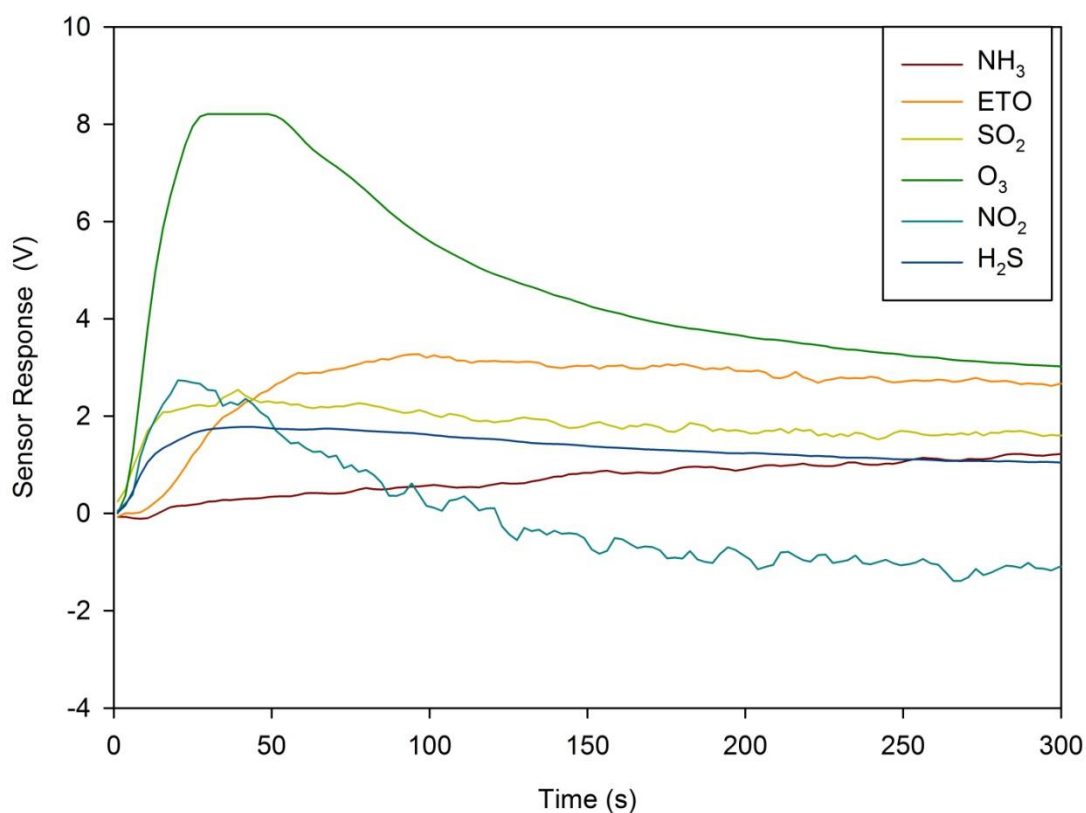


Figure 7.1: Voltage signals produced by the ISBs of a subset of WOLF 4.1 sensors from a urine sample

Figure 7.1 shows the change in analogue voltage outputs from a subset of the most responsive sensors upon the introduction of a urine headspace sample into the WOLF 4.1. There is generally a positive change in current produced from these sensors, which is expected considering an increase in analytes causes a larger ionic current within the cells. These responses are at least partially produced by an increase in humidity from the headspace sample, which rises from a baseline of approximately 6.8% to around 14%.

Experimental Testing of WOLF 4.1 and WOLF 3.1

However, individual sensor responses vary between different samples independently of humidity levels, proving the presence and detection.

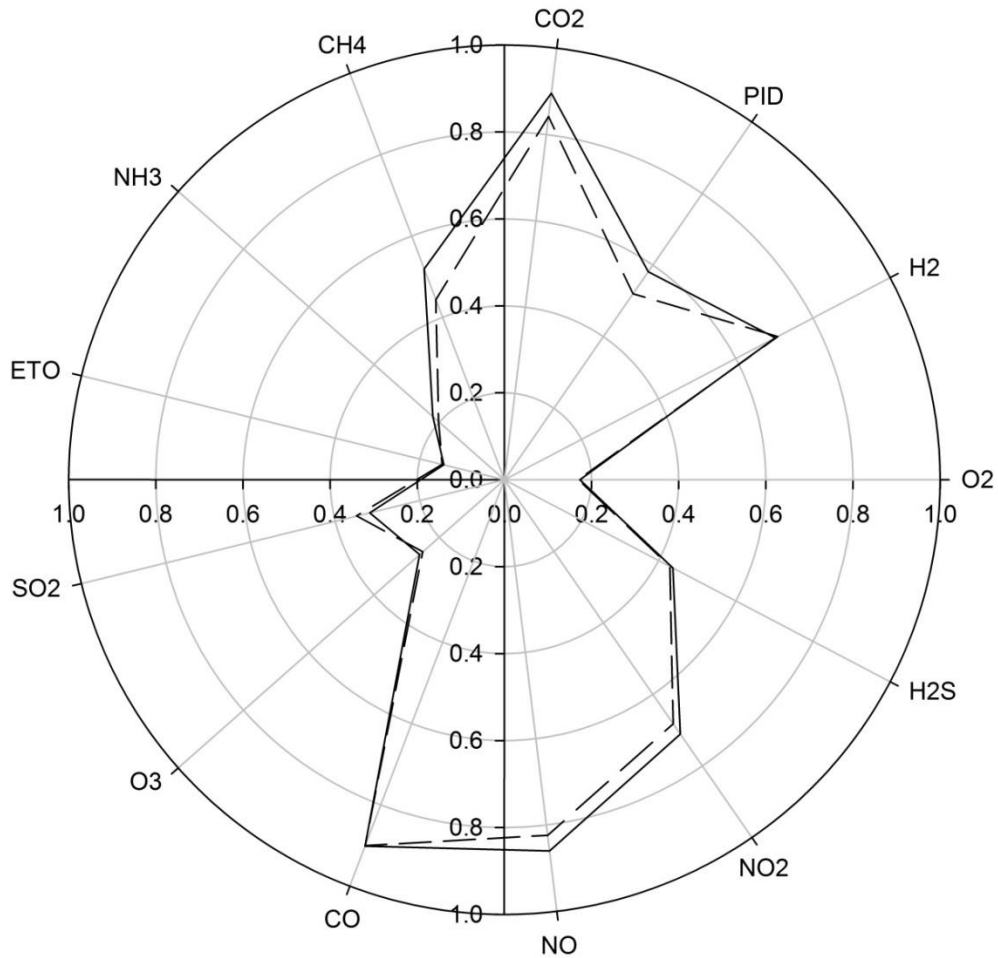


Figure 7.2: Radial plot of the average baseline-corrected response of all 13 WOLF 4.1 sensors to CRC (full line) and IBS (dashed line) urine samples

The baseline-corrected change in output voltage of the WOLF 4.1 sensors to IBS and CRC samples (with all responses averaged) is shown in Figure 7.2. This highlights both the overall similarities in response to all urine samples and the more subtle variations used to find distinction between these two disease groups. There is generally a positive change in current produced from these sensors, which is expected considering an increase in analytes

causes a larger ionic current within the cells. These responses are at least partially produced by an increase in humidity from the headspace of the sample (with approximate changes from 6.8% to 14%). However, individual sensor responses vary between different samples independently of humidity levels, proving the presence and detection of gases and volatile groups.

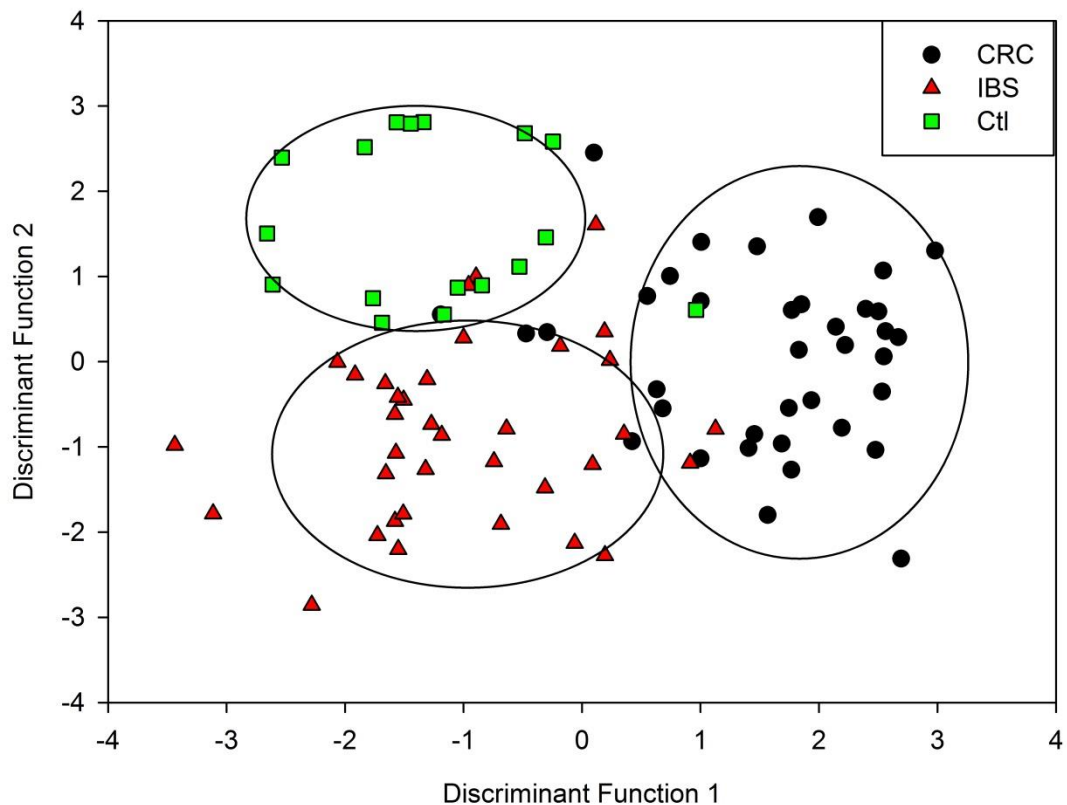


Figure 7.3: LDA classification separating all three sample groups of CRC, IBS and healthy controls (Ctl)

Figure 7.3 shows a full classification of all three sample groups from which a degree of class distinction can be seen. However, there is also a large amount of inter-class overlap and intra-class spreading in this diagram. The spread shown in IBS is in agreement with its pathological circumstances as a widely-variable collection of symptoms rather than a well-

Experimental Testing of WOLF 4.1 and WOLF 3.1

characterised disease state. The healthy control group also shows a larger variation in response, again supporting the results of previous investigations where this feature is particularly highlighted as compared to any disease group (1). A potential area for further study would be to investigate the three common subsets of IBS: IBS-D, IBS-C, and IBS-A to evaluate potential differences. The mean and average absolute deviations of the disease classes for each discriminant function in this LDA classification are shown in Table 7.2.

	Disease Groups	CRC	IBS	Volunteer
Discriminant Function 1	Mean Score	1.544	-1.001	-1.241
	Average Deviation from the Mean	0.791	0.820	0.737
Discriminant Function 2	Mean Score	0.071	-0.842	1.630
	Average Deviation from the Mean	0.831	0.791	0.845

Table 7.2: Average discriminant function scores for 3-group LDA classification

The LDA classification using only CRC and IBS groups is shown in Figure 7.4. This is the classification that most accurately represents the problem to be solved when patients enter a primary healthcare centre complaining of symptoms. Reasonable separation between the two groups is demonstrated as well as good clustering of similarly-classed samples, particularly in the case of CRC.

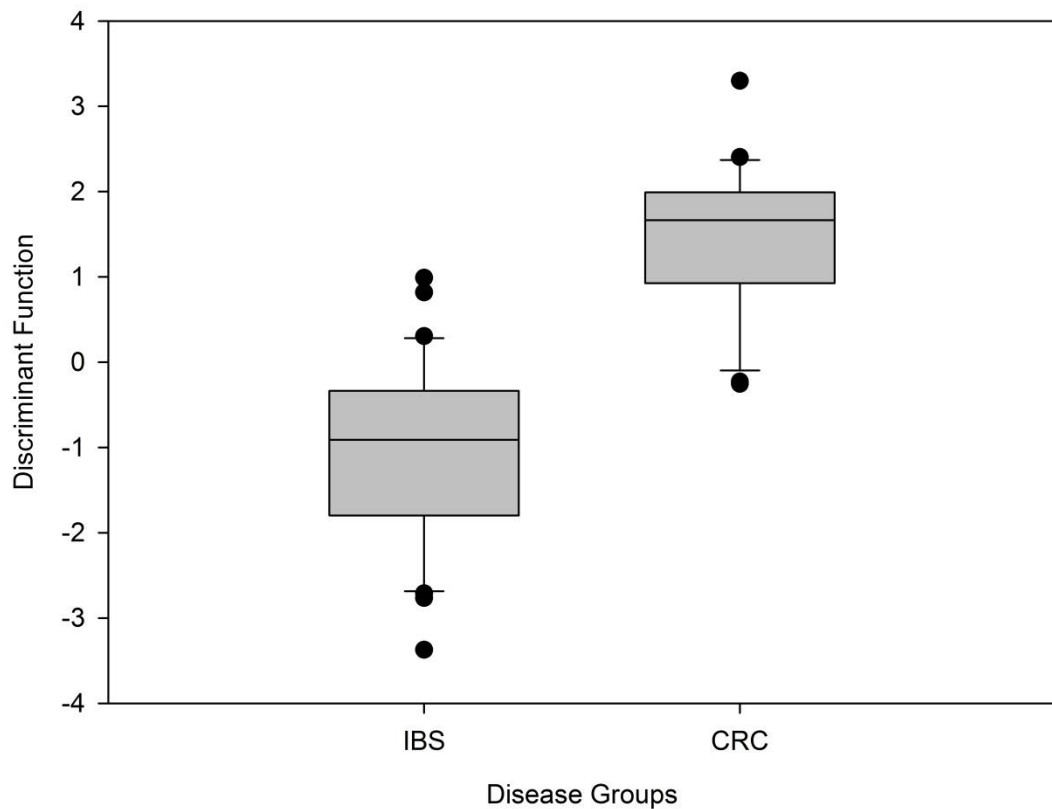


Figure 7.4: Box plot of LDA classification separating IBS and CRC sample groups

The basis for measuring the diagnostic merit of this method was the re-classification of individual samples that were taken out of the main “training set” one-by-one and re-introduced as unknowns. The system attempted to successfully choose the class for each unknown sample using an (n-1) K-nearest-neighbour algorithm for estimating from which group it likely belonged. Employing this technique, a sensitivity and specificity from this classification were found to be 78% and 79%, respectively. These compare favourably to other non-invasive screening techniques such as Faecal Occult Blood and Faecal Immunochemical Testing (FIT), with success measures that are similar or higher than what has been discovered in diagnostic review studies (2). The mean and average absolute deviations in discriminant function scores of both disease classes in this LDA classification are shown in Table 7.3.

	Disease Groups	CRC	IBS
Discriminant Function 1	Mean Score	1.459	-1.082
	Average Deviation from the Mean	0.717	0.845

Table 7.3: Average discriminant function scores for 2-group LDA classification

This initial training set of samples has established an effective set of LDA discriminant functions for distinguishing between CRC and IBS within this pilot cohort. A degree of individual variation was found in the profile of responses for urine samples in the same disease, which correlates with findings in other similar investigations (3). The sensitivities found in this study were much better than those shown with the Fox 4000, but were surpassed by those found using the Owlstone Lonestar FAIMS unit. This suggests that there may insufficient overall concentration of volatiles within the sensitive range of the chemically-driven sensors to compete with the measurement of the physical property of ion mobility, which provides very low resolution and a detection range only limited by ion mass and charge.

7.1.4. Conclusions

A cohort of 92 total urine samples have been run through the WOLF 4.1 system, based on state-of-the-art sensors and control hardware being driven by custom LabVIEW software interface. This new system was successfully tested to prove the sensitivity of the sensors to common volatile organic groups. LDA plots produced from the WOLF 4.1 urine data show a reasonable separation of all three groups included in this study, although there is a degree of inter-group overlapping due to a significant number of outliers. However, particularly well-clustered groups are shown when distinguishing colorectal cancer from irritable bowel syndrome. Re-classification of single unknown samples into this latter case produced 78% sensitivity and 79% specificity for detecting CRC, which accurately represents a situation requiring this new diagnostic tool within the clinical setting.

7.2. WOLF 3.1 Colorectal Cancer Distinction from Healthy and Diseased Controls

7.2.1. Introduction

Once the response of the sensors on the WOLF 3.1 had been characterised for a variety of different volatile groups and the level of distinction between them was found to be reasonable, testing was required to apply this distinction level to a diagnostic application. The most appropriate sample framework for these tests would be a population of urine samples including those from patients of target disease, CRC against controls of IBS. The experimental and statistical methods used to characterise the validity of this instrument must also be designed to emulate the comparative experiments run on the WOLF 4.1 and commercial machines as closely as possible to allow for a direct comparison to be made. The number of samples used in this investigation must also be at a similar level in order to maintain its statistical relevance when comparing to the other parallel studies with 25 - 50 samples per group. The clinical relevance of the proposed application has been explained in Chapter 2.

7.2.2. Materials and Methods

This set of experiments used the WOLF 3.1 GC/electronic nose developed in-house as described in Chapter 6 to use as the basis for classifying a set of urine samples from CRC and IBS patients. The pneumatic system is described in Section 6.6.2, and required a clean air supply from the laboratory (as described in Section 4.2.1) to be connected to the air supply port on the right hand side of the front face. Samples were connected to the centre and left side ports on the front of the machine, and the exhaust port at the rear was connected to a laboratory air exhaust line to remove the waste gas and volatile mix from the immediate area. The proposed experimental method for these test runs was

Experimental Testing of WOLF 4.1 and WOLF 3.1

programmed into the instrument from the touchscreen at the front, using the menu system detailed in Chapter 6.

Urine samples were brought to a temperature suitable for developing a headspace using a Dri-Block® DB-2D (Techne) heater with an adapted insert for holding the 22 mL vials used in this experiment.

7.2.2.1. Urine Samples

Urine samples were collected from pre-diagnosed patients recruited at the University Hospital of Coventry and Warwickshire, including a total of 26 CRC and 23 IBS patients (Ethical Approval Number: 09/H1211/38). Table 7.4 shows the demographics of each group. All cases of CRC (adenocarcinoma) were confirmed on colonoscopy and histology. All samples were collected alongside urine “dipstick” tests were conducted to rule out the presence of infection, diabetes or renal disease.

	CRC	IBS
Number	26	23
Mean BMI	28	25
Current Smokers	7.7%	17.4%
Alcohol - average units per week	9.5	4.1

Table 7.4: Patient demographics for urine sample cohort run through the WOLF 3.1

7.2.2.2. Experimental Method

Urine samples were stored frozen at -80 °C within 2 hours of being collected, and then defrosted overnight at 5 °C before experimental testing. Each sample was individually divided into 10 mL aliquots and pipetted into 22 mL screw lid glass vials for analysis. A modified screw lid was attached with a 1/8” Swagelok inlet and outlet port for attaching to the WOLF 3.1 and an added nitrile O-ring for holding the required internal pressure. The components of the modified lid were heated at 60 °C for 4 hours prior to analysis in order

Experimental Testing of WOLF 4.1 and WOLF 3.1

to remove any environmental volatile compounds being released from them. This lid was connected to the sample supply and inlet ports on the instrument, and the vial was placed into the Dri-Block® DB-2D heater insert held at a temperature of 40 °C for a period of 5 minutes, so that a sufficient headspace could be developed above the actual urine sample.

The WOLF 3.1 analysis method was started up simultaneously to the placement of the sample vial in the heater with a 300 second initial baseline time, so that sample introduction would occur at the correct time in terms of headspace development. The actual method run in the WOLF 3.1 was identical to that developed during single volatile testing as described in detail in Section 6.6.2.2.2 (GC heating method) and Section 6.6.2.1 (sample introduction and flow rates). This experimental method took a total of 25 minutes for each sample to be run through the instrument, with air blanks run in between each urine sample. This was done to ensure that all remaining artefacts of the previous samples had been purged before a new sample was run, thus avoiding sample cross-contamination. CRC and IBS samples were run in random groups allocated to each day of test, to avoid introducing an artificial separation of groups due to sensor drift or environmental changes across the experimental run time. The responses of all sensors from a single sample run were saved along with timestamps in tab delimited text files on the on-board SD card in the WOLF 3.1, with each file including a set of headers showing information on method conditions and sensors included.

7.2.2.3. Statistical Method

Statistical analysis was undertaken using multivariate techniques common to electronic noses. First, features were extracted from the raw data processed by the pre-classified technique Linear Discriminant Analysis, using Multisens Analyzer as a commercial software package (JLM Innovation, Germany). A wide variety of LDA classifications were attempted for distinguishing CRC samples from IBS controls using the data collected from the WOLF

3.1. The process began with dividing the raw responses of the sensors into slices of time length between 100 and 400 seconds. A class was set to each sample based on their disease state, and two or three features were extracted from some of their response slices. The number of features extracted depended on the full number of slices that were being used, in order to make a full set of features that were less than the number of samples included in the study for statistical validity. The LDA classification that achieved the highest success in sensitivity of CRC within a population of IBS controls used 100 second slices of the original sensor responses, and extracted features of “Sig-base3” and “Average” values. The definition of the feature “Sig-base3” is described in Section 4.2.4, and that of “Average” is shown in Equation 7.4 below:

$$Average(x) = \frac{\sum_{i=1}^{i_{max}} x_i}{i_{max}} \quad (7.4)$$

Similar to Section 7.1.2, the remainder of the statistical methods for processing the extracted features into an LDA plot and then qualifying it are equivalent to those described in Section 4.2.4. This resulted in an assessment based on sensitivity and specificity of Colorectal Cancer against the relevant controls.

7.2.3. Results and Discussion

Individual urine headspace samples of CRC and IBS patients were introduced to the machine after being allowed to develop for 5 minutes, which is 100 seconds after the start of the baseline. An example of the raw sensor response results from a single CRC sample is shown in Figure 7.5, which was run on an extended GC method of time length 2500 seconds, in order to further separate the individual peaks for better visual representation. While the response is dominated by the peaks in all sensors associated with the air gases and humidity sent from the sample, there are a large number of different peaks that can be

Experimental Testing of WOLF 4.1 and WOLF 3.1

picked out from individual sensors or distinctive sets. These unique responses generally appear after the humidity peak, which is expected as the column is designed to better retain the volatile groups of larger relative size than gaseous water. However, there are some variations in response earlier than this due to the inability of the column to retain chemical groups with a less significant polarity (4).

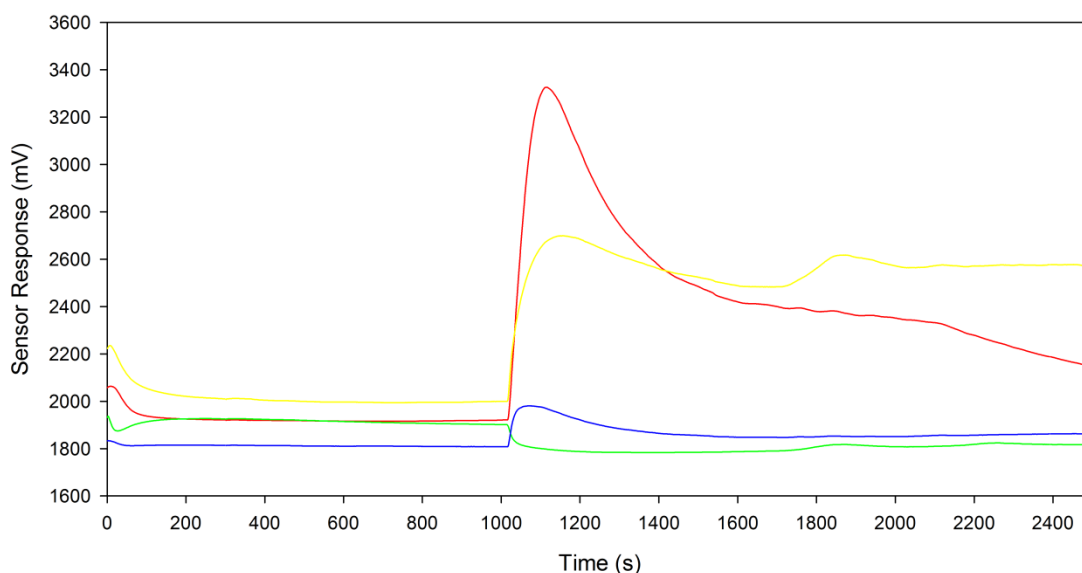


Figure 7.5: WOLF 3.1 sensor response to a CRC urine headspace sample (CRC232)

Figure 7.6 shows an example of the raw sensor responses from the WOLF 3.1 system after introduction of an IBS urine headspace sample. This sample was also run on an extended 2500-second GC method in order to improve visualisation of the temporal separation of responses due to retention. A number of unique responses can be seen along the graph both before and after the humidity peak seen at 1050 seconds, which include different populations of sensors for each. These are also markedly different from the responses seen in the CRC sample, giving support to the idea that statistically-valid distinction between these two groups can be achieved by this method.

Experimental Testing of WOLF 4.1 and WOLF 3.1

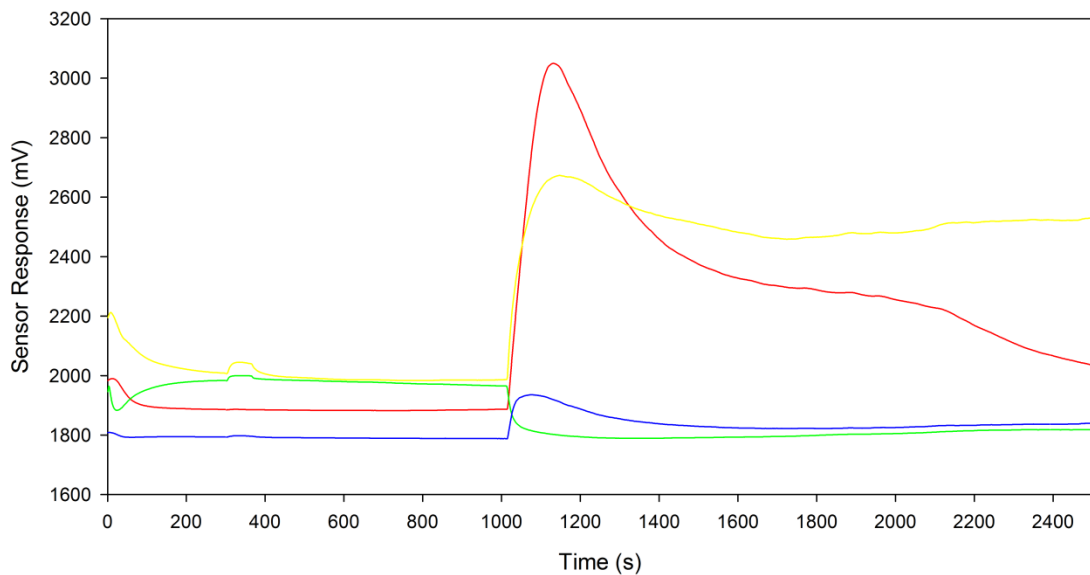


Figure 7.6: WOLF 3.1 sensor response to an IBS urine headspace sample (IBS150)

Figure 7.7 illustrates a box plot of the 2-group LDA classification of CRC and IBS samples using time slices of 100 seconds and extraction of “Sig-base3” and average value for each. There is generally a very good distinction between the disease groups, with no overlap seen in any of the samples in this population. There is also a promising level of clustering among samples in both groups. However, it is still unexpected that there is a greater spread in CRC samples as compared with IBS, as the nature of IBS as a collection of conditions based on widely-variable symptoms would have predicted the opposite to be true. The storage conditions and relative age of the CRC samples could potentially be causing this larger spread, as the variety in the sample age in the population is greater than that of the IBS samples (5).

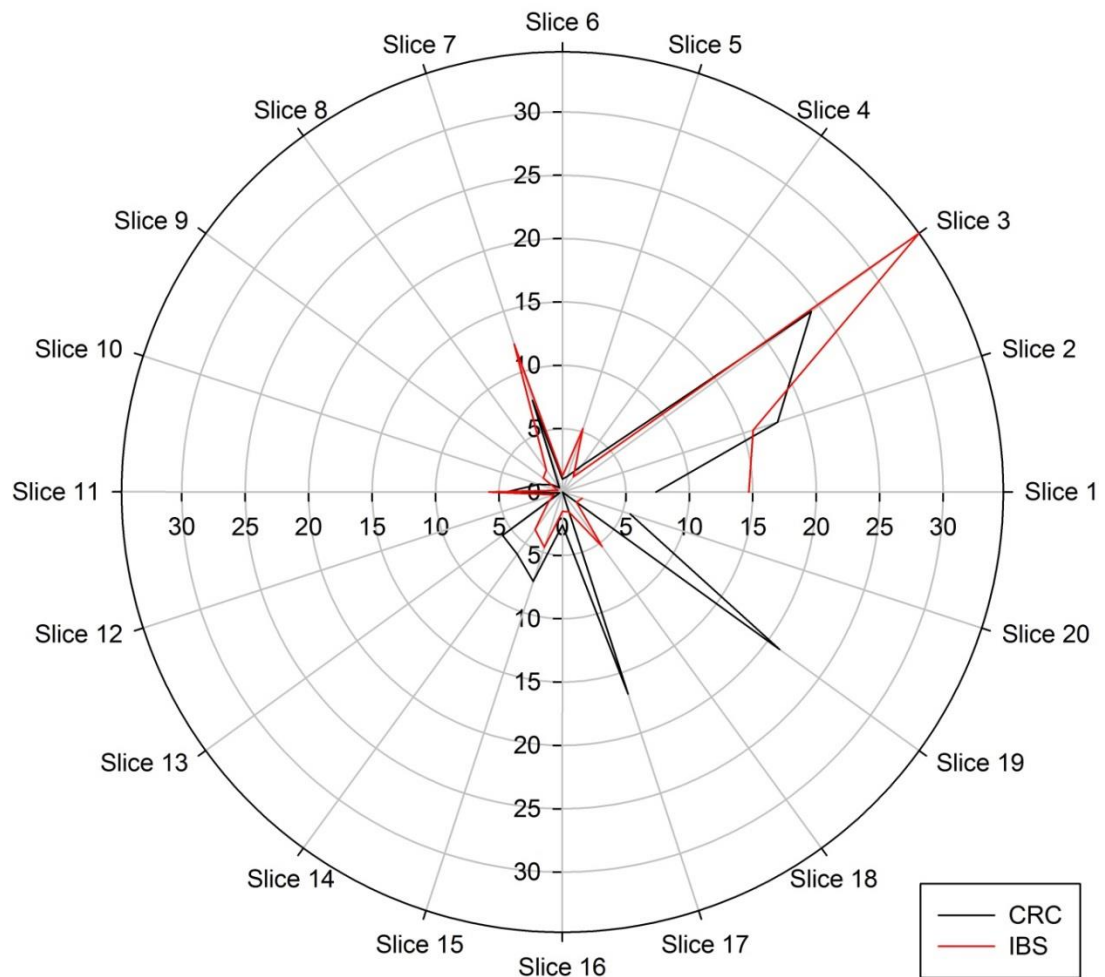


Figure 7.8: Mean values of “Sig-base3” for CRC and IBS samples across 20 included time slices

Both Figure 7.8 and Figure 7.9 show polar plots of the average feature values of CRC and IBS samples from each of the 20 slices included in the 2-group classification. The first of these figures illustrates the values produced by the “Sig-base3” feature calculation, while the latter shows the “average” feature for the time slices. The large difference in scales of the features included in the two polar plots makes it more obvious where the differences are in “Sig-base3” features than in “Average”. However, a large number of these features on both plots show a significant variation in average response between the two disease groups. This provides evidence to show that many of the features were instrumental in

distinguishing between CRC and IBS samples. The effectiveness of temporal separation of gases and volatile groups by GC is also shown by the large change in variation between disease groups amongst the slices of time within the responses.

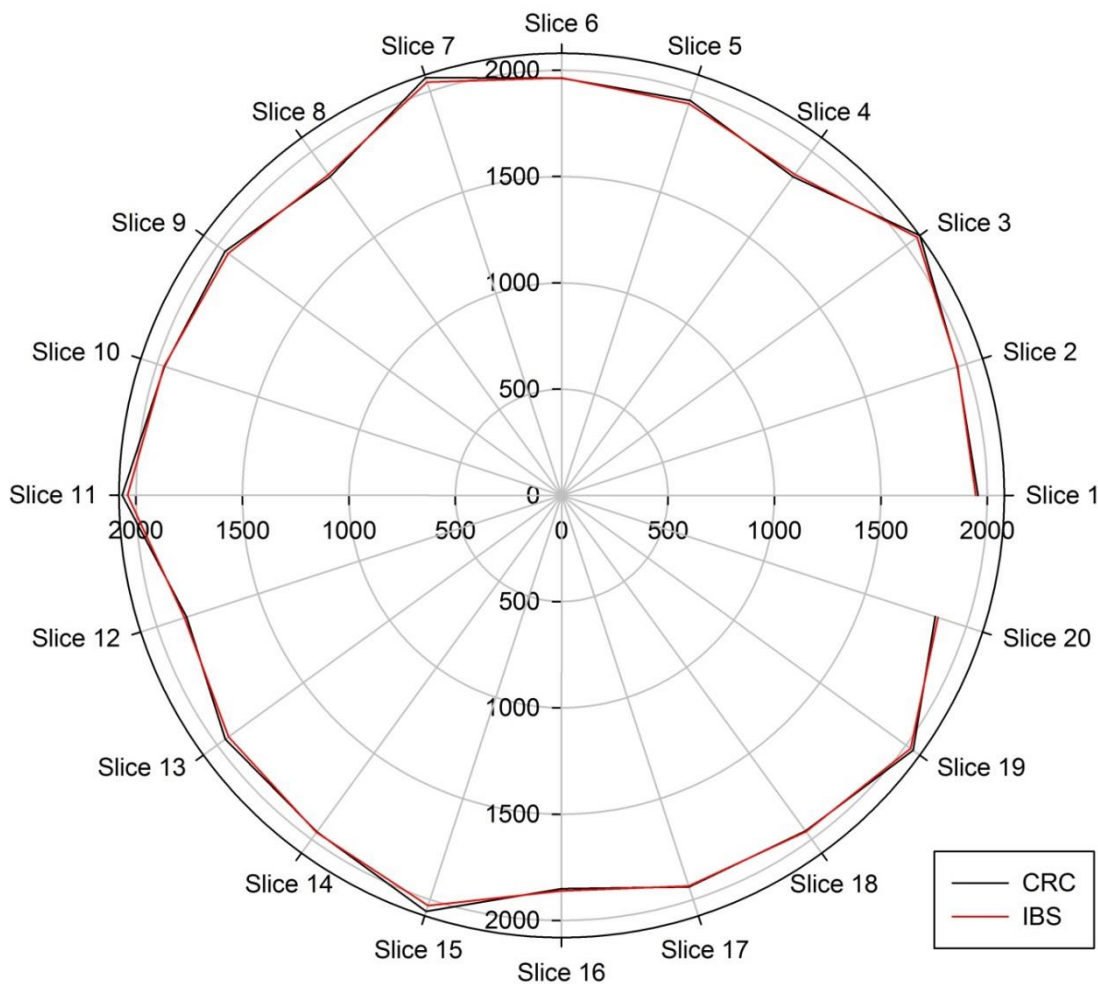


Figure 7.9: Mean values of “Average” for CRC and IBS samples across 20 included time slices

7.2.4. Conclusions and Future Work

A population of 49 urine samples from CRC and IBS patients have been successfully run through the WOLF 3.1, following from successful trials with single volatile samples. The 25-minute experimental method run internally on the instrument has been proven to

distinguish between distinct volatile groups, and the external experimental and statistical techniques were designed with a parallel comparison with the other urine cohort experiments in mind. LDA classification of these samples has yielded a method that shows very good clustering of both of the disease groups with no overlapped scatter. Resulting KNN re-classification of introduced unknowns into the main training set has revealed an impressive distinction level of CRC against IBS controls, with a resultant 92% sensitivity and 77% specificity. These results compare favourably against the other instruments tested comparatively in this study, and in studies performed by other groups.

This initial pilot investigation was useful in proof-of-concept of the diagnostic potential of this GC-electronic nose instrument, a more comprehensive study with larger sample populations is required to fully establish it as an effective method. Different digestive diseases may be introduced into the range of those run through the machine, either as controls against CRC detection or as separate target diseases. A great deal of more work could be done on developing a more appropriate GC method for the instrument using actual urine samples to maximise disease classification. After further optimisation of the experimental technique, prospective studies could be undertaken to indicate whether the WOLF 3.1 is capable of predicting the development of digestive disease in the future.

7.3. References

- 1) Arasaradnam, R.P., Covington, J.A., Harmston, C., Nwokolo, C.U. Review article: next generation diagnostic modalities in gastroenterology--gas phase volatile compound biomarker detection. 2014, *Aliment Pharmacol Ther.* 39, 780-9.
- 2) E2V Technologies (UK) Ltd., MiCS-2614 O₃ Sensor, September 2009, Version 2, E2V Technologies Plc.

Experimental Testing of WOLF 4.1 and WOLF 3.1

- 3) E2V Technologies (UK) Ltd., MiCS-4514 Combined CO and NO₂ Sensor, July 2008, Version 2, E2V Technologies Plc.

- 4) Brenner H, Tao S. Superior diagnostic performance of faecal immunochemical tests for haemoglobin in a head-to-head comparison with guaiac based faecal occult blood test among 2235 participants of screening colonoscopy. *Eur J Cancer*. 2013 49(14), 3049-54

- 5) Imperiale TF. Non-invasive screening tests for colorectal cancer. *Dig Dis*. 2012 30 Suppl 2, 16-26.

8. Conclusions and Further Work

The aim of this project has been to investigate electronic nose technologies for use as a point-of-care diagnostic tool to aid in the initial triage detection of colorectal cancer, against symptomatic and healthy controls. The current clinical diagnostic situation for lower gastro-intestinal diseases highlights that patients of lower gastro-intestinal diseases can exhibit a wide variety of overlapping symptoms. These conditions can be easily confused with each other, and the only current diagnostic options with a consistent sensitivity and specificity involve highly invasive and costly endoscopic techniques. Review of electronic nose and sensing technologies revealed omissions of suitable sensor technologies in the range of commercially-available instruments. The current literature includes a number of indirect reviews of different electronic nose technologies, some of which conclude that current technologies could be viable for clinical use. However, direct experimental comparisons between different sensing techniques for a particular application are rare.

The contents of urine headspace samples taken from 294 patients of a variety of lower gastro-intestinal diseases were analysed by gas chromatograph/mass spectrometer. A total of 10 candidate volatile compounds have been found to be common in a large majority of these samples (listed in Table 8.1), with each having been previously reported to be linked to diet and/or gut bacteria.

Conclusions and Further Work

Volatile Compound
Acetone
2-Pentanone
4-Heptanone
1,3,5,7-Cyclooctatetraene
Allyl Isothiocyanate
Oxime-, methoxy-phenyl-
1,3-Propanediamine
Carvone
Ethanone, 1,1'-(1,4-phenylene)bis
Phenol, 2,4-bis(1,1-dimethylethyl)-

Table 8.1: List of volatile chemicals found in urine headspace by GC-MS in this study

A comparative experimental study has been completed for a cohort of four electronic nose instruments, each making use of a different range of sensor technologies. An experimental testing rig was setup to produce accurate concentrations of single volatiles within a gaseous sample with a controlled environmental humidity. The humidity portion of the rig was developed in-house, and interfaced with control software to form an automated system for accurately testing electronic nose instruments. The single volatile samples produced by the rig were used to verify the sensitivity of the sensor technologies under test.

These instruments were each tested with a similarly-sized cohort of urine samples from the disease states of colorectal cancer, irritable bowel syndrome and healthy. The experimental methods used with all of them were designed to be parallel to each-other in every way possible in order to provide an accurate comparison. Where possible, a full 3-group linear discriminant analysis classification was made for all disease group samples run through a single instrument. However, the key metric for performance in detection of cancer was the sensitivity and specificity of a 2-group classification, in most cases comparing CRC and IBS samples.

Conclusions and Further Work

The first two of these are commercially available, and make use of an electro-resistive sensor array (Fox 4000 from Alpha MOS Ltd.) and field asymmetric ion mobility spectrometry (Lonestar from Owlstone Ltd.) as their respective sensing elements. The Fox 4000 performed very poorly in distinguishing colorectal cancer from controls of IBS, achieving a sensitivity of 54% and specificity of 48%. Only CRC patient and healthy volunteer data could be used from the Lonestar, for which the LDA classification yielded a sensitivity and specificity to the target of 88% and 60% respectively.

The other two instruments were developed and constructed in-house, and use different combinations of sensing elements commercially-available as individual packages. The first of these was based on an array of electro-chemical and optical sensors, and was built to house a built-in PC to allow a degree of portability within the clinical environment. This "WOLF 4.1" system was first tested with a series of single volatile samples at a range of ppm-level concentrations in order to test the sensitivity of its sensors to common volatile groups, with reasonable success in the case of most sensors. A cohort of urine headspace samples was then run through it, including the same disease groups used with the commercial instruments. A two-group LDA classification yielded a 78% sensitivity and 79% specificity for distinction of CRC against IBS controls, which is significantly higher than the results shown by the Fox 4000.

The last instrument to be developed and tested was a combined gas chromatography/electronic nose instrument that used a micropacked column for pre-separation before analysis with an array of micro-hotplate metal oxide sensors. The "WOLF 3.1" was housed in a portable desktop unit, with an on-board microcontroller and touchscreen system for independent use when provided with mains power supply. Initial testing with single volatile samples showed promise in terms of separation of volatiles by GC and sensitivity of the sensors. Testing was also done against a full urine cohort in this

Conclusions and Further Work

case, with samples of the same three disease states included. When testing for distinction of CRC against IBS controls, this technique yielded a sensitivity of 92% and a specificity of 77%. The sensitivity for the WOLF 3.1 in particular is considerably higher than the other instruments tested in this study, and is at an equal or higher level compared to non-invasive diagnostic techniques that are currently used in clinical practice.

Table 8.2 compares the four electronic noses tested in this investigation against the deliverables originally stated in Chapter 1. All machines used urine as a sample medium, which makes them all non-invasive techniques with a relatively high expected patient acceptance level (as discussed in Chapter 2). The Fox 4000 has clear shortcomings in terms of sensitivity and specificity to colorectal cancer. It is also a large (roughly 0.5 cubic metres) desktop machine that must have an uninterrupted supply of clean dry air, giving it issues with portability and the ability to function as a stand-alone device. The WOLF 4.1 is an improvement when compared to the Fox 4000 in sensitivity and specificity, but the reliance on clean air supply and external computing power for these two machines is essentially the same giving the WOLF 4.1 similar portability issues (dimensions 215 x 466 x 520 mm). The software was also designed with highly technical end users in mind, causing the current machine to require assumed knowledge that is unsuitable for clinical staff. The Lonestar provides an improved sensitivity and specificity to disease in a smaller package (383 x 262 x 195 mm) than the previous two instruments. However, the Lonestar also has very limited methodology options in terms of sampling and airflow without the peripheral equipment detailed in Chapter 4, which have the same air supply and space requirements as the WOLF 4.1 and Fox 4000. It has also currently only been tested against healthy controls and so is not directly comparable to the other machines. The WOLF 3.1 provides the best match to the list of deliverables, including the highest degree of sensitivity and a comparable specificity. Its dimensions (221.5 x 150 x 311 mm) give it a good degree of

Conclusions and Further Work

portability and its touchscreen interface can be operated independently by non-skilled users. One area that could be improved is the ability for it to perform statistical analysis on its own, but the hardware capability is already in-built to achieve this following further development of control software. This initial data shows promise for the suitability of GC/electronic nose instruments for aiding in triage and diagnosis of potential colorectal cancer patients within a point-of-care, primary healthcare environment.

Deliverables	AlphaMOS Fox 4000	Owlstone Lonestar	WOLF 4.1	WOLF 3.1
Technologies used	18 metal oxides	FAIMS	10 amperometric, 3 optical	GC, 5 metal oxides
Deliverables				
Sufficient sensitivity to detect patients that are suffering from colorectal cancer	54%	88%*	78%	92%
Sufficient specificity to screen out patients not suffering from colorectal cancer	48%	60%*	79%	77%
Ability to be used as a stand-alone device	Needs air supply + external PC	Needs air supply, external analysis	Needs air supply + regulation	Needs air supply
Non-invasive technique	Yes - urine	Yes - urine	Yes - urine	Yes - urine
Use of 'acceptable' medium for analysis	Yes - urine	Yes - urine	Yes - urine	Yes - urine
Reasonable degree of portability	Desktop w/ external PC	Portable, large setup peripherals	Desktop w/ external monitor	Portable
Low technical knowledge required for analysis	No for statistics	No for statistics	No	No for statistics
Relative low cost per treatment compared to colonoscopy	Scale-dependent	Scale-dependent	Scale-dependent	Scale-dependent
Reasonable analysis time	~10 minutes	~20 minutes	~10 minutes	~25 minutes
Ability to be serviced and maintained easily	Not tested	Not tested	Not tested	Not tested
Ability to store patient data for later use and updates	Yes	Yes	Yes	Yes
Robust design that cannot be easily damaged by contact	Not tested	Not tested	Not tested	Not tested

Table 8.2: Comparison of the tested electronic noses against original deliverables

* sensitivity/specificity of Lonestar not directly comparable

8.1. Recommendations and Further Work

The GC-MS analysis was only qualitative in nature due to a wide variation in a number of different environmental factors between all samples. Conditions such as pH and salt concentration should be controlled using experimental pre-processing techniques for GC-MS, so that full quantitative analysis can be done to give much more clarity to the urine content data. The GC-MS also has a limitation in sensitivity that caused difficulty in accurately detecting the urine headspace content, which was improved to some degree through the use of pre-concentration techniques such as ITEX and SPME.

Contamination of samples by additional compounds in the environment can occur during collection, while being put into storage (in addition to cross-contamination), and when being aliquoted for analysis. The results of this investigation could be improved through the use of air monitoring systems and barriers between individual samples and users (such as by using gloves) in order to minimise the risk of contamination. There are other confounding factors on the analysis of urine samples that cannot be controlled, including the level of water dilution in the samples. This effect occurs naturally as subjects will have varying levels of excess water to be excreted over time. The effect of this could be minimised in future work by lengthening headspace generation times to ensure that sufficient volatiles are present in all samples for suitable distinction.

The technologies combined together in the electronic nose instruments included in the study are by no means exhaustive; there are a large number of different permutations that could be considered. The combination of gas chromatography with a metal oxide sensor array was the most successful technique in this study, and so its use as a pre-separation technique for other sensing technologies such as ion mobility spectrometry or an amperometric sensor array could also achieve high diagnostic value.

Conclusions and Further Work

The Owlstone Lonestar only had useful data for colorectal cancer and healthy volunteer samples, but it would be much more coherent to have another dataset include IBS samples to give a better picture of clinical relevance. The choice of sensors on the “WOLF 4.1” instrument was based on the newest range of available electro-chemical and small optical sensors on the market. However, some of them did not respond with any reasonable sensitivity to the volatile markers in either the standard or urine samples. This list of sensors included in the array could be reduced without much effect on the overall sensitivity of the system, and those omitted could be replaced with sensors that may contribute to a greater extent. The single volatile samples used to determine sensitivity of the sensors in the WOLF 4.1 had concentrations calculated in volume of water, which did not result in a direct measure of sensor sensitivity. This led to the employment of a volatile standard generation rig to produce set concentrations in air on the WOLF 3.1; in future studies this rig could also be used on the WOLF 4.1 in order to directly compare the sensitivities of the two sensing methods.

The WOLF 3.1 produced the highest sensitivity and specificity levels as compared to the other electronic noses being tested, but there are a number of improvements that could still be made to its operation. The instrument’s electronic hardware has the capability to complete statistical analysis on-line, and an algorithm could be implemented in its software for future studies. Different combinations of sensors could also be tested in its array to investigate their diagnostic potential in conjunction with GC separation. Finally, a pumped pneumatic system could be better developed and tested in the WOLF 3.1 to prepare it for fully stand-alone usage in clinic.

There was also no exact overlap of samples run through all four instruments, although the experimental methods used were as similar as they could be. A more definitive parallel comparative experiment can be conducted with a single cohort of urine samples with

Conclusions and Further Work

separate aliquots being run through all machines, now that they are all fully developed. Further investigation could be undertaken to see the ability of the instruments to stage the disease progression using urine headspace samples, and to differentiate between different groups of diseases (including IBDs, for example). Finally, the sample numbers run through all of the instruments are currently at a very small scale, and their true sensitivities and specificities to colorectal cancer may be very different from the values shown here. There is scope for scaling up the size of cohorts run through the candidate WOLF 3.1 instrument, so that a more accurate picture of its diagnostic potential can be ascertained.

Appendix 1: Additional GC-MS Chromatograms and Mass Spectra

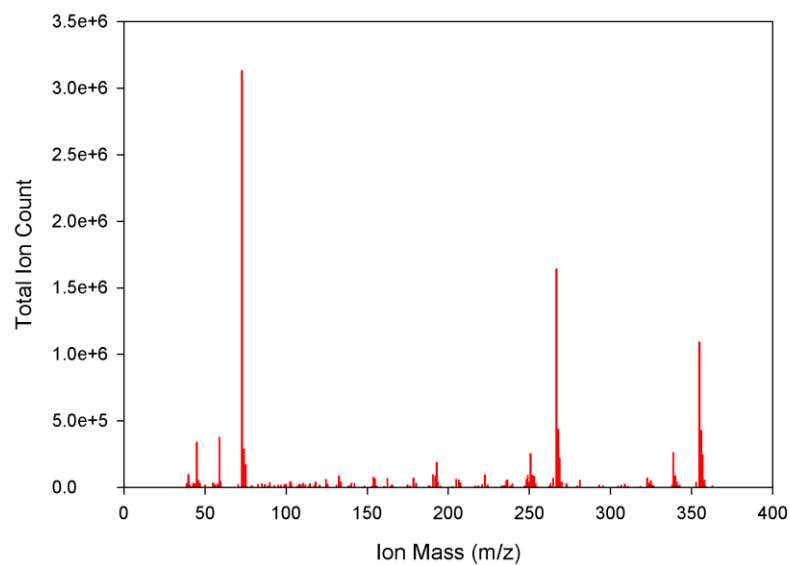


Figure 3.5: Example of the mass spectrum of an artefact peak found at 6.48 minutes

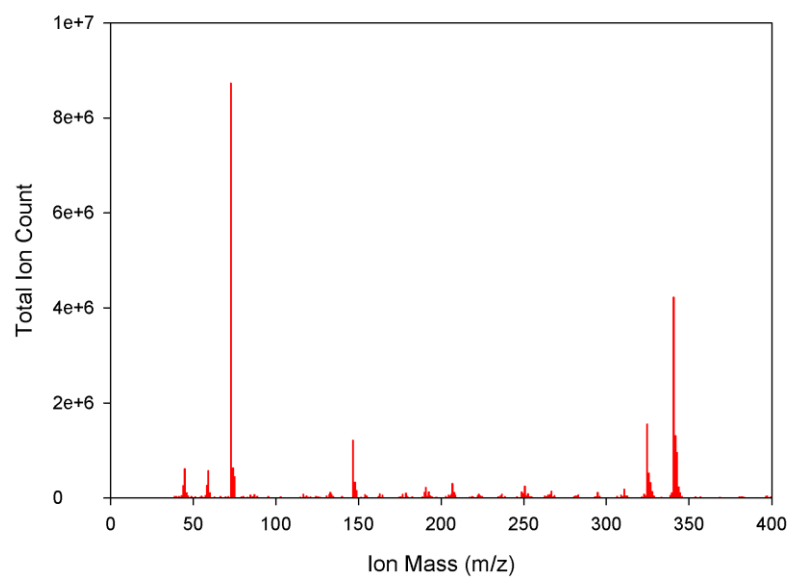


Figure 3.6: Example of the mass spectrum of an artefact peak found at 7.81 minutes

Appendix 1: Additional GC-MS Chromatograms and Mass Spectra

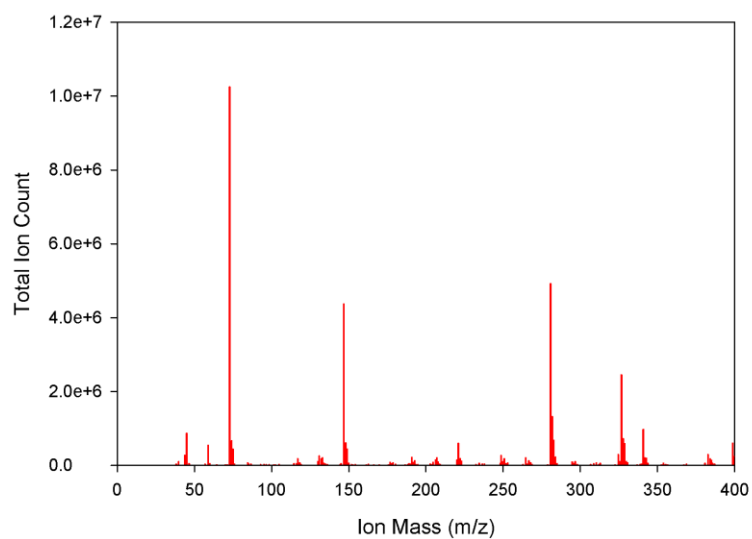


Figure 3.7: Example of the mass spectrum of an artefact peak found at 9.00 minutes

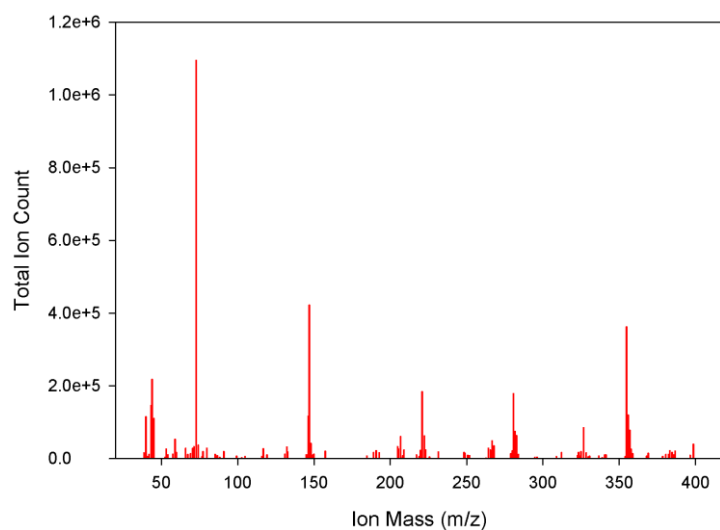


Figure 3.8: Example of the mass spectrum of an artefact peak found at 10.04 minutes

Common Peak Mass Spectra in Urine Samples

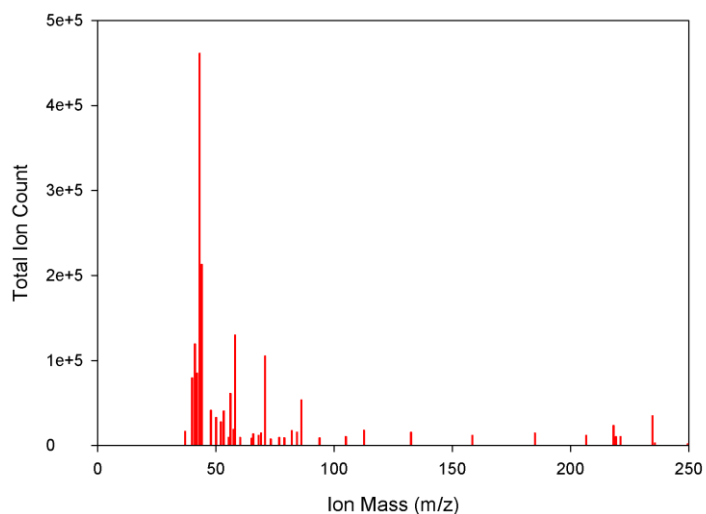


Figure 3.13: Example mass spectrum of an ITEX peak found at 2.83 minutes

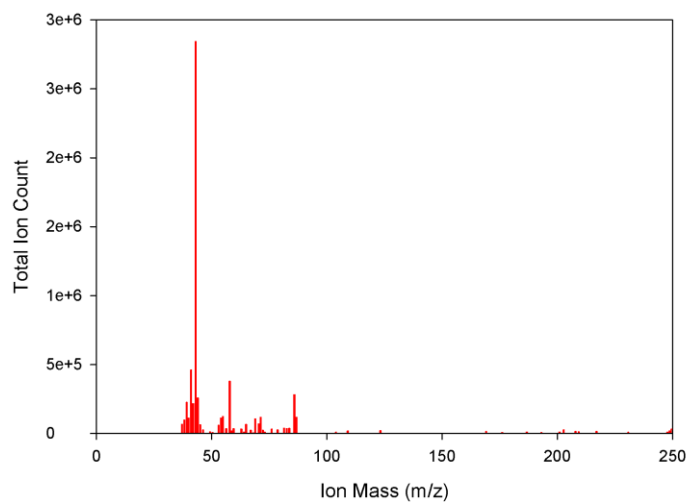


Figure 3.14: Example mass spectrum of an ITEX peak found at 2.95 minutes

Appendix 1: Additional GC-MS Chromatograms and Mass Spectra

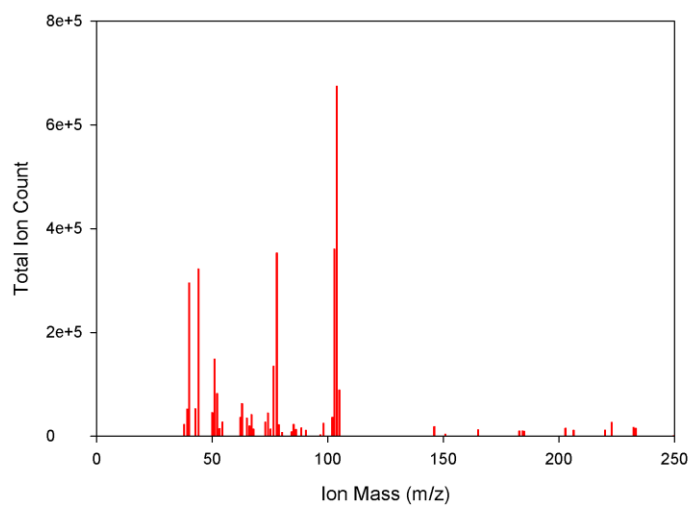


Figure 3.16: Example mass spectrum of an ITEX peak found at 4.70 minutes

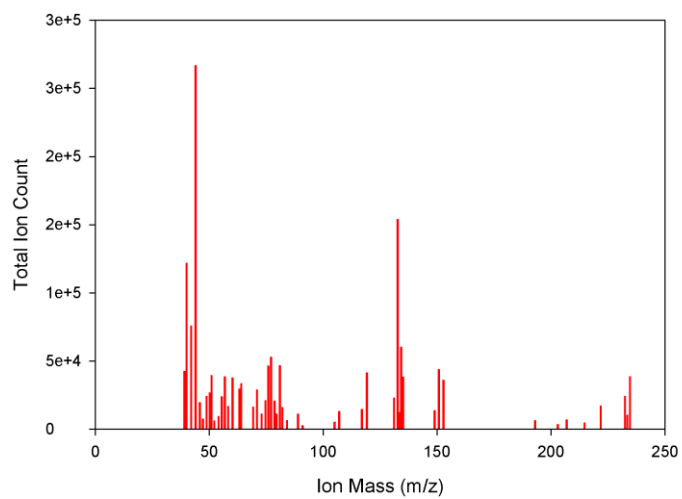


Figure 3.17: Example mass spectrum of an ITEX peak found at 5.30 minutes

Appendix 1: Additional GC-MS Chromatograms and Mass Spectra

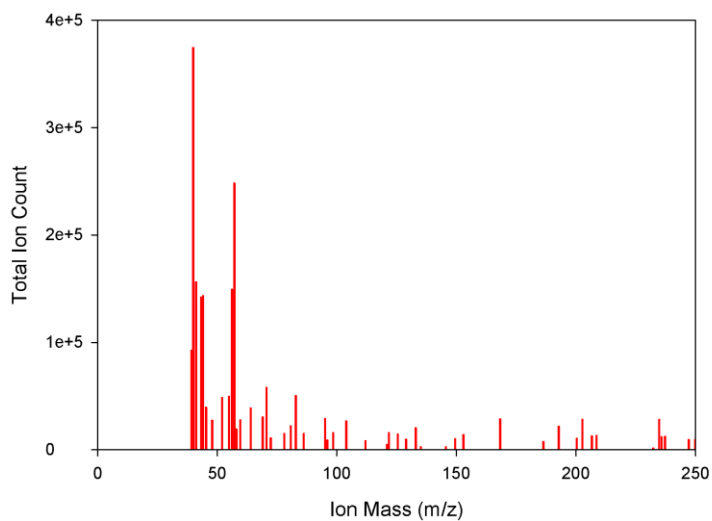


Figure 3.18: Example mass spectrum of an ITEX peak found at 5.37 minutes

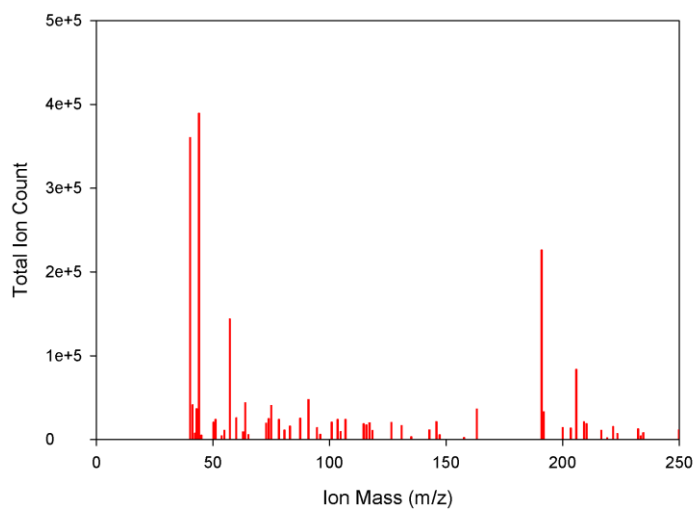


Figure 3.19: Example mass spectrum of an ITEX peak found at 9.75 minutes

Appendix 1: Additional GC-MS Chromatograms and Mass Spectra

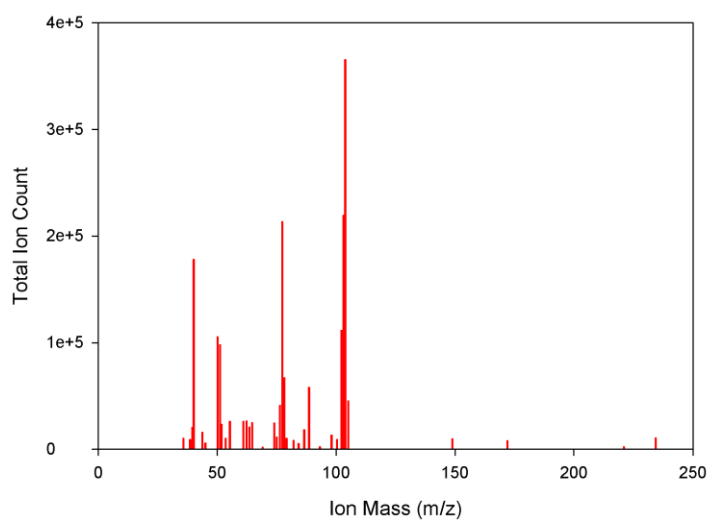


Figure 3.21: Example mass spectrum of a SPME peak found at 4.67 minutes

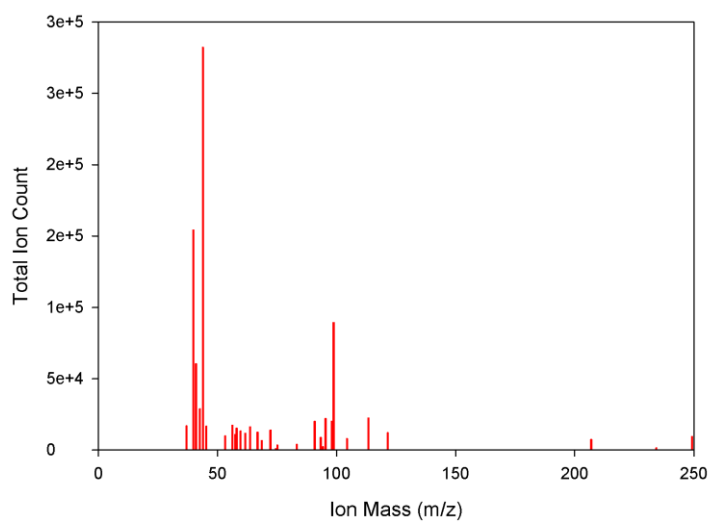


Figure 3.22: Example mass spectrum of a SPME peak found at 4.75 minutes

Appendix 1: Additional GC-MS Chromatograms and Mass Spectra

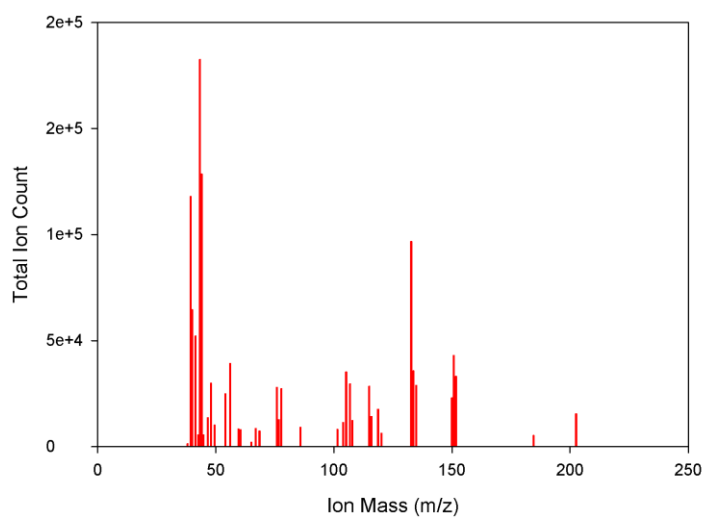


Figure 3.23: Example mass spectrum of a SPME peak found at 5.31 minutes

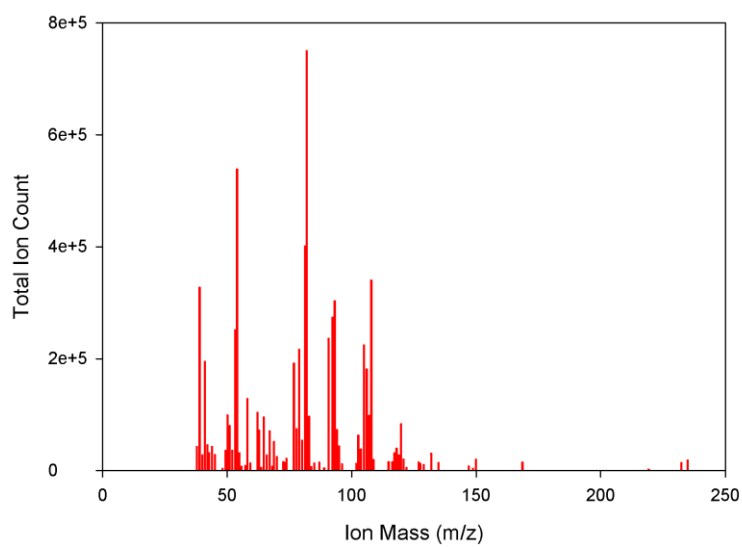


Figure 3.24: Example mass spectrum of a SPME peak found at 7.95 minutes

Appendix 1: Additional GC-MS Chromatograms and Mass Spectra

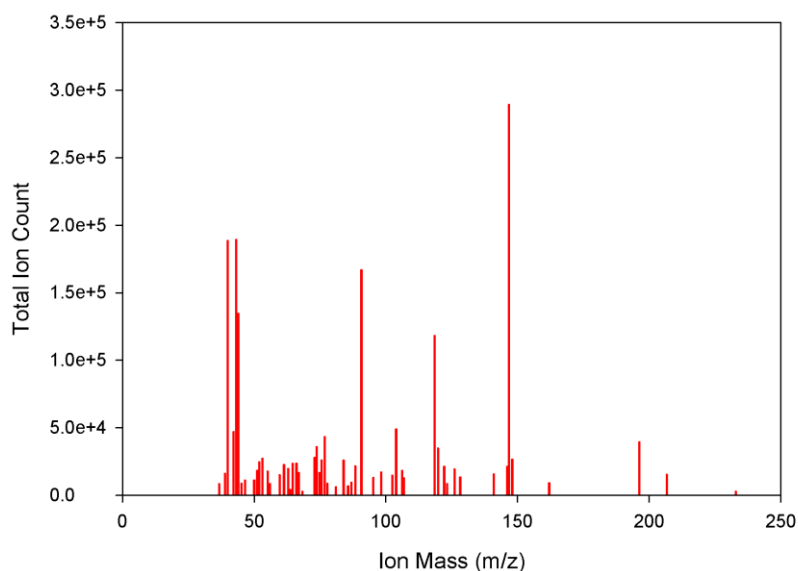


Figure 3.25: Example mass spectrum of a SPME peak found at 9.53 minutes

Peak at 5.37 minutes	
Tally Scores	Top Three Candidate Chemicals
9	1,2-Ethanediamine, N,N'-dimethyl-
8	Acetaldehyde
7	Ethylamine, 2-(adamantan-1-yl)-1-methyl-
Sample Set:	Rates of Incidence within Set
Full Set	22.6%
CRC	8.3%
IBS	29.8%
V	28.2%
CO	18.4%
CLD	15.4%

Table 1: List of top three tallied NIST classifications for ITEX peaks at 5.37 minutes and rates of incidence (low in red, normal in black, high in green)

Appendix 1: Additional GC-MS Chromatograms and Mass Spectra

Peak at 6.63 minutes	
Tally Scores	Top three Candidate Chemicals
22	1H-Pyrrole, 2,5-dihydro-1-nitroso-
20	Nonanal
14	8,9,9,10,10,11-Hexafluoro-4,4-dimethyl-3,5-dioxatetracyclo[5.4.1.0(2,6).0(8,11)]dodecane
Sample Set:	Rates of Incidence within Set
Full Set	42.1%
CRC	61.7%
IBS	49.1%
V	35.2%
CO	5.3%
CLD	50.0%

Table 2: List of top three tallied NIST classifications for ITEX peaks at 6.63 minutes and rates

of incidence (low in red, normal in black, high in green)

Peak at 6.71 minutes	
Tally Scores	Top three Candidate Chemicals
17	4-tert-butylamphetamine
17	Amphetamine
12	2,4-Bis(diazo)adamantane
Sample Set:	Rates of Incidence within Set
Full Set	25.8%
CRC	30.0%
IBS	21.1%
V	15.5%
CO	28.9%
CLD	34.6%

Table 3: List of top three tallied NIST classifications for ITEX peaks at 6.71 minutes and rates

of incidence (low in red, normal in black, high in green)

Peak at 6.89 minutes	
Tally Scores	Top three Candidate Chemicals
9	Ethyne, fluoro-
8	N-carbobenzyloxy-L-tyrosyl-L-valine
7	Amphetamine
Sample Set:	Rates of Incidence within Set
Full Set	25.0%
CRC	16.7%
IBS	24.6%
V	28.2%
CO	21.1%
CLD	42.3%

Table 4: List of top three tallied NIST classifications for ITEX peaks at 6.89 minutes and rates of incidence (low in red, normal in black, high in green)

Peak at 7.33 minutes	
Tally Scores	Top three Candidate Chemicals
13	1-Ethyl-1(1-cyclobutylidenethyl)cyclobutane
12	3-Nonyn-2-ol
11	Cyclohexanol, 1-methyl-4-(1-methylethyl)-
Sample Set:	Rates of Incidence within Set
Full Set	33.7%
CRC	13.3%
IBS	29.8%
V	31.0%
CO	36.8%
CLD	69.2%

Table 5: List of top three tallied NIST classifications for ITEX peaks at 7.33 minutes and rates of incidence (low in red, normal in black, high in green)

Appendix 1: Additional GC-MS Chromatograms and Mass Spectra

Peak at 7.64 minutes	
Tally Scores	Top three Candidate Chemicals
14	2-Propenoic acid, 3-[2-(aminocarbonyl)phenyl]-
12	Benzeneethanamine, 4-chloro- α -methyl-
12	Benzofuran, 4,7-dimethyl-
Sample Set:	Rates of Incidence within Set
Full Set	50.0%
CRC	70.0%
IBS	42.1%
V	42.3%
CO	36.8%
CLD	26.9%

Table 6: List of top three tallied NIST classifications for ITEX peaks at 7.64 minutes and rates of incidence (low in red, normal in black, high in green)

Peak at 8.51 minutes	
Tally Scores	Top three Candidate Chemicals
5	2,5-Pyrrolidinedione, 1-penta-3,4-dienyl-
5	4-Hydroxy-3-methylacetophenone
5	Cyclopropyl carbinol
Sample Set:	Rates of Incidence within Set
Full Set	18.7%
CRC	21.7%
IBS	21.1%
V	11.3%
CO	0.0%
CLD	38.5%

Table 7: List of top three tallied NIST classifications for ITEX peaks at 8.51 minutes and rates of incidence (low in red, normal in black, high in green)

Peak at 8.68 minutes	
Tally Scores	Top three Candidate Chemicals
13	Pentane-2,4-dione, 3-(1-adamantyl)-
11	2-n-butyladamantane
11	2-Methyl-2-butyl-1,3-benzodioxole
Sample Set:	Rates of Incidence within Set
Full Set	15.1%
CRC	1.7%
IBS	17.5%
V	14.1%
CO	15.8%
CLD	30.8%

Table 8: List of top three tallied NIST classifications for ITEX peaks at 8.68 minutes and rates of incidence (low in red, normal in black, high in green)

Peak at 8.79 minutes	
Tally Scores	Top three Candidate Chemicals
12	Ethanedial, dioxime
8	3,3-Dimethyl-4-methylamino-butan-2-one
5	1-Octadecanamine, N-methyl-
Sample Set:	Rates of Incidence within Set
Full Set	13.5%
CRC	8.3%
IBS	3.5%
V	7.0%
CO	28.9%
CLD	26.9%

Table 9: List of top three tallied NIST classifications for ITEX peaks at 8.79 minutes and rates of incidence (low in red, normal in black, high in green)

Peak at 9.83 minutes	
Tally Scores	Top three Candidate Chemicals
18	Ethanone, 1-[4-(1-hydroxy-1-methylethyl)phenyl]-
12	Benzeneethanol, α -methyl-3-(1-methylethyl)-
10	1-(3,5-Dimethyl-1-adamantanoyl)semicarbazide
Sample Set:	Rates of Incidence within Set
Full Set	18.3%
CRC	11.7%
IBS	26.3%
V	8.5%
CO	10.5%
CLD	38.5%

Table 10: List of top three tallied NIST classifications for ITEX peaks at 9.83 minutes and

rates of incidence (low in red, normal in black, high in green)